STAINLESS STEEL REINFORCEMENT AS A REPLACEMENT FOR EPOXY COATED STEEL IN BRIDGE DECKS

FINAL PROJECT REPORT – FHWA-OK-13-08

ODOT SP&R ITEM NUMBER 2231

Submitted to:
John R. Bowman, P.E.
Planning & Research Division Engineer
Oklahoma Department of Transportation

Submitted by:
David Darwin
Matthew O'Reilly
Isaac Somogie
Jayne Sperry
James Lafikes
Scott Storm
JoAnn Browning

University of Kansas Center for Research, Inc.
2585 Irving Hill Road
Lawrence, Kansas 66045-7563

August 2013

TECHNICAL REPORT DOCUMENTATION PAGE

1. Report No. FHWA-OK- 13-08	2. Government Accession No.	3. Recipient's Catalog No.
4. Title and Subtitle Stainless Steel Reinforcement as a Replacement for Epoxy Coated Steel in Bridge Decks		5. Report Date Aug 2013 6. Performing Organization Code
7. Author(s) David Darwin, Matthew O'Reilly, Isaac Somogie, Jayne Sperry, James Lafikes, Scott Storm, and JoAnn Browning		8. Performing Organization Report SM Report 105
9. Performing Organization Name and Address University of Kansas Center for Research, Inc. 2585 Irving Hill Road Lawrence, Kansas 66045-7563		10. Work Unit No. 11. Contract or Grant No. ODOT SP&R Item Number 2231
12. Sponsoring Agency Name and Address Oklahoma Department of Transportation Planning and Research Division 200 N.E. 21st Street, Room 3A7 Oklahoma City, OK 73105		13. Type of Report and Period Covered Final Report Oct 2010 - Jul 2013 14. Sponsoring Agency Code
15. Supplementary Notes Click here to enter text.		

16. Abstract

The corrosion resistance of 2304 stainless steel reinforcement and stainless steel clad reinforcement was compared to conventional and epoxy-coated reinforcement (ECR). 2304 stainless steel was tested in both the as-received condition (dark mottled finish) and repickled to a bright finish. Specimens were evaluated using rapid macrocell, Southern Exposure, and cracked beam tests. ECR and stainless steel clad specimens were evaluated with the coating having no intentional damage and with the coating or cladding penetrated. ECR with the coating penetrated is used to represent ECR that has undergone damage during construction. Clad bars were also bent to evaluate the corrosion resistance of the cladding after fabrication. Bars were tested for corrosion loss and chloride content at corrosion initiation. The critical chloride corrosion threshold for each system was established, as was an average corrosion rate after initiation. Results obtained from the southern exposure and cracked beam tests are used to the estimate cost effectiveness for each system under a 75-year and 100-year service life.

Epoxy-coated reinforcement and stainless steel clad bars with and without intentional penetrations in the coating, as well as 2304 stainless steel in the as-received and repickled conditions exhibit a significant increase in corrosion resistance and critical chloride corrosion threshold compared to conventional steel, with undamaged epoxy-coated specimens exhibiting the lowest corrosion rate. In the as-received condition, 2304 stainless steel did not satisfy the requirements of ASTM A955, while repickled 2304 did. The undamaged stainless steel clad bars satisfied the requirements of the rapid macrocell test in ASTM A955; however, some cracked beam specimens containing stainless steel clad bars exhibited corrosion rates greater than the maximum allowable value permitted by ASTM A955. Conventional reinforcing steel is the least cost-effective form of reinforcement, with 2304 stainless steel in the as-received condition, ECR with penetrations through the epoxy, correctly pickled 2304 stainless steel, and stainless steel clad reinforcement representing progressively more cost-effective materials. Stainless steel clad reinforcement, however, is not currently available, and its failure to pass ASTM A955 calls its long-term performance into question. Increasing the cover over the top mat of steel and considering partial-deck replacements, where applicable, are methods that should be considered to decrease life cycle costs.

17. Key Words Concrete, chlorides (or critical chloride corrosion threshold), corrosion, epoxy-coated reinforcement, stainless steel, stainless steel clad reinforcement	18. Distribution Statement No restrictions. This publication is available from the Planning & Research Div., Oklahoma DOT.		
19. Security Classif. (of this report) Unclassified	20. Security Classif. (of this page) Unclassified	21. No. of Pages 205	22. Price N/A

ACKNOWLEDGEMENTS

This study was supported by the Oklahoma Department of Transportation (ODOT SP&R Item Number 2231) and the University of Kansas Transportation Research Institute. Additional support was provided by Talley Metals, NX Infrastructure, the Concrete Reinforcing Steel Institute, ABC Coating Company of Tulsa Oklahoma, and Midwest Concrete Materials. Walter Peters, P.E. of ODOT provided data bridge construction costs in Oklahoma.

SI* (MODERN METRIC) CONVERSION FACTORS

APPROXIMATE CONVERSIONS TO SI UNITS				
SYMBOL	**WHEN YOU KNOW**	**MULTIPLY BY**	**TO FIND**	**SYMBOL**
LENGTH				
in	inches	25.4	millimeters	mm
ft	feet	0.305	meters	m
yd	yards	0.914	meters	m
mi	miles	1.61	kilometers	km
AREA				
in^2	square inches	645.2	square millimeters	mm^2
ft^2	square feet	0.093	square meters	m^2
yd^2	square yard	0.836	square meters	m^2
ac	acres	0.405	hectares	ha
mi^2	square miles	2.59	square kilometers	km^2
VOLUME				
fl oz	fluid ounces	29.57	milliliters	mL
gal	gallons	3.785	liters	L
ft^3	cubic feet	0.028	cubic meters	m^3
yd^3	cubic yards	0.765	cubic meters	m^3
NOTE: volumes greater than 1000 L shall be shown in m^3				
MASS				
oz	ounces	28.35	grams	g
lb	pounds	0.454	kilograms	kg
T	short tons (2000 lb)	0.907	megagrams (or "metric ton")	Mg (or "t")
TEMPERATURE (exact degrees)				
^oF	Fahrenheit	5 (F-32)/9 or (F-32)/1.8	Celsius	^oC
ILLUMINATION				
fc	foot-candles	10.76	lux	lx
fl	foot-Lamberts	3.426	candela/m^2	cd/m^2
FORCE and PRESSURE or STRESS				
lbf	pound force	4.45	newtons	N
lbf/in^2	pound force per square inch	6.89	kilopascals	kPa

APPROXIMATE CONVERSIONS FROM SI UNITS				
SYMBOL	**WHEN YOU KNOW**	**MULTIPLY BY**	**TO FIND**	**SYMBOL**
LENGTH				
mm	millimeters	0.039	inches	in
m	meters	3.28	feet	ft
m	meters	1.09	yards	yd
km	kilometers	0.621	miles	mi
AREA				
mm^2	square millimeters	0.0016	square inches	in^2
m^2	square meters	10.764	square feet	ft^2
m^2	square meters	1.195	square yards	yd^2
ha	hectares	2.47	acres	ac
km^2	square kilometers	0.386	square miles	mi^2
VOLUME				
mL	milliliters	0.034	fluid ounces	fl oz
L	liters	0.264	gallons	gal
m^3	cubic meters	35.314	cubic feet	ft^3
m^3	cubic meters	1.307	cubic yards	yd^3
MASS				
g	grams	0.035	ounces	oz
kg	kilograms	2.202	pounds	lb
Mg (or "t")	megagrams (or "metric ton")	1.103	short tons (2000 lb)	T
TEMPERATURE (exact degrees)				
^oC	Celsius	1.8C+32	Fahrenheit	^oF
ILLUMINATION				
lx	lux	0.0929	foot-candles	fc
cd/m^2	candela/m^2	0.2919	foot-Lamberts	fl
FORCE and PRESSURE or STRESS				
N	newtons	0.225	pound force	lbf
kPa	kilopascals	0.145	pound force per square inch	lbf/in^2

*SI is the symbol for the International System of Units. Appropriate rounding should be made to comply with Section 4 of ASTM E380.

TABLE OF CONTENTS

LIST OF FIGURES

LIST OF TABLES

1. INTRODUCTION AND PROBLEM STATEMENT

The use of deicing salts in the United States has resulted in the steady deterioration of roadway bridge decks due to the corrosion of reinforcing steel. Since the middle 1970s, the principal corrosion protection techniques for bridge decks have involved the use of epoxy-coated reinforcement (ECR) and increased cover over the reinforcing bars. The combination has greatly lengthened the life of bridge decks, but does not represent a perfect solution. The higher cover increases the bridge dead load and the cost of construction. Epoxy-coated reinforcement adds only slightly to the cost of bridge construction, but there are a number of well-documented cases in both the field and laboratory in which poorly adhering epoxy coatings have actually increased corrosion problems, and there is evidence that all epoxy coatings will eventually be susceptible to those shortcomings. As a result of these concerns, a number of other protective measures have been developed or are under development. These include the use of denser concretes, corrosion inhibitors, and corrosion-resistant steel alloys. Among the latter are various types of stainless steel, including 2304 duplex stainless steel and stainless steel clad reinforcing bars. Based on earlier studies, stainless steel reinforcement is generally less susceptible to corrosion than conventional and epoxy-coated reinforcement, but all stainless steels do not provide the same level of protection and their superiority to ECR has not been clearly demonstrated in all cases. 2304 duplex reinforcing bars and NX-SCR™ stainless steel clad bars (the only stainless steel clad reinforcement that was commercially available in the U.S. at the initiation of this study) have not undergone the same level of testing as other solid stainless steels and prototype clad bars in environments similar to those found in bridge decks. Combined with the additional initial cost of stainless steel compared to epoxy-coated reinforcement, there is a need to quantify the costs and benefits of using stainless steel reinforcement as a replacement for epoxy-coated steel in bridge decks.

1.1 OBJECTIVES

This study was undertaken with the following objectives:

1.1.1 Determine the corrosion resistance of 2304 duplex stainless steel reinforcement and NX-SCR™ stainless steel clad bars compared to conventional and epoxy-coated reinforcement in reinforced concrete bridge decks.

1.1.2 Estimate the life expectancy and cost effectiveness of 2304 duplex stainless steel, NX-SCR™ stainless steel clad reinforcement, epoxy-coated reinforcement, and mild steel reinforcement in bridge decks in Oklahoma.

1.2 PREVIOUS WORK

In 1979, the cost of bridge repairs in the federal-aid system due to all types of corrosion damage was estimated to be $6.3 billion (Locke 1985). By 1986, the estimated cost was $20 billion and was forecast to increase at the rate of $500 million per year (Cady and Gannon 1992). By 1992, the estimated total repair cost had risen to $51 billion (Fliz et al. 1992). In 2002, these figures translated into annual costs of $1.07 to $2.93 billion for maintenance and cost of capital for concrete bridge decks alone (Yunovich et al. 2002). As a result, methods that can significantly reduce or halt chloride-induced corrosion have been pursued aggressively for well over 30 years.

The methods used to reduce corrosion of reinforcing steel may be divided into two categories. The first includes methods that slow the initiation of corrosion, that is, the time it takes the chlorides in the deicers to reach a concentration that is high enough to cause corrosion of the reinforcing steel. The second includes methods that lengthen the corrosion period, the time between initiation of corrosion and the end of service life. Both the use of

epoxy-coated reinforcement and increased cover over the reinforcing bars slow the initiation of corrosion and lengthen the corrosion period. Increased cover increases the time required for chlorides to reach the reinforcing steel and lowers the rate at which oxygen and moisture are available to participate in the corrosion process. The epoxy coating also limits access of chlorides, oxygen, and moisture to the surface of the reinforcing steel. In regions where the chlorides have access to the steel at breaks in the coating, corrosion is slowed because the epoxy coating still limits access of oxygen and moisture, which are required for active corrosion. Problems with epoxy-coated reinforcement usually involve small breaks in the coating that allow the bond between the coating and the steel to be lost. The coating remains generally intact, but a chloride concentration cell forms underneath the coating in an environment that is low in oxygen. The result is crevice corrosion, which essentially involves hydrochloric acid attack of the steel. This happened for poorly applied coatings in substructures in Florida (Sagues et al. 1994). There is clear evidence that given enough time even well-applied coatings will lose adhesion (Manning 1996, Smith and Virmani 1996, Darwin et al. 2011. The problem appears to be worse for bars located directly under transverse cracks in decks (Darwin et al. 2011).

Conventional reinforcing steel embedded in concrete is normally in a passive or noncorrosive condition due to the high pH of the concrete pore solution. Passivation involves the formation of a tightly adhering iron-oxide layer on the reinforcing steel surface, which protects the iron from corrosion. To obtain a passive condition, the pH must be between 12.5 and 13.8 (Jones 1992). If the pH of the concrete solution is lowered, the iron-oxide layer becomes unstable, and corrosion will occur.

The pH of concrete can be lowered in two ways: by carbonation due to the penetration of CO_2 into the concrete; or indirectly, by the presence of aggressive ions like Cl^-, found in deicing salts. Chloride ions also weaken the iron-oxide layer, allowing chloride ions to react with available iron cations on the bar surface to form an iron-chloride complex. In the presence of hydroxyl ions, the iron-chloride reacts with hydroxyl ions to form ferrous hydroxide and release the chloride ions, which, in turn, again react with available iron cations. As a result, the passive iron-oxide layer is dissolved, initiating corrosion. The corrosion can be one of two forms: microcorrosion, in which the anode (corrosion site) is located nearby the cathode (location at which oxygen and moisture are converted to hydroxyl ions); or macrocell corrosion, in which large regions of the steel serve as anodes or cathodes. In a bridge deck, typically the upper layer of steel serves as the anode, while the lower layer of steel serves as the cathode. Studies of solid stainless steel reinforcement in concrete have demonstrated that 304 and 316 austenitic stainless steels (McDonald, Pfeifer, and Sherman 1998) and 2205 duplex stainless steel (Ji et al. 2005) provide superior corrosion resistance. [For duplex stainless steels, the numbering system indicates the quantities of chromium and nickel. For example, 2205 represents a steel that consists of 22% chromium and 5% nickel.] That work also showed, however, that 304 stainless steel does not perform well when combined in a macrocell with conventional steel, while 316 and 2205 stainless steels are not affected by such a combination. Prototype 304 stainless steel clad reinforcement performed well in preliminary tests at the University of Kansas (Darwin et al. 1999, Kahrs, Darwin, and Locke 2001). Based on recommendations by Darwin et al. (1999) that were, in turn, based on the observations by McDonald et al. (1998), the producer chose to switch to a 316L stainless steel cladding when the bars went into production. Research at the University of Kansas performed for the South Dakota Department of Transportation (Darwin et al. 2007) indicated that the resulting SMI-316 SC™ reinforcement provides high resistance to both microcell and macrocell corrosion. Unfortunately, due to high costs and production problems, SMI-316 SC™ reinforcement is no longer in production.

In recent years, other studies have addressed the use of stainless steel and stainless steel clad reinforcement as potential replacements for epoxy-coated and conventional reinforcing bars. Clemeña (2002) found that the corrosion performance of one type of 316 stainless steel clad reinforcement was the equal of similar solid reinforcement, although the

same reinforcement was found unsatisfactory by Cross et al. (2001) for reasons of poor structural performance. That reinforcement is the predecessor of NX-SCR™ bars proposed for evaluation in the current study. The current NX-SCR™ bars are said by the manufacturer to be fabricated to a much higher quality than those tested nearly a decade ago.

Scully and Hurley (2007) evaluated 316LN solid stainless steel, 316L stainless steel clad, 2101 solid duplex stainless steel, and low carbon, chromium (MMFX-2) and conventional reinforcing steel in saturated calcium hydroxide (used as a proxy for concrete pore solution). Those tests indicated superior performance by the 316LN solid stainless steel bars but lower levels of performance by the 316L stainless steel clad bars and the 2101 duplex and MMFX-2 bars. The lower performance of the stainless steel clad reinforcement was the result of defects along a seam in the cladding. The bars are manufactured by first forming 316L stainless steel pipe (with a seam) that is filled with steel turnings produced during the fabrication of machine parts. The turnings are physically compacted within the stainless steel pipe. The composite is then heated and rolled in the same fashion as conventional reinforcing steel.

In 2009, Hartt et al. reported on a long-term FHWA study on corrosion resistant steels for reinforced concrete. The study included two lower grades of stainless steel (3Cr12 and 2101) and higher grades of solid stainless steel, 2205 and 316L, along with two 316 stainless steel clad bars, and MMFX-2 reinforcement. Conventional reinforcing steel was used to provide a baseline. The study also included three small slab specimens containing 2304 stainless steel reinforcement, which were apparently added late during the specimen fabrication phase of the work. The tests were performed in concrete but did not include Southern Exposure or cracked beam tests, which are used in most reinforcing bar corrosion protection systems studies. Prior to this study, the 2304 specimens represented the only specimens of 2304 solid stainless steel ever tested in concrete, but were exposed to only about one-half of the chloride content of the 2205 and 316L solid stainless steel bars, and the specimens were not designed to measure corrosion current, a measurement that was made for the other reinforcement in the study.

Recent tests at the University of Kansas have evaluated stainless steels in simulated concrete pore solution in accordance with ASTM A955. O'Reilly et al. (2010) evaluated 2101 and 2205 stainless steel bars and found that both steels exhibited increased corrosion resistance, with 2205 stainless steel outperforming 2101. Sturgeon et al. (2010a, 2011) evaluated multiple stainless steels – XM-28, XM-29, 316LN, and 2205 – in simulated pore solution with chlorides and found all stainless steels performed better than conventional reinforcement. One heat of XM-28 bars, however, performed poorly, likely due to a poor cleaning of the stainless steel surface. A second heat of XM-28 performed comparably to the other stainless steels.

O'Reilly et al. (2011) tested 2205 stainless steel in Southern Exposure and cracked beam tests, as well as in field slabs exposed to the same conditions as a typical Kansas bridge deck. In all specimens, 2205 stainless steel exhibited improved corrosion resistance when compared to conventional and epoxy-coated reinforcement. Of the 11 Southern Exposure specimens with 2205 stainless steel, seven specimens did not initiate corrosion after over 300 weeks of testing. The four specimens that initiated corrosion did so at an average age over 10 times greater than conventional reinforcement and an average chloride content over 15 times greater than conventional reinforcement. Cracked beam specimens and field specimens containing 2205 stainless steel showed similar improvements over specimens containing conventional steel.

2. EXPERIMENTAL WORK

The bars evaluated in this study are described in Section 2.1 The test methods, the rapid macrocell, bench scale (Southern Exposure and cracked beam), and linear polarization resistance tests are described in Sections 2.2 through 2.5.

2.1 MATERIALS

Tests were performed on 2304 duplex stainless steel bars in the as-received and repickled conditions and on NX-SCR™ stainless steel clad bars in the intentionally damaged, undamaged, and uncapped conditions, as well as on conventional steel reinforcement and on epoxy-coated reinforcement (ECR) in the damaged and undamaged conditions. The stainless steel cladding is Type 316L austenitic stainless steel with an average thickness of 19.1 mils. The ECR coating is DuPont™ Nap-Gard® 7-2719 Epoxy Powder with an average thickness of 11.2 mils. The thickness of the stainless steel cladding and epoxy coating were measured with a pull-off gage, per ASTM A775. The conventional steel and ECR bars are from the same heat of steel. The chemical compositions of the bars used for the study are listed in Table 1.

Table 1: Chemical compositions of steels (provided by manufacturer)

Material	C	Mn	P	S	Si	Cu	Cr	Ni	Mo	V	Co	Sn	Al	N	B
ECR and Conventional	0.39	1.18	0.01	0.037	0.23	0.31	0.16	0.15	0.045	0.002	0.001	0.012	0.002	-	-
2304	0.02	1.72	0.02	0.001	0.41	0.3	22.71	3.58	0.25	-	-	-	-	0.18	0.002
NX-SCR™ - cladding	0.018	1.37	0.034	0.003	0.37	-	16.87	10	2	-	-	-	-	0.058	-
NX-SCR™ core	0.34	1.04	0.014	0.026	0.25	-	-	-	-	-	-	-	-	-	-

All tests were performed on No. 5 bars (nominal diameter = 0.625 in.), with the exception of the NX-SCR™ stainless steel clad bars, which, based on weight per unit length, had an average diameter of 0.673 in.

The stainless steel clad bars, conventional reinforcement, and ECR were inspected upon arrival and found to be in good condition. The 2304 bars arrived with a dark and mottled appearance, possibly due to incomplete pickling. As a result, some tests were performed on the 2304 stainless steel bars in both the as-received condition and after repickling.

Repickling was performed at the University of Kansas. The procedure consisted of submerging the bars in a solution of 25% nitric acid and 5% hydrofluoric acid for thirty minutes at room temperature (72° F). The bars were then removed from the solution and rinsed thoroughly with distilled water, producing a bright, shiny surface on the metal. Figure 1 shows 2304 bars in the as-received and repickled conditions.

Figure 1: 2304 duplex stainless steel bars in the as-received (left) and repickled (right) conditions

To protect the exposed steel at the submerged ends of the ECR and stainless steel clad bars in the rapid macrocell tests, one end of each bar was covered with a protective cap. To apply the cap, 3M Scotchkote Liquid Epoxy Coating Patch Compound 323R was applied to the exposed ends and left to dry overnight. A second coat of the epoxy patch compound was then applied to the ends, and a 0.5-in. deep vinyl cap, half-filled with the epoxy, was placed on the end of the bar. One set of stainless steel clad specimens was tested without the use of the protective cap.

The coating on most ECR bars and the cladding on some of the NX-SCR^{TM} bars were penetrated using a 1/8-in. diameter four-flute drill bit to simulate damage that may occur in the field. The number and spacing of the drilled holes varied between the rapid macrocell specimens and bench-scale specimens.

For the rapid macrocell specimens, two holes were placed on each side of a bar, for a total of four holes, exposing 0.83% of the submerged bar area. The holes were located approximately 1 in. from the bottom end of the bar with the second spaced 1 in. from the first hole. For the bench-scale specimens, the number of holes varied based on steel type. The coating on selected ECR specimens was penetrated with five evenly spaced holes on both the top and bottom sides of the bar, exposing 0.5% of the bar area. Selected stainless steel clad specimens had two evenly spaced holes drilled on the top and bottom sides of the bar, exposing 0.2% of the bar area. The reduced number of holes was chosen to reflect the cladding's increased resistance to damage compared to ECR. Holes were drilled to a depth so as to expose the underlying conventional steel. For the rapid macrocell specimens, holes were located approximately 1.5 in. and 2.5 in. from the bottom end of the bar. The exact spacing of the holes varied slightly to avoid drilling at deformations, as shown in Figure 2.

Figure 2: Rapid macrocell specimens, ECR and NX-SCR^{TM} stainless steel clad bars with holes in the coating (0.83% exposed area)

2.2 RAPID MACROCELL TEST

2.2.1 Experimental Procedure

Six specimens for each of the series of specimens were tested in accordance with the rapid macrocell test outlined in Annexes A1 and A2 of ASTM 955/A955M-10 and illustrated in Figure 3, with the exception of undamaged ECR, mixed NX-SCR™ stainless steel/conventional and mixed 2304 duplex stainless steel/conventional specimens for which three specimens were tested.

The bars used in the rapid macrocell test are cut to a length of 5 in. (127 mm) and drilled and tapped at one end to accept a 0.5-in., 10-24 stainless steel machine screw. To remove any oil and surface contaminants introduced when machining the bars, conventional, stainless steel clad, and 2304 specimens are cleaned with acetone prior to testing. ECR bars are cleaned with soap and water. A length of 16-gauge insulated copper wire is attached to each bar with a machine screw. To prevent corrosion from occurring at the electrical connection, 3M Scotchkote Liquid Epoxy Coating Patch Compound 323R is used to thoroughly coat the tops of the bars. After the first coat of epoxy has dried overnight, a second coat is applied to ensure complete coverage.

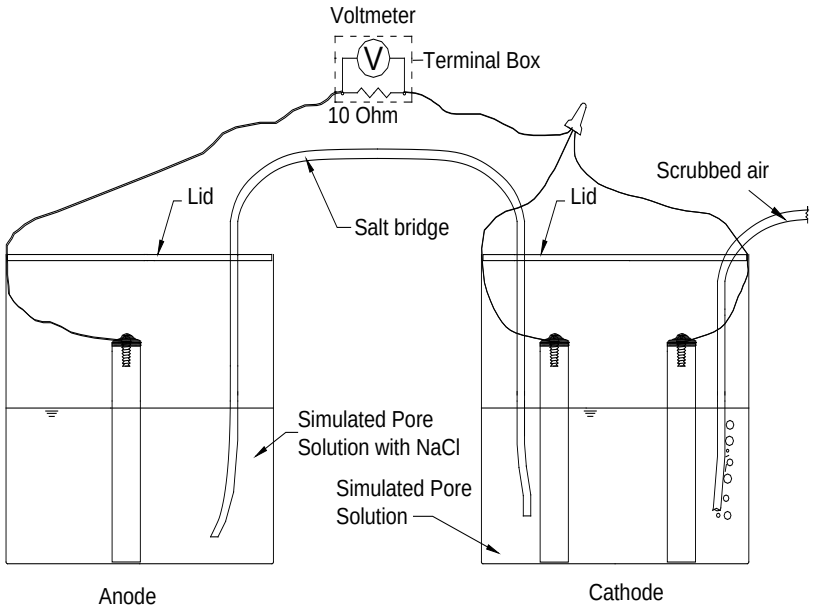

Figure 3: Rapid macrocell test

Extra precautions are taken when preparing the ECR specimens. To avoid coating damage where the bar is clamped in the lathe for drilling and tapping, the bars are cut to a length in excess of 5 in. The area that is damaged by the clamp is then removed, providing the 5-in. specimen with, at most, minimal unintentional damage to the epoxy coating. When selecting anode and cathode bars, the bars with minimal damage to the epoxy coating are used as cathode bars, while the bars with no damage are used as anode bars. Unintentional damage is patched prior to testing, and bars with excessive damage are not used. Prior to testing, the ECR bars are inspected to ensure that no perforations in the coating, other than drilled holes, are present.

To prepare the bent stainless steel clad bars, the specimens are initially cut to a length of 18 in. The specimens are then bent to form a 180° bend around a 3.25-in. diameter pin. The

excess length of bar is then removed with a band saw, providing a specimen that fits in the testing container. One end of the bent bar is drilled and tapped, thus allowing it to accept a machine screw for the electrical connection. The end that is to be electrically connected receives multiple coats of the epoxy patch compound, as described earlier. The other end of the bar is fit with the protective capping system. The cap is then clipped with an alligator clamp and attached to a wire, which is used to stabilize the specimen in the container by securing the wire to the lid. No electrical connection is made between the specimen and the second wire. A rapid macrocell test on a bent bar is shown in Figure 4.

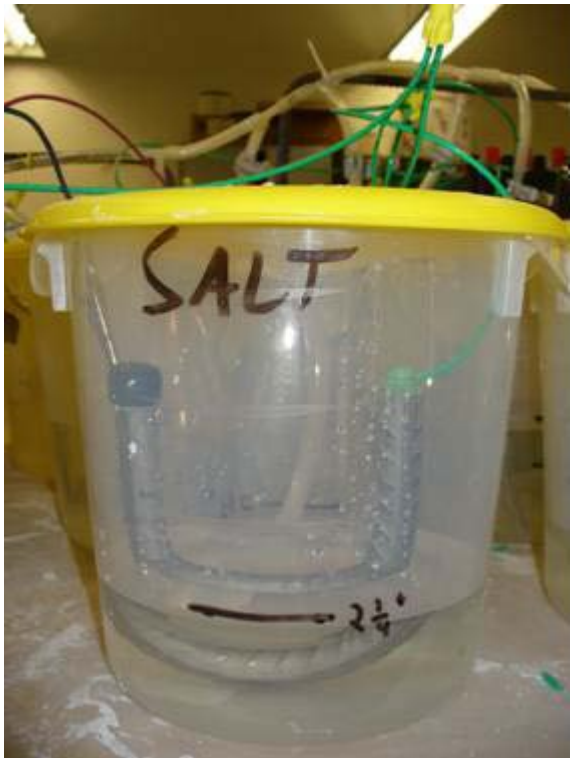

Figure 4: Macrocell test of a bent bar

2.2.2 Test Procedure

A single rapid macrocell test consists of an anode and a cathode, as shown in Figure 3. The cathode consists of two bars placed in a plastic container, which are submerged in simulated concrete pore solution. One liter of pore solution consists of 974.8 g of distilled water, 18.81 g of potassium hydroxide, and 17.87 g of sodium hydroxide. The solution has a pH of 13.9. Air, which is scrubbed to remove carbon dioxide, is bubbled into the cathode solution. The anode consists of a single bar submerged in the simulated concrete pore solution with 15 percent sodium chloride solution. The "salt" solution is prepared by adding 172.1 g of NaCl to one liter of pore solution. To limit the effects of carbonation, the solutions are changed every five weeks. The anode and cathode are electrically connected across a 10-ohm resistor. An ionic connection is provided between the anode and cathode using a potassium chloride salt bridge (Figure 3).

In accordance with Annex A2 of ASTM 955, bars are submerged in the solution to a depth of 3 in., which exposes 6.20 in.^{2} to the solution. In the case of the ECR and stainless steel clad bars that receive a protective cap, the solution depth is 3.5 in., which provides a nearly equal amount of exposed area as obtained for bars without a vinyl cap. The capped specimens submerged to a depth of 3.5 in. have roughly 4% less exposed area than the typical specimens

submerged to a depth of 3 in.. This small difference in exposed area is included in the expressions when calculating corrosion rates. The slightly larger diameter of the NX-SCR™ stainless steel has an exposed area of 6.34 in.^{2} when submerged to an exposed length of 3 in., as well. The bent stainless steel clad bars are placed in a solution to a depth of 2.25 in., which provides an exposed area of 12.7 in.^{2}. The exposed areas are used to calculate the corrosion rate, which is calculated based on the voltage drop measured across the 10-ohm resistor using Faraday's equation.

$$\text{Rate} = K \frac{V \cdot m}{n \cdot F \cdot D \cdot R \cdot A} \quad (1)$$

where the Rate is given in μm/yr,
K = conversion factor = $31.5 \cdot 10^4$ amp·μm ·sec/μA·cm·yr
V = measured voltage drop across resistor, millivolts
m = atomic weight of the metal (for iron, m = 55.8 g/g-atom)
n = number of ion equivalents exchanged (for iron, n = 2 equivalents)
F = Faraday's constant = 96485 coulombs/equivalent
D = density of the metal, g/cm^3 (for iron, D = 7.87 g/cm^3)
R = resistance of resistor, ohms = 10 ohms for the test
A = surface area of anode exposed to solution

In addition to determining the corrosion rate by taking voltage readings across the 10-ohm resistor, the corrosion potential is measured at both the anode and cathode using a saturated calomel electrode (SCE). Voltage drop and potential readings are taken daily for the first week and then weekly thereafter for a total of 15 weeks. Linear polarization resistance (LPR) tests are performed every 3 weeks. The LPR test procedure is described in Section 2.4.5.

For stainless steels to qualify in accordance with the rapid macrocell test guidelines listed in ASTM A955, the corrosion rate of the individual specimens may not exceed 0.50 μm/yr, and the average corrosion rate for all specimens in a series may not exceed 0.25 μm/yr. In some cases, the corrosion current is negative. This, however, does not indicate negative corrosion; rather it is caused by minor differences in the oxidation rate between the single anode bar and the two cathode bars.

2.3 BENCH-SCALE TESTS

2.3.1 General

The bench-scale tests in this study are the Southern Exposure (SE) and cracked beam (CB) tests. These tests take approximately two years to complete. During this period, the specimens are exposed to alternate ponding and drying cycles with a 15% sodium chloride solution. The data collected allows the corrosion rate to be monitored via the voltage drop between top and bottom bars in the specimen. Mat-to-mat resistances and corrosion potentials are also recorded. In addition to these readings, the Southern Exposure specimens are sampled for chlorides at corrosion initiation and at the end of the test.

2.3.2 Concrete mix design and aggregate properties

The concrete used in the study matches that used in bridge decks. The materials used in the concrete mixtures were:
Water – Municipal tap water from the City of Lawrence.
Cement – Type I/II portland cement.

Coarse Aggregate – Crushed limestone from Fogle Quarry. Nominal maximum size = 0.75 in., bulk specific gravity (SSD) = 2.58, absorption = 2.3%, unit weight = 95.9 lb/ft^3.

Fine Aggregate – Kansas River sand. Bulk specific gravity (SSD) = 2.62, absorption = 0.8%, fineness modulus = 2.51.

Air-Entraining Agent – Daravair 1400, a saponified rosin-based air-entraining agent manufactured by W. R. Grace.

The concrete mixture proportions are detailed in Table 2. The concrete for all test specimens has a water-cement ratio of 0.45, a target slump of 3 ± 0.5 in. (75 ± 13 mm), a target air content of 6 ± 1%, and a target 28-day compressive strength of 4000 psi.

Table 2: Mixture proportions for lab and field specimens based on SSD aggregate

Mix	Water lb/yd^3	Cement lb/yd^3)	Coarse Aggregate lb/yd^3	Fine Aggregate lb/yd^3	Air-entraining Agent oz/yd^3
Batch 1-7	269	598	1484	1435	2.33

2.4 SOUTHERN EXPOSURE (SE) AND CRACKED BEAM (CB) TESTS

2.4.1 Description

The Southern Exposure (SE) and cracked beam (CB) tests expose the test specimen to cyclic ponding and drying with a 15% sodium chloride (NaCl) solution. Southern Exposure specimens (Figure 5) are prisms measuring 12 × 12 × 7 in. No. 5 reinforcing bars are cast in the specimen in two mats and measure 12 in. in length. The top and bottom mats consist of two and four bars, respectively, each with 1-in. clear cover. The bars in each mat are centered horizontally within the prism and are spaced 2.5 in. from each other. The bars in the top and bottom mats are electrically connected though a terminal box across a 10-ohm resistor to allow for macrocell corrosion rate measurements. A 0.75-in. deep concrete dam is integrally cast with the specimen to contain the ponded salt solution. Southern Exposure tests represent conditions in uncracked reinforced concrete.

Cracked beam specimens (Figure 6) are half the width of the Southern Exposure specimens, measuring 12 × 6 × 7 in.. These specimens contain two mats of steel. The top mat consists of a single No. 5 bar; the bottom mat consists of two No. 5 bars. This test simulates exposure conditions in cracked concrete. Prior to casting, a 12-mil thick × 6-in. long stainless steel shim is affixed in the mold in direct contact with the top reinforcing bar. The shim is removed about 12 hours after casting. This results in direct infiltration of chlorides at the beginning of the test.

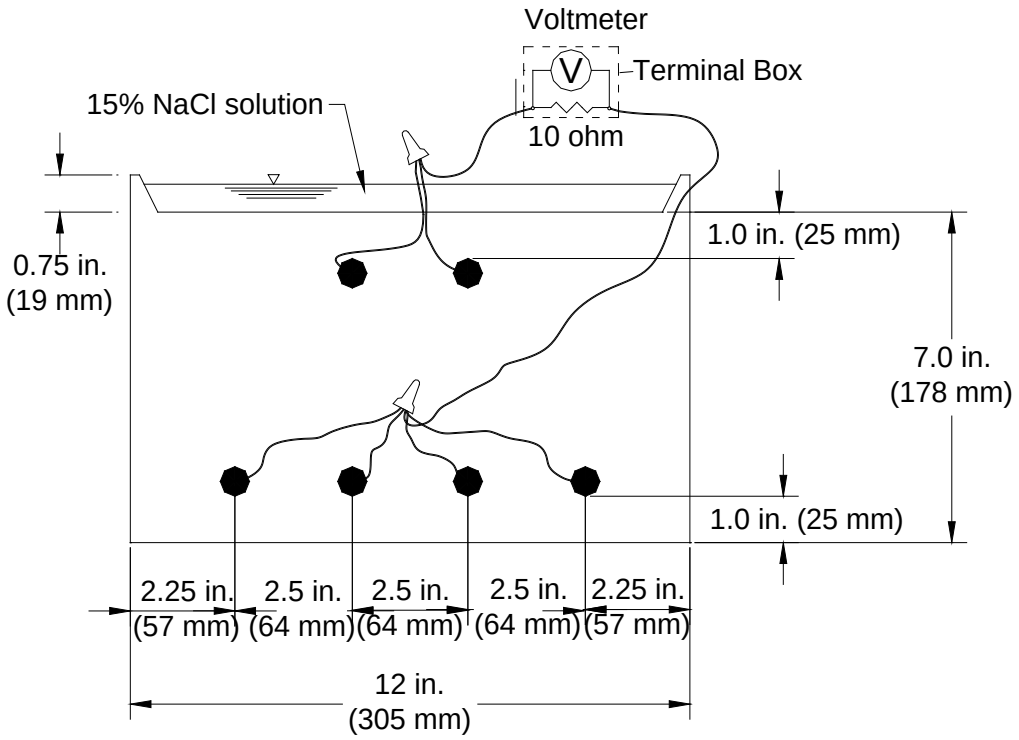

Figure 5: Southern Exposure (SE) specimen

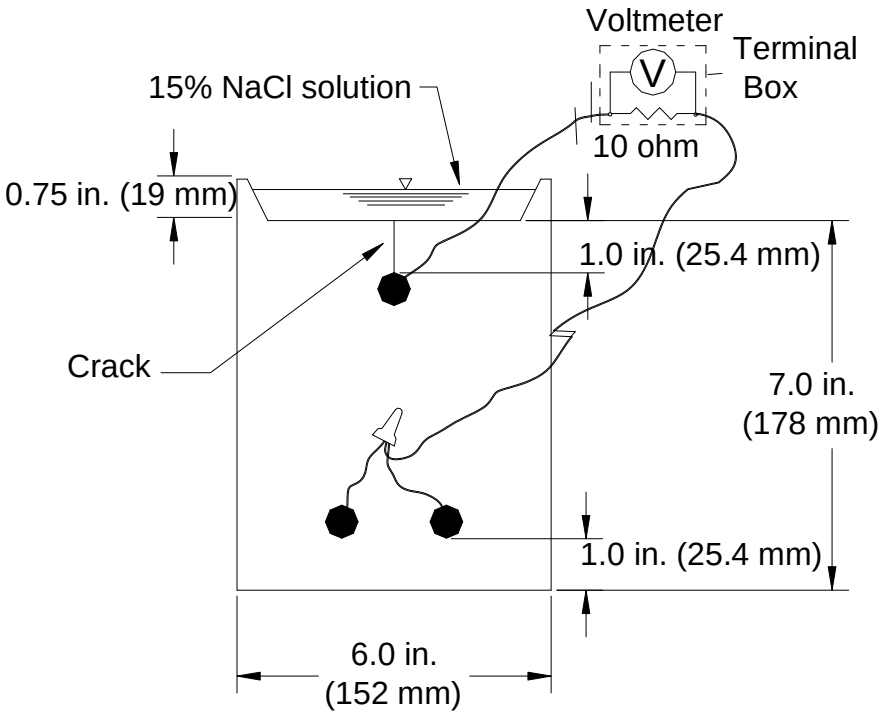

Figure 6: Cracked Beam (CB) specimen

2.4.2 Fabrication

Fabrication for Southern Exposure and cracked beam specimens proceeds as follows:

1. Reinforcing bars are cut to 12 in. with a band saw.
2. Both ends of each bar are drilled and tapped to a 0.75-in. depth with 10-24 threading.
3. When appropriate, holes are drilled through the coating on epoxy-coated and stainless steel clad bars, as previously described.
4. Epoxy-coated bars are cleaned with warm soapy water, rinsed, and allowed to dry. Conventional, stainless steel, and stainless steel clad bars are soaked in acetone for a minimum of two hours and scrubbed to remove any oil.
5. The forms are assembled, and the reinforcement is attached. Reinforcing bars with penetrations in the coating or cladding are aligned so that the holes face the top and bottom of the specimen. Forms and reinforcement are held in place using 1.25-in. long 10-24 threaded stainless steel machine screws.
6. Specimens are cast using concrete with the mixture proportions shown in Table 2. Specimens are filled in two layers, with each layer consolidated using a 0.75-in. diameter vibrator. The free surface of the concrete (the bottom of the specimen) is finished with a trowel.
7. Specimens are cured for 24 hours at room temperature. A plastic cover is used to minimize evaporation. Stainless steel shims are removed from CB specimens after 12 hours, when the concrete has set.
8. Formwork is removed after 24 hours.
9. Specimens are cured for an additional two days in a plastic bag containing deionized water, then air-cured for 25 days.
10. Prior to test initiation, wire leads are connected to the test bars using 10-24 × 0.5 in. stainless steel screws and a No. 10 stainless steel washer. Sewer Guard HBS 100 Epoxy is applied to the vertical sides of the specimens, while the top and bottom of the specimens are left uncoated. The top surface is lightly sanded to remove the outer layer of cement paste.
11. The two mats of steel are connected to the terminal box. Specimens are left connected across the 10-ohm resistor, except when readings are taken (see the section on Corrosion Measurements). Specimens are placed on 2 × 2 studs to allow air flow under the specimens. Tests begin 28 days after casting.

2.4.3 Test Procedure

The Southern Exposure and cracked beam tests involve alternate cycles of ponding and drying. The tests begin with 12 weeks of ponding and drying, followed by another 12 weeks of ponding. The 24-week exposure regime is then repeated for the duration of testing. The tests conclude after 96 weeks. The procedures are described below.

Ponding and Drying Cycle:

A 15% NaCl solution is ponded on the surface of the specimens. SE specimens receive 600 mL of solution; CB specimens receive 300 mL of solution. The specimens are covered with plastic sheeting during ponding to minimize evaporation. Readings are taken on day 4. After all readings are completed, the specimens are vacuumed to remove the salt solution, and a heat tent (described below) is placed over the specimens. The heat tent keeps the specimens at 100 ± 3° F for three days. The tent is then removed, and the specimens are again ponded with the NaCl solution to start the second week of testing. Ponding and drying cycles continue for 12 weeks.

Ponding Cycle:

After 12 weeks of the ponding and drying, specimens are ponded for 12 weeks with the 15% NaCl solution and covered with plastic sheeting. The NaCl solution remains on the specimens throughout the 12 weeks at room temperature. Readings continue to be taken on a weekly basis. Deionized water is added to maintain the desired solution depth on the specimens during this time. After 12 weeks, the specimens are again subjected to the weekly ponding and drying cycle. The two testing cycles are repeated for a total of 96 weeks.

2.4.4 Corrosion Measurements

The measurements taken weekly on the Southern Exposure and cracked beam specimens include macrocell voltage drop, mat-to-mat resistance, corrosion potential, and linear polarization resistance. The macrocell corrosion rate is determined from the voltage drop, based on Faraday's Law.

Following the measurement of the voltage drop, the electrical connection is interrupted to measure mat-to-mat resistance. This is completed using the ohmmeter. The specimens then remain disconnected for a minimum of two hours before measuring corrosion potentials and a minimum of thirty minutes before obtaining linear polarization resistance (LPR) readings. Potentials and LPR are measured with respect to a saturated calomel electrode. After these readings are taken, the mats are then reconnected using the switch on the terminal box.

2.4.5 Linear Polarization Resistance

Linear Polarization Resistance (LPR) provides a means by which the total corrosion rate (macrocell and microcell) of a metal can be determined by measuring the metal's response to an applied voltage (polarization). Without an externally applied voltage, a metal will corrode with a given current density, i_{corr}, and potential, E_{corr}. Applying the external voltage will cause the potential to shift by $\Delta\varepsilon$ which will in turn cause the current density to shift by some amount Δi. The polarization resistance is defined as the slope of the potential-current function, also known as the polarization curve (Jones 1996). For small changes in potential, the polarization curve is linear. It is in this linear region that the polarization resistance is inversely proportional to the corrosion current density. The polarization resistance can be measured by applying a range of potential shifts and measuring the current density at each potential or by applying a range of currents to the sample and measuring the resultant voltage shifts. Plotting the data and finding the slope of the linear region results in the polarization resistance, R_p, which can be used in Eq. (2) to find the corrosion current density.

$$i_{corr} = \frac{\beta_a \beta_c}{2.3 R_p (\beta_a + \beta_c)} \tag{2}$$

Values of 0.12 V/decade for both the anodic and cathodic Tafel constants β_a and β_c have been shown to give a linear region for the polarization curve over a region of approximately $\pm$10 mV with respect to E_{corr}. With these values Eq. (2) yields

$$i_{corr} = \frac{0.026}{R_p} \tag{3}$$

Equation (3) is used to determine corrosion current densities for LPR data presented in this report.

2.4.6 Chloride Sampling for SE Specimens

Southern Exposure specimens are sampled for chlorides at the level of the top mat of steel upon the initiation of corrosion and at the end of the test. Cracked beam specimens are not sampled for chlorides, because the simulated crack allows for direct infiltration of the salt solution. Corrosion initiation for conventional steel is marked by voltage drops that signify macrocell corrosion rates above 0.3 µm/yr and top-mat corrosion potentials more negative than –0.275 V with respect to a saturated calomel electrode, as per ASTM C876. For other steels, corrosion initiation is marked by an increase in corrosion rate with a corresponding drop in potential.

2.4.7 Chloride Sampling Procedure

Chloride sampling is performed after all corrosion measurements are taken for a SE specimen. Prior to sampling, the specimen is rinsed on all four sides with tap water and again rinsed with deionized water. Samples are obtained from the sides of the specimen, perpendicular to the mat of steel, with a 0.25-in. masonry drill bit aligned such that the top of the drill bit is even with the top of the reinforcing steel (Figure 7). Three or five samples are taken from each side of the specimen, for a total of six or ten samples. Sample sites are randomly chosen along the side of the specimen, with the exception that no samples are taken within 1.5 in. of the edge of the specimen.

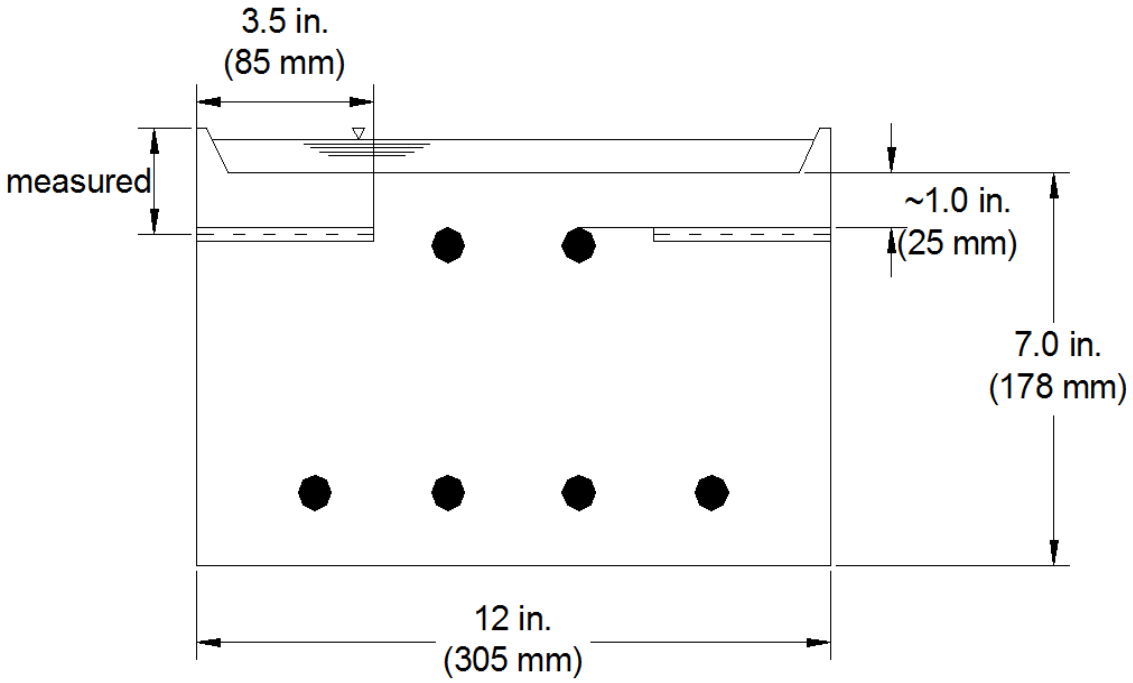

Figure 7: Southern Exposure specimen chloride sampling

For each sample site, a 0.5-in. deep hole is initially drilled. The resulting powder is removed and discarded. The drill bit is then rinsed, dried, reinserted, and used to penetrate to a depth of 3.5 in. This sample is collected in a plastic bag and labeled for analysis. Each sample provides approximately four grams of material. The drill bit is rinsed between specimens with reverse osmosis filtered water. The holes left from drilling are filled with modeling clay, and the specimen is reconnected for continued testing, as appropriate.

2.4.8 Chloride Analysis

Concrete samples are analyzed for water-soluble chloride content using Procedure A of AASHTO T 260-97, "Standard Method of Test for Sampling and Testing for Chloride Ion in Concrete and Concrete Raw Materials." Each chloride sample is boiled in reverse osmosis water to free any water-soluble chlorides. Solutions rest for 24 to 28 hours after boiling and are then filtered. The solution is acidified with nitric acid and then titrated with silver nitrate ($AgNO_3$). The potential with respect to a chloride sensitive electrode is measured throughout titration. For an incremental addition of silver nitrate, the change in potential with respect to each endpoint is indicated by the inflection point of the potential-volume curve. This point is indicated by the greatest change in potential for a given incremental addition of silver nitrate. This procedure gives the chloride concentration in terms of percent chloride by mass of sample. In this study, values are presented in lb/yd^3 by multiplying by the unit weight of concrete, taken as 3786 lb/yd^3.

2.5 TEST EQUIPMENT

The following materials and equipment are used for the rapid macrocell and bench-scale tests.

Wire – The anode and cathode in rapid macrocell test and top and bottom mats of steel in the bench-scale tests are connected to a terminal box using 16-gauge multi-strand copper wire.

Terminal Box – To provide an electrical connection between the bars, each specimen is connected to an individual station in the terminal box. The terminal box allows the bars to be connected across a 10-ohm resistor. Internal box connections are made using solid 22-gauge copper wire. All connections are housed within the terminal box to protect the connections from unintentional salt exposure. This arrangement allows the voltage drop across the 10-ohm resistor to be measured. A switch is provided to interrupt the connection between the two bars to obtain corrosion potential, linear polarization resistance measurements, and in the case of bench-scale specimens, mat-to-mat resistance.

Voltmeter – An Agilent model 34401A nanovoltmeter is used to measure voltage drop and corrosion potential.

Ohmmeter – An Agilent 4338B milliohmmeter is used to measure mat-to-mat resistance of SE and CB specimens.

Reference Electrode – A saturated calomel electrode (SCE) is used for corrosion potential measurements.

Epoxy – Sewer Guard HBS 100 Epoxy, manufactured by BASF, is used on the sides of the specimen to confine the chlorides within the specimen and to prevent corrosion of electrical connections.

Epoxy Patch – Scotchkote Liquid Epoxy Coating Patch Compound 323R, manufactured by 3M, is used to prevent corrosion of the specimen electrical connections and also to apply the protective cap to the bottom of the rapid macrocell specimens.

Stainless Steel Screws/Washers – These are used to hold reinforcement in place in the formwork and to connect wires to specimens during testing. The fabrication procedure is described further in the section on Fabrication.

Wet/Dry Vacuum – A wet/dry vacuum is used to remove the salt solution from the bench-scale specimens, as described in the section on Test Procedure.

Potentiostat and Measuring System– A PC4/750 Potentiostat is used in obtaining Linear Polarization Resistance readings. The potentiostat forces the specimen away from

equilibrium potential and a DC105 computer-controlled corrosion measurement system measures the resulting change in current.

Heating Tent – Heating tents are used to expose bench-scale specimens to a temperature of 100 ± 3° F during drying. A schematic is shown in Figure 8. The tents are 8 ft long by 4 ft wide by 3.5 ft high. The faces and roofs of the tents are fabricated using 0.75-in. plywood with six 2 x 4 studs bracing the tent. Two sheets of plastic sheeting cover the space between the studs. Three 250-watt heat lamps are spaced along the inside roof of the tent to provide heat. The lamps are 1.5 ft above the surface of the bench-scale specimens. Temperature is controlled with a thermostat.

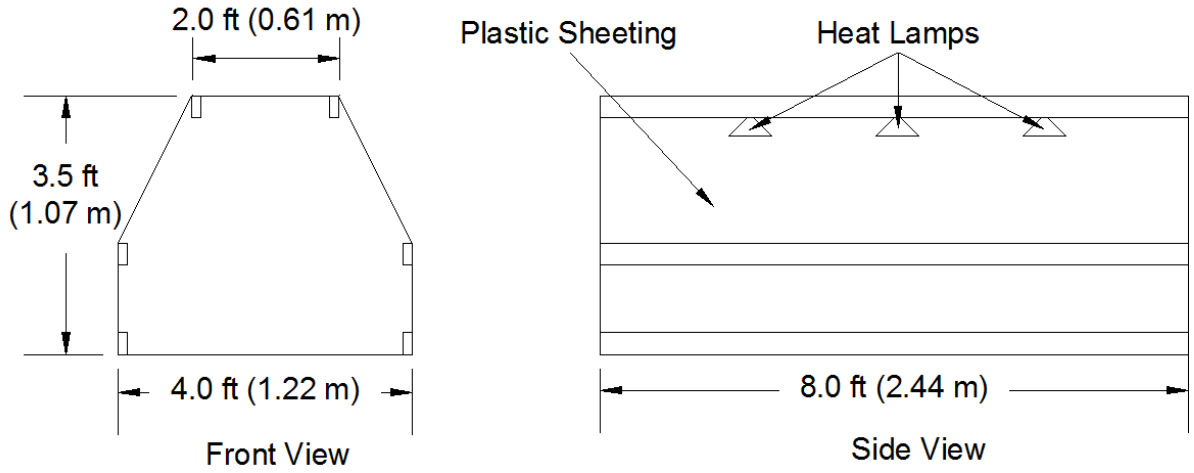

Figure 8: Heat tent dimensions

Formwork – The formwork for the bench-scale specimens is constructed using 0.75-in. plywood, sealed with polyurethane. The forms consist of four face pieces and a base. The specimens are cast upside-down. The formwork has tapered inserts centered and affixed to the base to create the concrete dam used to pond the solution on the specimen. SE formwork inserts measure 10.5 × 10.5 × 0.75 in., and CB formwork inserts measure 4.5 × 10.5 × 0.75 in. at their widest dimensions. CB forms also contain a slot centered and cut in the tapered insert to accommodate the 12-mil shim. Holes are drilled on two opposing faces to allow for the reinforcement to be held in place during casting. The faces and base are held together using 10-24 stainless steel machine screws that connect to threaded inserts in the sides of the forms. Prior to placement of the reinforcement and casting of the concrete, the interior surfaces of the forms are coated with mineral oil and the metal shim is affixed for the CB specimens.

3. TEST PROGRAM

Rapid macrocell tests were performed on six specimens of each type, with the exception of the undamaged ECR, mixed NX-SCR^{TM} stainless steel clad/conventional and mixed 2304 duplex stainless steel/conventional specimens, for which tests were run on three specimens, as shown in Table 3, which includes the specimen designations used for the study (Conv., ECR, ECR-ND, 2304, 2304-p, SSClad, SSClad-NC, SSClad-4h, 2304/Conv., Conv./2304, SSClad/Conv., and Conv./SSClad). An additional mixed stainless steel clad/conventional specimen was tested, as one specimen demonstrated possibly errant results.

Bench-scale tests (also shown in Table 3) were performed on six specimens of each type for both Southern Exposure and cracked beam tests, with the exception of undamaged ECR, mixed NX-SCR^{TM} stainless steel/conventional and mixed 2304 duplex stainless steel/conventional specimens, for which tests were run on three specimens. This distribution of specimens among separate batches was designed to minimize the effect of differences in concrete properties for the different types of steel.

The casting schedule for the bench-scale specimens, summarized in Table 4, was established to reduce possible effects of variations in concrete properties from batch to batch. One specimen of each type was cast in each batch with the exception of the ECR-ND specimens, which were cast in the first three batches, and the mixed specimens, Conv./2304, 2304/Conv., Conv./SSClad, and SSClad/Conv., which were to be cast in every other batch. The mixed specimens were not included in some batches, however, requiring additional specimens to be cast in Batch 7. The repickled 2304 stainless steel bars were case at a later date as Batch 8.

The concrete mixture, as described earlier, had a water-cement ratio of 0.45, a target slump of 3 ± 0.5 in., a target air content of 6 ± 1%, and a target 28-day compressive strength of 4000 psi. The measured slump ranged from 1.75 in. to 6.5 in., with an average of 3.9 in. The measured air content ranged from 5.4% to 6.1%, with an average of 5.8%. At 28 days, the compressive strengths ranged from 3900 to 5160 psi, with an average of 4650 psi. Table 5 summarizes the resulting concrete properties.

Table 3: Test Program – number of test specimens

Test	Macrocell		Southern Exposure[a]		Cracked Beam[a]
System	Straight Bar	Bent Bar	Straight Bar	Bent Bar	Straight Bar
Conventional reinforcement (Conv.)	6	--	6	--	6
ECR (ECR and ECR-ND)[b]	9	--	9	--	9
2304 stainless steel (2304)	6	--	6	--	6
Repickled 2304 stainless steel (2304-p)[c]	6	--	--	--	6
2304 stainless steel/conventional steel (2304/Conv.)[d]	3	--	3	--	--
Conv./2304 stainless steel (Conv./2304)[d]	3	--	3	--	--
NX-SCR™ stainless steel clad (SSClad)	6	6	6	6	6
NX-SCR™ stainless steel clad with 4 holes in the cladding (SSClad-4h)[e]	6	--	6	--	--
NX-SCR™ without a cap at the end of the bar (SSClad-NC)	6	--	--	--	--
NX-SCR™/conventional steel (SSClad/Conv.)[d]	4	--	5	--	--
Conventional/NX-SCR™ (Conv./SSClad) [d]	3	--	3	--	--

[a] Water cement ratio = 0.45. Epoxy-coated bars have ten 1/8-in. (3-mm) diameter holes in coating.

[b] For ECR bars, three specimens with undamaged coating (ECR-ND), six specimens with four (macrocell) or ten (Southern Exposure) 1/8-in. (3-mm) diameter holes in coating (ECR).

[c] 2304-p stainless steel designates 2304 steel that was pickled a second time at the University of Kansas

[d] Mixed steel specimen titles are written with the first steel as the anode and section steel as the cathode, i.e. anode/cathode

[e] Stainless steel clad reinforcement with four 1/8-in. (3-mm) diameter holes through the cladding

Table 4: Casting schedule

Steel Type[a]	Batch 1	Batch 2	Batch 3	Batch 4	Batch 5	Batch 6	Batch 7	Batch 8
Conv.	1	1	1	1[b]	1	1	1	-
ECR	1	1	1	1	1	1	-	-
ECR-ND	1	1	1	-	-	-	-	-
2304	1	1	1	1	1	1	-	-
2304-p	-	-	-	-	-	-	-	6
SSClad-4h	1	1	1	1	1	1	1[c]	-
SSClad-ND	1	1	1	1	1	1	-	-
SSClad-b	1	1	1	1	1	1	-	-
Conv./2304	-	1	1	1	1[b]	1[b]	1	-
2304/Conv.	1	-	-	-	-	-	2	-
Conv./SSClad	1	-	-	-	-	-	2	-
SSClad/Conv.	-	1	1	1	1[c]	1[c]	-	-

[a] Conv. = conventional reinforcement, ECR = epoxy-coated reinforcement with ten 1/8-in. diameter holes through the epoxy, ECR-ND = undamaged ECR, 2304 = 2304 stainless steel, SSClad-4h = NX-SCR™ stainless steel clad reinforcement with four 1/8-in. diameter holes through the cladding, SSClad = undamaged NX-SCR™ stainless steel clad reinforcement, SSClad-b = bent NX-SCR™ stainless steel clad reinforcement. For mixed specimens, the reinforcement in the top mat is listed first.
[b] Corrosion observe at electrical connection – specimen taken out of testing
[c] Extra specimens

"-" = No specimen cast in this batch.

Table 5: Concrete properties

	Batch 1	Batch 2	Batch 3	Batch 4	Batch 5	Batch 6	Batch 7	Batch 8
Casting Date:	12/3/10	12/10/10	12/17/10	12/24/10	1/4/11	1/10/11	4/18/11	12/12/11
Slump (in.)	2.75	3	2	1.75	5.25	6.5	6	2.25
Temp. (^{o}F)	53	63	60	64	55	45	65	75
Air content (%)	5.4	5.5	6.0	5.8	6.0	5.9	6.1	5.8
Unit wt. (lb/ft^3)	143.9	144.4	142.2	142.7	143.9	142.6	143.3	142.8
Strength (psi)								
7-day	3880	3560	3780	3680	3400	3290	3340	4010
28-day	4990 4770 4950	4370 4580 5080	4850 4850 4830	4910 4950 5160	4290 4470 4810	4200 4460 4440	4400 4340 3900	5230 5360 4730
Avg. 28-day	4900	4680	4840	5010	4520	4370	4210	5110

4. RESULTS

This chapter presents the results of the rapid macrocell, Southern Exposure, and cracked beam tests. The three test methods were used to evaluate conventional reinforcement, epoxy-coated reinforcement, 2304 stainless steel, and stainless steel clad reinforcement. Southern Exposure and rapid macrocell tests were used to investigate the possibility of a galvanic effect between conventional reinforcement and 2304 or stainless steel clad reinforcement that might result in accelerated corrosion. Corrosion rate, corrosion loss, and corrosion potential were measured for each specimen. Most of the results presented in this chapter represent the average of multiple specimens containing a given type of reinforcement. Results for individual specimens are presented in Appendix A.

4.1 RAPID MACROCELL TESTS

The individual corrosion losses for macrocell specimens are listed in Table 6. Some specimens listed in the table show negative losses. The negative values can result from corrosion occurring at the location of the electrical connection or can be caused by minor differences in the oxidation rates of the single anode bar and two cathode bars. Upon completion of the test, all specimens were autopsied and no corrosion at an electrical connection was found. The negative readings, therefore, are likely caused by current drift due to differences in oxidation rates between the single anode bar and the two cathode bars and do not actually indicate “negative” corrosion.

Conventional steel displayed the greatest corrosion loss, with values ranging from 6.21 µm to 12.4 µm with an average corrosion loss of 10.9 µm (Table 6). Corrosion losses for ECR with holes in the coating based on total area of the bar ranged from 0.037 µm to 0.244 µm, with an average of 0.107 µm. Corrosion losses for NX-SCR^{TM} stainless steel clad reinforcement with four 1/8-in. holes through the cladding ranged from –0.005 µm to 0.803 µm, with an average of 0.195 µm. Conventional steel with 2304 stainless steel as the cathode (Conv./2304) exhibited corrosion losses very similar to those of conventional steel alone, with a mean corrosion loss of 10.4 µm. Also, conventional steel bars with stainless steel clad bars as the cathode showed relatively high corrosion losses, with an average of 4.63 µm; however, the average loss was somewhat lower than for conventional steel alone. Both of the “mixed” specimen sets with conventional steel at the cathode (2304/Conv. and SSClad/Conv.) had corrosion losses significantly below those for the mixed specimen sets with conventional steel as the anode but higher than the values recorded for specimens with 2304 stainless steel bars or SSClad bars at both the anode and the cathode suggesting the possibility of a galvanic effect due to the combination of the stainless steels with conventional steel. The rest of the specimens had minimal corrosion losses.

Figures 9 and 10 show the average corrosion loss based on total area for the control specimens, conventional, ECR, and undamaged ECR rapid macrocell specimens. Conventional steel exhibited a corrosion loss of 10.9 µm. The ECR specimens exhibited average corrosion losses of 0.107 µm, while undamaged ECR exhibited no significant losses. Individual corrosion rate data support these findings, with conventional steel exhibiting very high corrosion rates and ECR and undamaged ECR exhibiting much lower corrosion rates.

Table 6: Corrosion losses at 15 weeks based on total area for macrocell specimens

System[a]	Specimen						Average	Standard Deviation
	1	2	3	4	5	6		
	Corrosion Loss (µm)							
Conv.	9.09	12.4	10.9	15.5	6.21	11.1	10.9	3.12
ECR	0.072	0.058	0.104	0.037	0.127	0.244	0.107	0.0744
ECR-ND	0	0	-0.010	-	-	-	-0.0033	0.00577
2304	0.099	-0.101	0.008	-0.092	-0.018	-0.200	-0.0507	0.103
2304-p	-0.012	-0.025	-0.035	-0.030	-0.031	-0.007	-0.0233	0.0113
2304/Conv.	0.058	-0.066	0.490	-	-	-	0.161	0.292
Conv./2304	10.9	9.61	10.8	-	-	-	10.4	0.697
SSClad-4h	0.163	0.055	0.803	0.105	0.050	-0.005	0.195	0.303
SSClad	-0.028	-0.029	-0.076	-0.052	-0.004	0.063*	-0.021	0.0478
SSClad-b	-0.013	-0.096	-0.067	-0.066	-0.038	-0.044	-0.054	0.0289
SSClad-NC	0.014	1.205	0.061	2.340	0.776	1.864	1.043	0.946
SSClad/Conv.	0.172	1.11	0.011	0.445	-	-	0.435	0.487
Conv./SSClad	4.88	4.69	4.35	-	-	-	4.63	0.268

[a] Conv. = conventional reinforcement, ECR = epoxy-coated reinforcement with four 1/8-in. diameter holes through the epoxy, ECR-ND= undamaged ECR, 2304 = 2304 stainless steel, 2304-p = repickled 2304 stainless steel, SSClad-4h = stainless steel clad reinforcement with four 1/8-in. diameter holes through the cladding, SSClad = undamaged stainless steel clad reinforcement, SSClad-b = bent stainless steel clad reinforcement, SSClad-NC = stainless steel clad reinforcement with no protective cap on the cut end.
For mixed specimens, the reinforcement on the top mat is listed first.
"-" = No specimen tested in this set.
*Specimen exhibited corrosion at electrical connection.

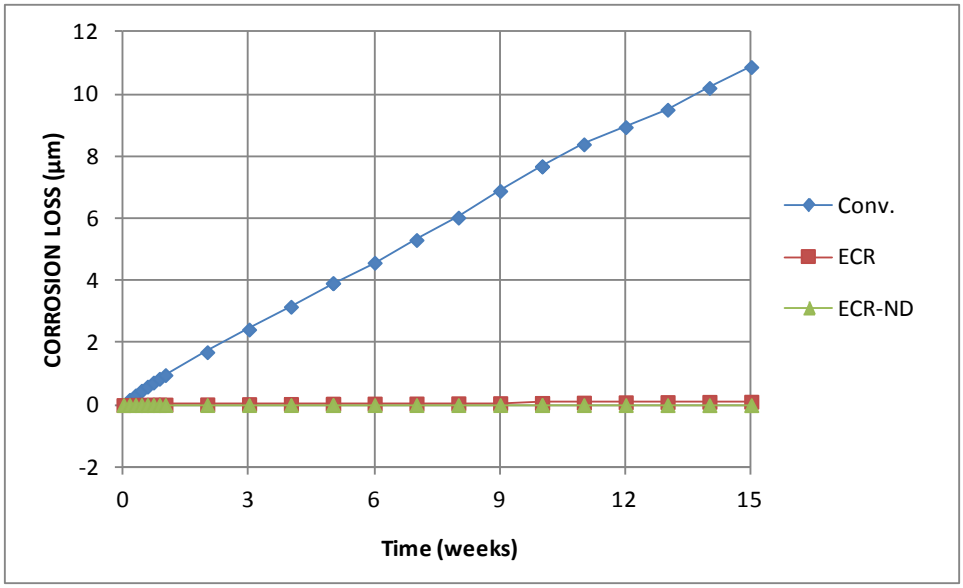

Figure 9: Average corrosion losses based on total area for conventional, ECR, and undamaged ECR rapid macrocell specimens

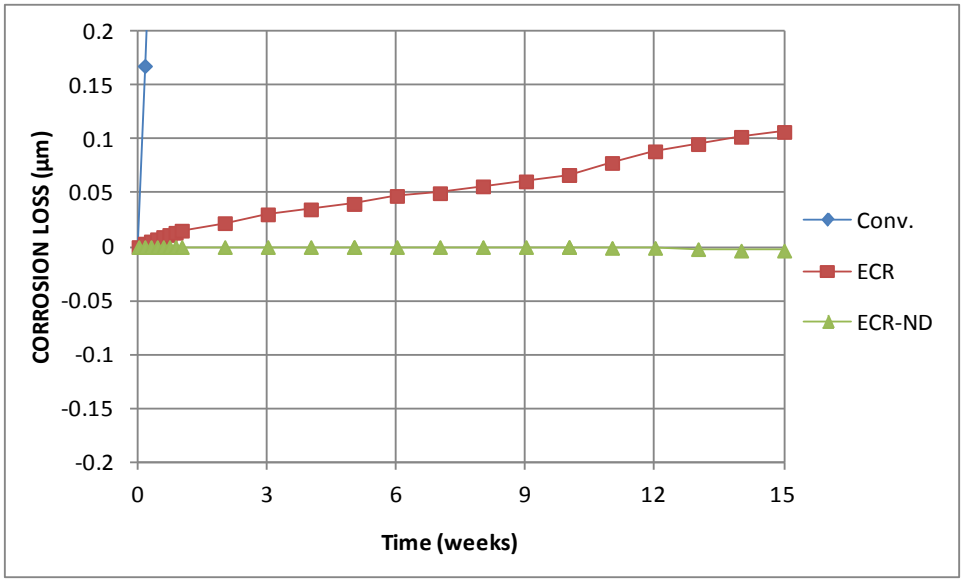

Figure 10: Average corrosion losses based on total area for conventional, ECR, and undamaged ECR rapid macrocell specimens (different scale)

Figures 11 and 12 show the corrosion losses based on total area for conventional, 2304 stainless steel, repickled 2304 stainless steel, and mixed 2304/Conv. and Conv./2304 stainless steel rapid macrocell specimens. The Conv. and Conv./2304 stainless steel specimens exhibited relatively high corrosion losses of about 11 and 10 µm, respectively (Figure 11). As shown in Figure 12, the 2304 and 2304-p rapid macrocell specimens exhibited slightly negative losses, most likely due to the different oxidation rates of the anode and cathode bars, as discussed earlier. The mixed 2304/Conv. specimens exhibited minimal losses until week 12 with an average loss of about 0.15 µm at week 15. This increase in average corrosion loss is due to one specimen, which exhibited staining and a significant increase in corrosion rate at week 12, as will be demonstrated later in this section.

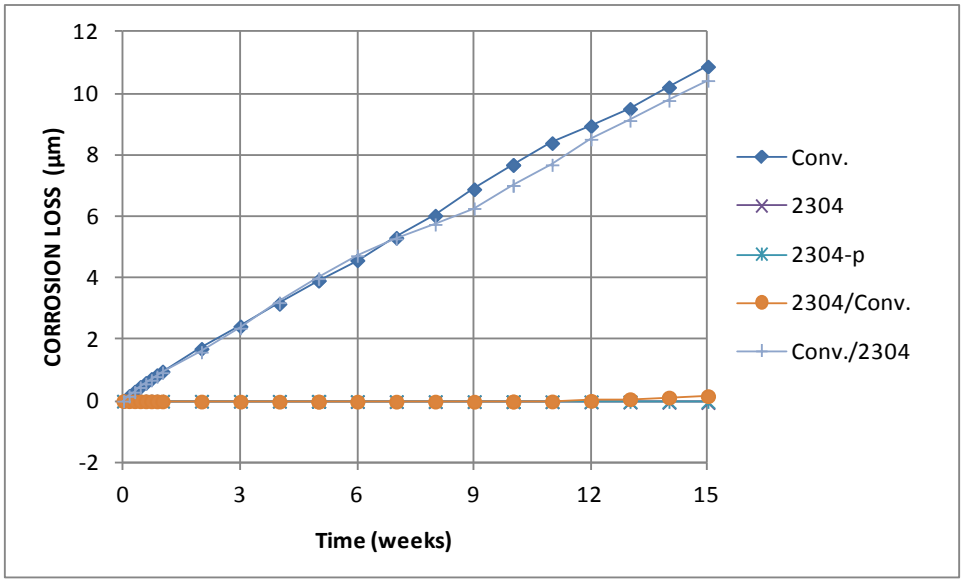

Figure 11: Average corrosion losses based on total area for conventional, 2304, 2304-p, mixed 2304/conventional, and mixed conventional/2304 rapid macrocell specimens

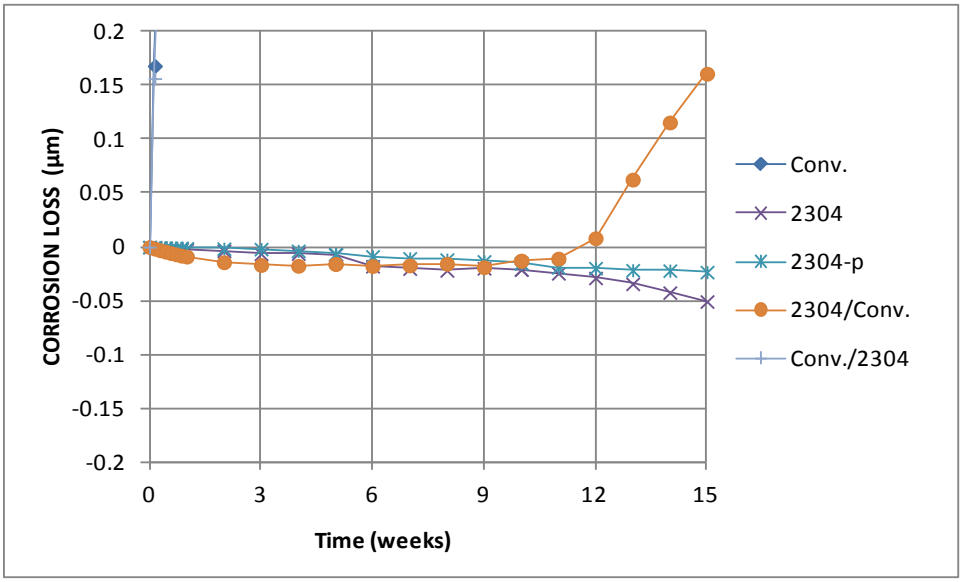

Figure 12: Average corrosion losses based on total area for conventional, 2304, 2304-p, mixed 2304/conventional and mixed conventional/2304 rapid macrocell specimens (different scale)

Figures 13 and 14 show the corrosion losses based on total area for conventional, undamaged stainless steel clad, stainless steel clad bars with four holes, uncapped stainless steel clad, bent stainless steel clad, and mixed stainless steel clad/conventional specimens. The mixed Conv./SSClad specimens exhibited roughly half of the corrosion losses of conventional steel (Conv.), or 4.6 µm, over the course of the 15 week test (Figure 13). The uncapped stainless steel clad (SSClad-NC) specimens exhibited the highest losses of the specimens with stainless steel clad bars at the anode, with an average corrosion loss of 1.04 µm. The other specimens, which include SSClad, SSclad-4h, SSClad-b, and mixed SSClad/Conv., exhibited average corrosion losses under 0.5 µm (Figure 14). The undamaged stainless steel clad and bent stainless steel clad reinforcement specimens exhibited slightly negative corrosion losses. Stainless steel clad reinforcement with the cladding penetrated exhibited average corrosion losses of 0.20 µm, which is roughly half of the 0.42 µm loss recorded for the mixed SSClad/Conv. specimens.

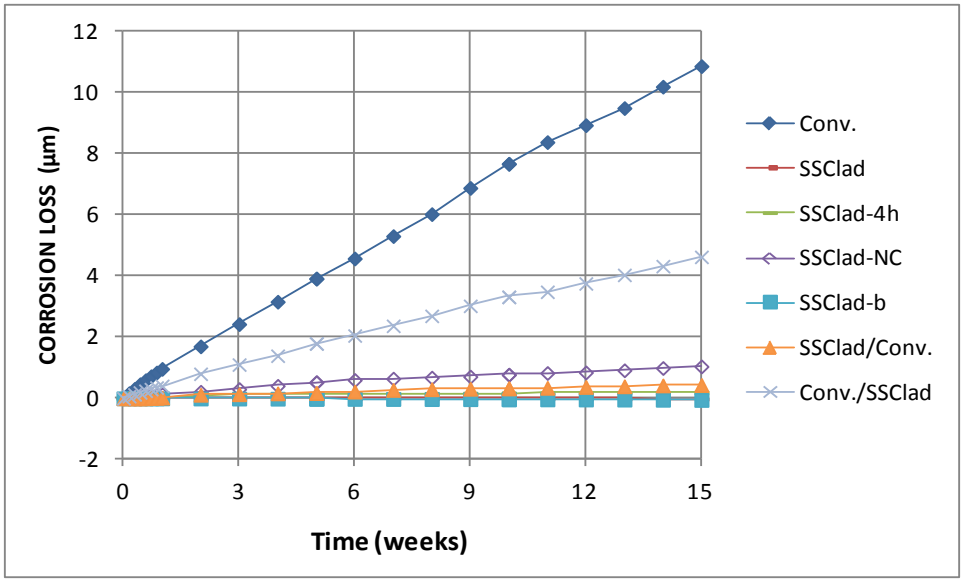

Figure 13: Average corrosion losses based on total area for conventional, stainless steel clad, stainless steel clad with four holes through the cladding, uncapped stainless steel clad, bent stainless steel clad, mixed stainless steel clad/conventional, and mixed conventional/stainless steel clad rapid macrocell specimens

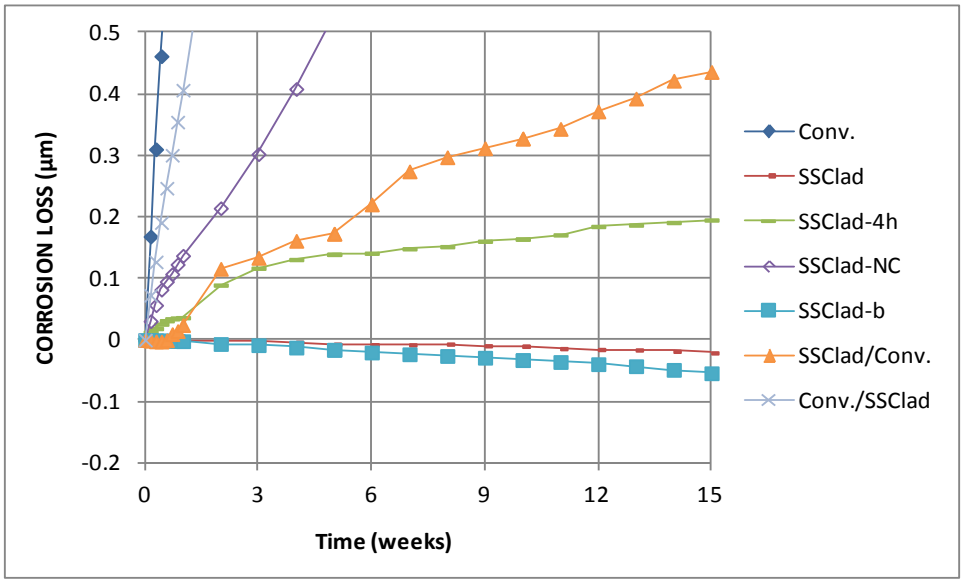

Figure 14: Average corrosion losses based on total area for conventional, stainless steel clad, stainless steel clad with four holes through the cladding, uncapped stainless steel clad, bent stainless steel clad, mixed stainless steel clad/conventional, and mixed conventional/stainless steel clad rapid macrocell specimens (different scale)

4.1.1 Control Specimens

The control specimens include conventional steel (Conv.), epoxy-coated reinforcement with 1/8-in. diameter holes through the epoxy (ECR), and undamaged epoxy-coated reinforcement (ECR-ND). As stated earlier, all specimens tested in the control group are from the same heat of steel. Figures 15 and 16 show the average corrosion rates of the control

group. As shown in Figure 15, the conventional steel specimens exhibited an average corrosion rate of about 60 µm/yr at the beginning of the test, which dropped, with some variations, to about 40 µm/yr for the duration of the test. The ECR specimens exhibited an average corrosion rate of about 1.2 µm/yr at the beginning of the test, dropping to about 0.3 µm/yr for the duration of the test (Figure 16). ECR-ND had an average corrosion rate near zero for the entire test, with a slight negative average corrosion rate from week 10 until the end of the test (Figure 16). The ECR-ND bars were autopsied at the end of the test. No signs of corrosion were observed on any ECR-ND specimen. The slight negative corrosion readings may be due to a small amount of current drift between the anode and the cathodes.

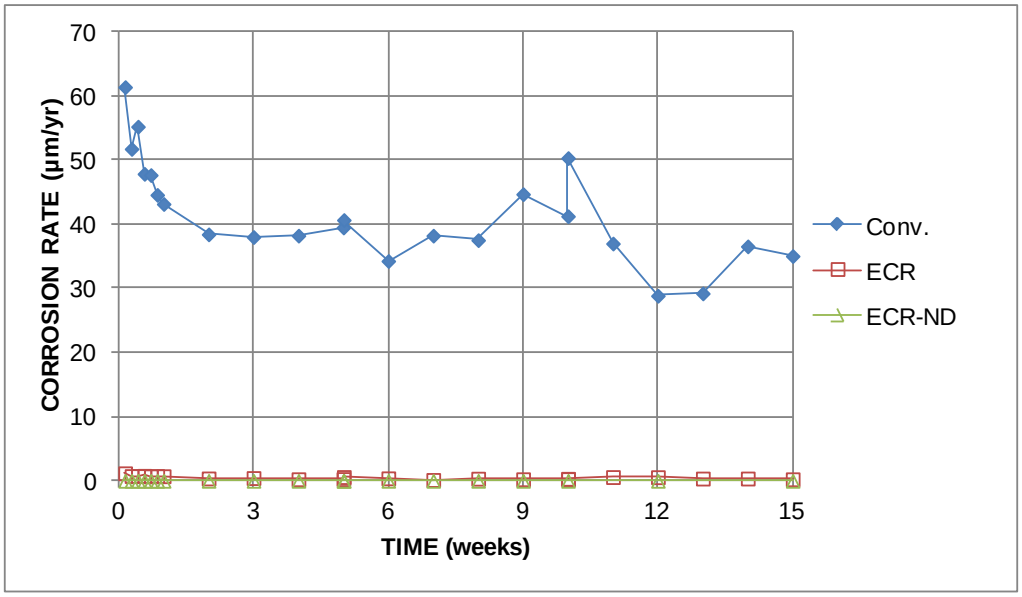

Figure 15: Average corrosion rates of conventional, ECR, and undamaged ECR rapid macrocell specimens

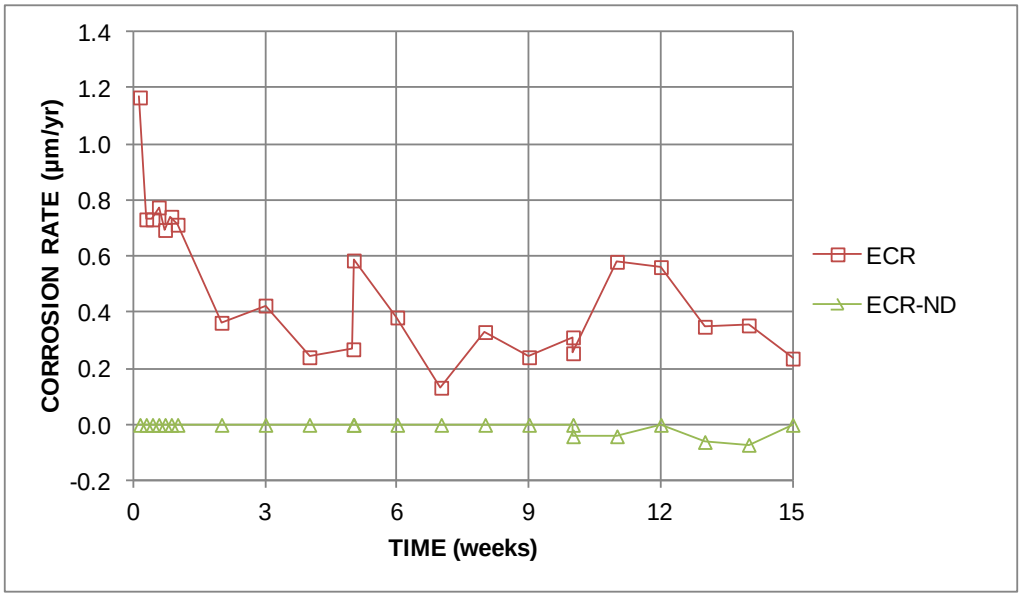

Figure 16: Average corrosion rates of ECR and undamaged ECR rapid macrocell specimens

4.1.2 2304 Stainless steel

The average corrosion rates for the specimens containing 2304 stainless steel are shown in Figures 17 and 18. The rates for the conventional, ECR, and ECR-ND specimens are also plotted for comparison. The average corrosion rate of all stainless steel specimen sets must be below +0.25 µm/yr for the steel to qualify under the provisions of ASTM A955.

The behavior of the mixed Conv./2304 specimens is similar to that of the Conv. specimens, which demonstrate average corrosion rates between 25 and 60 µm/yr throughout the test. The mixed 2304/Conv. specimens exhibited an average corrosion rate between –0.6 and 3.0 µm/yr. The 2304/Conv. specimens exhibited average corrosion rates that were in excess of the +0.25 µm/yr threshold specified in ASTM A955, although mixed-steel tests are not required by ASTM A955. As shown in Figure 18, the average corrosion rates of the 2304 and 2304-p specimens were nearly equal to that of the ECR-ND specimens. The 2304 and 2304-p specimens exhibited average corrosion rates of less than +0.25 µm/yr throughout the 15-week test, satisfying this requirement of ASTM A955.

The individual corrosion rates for the 2304 stainless steel specimens in the as-received condition are shown in Figure 19. As discussed earlier, most values were “negative,” which is caused by minor differences in the oxidation rates of the single anode bar and the two cathode bars. The rates exhibit significant scatter, with values ranging between 1.10 µm/yr and –2.60 µm/yr. While these data points may appear to be outliers, several specimens consistently exhibited corrosion rates in excess of +0.50 µm/yr maximum permitted by ASTM A955. Specimens 1, 2, and 3 exceeded +0.50 µm/yr one or more times during the test, although no corrosion products were observed on the bars.

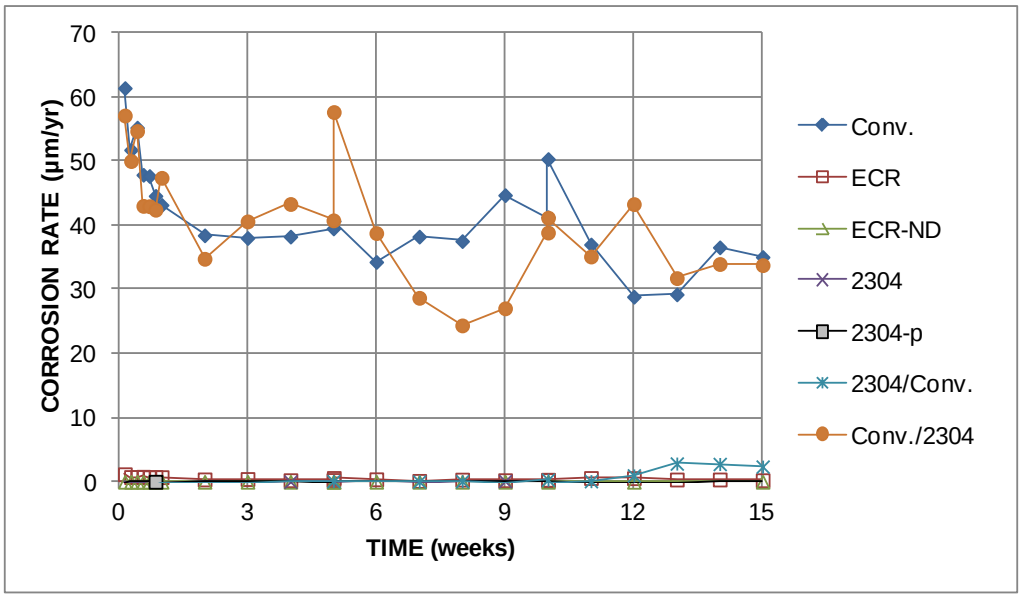

Figure 17: Average corrosion rates of conventional, ECR, ECR-ND, 2304, 2304-p, mixed 2304/conventional, and mixed conventional/2304 rapid macrocell specimens.

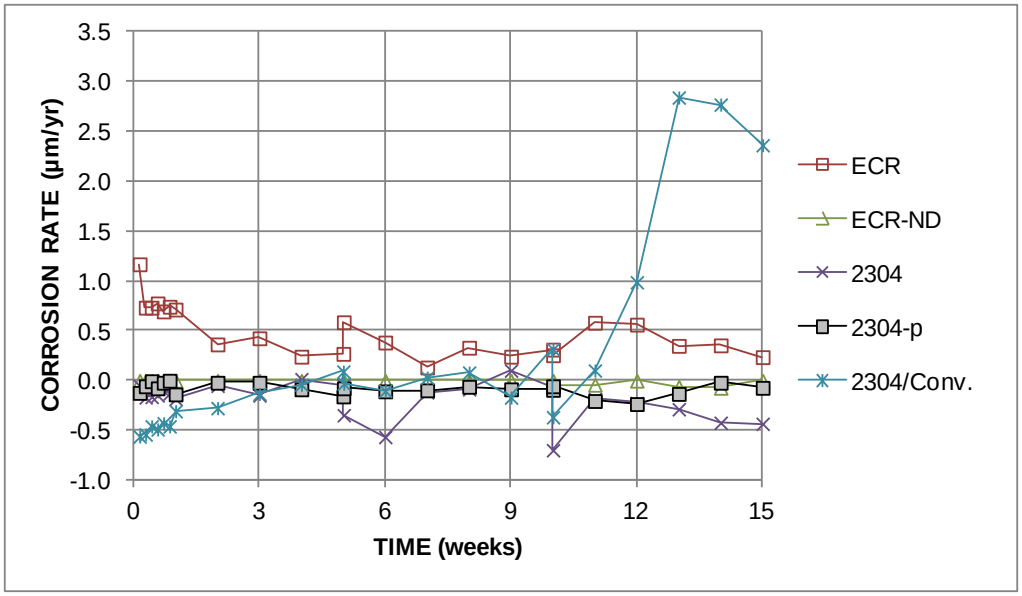

Figure 18: Average corrosion rates of, ECR, ECR-ND, 2304, 2304-p, and mixed 2304/conventional rapid macrocell specimens (different scale)

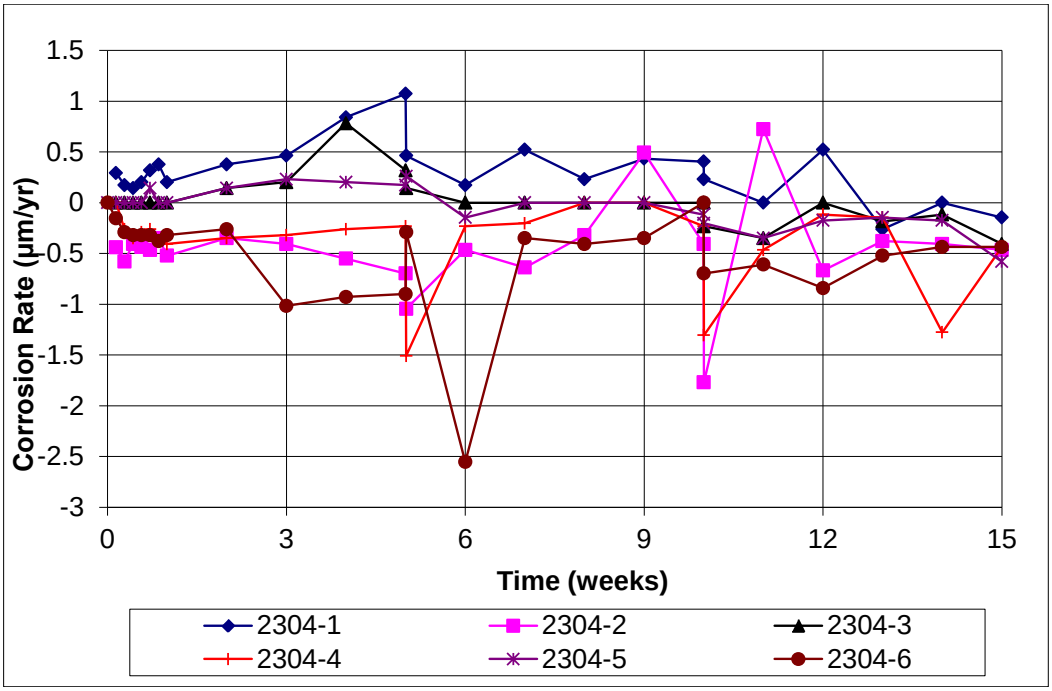

Figure 19: Individual corrosion rates of 2304 stainless steel rapid macrocell specimens 1-6

As described earlier, the 2304 stainless steel in the as-received condition had a dull, mottled finish. As a result, a set of specimens was repickled to a bright, uniformly light surface. The individual corrosion rates for the repickled 2304 stainless steel bars are shown in Figure 20. The individual corrosion rates for the 2304-p specimens range between +0.15 and –0.50 µm/yr, with the largest scatter in the corrosion rates occurring in the first week of the test. Thereafter,

individual corrosion rates of the repickled 2304 stainless steel were very tightly grouped, with values ranging for the most part between 0 and –0.30 µm/yr. The criteria for qualifying stainless steel per ASTM A955 were met, with no individual reading exceeding +0.50 µm/yr (Figure 20) and the average not exceeding +0.25 µm/yr during the test (Figure 18).

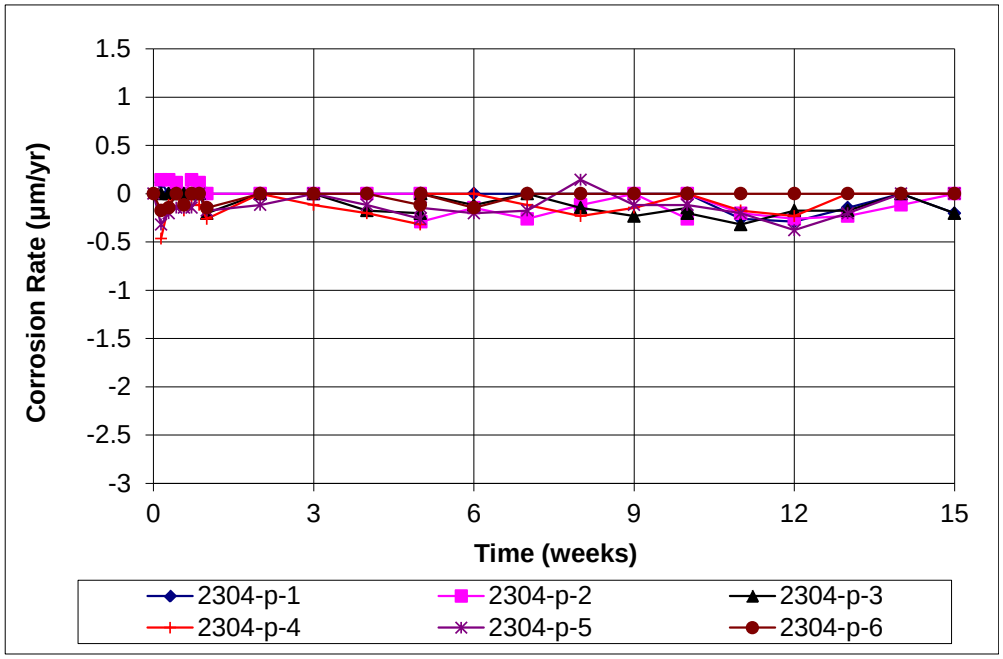

Figure 20: Individual corrosion rates of repickled 2304 stainless steel rapid macrocell specimens 1-6

To assess the potential for galvanic effects, mixed-steel specimens were tested that included both conventional and 2304 stainless steel reinforcement. The 2304 stainless steel used in the mixed tests was tested in the as-received condition. Three specimens were tested with 2304 stainless steel as the anode and conventional reinforcement as the cathode, and three sets of specimens were tested with conventional reinforcement as the anode and 2304 stainless steel as the cathode.

The individual corrosion rates for the six mixed specimens are shown in Figures 21 and 22. In Figure 21, the corrosion rates of the Conv./2304 specimens are similar to those of conventional reinforcement. As shown in Figure 22, three of the 2304/Conv. specimens have corrosion rates that are similar to those of the 2304 stainless steel specimens in the as-received condition; the three mixed 2304/Conv. specimens exhibited individual corrosion rates in excess of +0.50 µm/yr at least once during the 15-week test. After week 12, specimen 2304/Conv.-3 corroded at rates exceeding 1.5 µm/yr, with a spike at week 12, reaching a maximum of 10 µm/yr in week 14. Staining of the anode was observed, as shown in Figure 23. As a result, the average corrosion rate of all the 2304/Conv. specimens is in excess of +0.25 µm/yr (Figure 18).

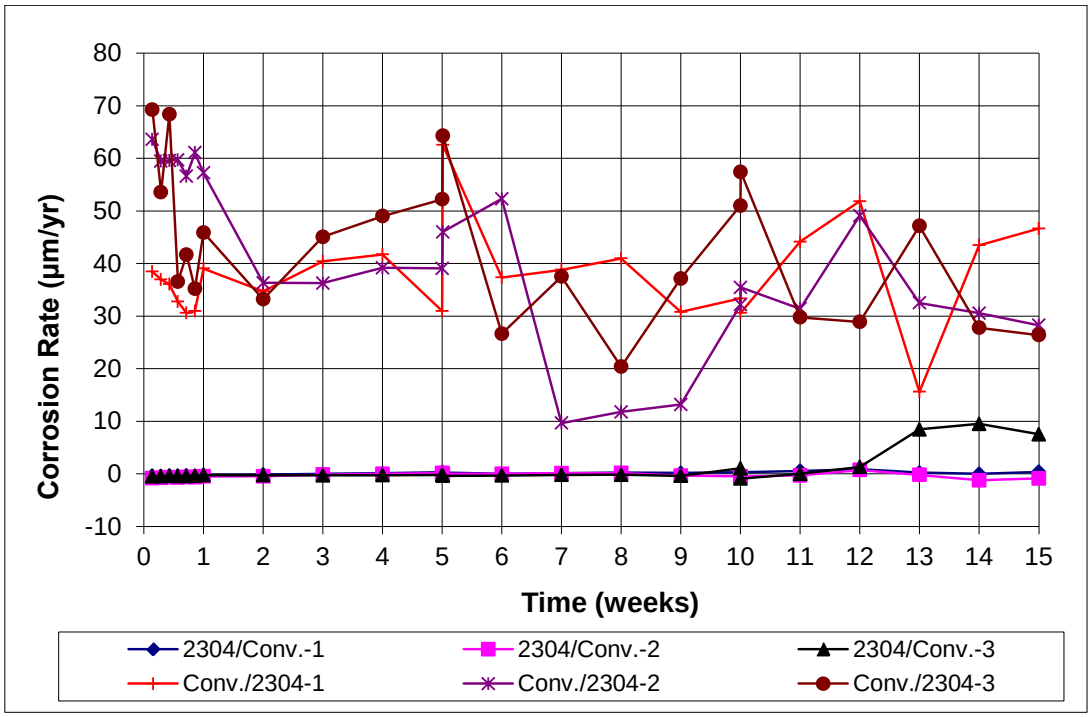

Figure 21: Individual corrosion rates of mixed 2304 stainless steel (anode/cathode) rapid macrocell specimens 1-6

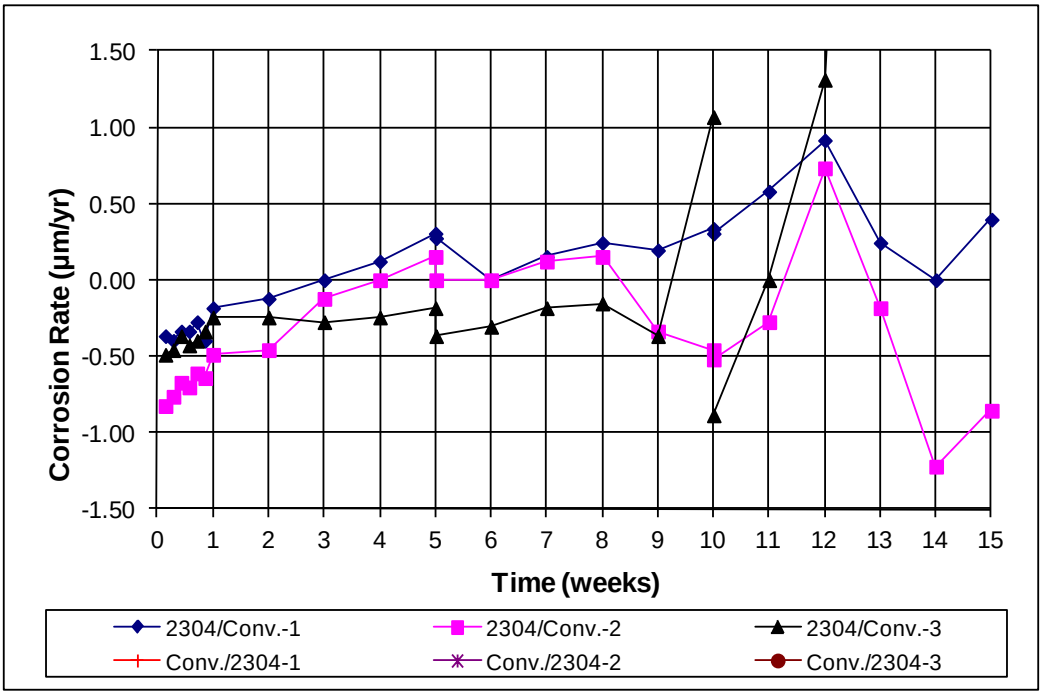

Figure 22: Individual corrosion rates of mixed 2304 stainless steel (anode/cathode) rapid macrocell specimens 1-6 (different scale)

Figure 23: Staining of anode of 2304 stainless steel, mixed 2304/conventional steel macrocell specimen

4.1.3 NX-SCR™ stainless steel clad reinforcement

The average corrosion rates for the specimens containing NX-SCR™ stainless steel clad reinforcement (SSClad) are shown in Figures 24 and 25. The results of the control specimens, conventional, ECR, and ECR-ND, are also plotted for comparison.

The mixed Conv./SSClad specimens exhibited the highest average corrosion rate among rapid macrocell specimens containing stainless steel clad reinforcement. The average corrosion rate, which ranged between 9 and 26 µm/yr during the test, was roughly half of the average corrosion rate of conventional steel.

The SSClad-NC and SSClad-4h bars had conventional steel exposed at the uncapped ends of the bars or at the holes drilled through the cladding. The SSClad-NC specimens exhibited average corrosion rates between 1 and 12 µm/yr, and the SSClad-4h specimens exhibited average corrosion rates between 0.2 and 5 µm/yr.

The average corrosion rates of the undamaged and bent stainless steel clad specimens never exceeded zero for the duration of the test. This seemingly “negative” corrosion has been discussed previously. Moreover, the average corrosion rate of both the undamaged and bent stainless steel clad reinforcement remained below +0.25 µm/yr throughout the duration of the test, satisfying this requirement of ASTM A955.

The corrosion rates for the individual SSClad specimens are shown in Figure 26. Individual corrosion rates range from –0.60 to +0.90 µm/yr, although only one specimen exhibited corrosion rates above 0.42 µm/yr. Upon completion of the evaluation, the specimens were autopsied and the protective caps on both the anode bar and two cathode bars were removed to inspect the bar ends for signs of corrosion. Specimens showed little to no corrosion under the protective cap, as shown in Figure 27. All specimens, with the exception of Specimen 6, performed satisfactorily, in that the individual corrosion rate did not exceed +0.50 µm/yr. Specimen 6, which exhibited very minor corrosion staining at the electrical connection of the anode and significant staining along the side of a cathode bar, is shown in Figures 28a through 28c. Due to the corrosion at the electrical connection, the failure of this specimen to meet the 0.50 µm/yr limit is not considered as representing a failure of the SSClad bars.

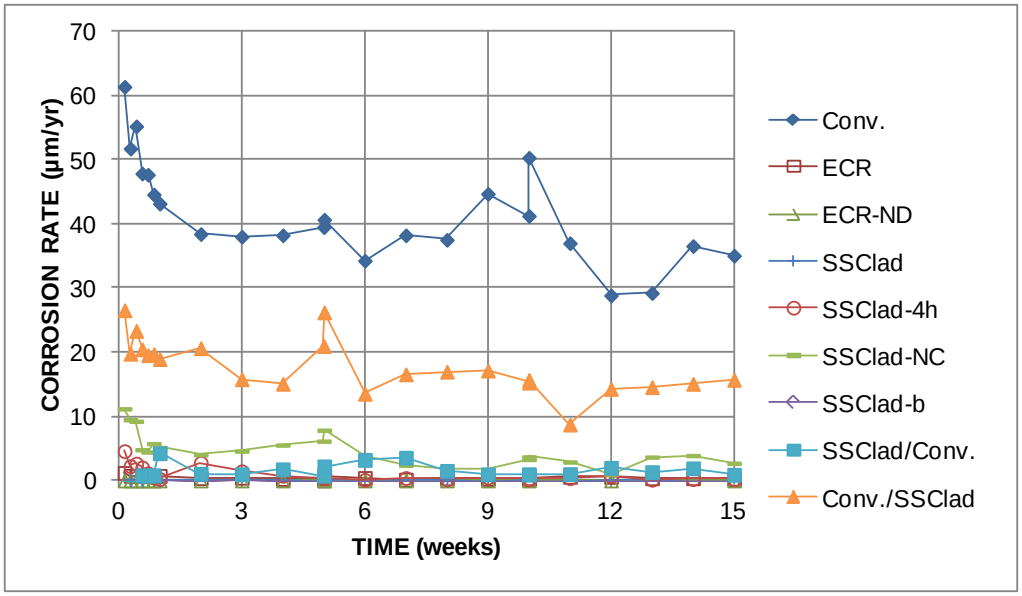

Figure 24: Average corrosion rate of conventional, stainless steel clad, stainless steel clad with four holes through the cladding, uncapped stainless steel clad, bent stainless steel clad, mixed stainless steel clad/conventional, and mixed conventional/stainless steel clad rapid macrocell specimens

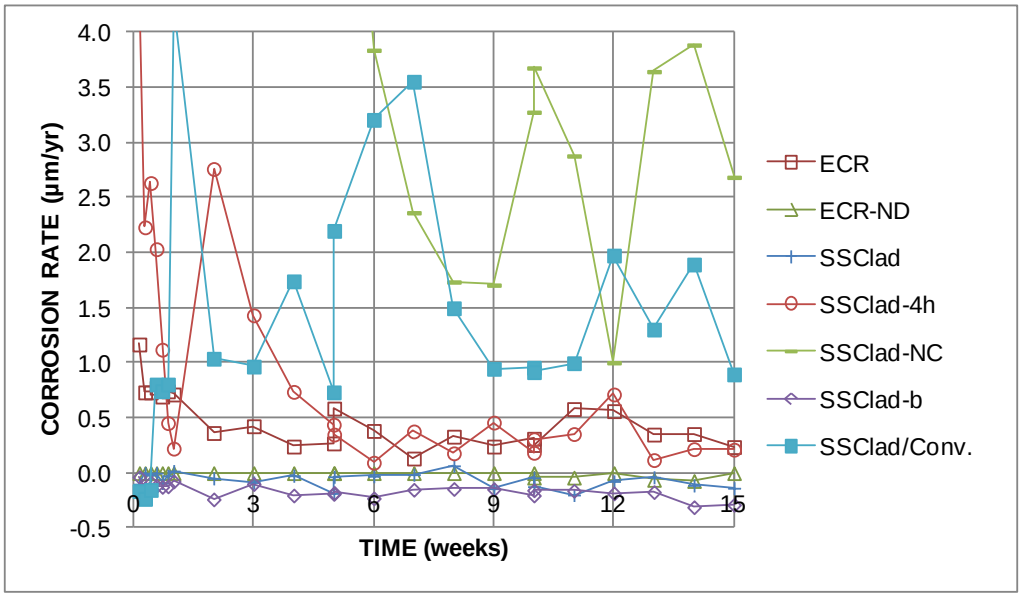

Figure 25: Average corrosion rate of stainless steel clad, stainless steel clad with four holes through the cladding, uncapped stainless steel clad, bent stainless steel clad, and mixed stainless steel clad/conventional rapid macrocell specimens (different scale)

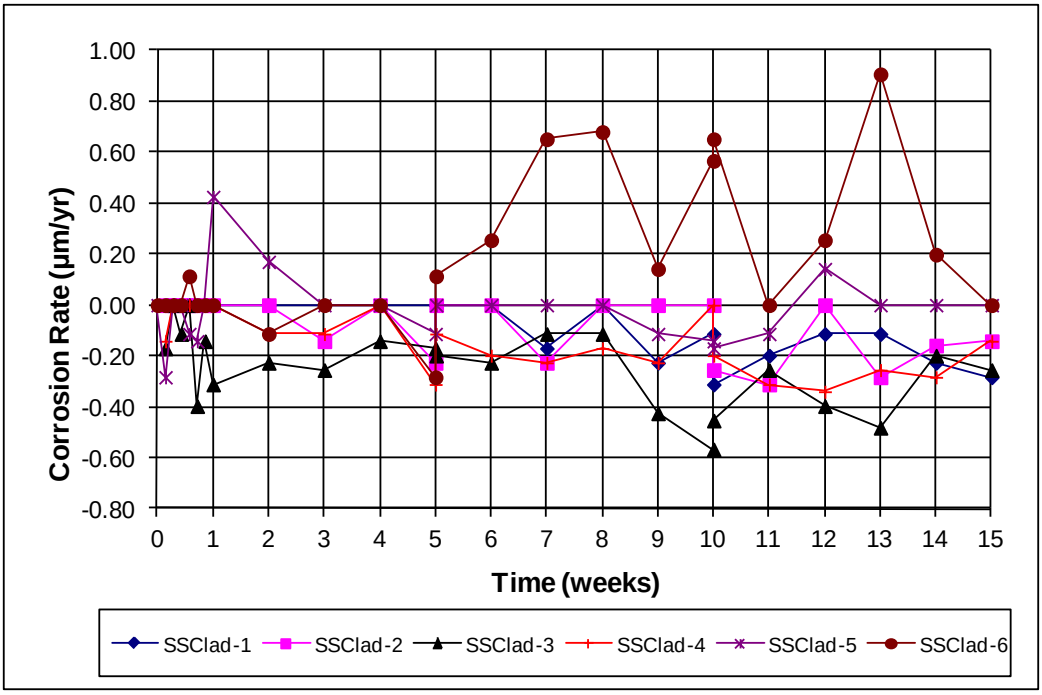

Figure 26: Macrocell individual corrosion rates of undamaged NX-SCR^{TM} stainless steel clad bars, specimens 1-6. Note: Specimen 6 exhibited corrosion at electrical connection of anode

Figure 27: Bar end with protective cap removed at end of rapid macrocell test, NX-SCR^{TM} stainless steel clad (cathodes)

Figure 28a: Photograph of specimen 6 upon completion of the rapid evaluation test, NX-SCR^{TM} stainless steel clad (anode on top, cathode on bottom)

Figure 28b: Photograph of specimen 6 upon completion of the rapid evaluation test, NX-SCR^{TM} stainless steel clad (close-up of cathode)

Figure 28c: Photograph of specimen 6 upon completion of the rapid evaluation test, NX-SCR™ stainless steel clad showing corrosion at electrical connection

Individual corrosion rates are shown for the uncapped stainless steel clad bars in Figure 29. Corrosion rates were highest in week 1, reaching values in excess of 25 µm/yr. Although the individual corrosion rates of the specimens was rather high due to the exposed conventional steel core of the NX-SCR™ stainless steel clad bars, the individual corrosion rates were much lower than the conventional reinforcement. Upon autopsy of the bars, it was discovered that a significant amount of corrosion was present at the location of the uncapped bar ends, as shown in Figure 30.

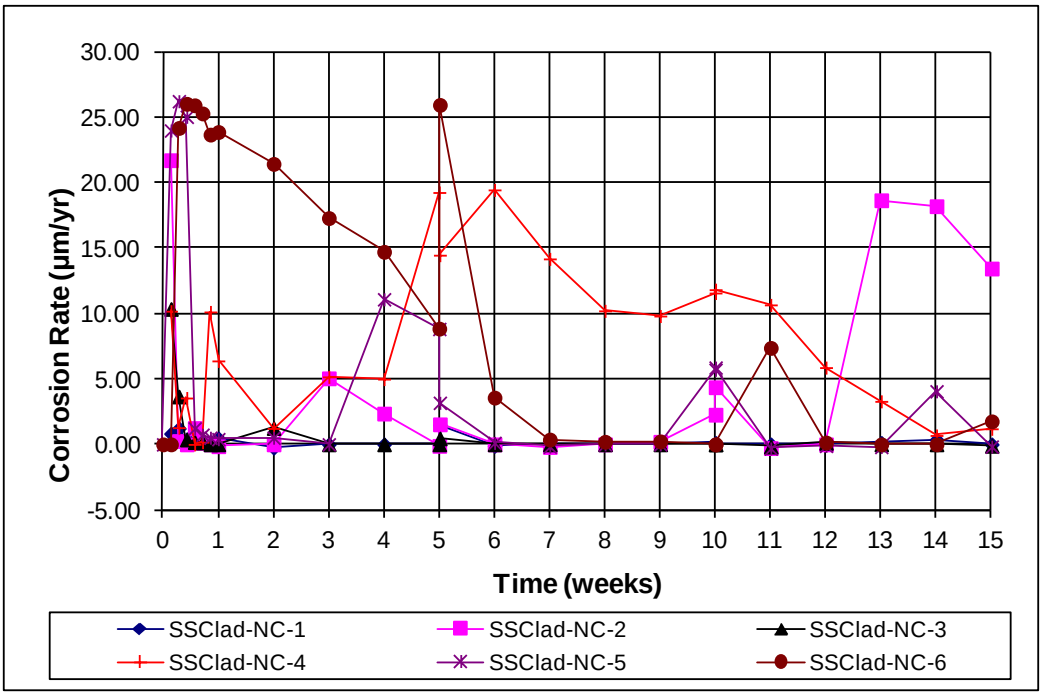

Figure 29: Macrocell individual corrosion rates of uncapped NX-SCR™ stainless steel clad bars, specimens 1-6

Figure 30: Uncapped bar end upon autopsy, NX-SCR™ stainless steel clad bar

The corrosion rates for the individual bent NX-SCR™ stainless steel clad (SSClad) bars are shown in Figure 31. The individual corrosion rates ranged from +0.40 to –0.47 µm/yr, satisfying the maximum value of +0.50 µm/yr in accordance with ASTM A955. Minimal corrosion staining was observed on the bent stainless steel clad bars, possibly due to damage caused by the bending operation. A typical specimen is shown in Figure 32.

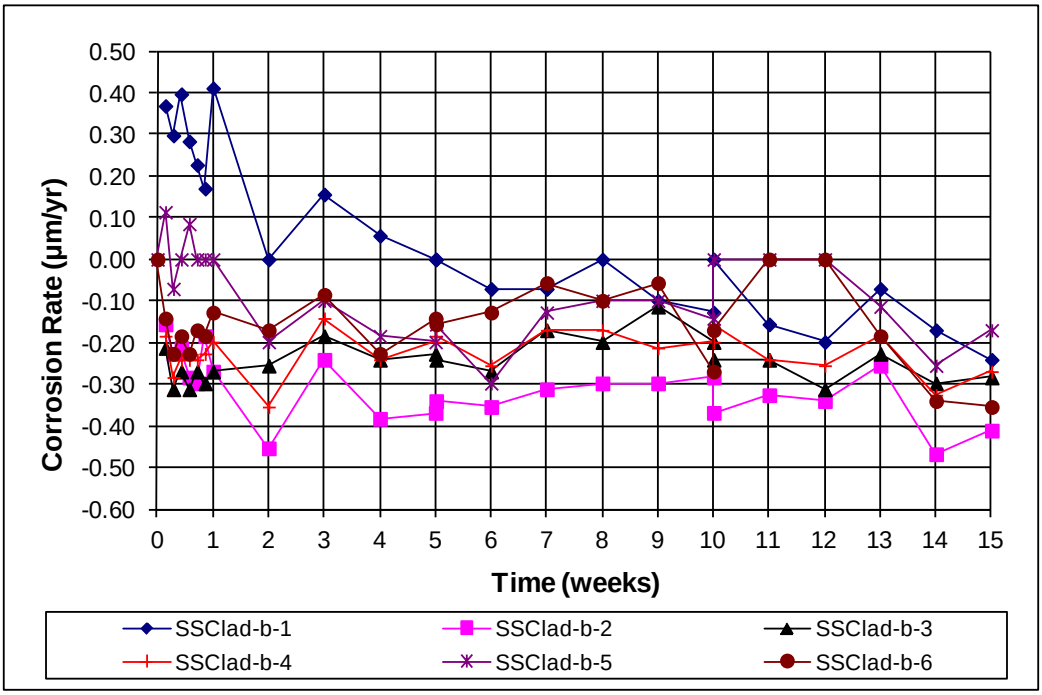

Figure 31: Macrocell individual corrosion rates of bent NX-SCR™ stainless steel clad bars, specimens 1-6

Figure 32: Corrosion staining on bent section upon autopsy, bent NX-SCR™ stainless steel clad bar (close-up)

The corrosion rates for the individual NX-SCR™ stainless steel clad specimens with four holes through the cladding (SSClad-4h) are shown in Figure 33. Some individual corrosion rates, which range from just below 0 to over 15 µm/yr, are rather high due to the exposed conventional steel core. Some specimens showed light to moderate corrosion at some of the damage sites on the anode bar (see left hole on top bar in Figure 34); other specimens showed no corrosion at any damage site. As was the case for the undamaged, capped stainless steel clad (SSClad) bars, the bar caps were removed during the autopsy to determine if corrosion had occurred beneath the protective cap. No corrosion was discovered under the caps.

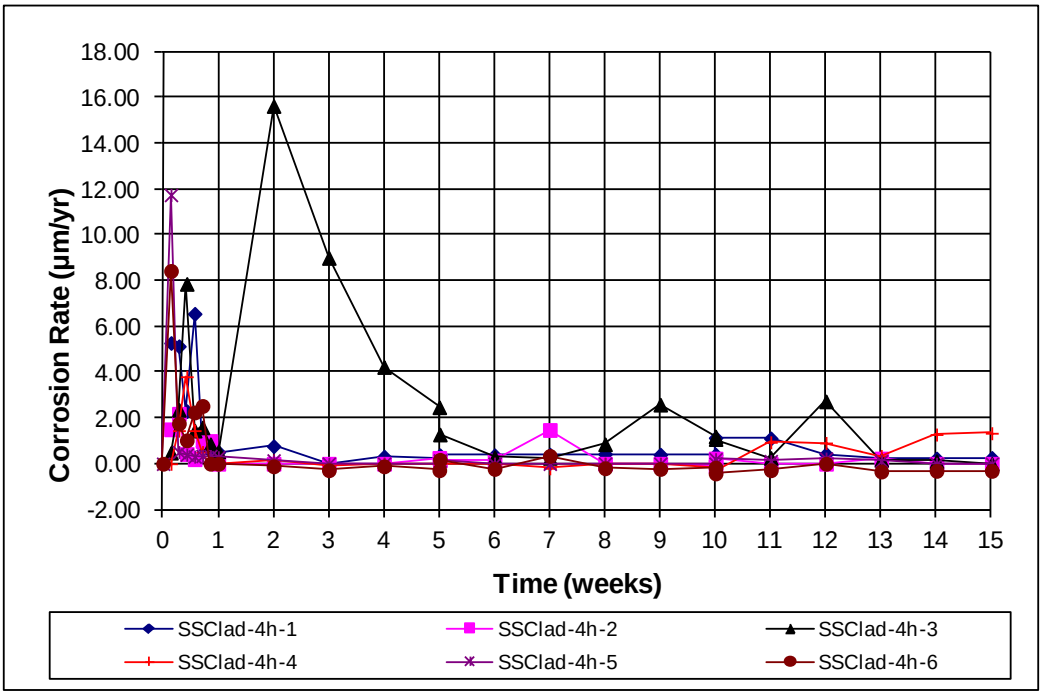

Figure 33: Macrocell individual corrosion rates of 0.83% exposed area NX-SCR™ stainless steel clad bars, specimens 1-6

Figure 34: Photograph of specimen SSClad-4h-5 upon completion of the rapid evaluation test, NX-SCR^{TM} stainless steel clad with four holes through the cladding (anode on top, cathode on bottom)

The corrosion rates for the individual SSClad/Conv. and Conv./SSClad specimens are shown in Figures 35a and 35b. As shown in Figure 35a, the specimens with a conventional bar as the anode performed similarly to the Conv. specimens, with corrosion rates of about 35 µm/yr at the onset of the test, settling to about 15 µm/yr after about 6 weeks.

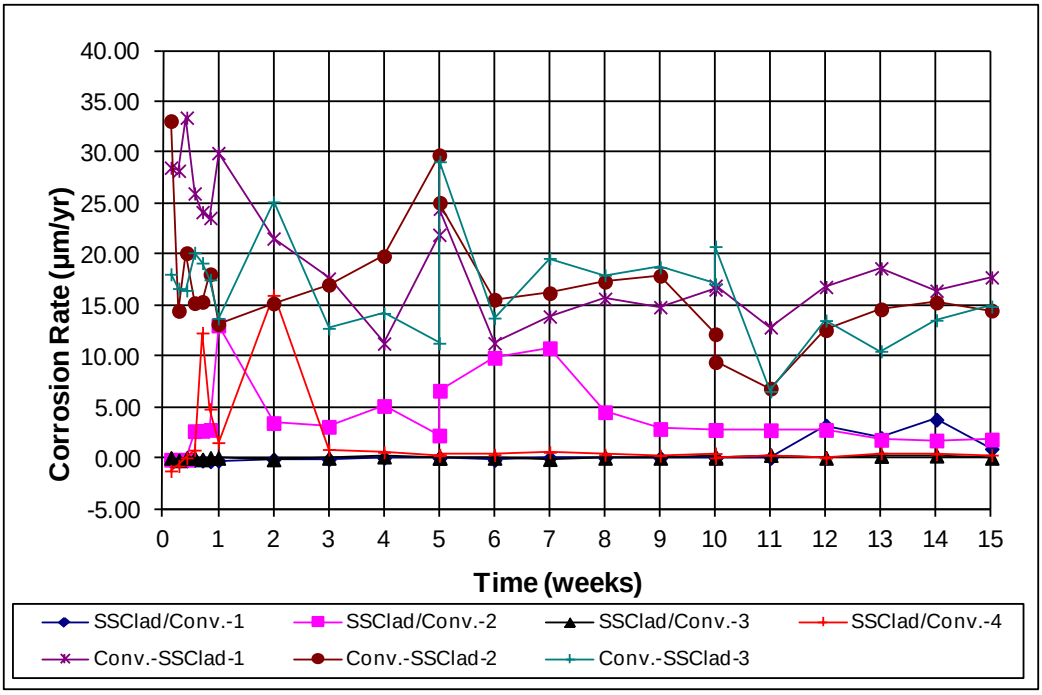

Figure 35a: Macrocell individual corrosion rates of mixed NX-SCR™ stainless steel clad bars (anode/cathode), specimens 1-6

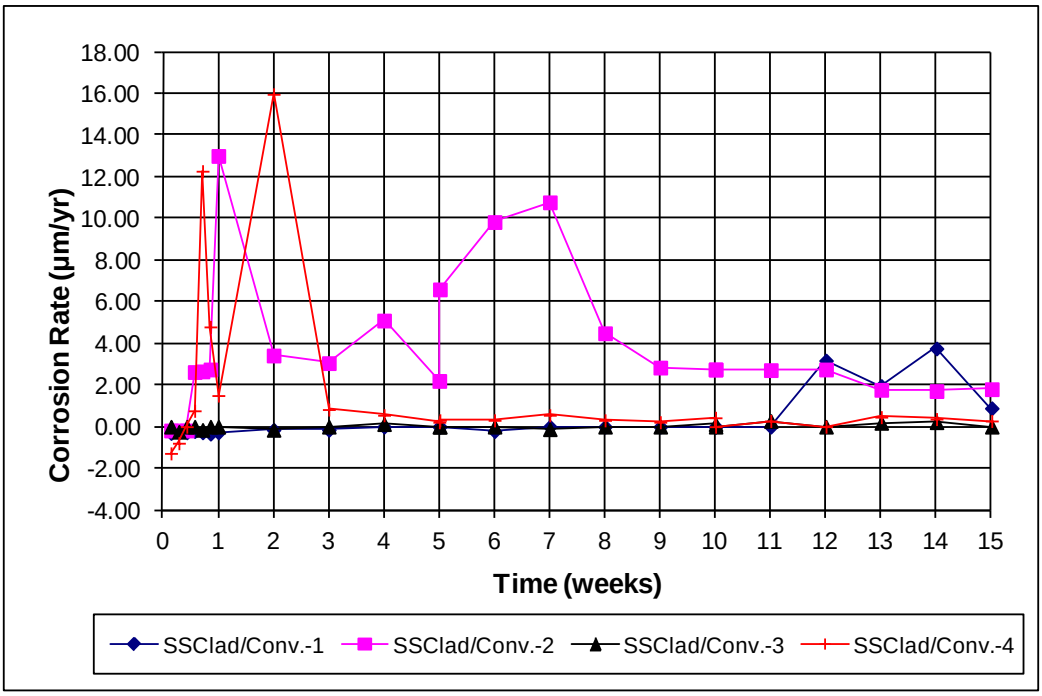

Figure 35b: Macrocell individual corrosion rate of mixed NX-SCR™ stainless steel clad bars (anode/cathode), specimens 1-6 (different scale)

The mixed specimens with a stainless steel clad bar as the anode (SSClad/Conv.) exhibited significantly lower corrosion rates than the specimens with conventional steel at the anode (Conv./SSClad); however, as shown in Figure 35b, several specimens exhibited spikes in

corrosion rate during testing. Specimen SSClad/Conv.-2 had a corrosion rate of approximately 3 µm/yr during most of the test, with a spike in corrosion rate at week 7 to approximately 10 µm/yr. Because this specimen experienced such a high corrosion rate, it was thought that the protective cap on the end of this stainless steel clad bar may have been ineffective. As a result, an additional mixed SSClad/Conv. reinforcement specimen was tested (SSClad/Conv.-4), but it also exhibited a high corrosion rate. Upon autopsy of specimen SSClad/Conv.-2, a significant amount of corrosion was discovered underneath the protective cap (Figure 36) indicating that the cap rather than the bar failed. Specimen SSClad/Conv.-4 and SSClad/Conv.-1 also exhibited a small amount of corrosion under the cap, suggesting that the corrosion observed for those specimens was also caused by a failure of the cap. All specimens that exhibited corrosion rates greater than 0.5 µm/yr later exhibited corrosion under the cap. The nonstandard bar size resulted in a poor cap fit and a higher than normal failure rate. Since the corrosion was due to the failure of the cap and not the cladding, this should not be interpreted as the bars failing ASTM A955.

Figure 36: Corrosion under protective cap at end of evaluation, NX-SCR™ stainless steel clad bar, Specimen 2 (close-up)

4.1.4 Linear Polarization Resistance (LPR) Results

Individual and average total corrosion losses at 15 weeks as measured by linear polarization resistance (LPR) are shown in Table 7. Conventional reinforcement specimens exhibited an average LPR corrosion loss of 13.6 µm. The mixed Conv./SSClad specimens with conventional steel at the anode had similar losses at 15 weeks, 14.2 µm. The mixed Conv./2304 specimens, however, exhibited an average loss of 27.3 µm, twice the loss observed for conventional reinforcement alone. This suggests a galvanic corrosion effect is occurring, resulting in the accelerated corrosion of conventional reinforcement when paired with 2304 stainless steel. Among the epoxy-coated specimens, ECR exhibited an average LPR loss of 0.322 µm. No significant losses were observed on undamaged ECR.

Among specimens with 2304 stainless steel at the anode, mixed 2304/conv. specimens had the greatest average loss, 1.57 µm. The 2304 and 2304p specimens had average losses of 0.723 µm and 0.580 µm, respectively.

Among specimens with NX-SCR™ stainless steel clad bars as the anode, the specimens with an unprotected cut end (SSClad-NC) had the greatest losses, averaging 1.51 µm. The SSClad-b and SSClad/Conv. specimens had average losses of 0.601 µm and 0.505 µm, respectively. The SSClad specimens with four holes in the cladding had average losses of 0.221 µm, and the undamaged SSClad specimens had the lowest losses of the SSClad specimens, 0.212 µm.

Table 7: Total (LPR) Corrosion Losses (µm) at 15 Weeks for Rapid Macrocell Specimens

Specimen[a]	Specimen						Average	Standard Deviation
	1	2	3	4	5	6		
Conv.	16.2	12.3	21.1	6.27	11.1	14.9	13.6	5.04
ECR	0.419	0.313	0.446	0.127	0.249	0.379	0.322	0.120
ECR-ND	0.001	0.000	0.000	-	-	-	0.000	0.000
2304	1.01	0.623	0.528	0.712	0.737	0.733	0.723	0.160
2304p	0.501	0.377	0.811	0.502	0.532	0.754	0.580	0.167
2304/Conv.	1.46	1.29	1.96	-	-	-	1.57	0.348
Conv./2304	23.7	46.8	11.4	-	-	-	27.3	17.9
SSClad-4h	0.099	0.344	0.492	0.122	0.071	0.201	0.221	0.165
SSClad	0.284	0.184	0.313	0.118	0.277	0.094	0.212	0.093
SSClad-NC	2.87	2.22	0.183	1.79	0.223	1.78	1.51	1.09
SSClad-b	0.342	0.876	0.541	0.526	0.220	1.098	0.601	0.330
SSClad/Conv.	0.089	1.401	0.131	0.398	-	-	0.505	0.613
Conv./SSClad	10.5	20.4	11.8	-	-	-	14.2	5.36

[a] Conv. = conventional reinforcement, ECR = epoxy-coated reinforcement with ten 1/8-in. diameter holes through the epoxy, ECR-ND= undamaged ECR, 2304 = 2304 stainless steel, SSClad-4h = stainless steel clad reinforcement with four 1/8-in. diameter holes through the cladding, SSClad = undamaged stainless steel clad reinforcement, SSClad-b = bent stainless steel clad reinforcement, SSClad-NC=clad reinforcement with no cap over the cut end.

For mixed specimens, the reinforcement on the top mat is listed first.

A comparison between macrocell (losses from voltage drop readings) and total (LPR) corrosion losses is shown in Figures 37a and 37b, respectively. All systems in this study show average LPR corrosion losses greater than macrocell losses. Considering all specimens (Figure 37a), average total losses are 2.07 times macrocell losses as determined by a best fit line. Removing specimens with conventional reinforcement as the anode (Figure 37b), average total losses are 4.47 times macrocell losses. This suggests that localized corrosion is a greater percentage of total corrosion on ECR and stainless steel reinforcement than on conventional reinforcement. Conv./2304 specimens exhibited the greatest average macrocell and total corrosion loss. With the exception of specimens containing 2304 reinforcement, all specimens exhibited similar behavior in terms of macrocell and total corrosion loss. Specimens with 2304 at the anode (2304, 2304/Conv.) exhibit relatively low macrocell corrosion losses, but somewhat higher total losses.

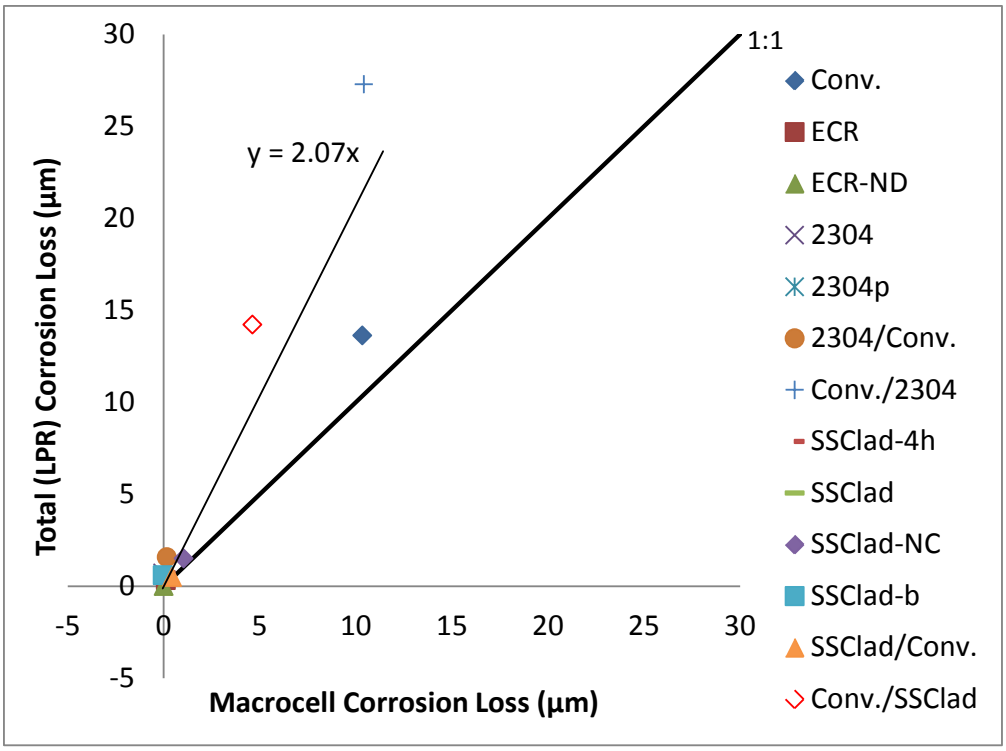

Figure 37a: Rapid macrocell test-comparison between corrosion loss (µm) from macrocell and total corrosion loss readings

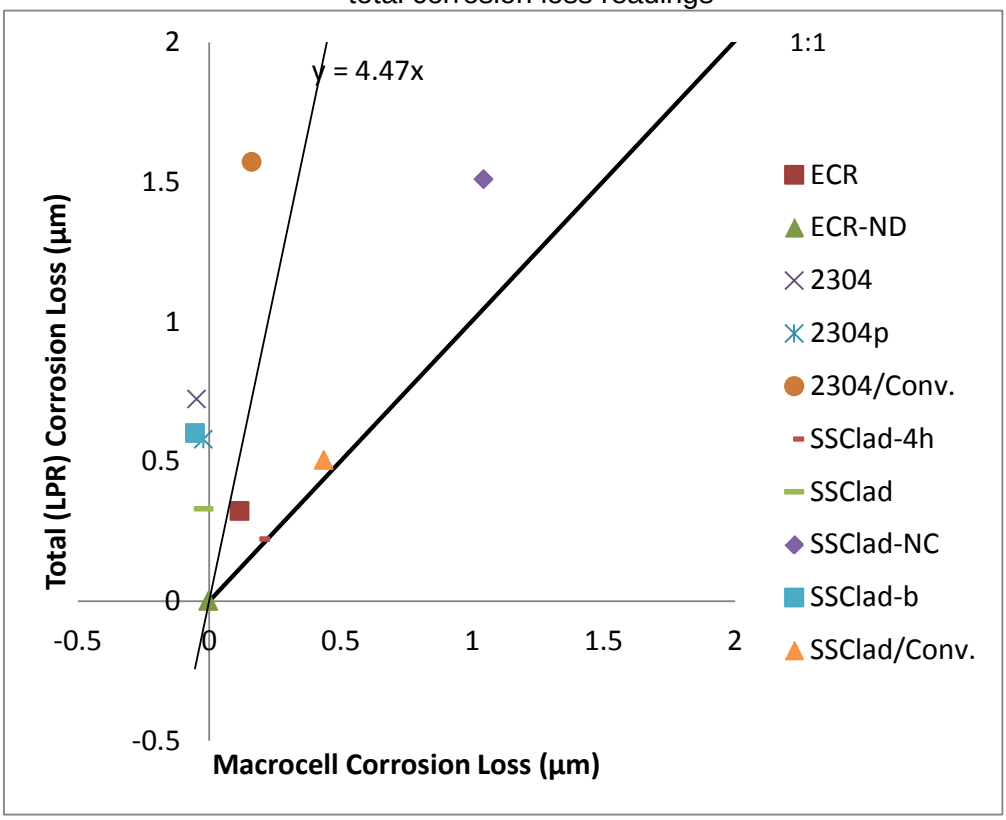

Figure 37b: Rapid macrocell test-comparison between corrosion loss (µm) from macrocell and total corrosion loss readings (different scale)

4.1.5 Autopsy

Upon completion of the 15-week rapid macrocell tests, all specimens were autopsied, using the following procedure:

1. Specimens are removed from the solution and patted dry with paper towels.
2. The electrical connection of each specimen is closely examined for signs of corrosion.
3. Photographs are taken of each specimen on two sides.
4. In the case of capped specimens, the protective caps on the ends are removed with a pen knife and inspected for signs of corrosion.
5. If applicable, photographs are taken of each specimen that has noteworthy corrosion staining.
6. In the case of ECR and ECR-ND specimens, disbondment tests are performed upon each anode bar.

The disbondment test is performed at the four locations where the on ECR bars is penetrated and at the same locations on the undamaged ECR-ND bars. At each test site, a sharp utility knife is used to make two cuts through the epoxy at 45° from the axis of the bar, forming an "X" centered on the hole. An attempt is made to peel back the epoxy coating with the knife around the "X" until either (1) the coating will no longer peel back or (2) a longitudinal rib is reached in the circumferential direction or the second deformation on either side of the hole is reached along the specimen. In the case of the ECR-ND specimens, the coating was scraped with a pen knife to detect any softening of the coating that may be present. The disbonded area is measured with 0.01-in. (0.254-mm) grid paper. The 1/8-in. diameter hole area is not included in the disbonded area. The values of the disbonded area for each of the ECR specimens with penetrations in the coating are shown in Table 8. The originally undamaged bars exhibited no disbondment.

Table 8: Disbonded area (in.^{2})* for ECR specimens 1-6

Specimen	Site 1	Site 2	Site 3	Site 4	Average
1	0.18	0.14	0.13	0.13	0.15
2	0.16	0.19	0.17	0.22	0.19
3	0.11	0.21	0.10	0.26	0.17
4	0.19	0.08	0.15	0.08	0.13
5	0.06	0.32	0.09	0.09	0.14
6	0.33	0.20	0.52	0.09	0.29

*Values do not include area of original hole.

As mentioned earlier, each specimen is photographed on two sides upon completion of the rapid macrocell test. Typical specimens are presented in Figures 38 through 52; anomalies observed during the autopsy were discussed earlier in this chapter. Where corrosion products and staining are shown, it can be inferred that these effects were observed for all specimens in a set.

Figure 38 shows a specimen with conventional reinforcement upon completion of the rapid macrocell test. As can be seen, the anode bar had corrosion products along the length of the bar, while the cathode bars did not exhibit corrosion products.

Figure 39 shows an undamaged ECR specimen upon completion of the test. These specimens performed very well and did not exhibit any corrosion or disbondment of the epoxy coating. The ECR specimens with penetrations in the coating did, however, experience some disbondment, as shown in Figure 40.

Figure 38: Rapid macrocell specimen upon completion of test, conventional steel (anode on top, cathode on bottom)

Figure 39: Rapid macrocell specimen upon completion of test, undamaged ECR (anode on top, cathode on bottom)

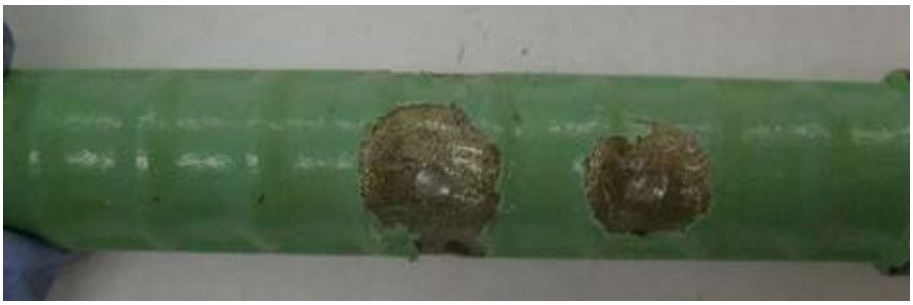

Figure 40: Rapid macrocell specimen upon completion of test, ECR (close-up of damage site after disbondment test)

Figures 41 and 42 show the 2304 and 2304-p specimens, respectively, upon completion of the test. Figure 41 is representative of the as-received 2304 specimens that passed the rapid macrocell test. The specimens that failed the test were discussed earlier (Figure 23).

Figure 41: Rapid macrocell specimen upon completion of test, 2304 stainless steel (anode on top, cathode on bottom)

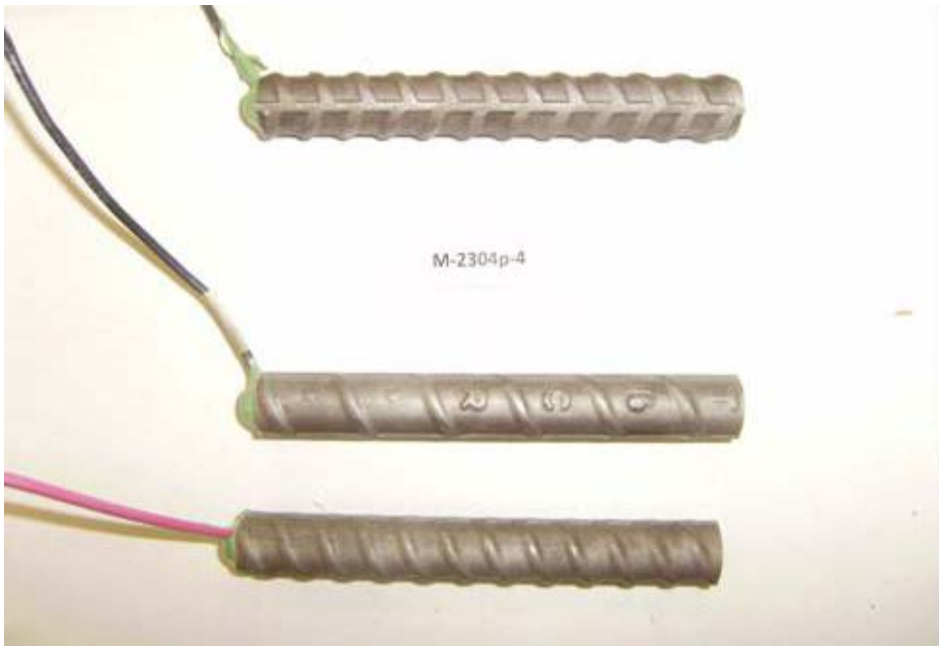

Figure 42: Rapid macrocell specimen upon completion of test, repickled 2304 stainless steel (2304-p) (anode on top, cathode on bottom)

Figures 43 and 44 show the mixed specimens containing 2304 stainless steel and conventional steel. As shown in Figure 44, the specimens with conventional steel as the anode bar show significant corrosion product on the anode bar. The cathode bars in both cases show no significant corrosion products.

Figure 43: Rapid macrocell specimen upon completion of test, mixed 2304/conventional steel (anode on top, cathode on bottom)

Figure 44: Rapid macrocell specimen upon completion of test, mixed conventional/2304 stainless steel (anode on top, cathode on bottom)

The undamaged stainless steel clad specimens upon completion of the test can be seen in Figures 45 and 46. Figure 46 shows the end of the specimen after removal of the cap. As can be seen, there is no corrosion product under the cap.

Figure 45: Rapid macrocell specimen upon completion of test, undamaged stainless steel clad reinforcement (anode on top, cathode on bottom)

Figure 46: Rapid macrocell specimen upon completion of test, undamaged stainless steel clad reinforcement (close-up of bar end after cap has been removed)

The stainless steel clad specimens with four holes through the cladding are shown in Figure 47. As discussed earlier, there were no signs of corrosion at the holes or under the caps

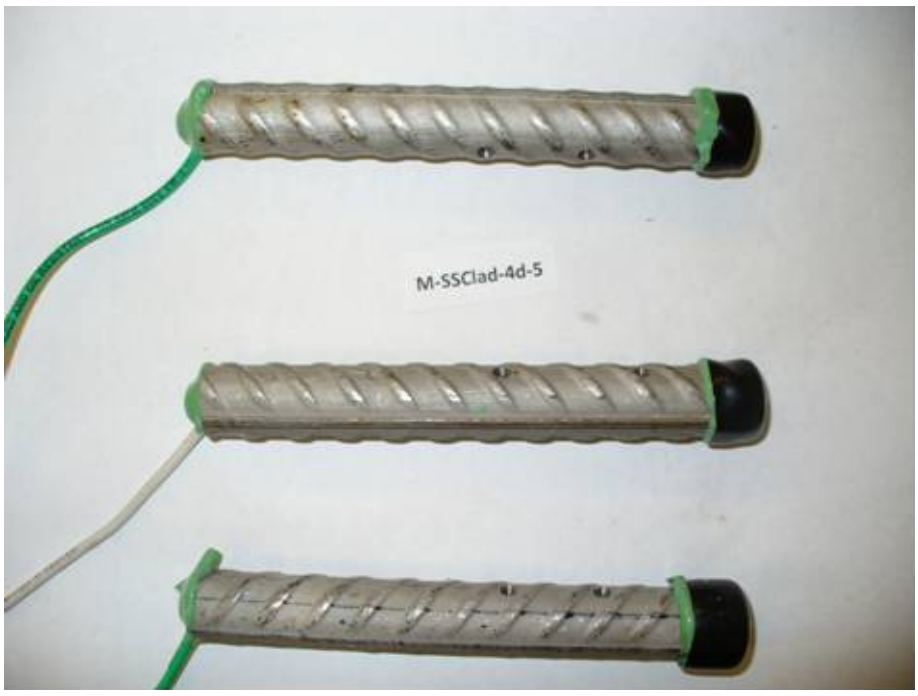

Figure 47: Rapid macrocell specimen upon completion of test, stainless steel clad reinforcement with four holes through the cladding (anode on top, cathode on bottom)

Figures 48 and 49 show the uncapped stainless steel specimens. These specimens showed signs of corrosion at the ends where the conventional core was exposed (Figure 49).

Figure 48: Rapid macrocell specimen upon completion of test, uncapped stainless steel clad reinforcement (anode on top, cathode on bottom)

Figure 49: Rapid macrocell specimen upon completion of test, uncapped stainless steel clad reinforcement (close-up of bar end)

Figure 50 shows a bent stainless steel specimen upon completion of the rapid macrocell test. As discussed earlier, there was minor staining on the bend of most specimens. The corrosion rate of all specimens remained below the limit set by ASTM A955, although bent specimens are not covered by this standard.

Figure 50: Rapid macrocell specimen upon completion of test, bent stainless steel clad reinforcement (anode)

Figures 51 and 52 show the mixed specimens containing stainless steel clad and conventional specimens. As was the case with the Conv./2304 specimens, the specimens containing conventional steel as the anode and stainless steel clad bars as the cathode showed significant corrosion products on the anode bar, while the cathode bars had no corrosion products (Figure 51). There was slight staining on the cathode bars of those specimens containing stainless steel clad bars as the anode and conventional steel as the cathode (Figure 52). Some of these specimens did, however, show staining under the cap of the stainless steel bar (Figure 36).

Figure 51: Rapid macrocell specimen upon completion of test, mixed conventional/stainless steel clad reinforcement (anode on top, cathode on bottom)

Figure 52: Rapid macrocell specimen upon completion of test, mixed stainless steel clad/conventional steel (anode on top, cathode on bottom)

4.2 BENCH-SCALE TESTS

4.2.1 Corrosion losses

With the exception of the repickled 2304 (2304-p) cracked beam specimens, which were added to the test program after the relatively poor performance of the 2304 bars was observed, all bench-scale tests have completed the 96 week test. All ECR-ND specimens and three SE-2304 specimens (SE-2304-4, SE-2304-5, and SE-2304-6) have been continued until week 120 to collect additional data. Corrosion losses at week 96 for the individual Southern Exposure and cracked beam specimens are listed in Tables 9 and 10, respectively. Some specimens in the tables list negative loss values. Negative readings can result from corrosion at the external wiring or in the bottom mat of steel. For the case of the SSClad/Conv. specimens, upon autopsy of the specimens, there was evidence of corrosion of the conventional cathode bars. Inspections of the other specimens showed no signs of corrosion of the wiring or bottom mat of steel. These readings are likely due to drift in the current because of the greater number of bars in the bottom mat of steel and do not actually indicate “negative corrosion”.

Table 9 shows the corrosion losses for the individual Southern Exposure specimens through 96 weeks. The values were obtained by integration of the corrosion rates that are measured on a weekly basis. Corrosion initiated in all Conv., ECR, Conv./2304, Conv./SSClad, and SSClad-4h specimens and in specimens SSClad-b-2 and SSClad-b-3 as well as 2304/Conv.-2, 2304/Conv.-3, 2304-2, and 2304-3 during the 96-week test. Specimen 2304-5 also initiated corrosion but after standard 96 weeks, at week 98, as did specimen 2304-6 at 116 weeks. Losses for the Conv. specimens ranged between 12.3 and 21.0 µm, representing specimens Conv.-1 and Conv.-3, respectively. Losses for the three Conv./2304 specimens exceeded the losses exhibited by all of the Conv. specimens, indicating some galvanic corrosion effect is present. Conv./SSClad-1 had a loss of 18.2 µm, which was also greater than the losses of all Conv. Specimens, except Conv.-3. The remaining two Conv./SSClad specimens had losses equal to or lower than the Conv specimens, suggesting no galvanic corrosion had occurred between the conventional and clad bars. Losses for all other Southern Exposure specimens were less than 1 µm, with the exception of specimens SSClad-4h-3 and SSClad-4h-6, which had losses of 1.84 µm and 2.04 µm, respectively.

Corrosion losses for the individual cracked beam specimens are presented in Table 10. The greatest corrosion loss was exhibited by specimen Conv.-1 (42.2 µm). Specimens containing ECR with 10 1/8-in. diameter holes through the epoxy (ECR) exhibited losses between 0.204 and 1.25 µm based on the total area of the bar. The undamaged ECR (ECR-ND) specimens have exhibited no significant corrosion losses to date. The corrosion losses for 2304 stainless steel ranged between 0.216 and 3.29 µm with corrosion product showing in the crack of specimens 1 and 5, the specimens exhibiting the highest corrosion losses. Specimens containing stainless steel clad reinforcement (SSClad) exhibit losses between –0.172 and 0.233 µm.

Table 9: Corrosion losses based on total area for Southern Exposure specimens

System[a]	Specimen						Average	Standard Deviation
	1	2	3	4	5	6		
	Corrosion Loss (µm)							
Conv.	12.3	16.4	21.0	20.4	14.6	13.5	16.4	3.59
ECR	0.238	0.624	0.309	0.170	0.175	0.536	0.342	0.193
ECR-ND	-0.036	-0.021	-0.023	-	-	-	-0.027	0.008
2304	-0.070	0.246	-0.044	-0.033	0.042	-0.165	-0.004	0.140
2304/Conv.	-0.015	0.216	0.219	-	-	-	0.140	0.134
Conv./2304	-	24.0	28.4	21.9	-	-	24.8	3.32
SSClad-4h	0.404	0.138	1.84	0.026	-0.014	2.042	0.739	0.943
SSClad	-0.043	-0.017	-0.080	-0.157	-0.036	0.197	-0.023	0.119
SSClad-b	0.006	0.364	0.098	-0.152	-0.077	-0.085	0.026	0.187
SSClad/Conv.	-	-0.172	-0.019	-0.535	-0.056	-0.431	-0.242	0.230
Conv./SSClad	18.2	11.7	12.6	-	-	-	14.2	3.54

[a] Conv. = conventional reinforcement, ECR = epoxy-coated reinforcement with ten 1/8-in. diameter holes through the epoxy, ECR-ND= undamaged ECR, 2304 = 2304 stainless steel, SSClad-4h = stainless steel clad reinforcement with four 1/8-in. diameter holes through the cladding, SSClad = undamaged stainless steel clad reinforcement, SSClad-b = bent stainless steel clad reinforcement.

For mixed specimens, the reinforcement on the top mat is listed first.

"-" = No specimen cast in this batch.

Table 10: Corrosion losses based on total area for cracked beam specimens

System[a]	Specimen						Average	Standard Deviation
	1	2	3	4	5	6		
	Corrosion Loss (µm)							
Conv.	42.2	33.4	28.6	22.9	30.9	22.5	30.1	7.35
ECR	0.230	0.316	1.25	0.204	0.426	0.288	0.453	0.400
ECR-ND	-0.070	-0.077	-0.041	-	-	-	-0.063	0.019
2304	2.91	1.31	0.216	1.39	3.29	0.707	1.64	1.22
SSClad	0.233	0.097	-0.168	0.056	-0.059	-0.172	-0.002	0.160

[a] Conv. = conventional reinforcement, ECR = epoxy-coated reinforcement with ten 1/8-in. diameter holes through the epoxy, ECR-ND= undamaged ECR, 2304 = 2304 stainless steel, SSClad = undamaged stainless steel clad reinforcement.

"-" = No specimen cast in this batch.

Figure 53 shows the average corrosion losses for the Southern Exposure specimens. Figure 53a shows the average corrosion losses for the control specimens, Conv., ECR, and ECR-ND, in the Southern Exposure test. Conventional reinforcement exhibited an average loss

of 15.6 µm at the end of the test. The ECR specimens exhibited an average loss of 0.342 µm, while the ECR-ND specimens exhibited no significant losses.

Figure 53b shows the average losses for the Southern Exposure specimens containing 2304 stainless steel, a mix of 2304 and conventional reinforcement, and conventional reinforcement alone. Mixed specimens with conventional steel in the top mat and 2304 stainless steel in the bottom mat exhibited average losses of 24.8 µm upon completion of the test, which was greater than the value for conventional reinforcement alone (15.6 µm). The Conv./2304 specimens from the rapid macrocell test exhibited an average loss similar to that of the Conv. specimens at the conclusion of testing. The specimens containing 2304 in the top mat and conventional reinforcement in the bottom mat (2304/Conv.) had an average corrosion loss of 0.140 µm at the end of testing. The 2304 specimens showed losses of less than 0.01 µm. The latter trends are similar to those observed for losses in the rapid macrocell test.

Figure 53c shows the average losses for the Southern Exposure specimens containing stainless steel clad reinforcement (SSClad), a mix of SSClad and conventional reinforcement, and conventional reinforcement alone. None of the specimens with stainless steel clad reinforcement in the top mat, SSClad, SSClad-b, or SSClad/Conv., exhibited significant losses. The Conv./SSClad specimens exhibited an average loss of 14.2 µm at the end of the test, similar to conventional reinforcement (15.6 µm). This suggests there is no galvanic effect between conventional and stainless steel clad reinforcement, matching the results of the rapid macrocell test. The Conv./SSClad specimens in the rapid macrocell test also exhibited significant losses.

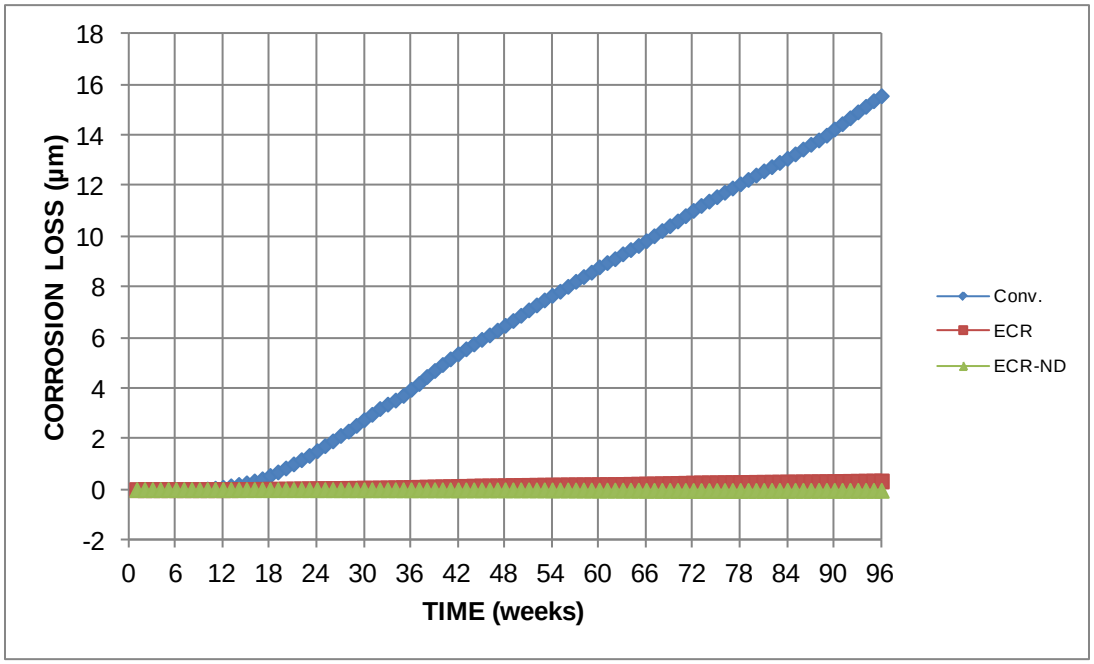

Figure 53a: Average corrosion losses (µm) based on total area for Southern Exposure specimens with conventional and epoxy-coated reinforcement

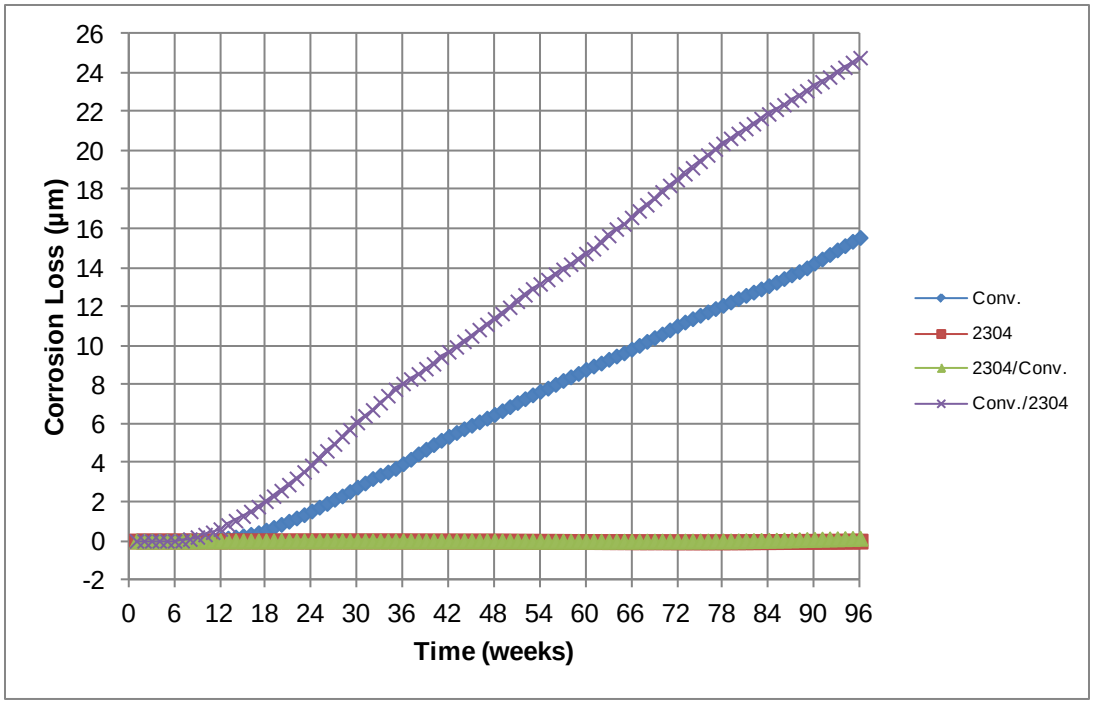

Figure 53b: Average corrosion losses based on total area for Southern Exposure specimens with conventional and 2304 stainless steel reinforcement

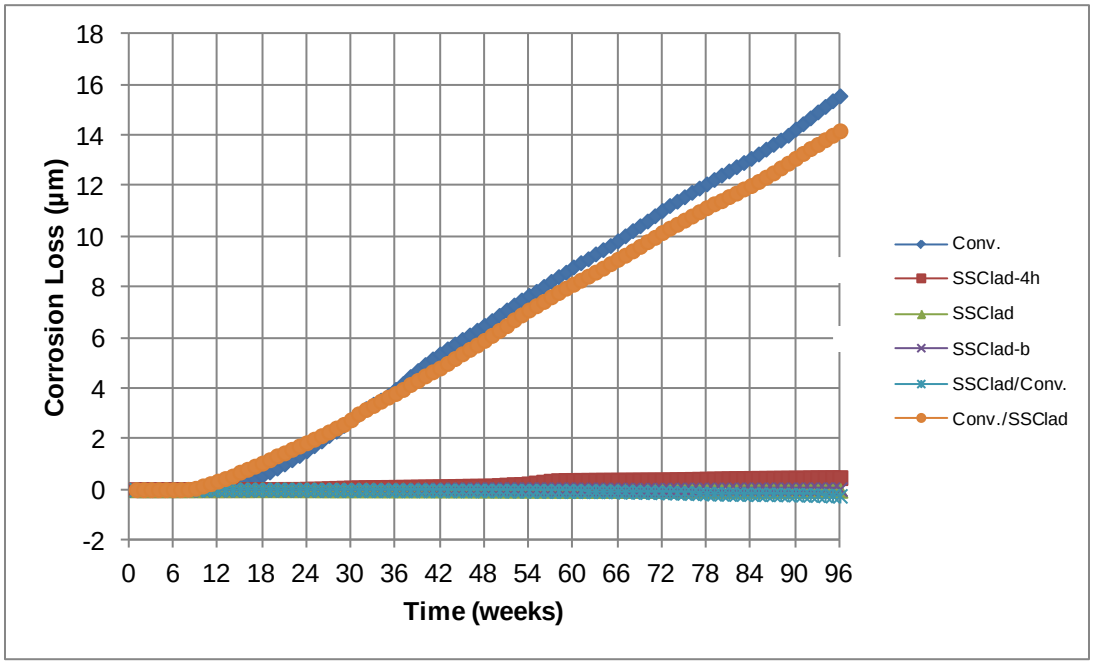

Figure 53c: Average corrosion losses based on total area for Southern Exposure specimens with conventional and stainless steel clad reinforcement

Figures 54a and 54b show the average losses for the cracked beam specimens. Figure 54a shows that conventional reinforcement exhibited an average corrosion loss of 30.0 µm at 96 weeks, far greater than the other systems upon completion of the test. Figure 54b examines the

average losses of the more corrosion-resistant steels at a different scale. The 2304 specimens had the second greatest losses, at 1.64 µm, followed by ECR at 0.453 µm. The undamaged ECR and the stainless steel clad reinforcement exhibited corrosion losses very near zero throughout the test. As of 74 weeks, the repickled 2304 (2304-p) specimens exhibited corrosion losses near zero, as well.

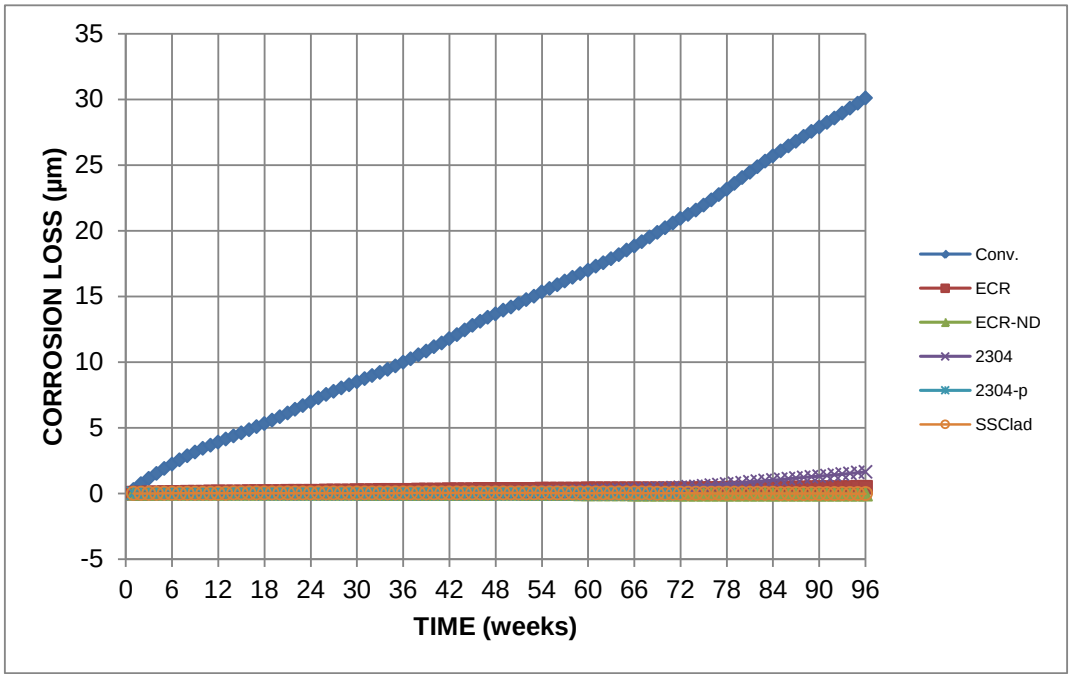

Figure 54a: Average corrosion losses based on total area for cracked beam specimens

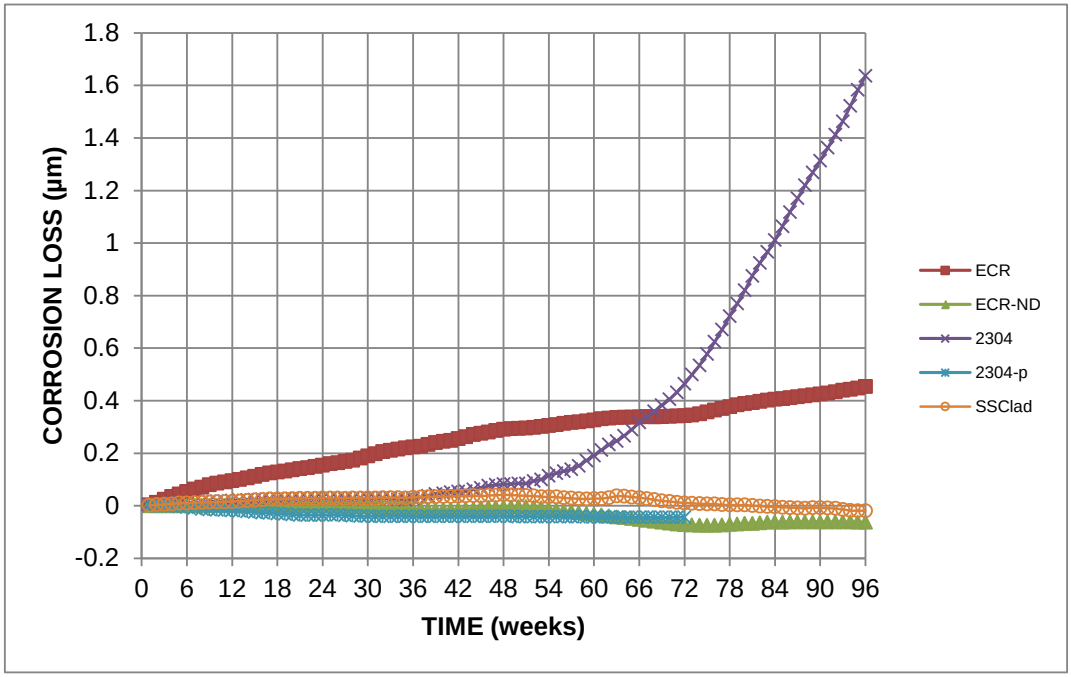

Figure 54b: Average corrosion losses based on total area for cracked beam specimens (different scale)

4.2.2 Mat-to-mat resistance

Figures 55a through 55c show the average mat-to-mat resistances for the Southern Exposure specimens. The resistances for the epoxy-coated bars were considerably higher than those for uncoated reinforcement. The ECR-ND specimens exhibited the highest average resistance during the first 43 weeks, but dropped to levels near that of ECR for several weeks. At week 44, the average resistance of both ECR-ND and ECR were approximately equal until week 53 when the average resistance for ECR-ND dropped below the value for ECR. The drop may indicate some penetration of ions through the undamaged coating; however, the variations in mat-to-mat resistance among individual specimens (Appendix B) are far greater than the apparent drop in resistance among ECR-ND specimens, suggesting this drop is not a statistically significant event. At 96 weeks, average resistances of 428, 7658, and 5163 ohms are observed for the Conv., ECR, and ECR-ND specimens, respectively.

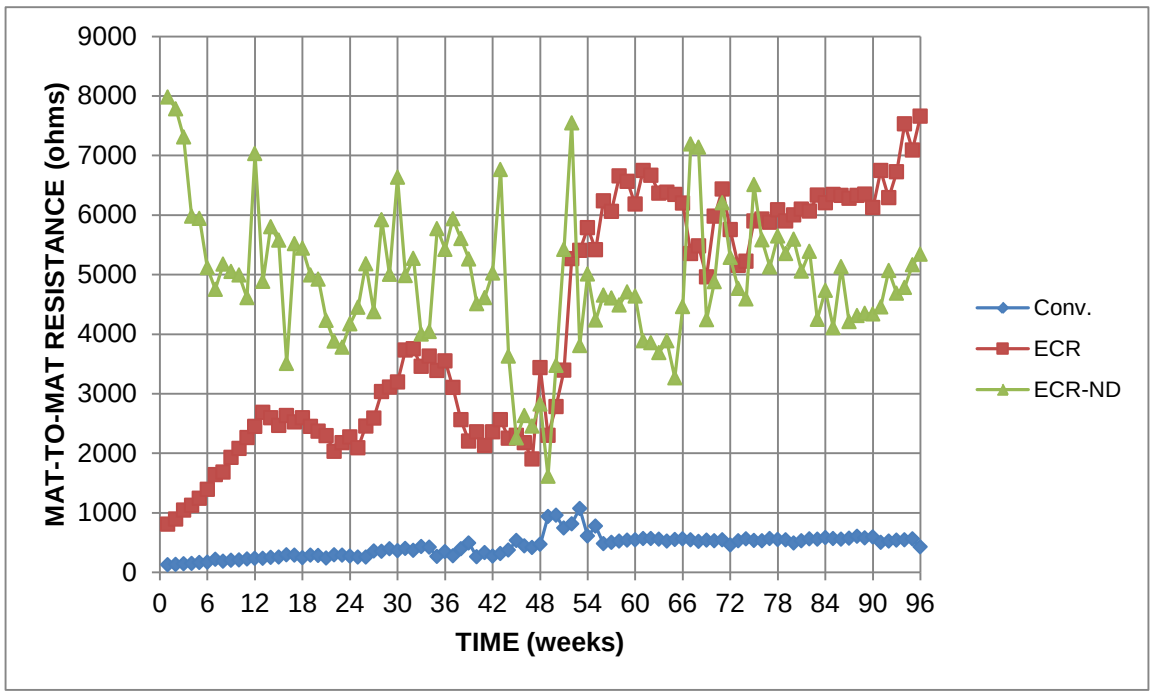

Figure 55a: Average mat-to-mat resistances for Southern Exposure specimens with conventional and epoxy-coated reinforcement

Figure 55b shows mat-to-mat resistances for specimens with conventional and 2304 stainless steel reinforcement. These specimens exhibited similar mat-to-mat resistances until week 55, after which the Conv./2304 specimens exhibited a lower average resistance than the other specimens. The mat-to-mat resistances increased throughout the tests. For the first 55 weeks, the Conv. specimens exhibited somewhat higher resistances than the other specimens, with a spike in resistance during weeks 49-55. However, at week 56, the average resistances for the 2304 specimens and the 2304/Conv. specimens were greater than that for the Conv. specimens. As shown in Figure 55c, the stainless steel clad specimens exhibited similar but somewhat lower values of mat-to-mat resistance than those containing 2304 bars. The mat-to-mat resistances increased throughout the tests, and like the Conv./2304 specimens, the Conv./SSClad specimens had the lowest average resistance after about the mid-point of the test period.

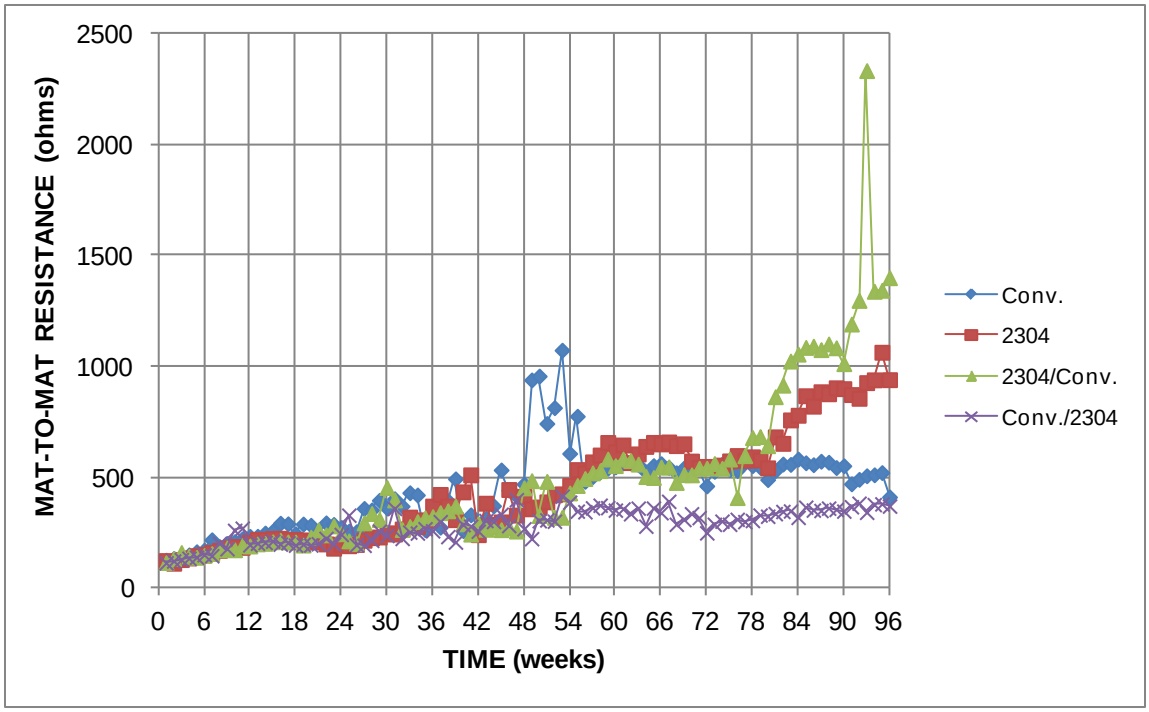

Figure 55b: Average mat-to-mat resistances for Southern Exposure specimens with conventional and 2304 stainless steel reinforcement (different scale)

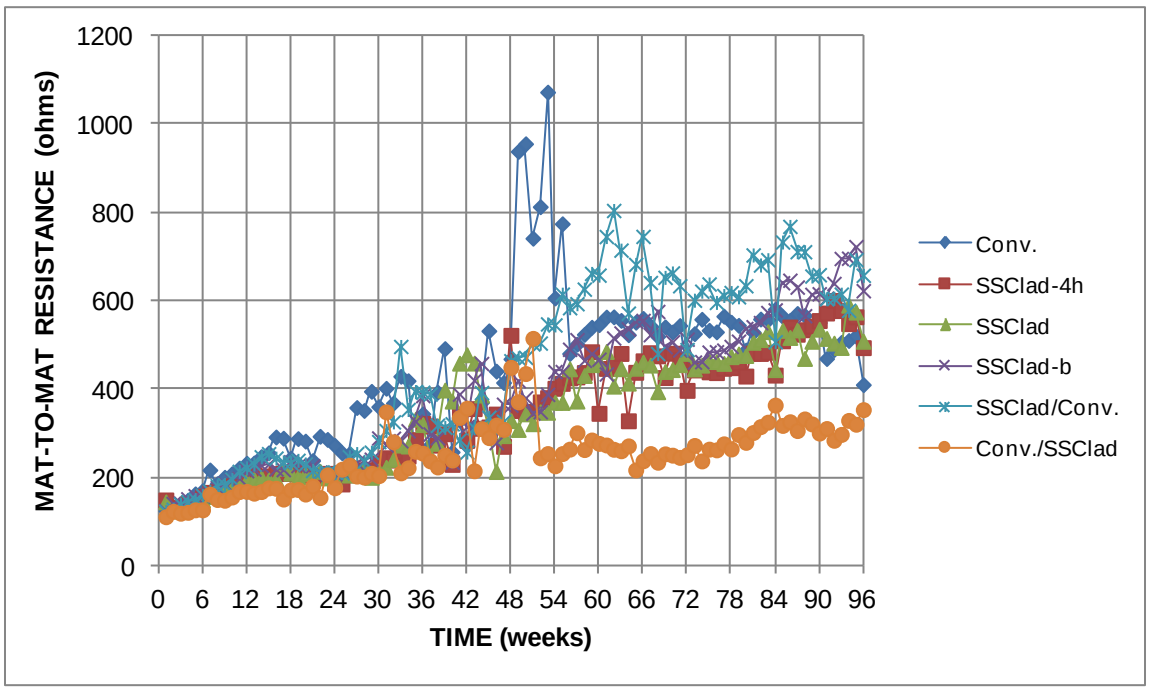

Figure 55c: Average mat-to-mat resistances for Southern Exposure specimens with conventional and stainless steel clad reinforcement (different scale)

The average mat-to-mat resistances for the cracked beam specimens are shown in Figure 56. As for the Southern Exposure specimens, the ECR-ND cracked beam specimens began with the highest values, which dropped to values similar to ECR until week 56 and

remained relatively constant with a slight decrease while the average resistance increased for ECR, possibly due to buildup of corrosion products around the damage sites. Uncoated bar specimens, Conv., 2304, 2304-p, and SSClad, exhibited low values of resistance, with the Conv. specimens showing the lowest average resistance at 461 ohms, the 2304 specimens averaging 2291 ohms, and the SSClad specimens averaging 1565 ohms at the end of the test.

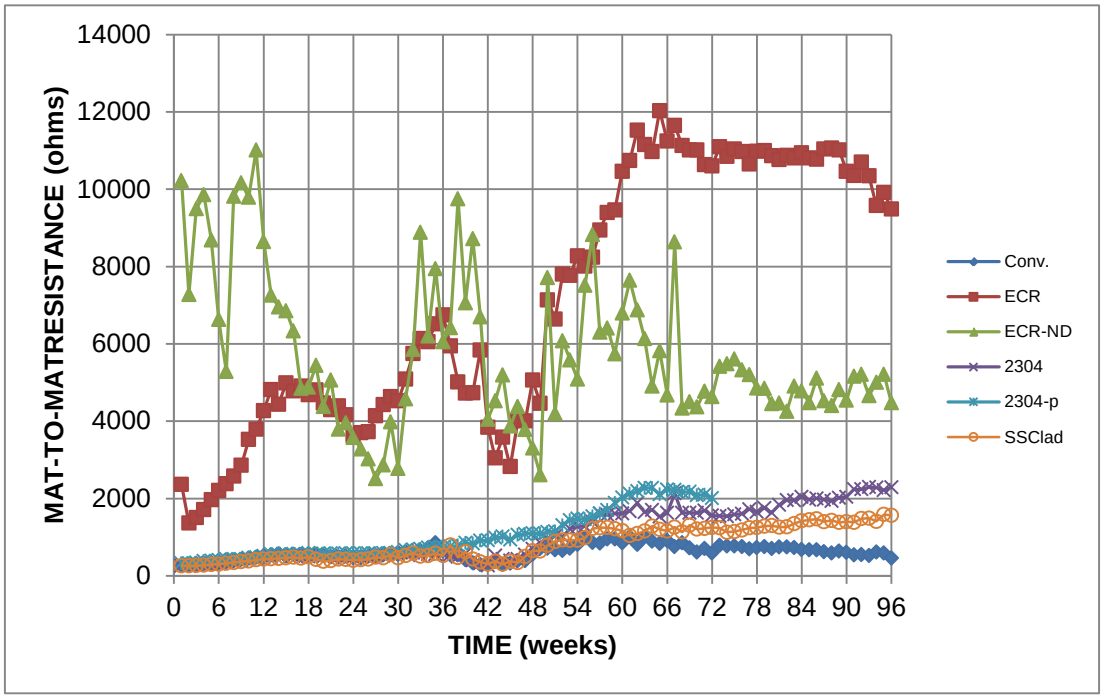

Figure 56: Average mat-to-mat resistances for cracked beam specimens

4.2.3 Corrosion potential

Figure 57a compares the top-mat potentials with respect to a copper-copper sulfate electrode (CSE) for the Southern Exposure specimens with conventional and epoxy-coated reinforcement. Figures 57b and 57c compare the top-mat potentials for specimens containing, respectively, 2304 and SSClad bars with those containing only conventional bars. As the potential of a bar or mat becomes more negative, the probability of corrosion increases. Throughout the tests, the top-mat potentials dropped for specimens with exposed conventional steel in the top mat. Although the ECR-ND specimens did not exhibit significant corrosion, the average top-mat potential was lower than that of the specimens with stainless steel in the top mat, as shown in Figures 57b and 57c. For the 2304 and mixed Conv./2304 and 2304/Conv. specimens, those with higher corrosion rates (Conv. and Conv./2304) showed the most negative corrosion potentials after the specimens initiated corrosion, with these potentials ranging between –0.51 and –0.63 V. Two 2304 specimens and two 2304/Conv. specimens initiated corrosion. For the 2304 and 2304/Conv. specimens, top-mat potentials remained more positive than Conv. specimens, with no value more negative than –0.30 V (for 2304/Conv. at 13 weeks and 87 weeks). The same trends can be seen in Figure 57c for specimens with SSClad reinforcement. Again, the Conv. and Conv./SSClad specimens showed the most negative potentials throughout the test. All of the stainless steel clad specimens with four holes through the cladding initiated corrosion and exhibited the next lowest potentials. Two SSClad-b specimens (SSClad-b-2 and SSClad-b-3) initiated corrosion but the average top-mat potential was similar to those of the SSClad and SSClad/Conv. specimens. The SSClad and

SSClad/Conv. specimens did not initiate corrosion and did not have potentials lower than –0.30 V.

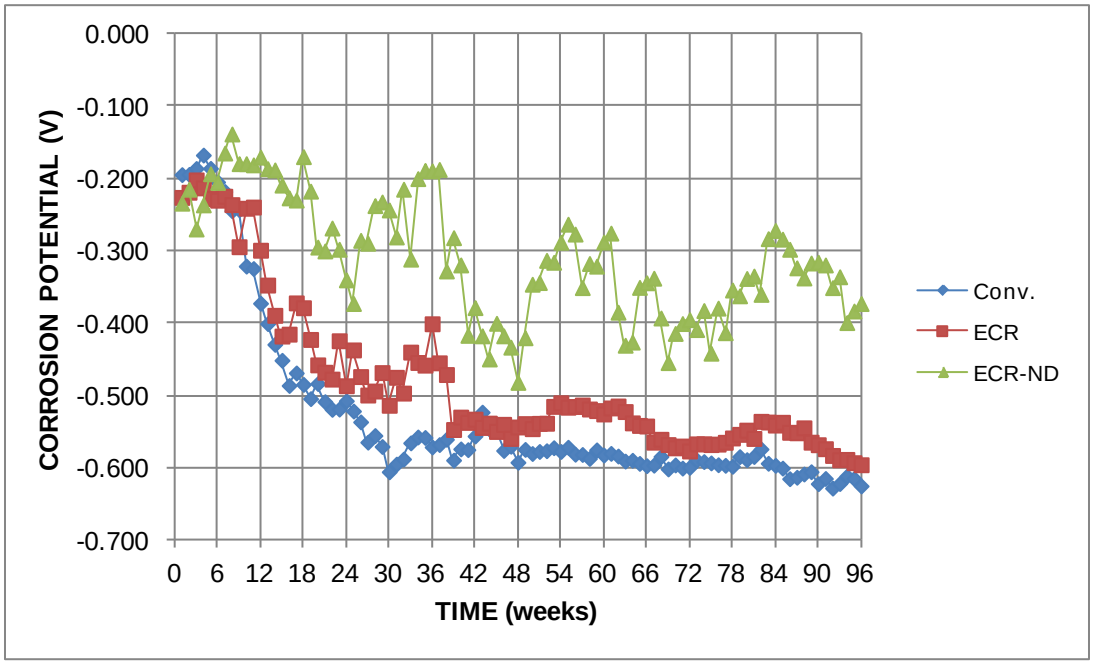

Figure 57a: Average top-mat potentials with respect to CSE for Southern Exposure specimens with conventional and epoxy-coated reinforcement

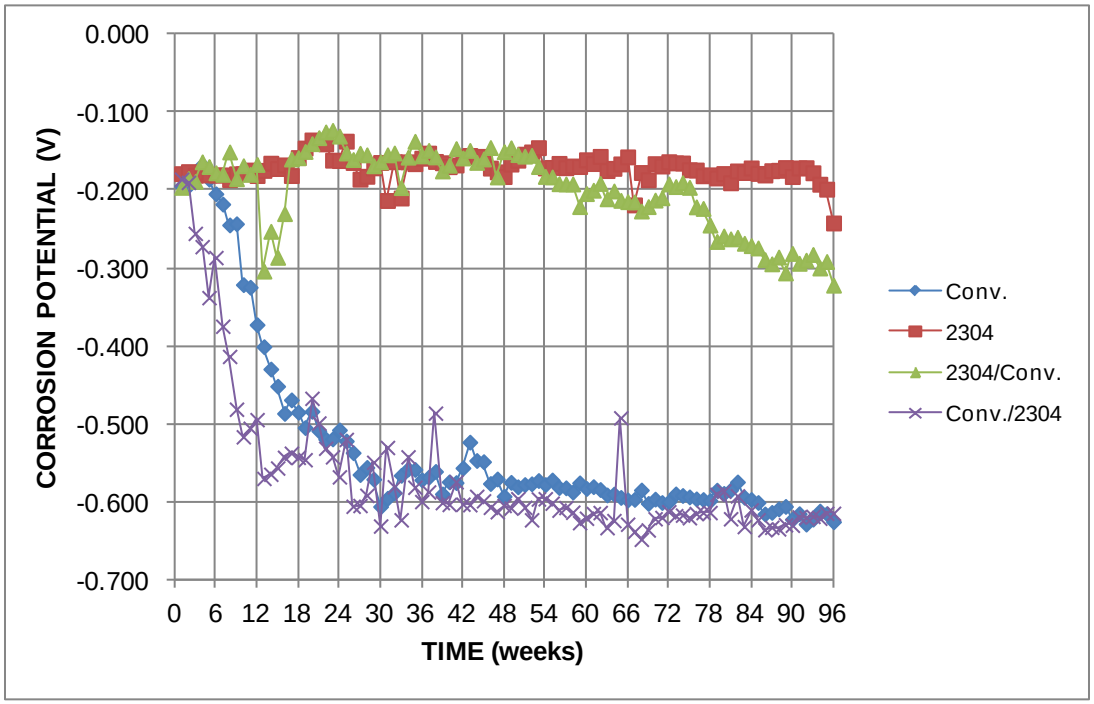

Figure 57b: Average top-mat potentials with respect to CSE for Southern Exposure specimens with conventional and 2304 stainless steel reinforcement

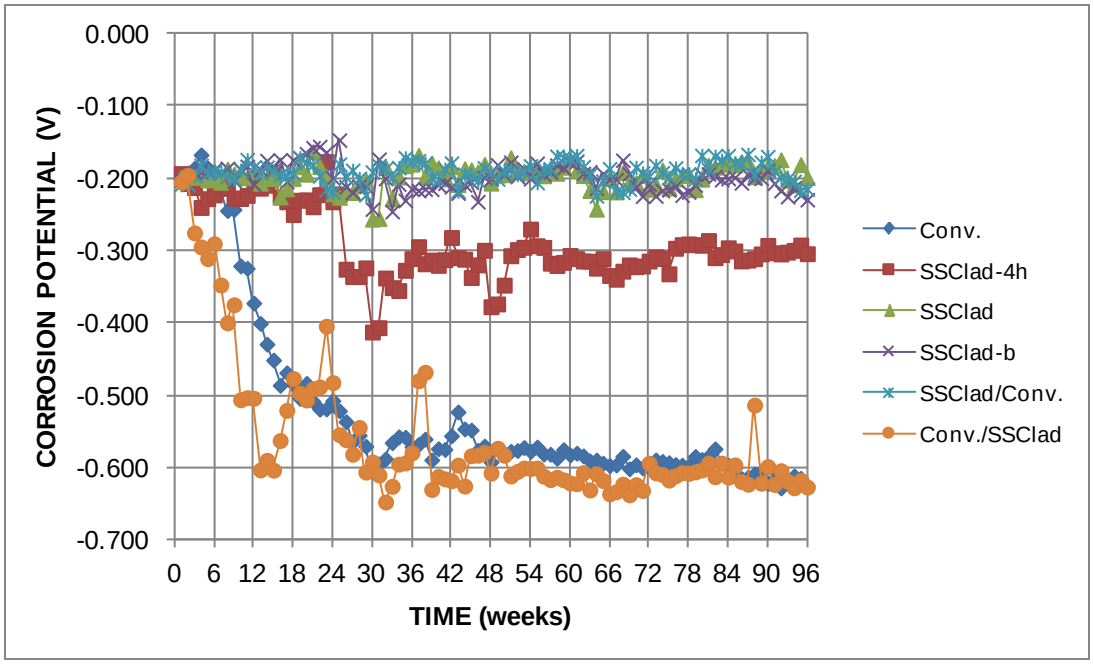

Figure 57c: Average top-mat potentials with respect to CSE for Southern Exposure specimens with conventional and stainless steel clad reinforcement

The top-mat potentials for the cracked beam specimens are shown in Figure 58. As for the Southern Exposure specimens, conventional reinforcement and epoxy-coated reinforcement exhibited the most negative corrosion potentials throughout the test. The potentials for the ECR-ND specimens were higher than for the ECR and Conv. specimens but were below –0.30 V beginning in week 14. The potentials for the 2304 and SSClad specimens were similar until week 52 when the potentials for 2304 began to drop. The SSClad specimens showed average potentials above –0.30 V throughout testing. The average potential for the 2304 specimens dropped below –0.30 V at week 74 and remained that value through week 96. At the end of testing, the 2304 and SSClad specimens exhibited average corrosion potentials of –0.417 V and –0.177 V, respectively. Through week 72, the 2304-p specimens have exhibited an average corrosion potential above –0.25 V.

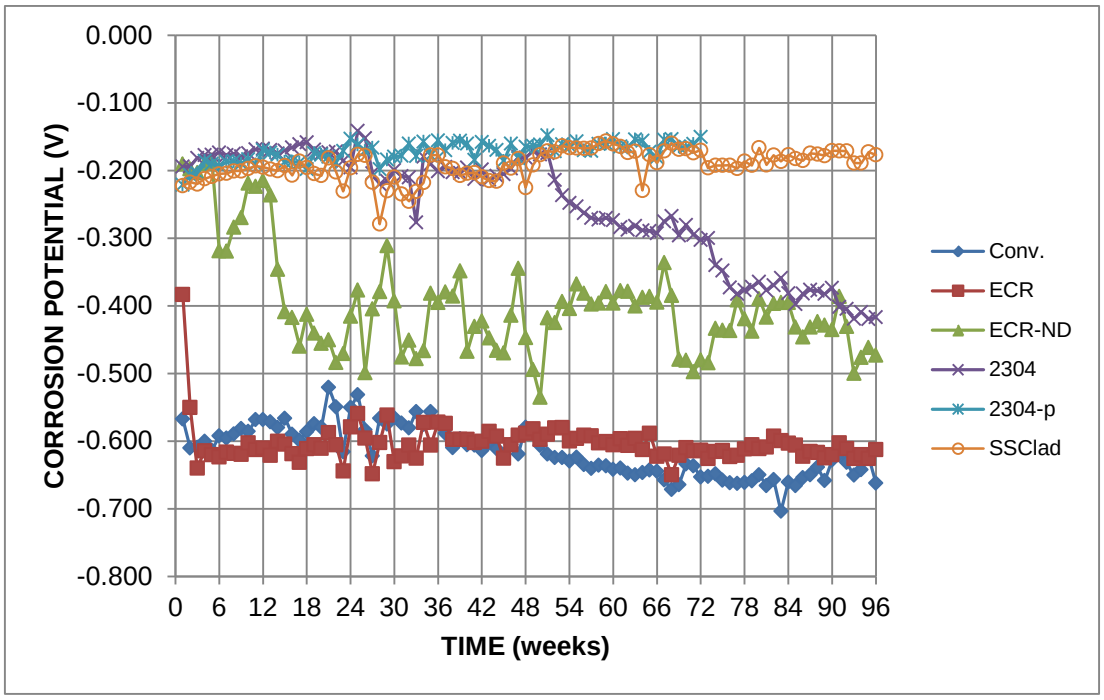

Figure 58: Average top-mat potentials with respect to CSE for cracked beam specimens

The bottom-mat corrosion potentials were typically more positive than the top-mat potentials for all specimens, indicating a greater tendency to corrode in the top mat. For conventional and epoxy-coated reinforcement, shown in Figure 59a, the average bottom-mat potentials exhibited similar values throughout testing, most between –0.200 V and –0.350 V, with the exception of ECR-ND at week 26, where the average bottom-mat potential was –0.56 V, and at weeks 64 through 71 where ECR-ND exhibited slightly lower potentials than Conv. and ECR.

For the stainless steel specimens, the average bottom-mat potentials remained in roughly the same range throughout the test, with most between –0.150 V and –0.250 V, as shown in Figures 59b and 59c. The bottom-mat potentials for the 2304 and SSClad specimens remained higher than those of the Conv. specimens throughout the test.

The average bottom-mat potentials for the cracked beam specimens are shown in Figure 60. As for the Southern Exposure specimens, the 2304 and SSClad specimens exhibited the highest (most positive) average potentials, with most values ranging between –0.150 V and –0.200 V; the 2304-p specimens have exhibited similar bottom-mat potentials through week 72. For the ECR and ECR-ND specimens, average values were closely grouped – on the order of –0.10 to –0.20 V lower than those of the stainless steel specimens. The bottom-mat potentials for the Conv. specimens continuously decreased throughout the test. The Conv. specimens exhibited the lowest bottom-mat potential (–0.500 V) at the end of the test.

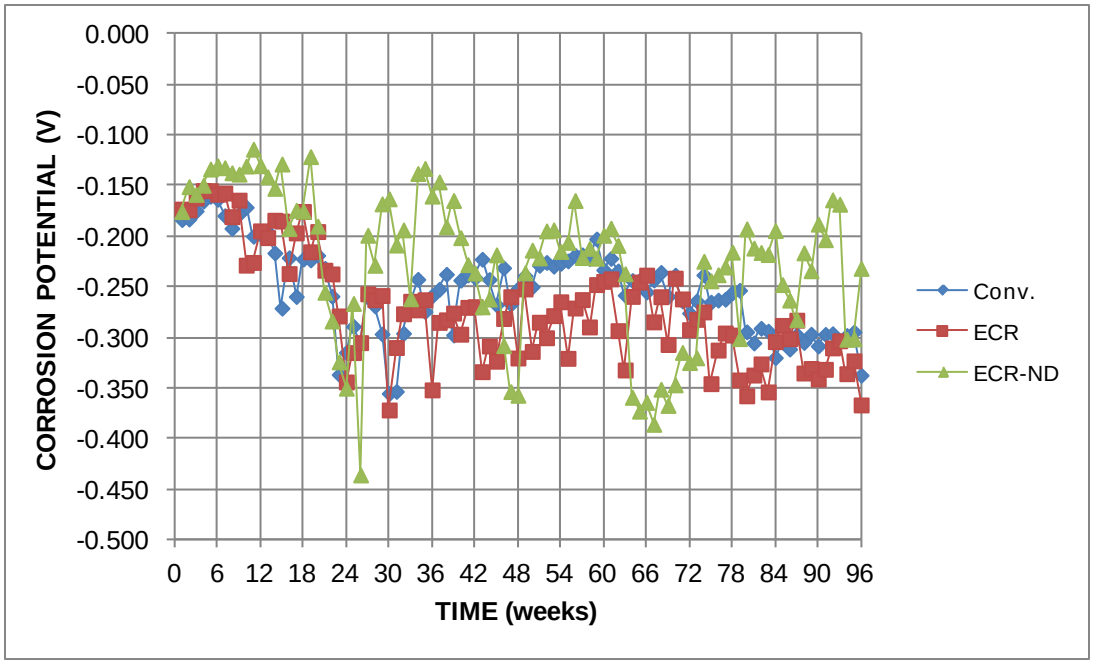

Figure 59a: Average bottom-mat potentials with respect to CSE Southern Exposure specimens with conventional and epoxy-coated reinforcement

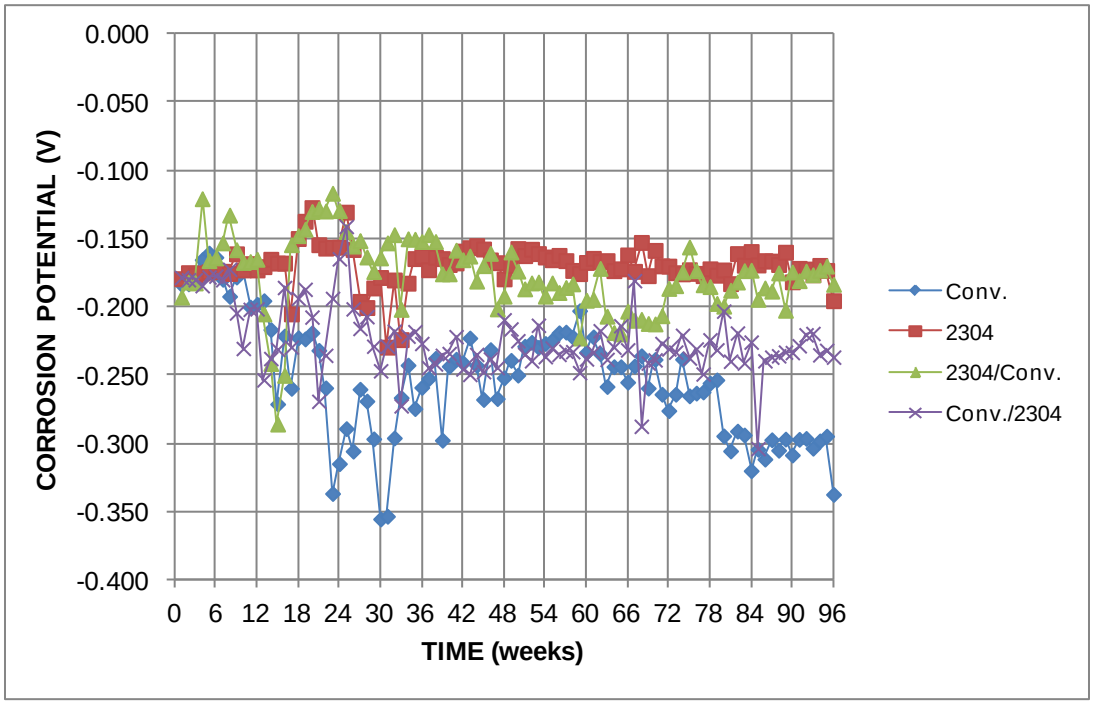

Figure 59b: Average bottom-mat potentials with respect to CSE Southern Exposure specimens with conventional and 2304 stainless steel reinforcement

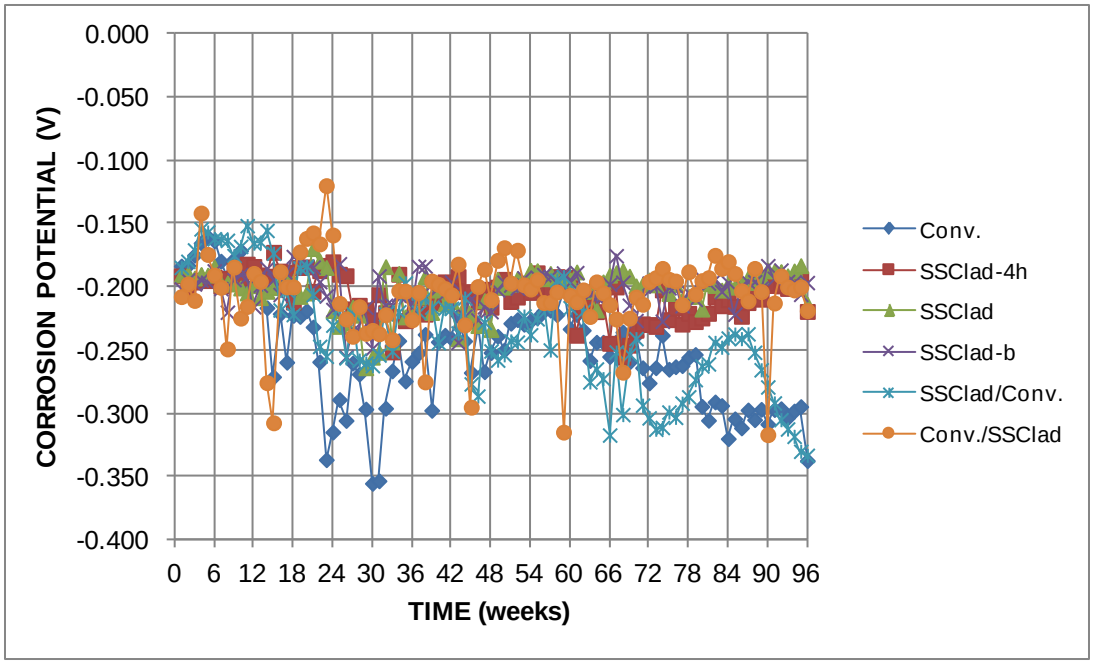

Figure 59c: Average bottom-mat potentials with respect to CSE Southern Exposure specimens with conventional and stainless steel clad reinforcement

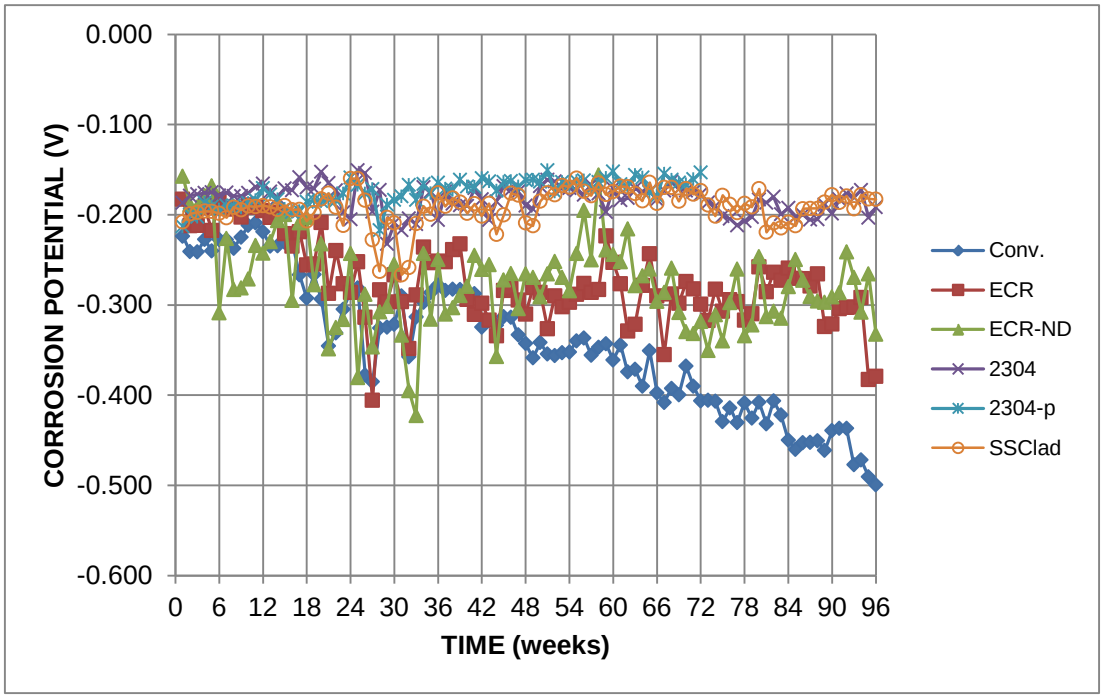

Figure 60: Average bottom-mat potentials with respect to CSE for cracked beam specimens

4.2.4 Corrosion rates

4.2.4.1 Control Specimens

The control specimens include conventional steel (Conv.), epoxy-coated reinforcement with 1/8-in. (3.2-mm) diameter holes through the epoxy (ECR), and undamaged epoxy-coated reinforcement (ECR-ND). As stated earlier, all specimens tested in the control group are from the same heat of steel. Figures 61a and 61b show the average corrosion rates of the Southern Exposure control group. As shown in Figure 61a, the conventional steel specimens exhibited an average corrosion rate between 8 and 12 µm/yr for the majority of the test. The ECR specimens exhibited an average corrosion rate of 0.1 to 0.4 µm/yr (Figure 61b), while the ECR-ND specimens had an average corrosion rate close to zero for the entire test, with a slight negative average corrosion rate from weeks 53 to 75 (Figure 61b). The slight negative corrosion readings may be due to a small amount of current drift between the anodes and the cathodes. At week 77, the average corrosion rate increased to 0.08 µm/yr, the highest average corrosion rate experienced by the ECR-ND specimens. The tests for the ECR-ND specimens were extended through week 144. No signs of corrosion have been observed.

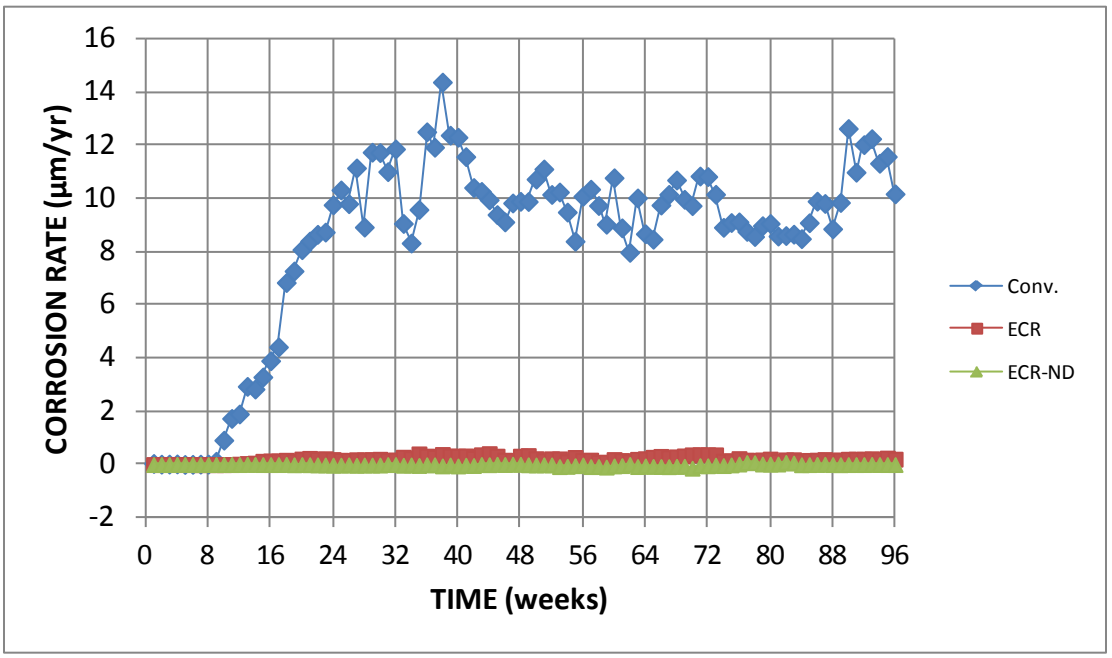

Figure 61a: Average corrosion rates of conventional, ECR, and undamaged ECR Southern Exposure specimens

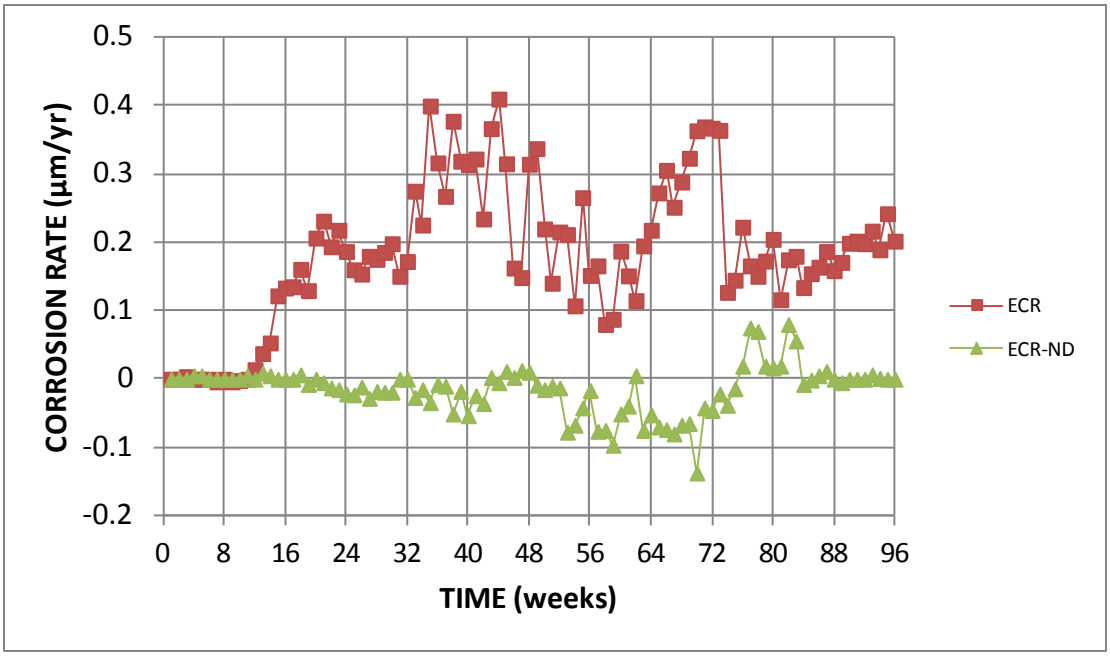

Figure 61b: Average corrosion rates of ECR and undamaged ECR Southern Exposure specimens (different scale)

Figures 62a and 62b show the average corrosion rate of the cracked beam specimens containing the Conv., ECR, and ECR-ND bars. As with the Southern Exposure specimens, conventional steel exhibited the highest corrosion rate, with values ranging from 12 µm/yr to 23 µm/yr, during the test. Figure 62b shows the average corrosion rate for the ECR and ECR-ND specimens on a different scale. The ECR specimens had an average corrosion rate between 0.1 and 0.4 µm/yr for the majority of the test with a few fluctuations above (weeks 2-9 and 29-32) and below (weeks 63-72) that range. The greatest individual corrosion rate, 2.02 µm/yr, occurred in specimen 3 at week 75 (Figure 62c). The ECR-ND specimens exhibited no significant corrosion. The highest average corrosion rate experienced by the ECR-ND specimens was at week 45 with an average corrosion rate of 0.19 µm/yr. As stated earlier, the negative corrosion rates are likely due to current drift because of the greater number of bars in the bottom mat.

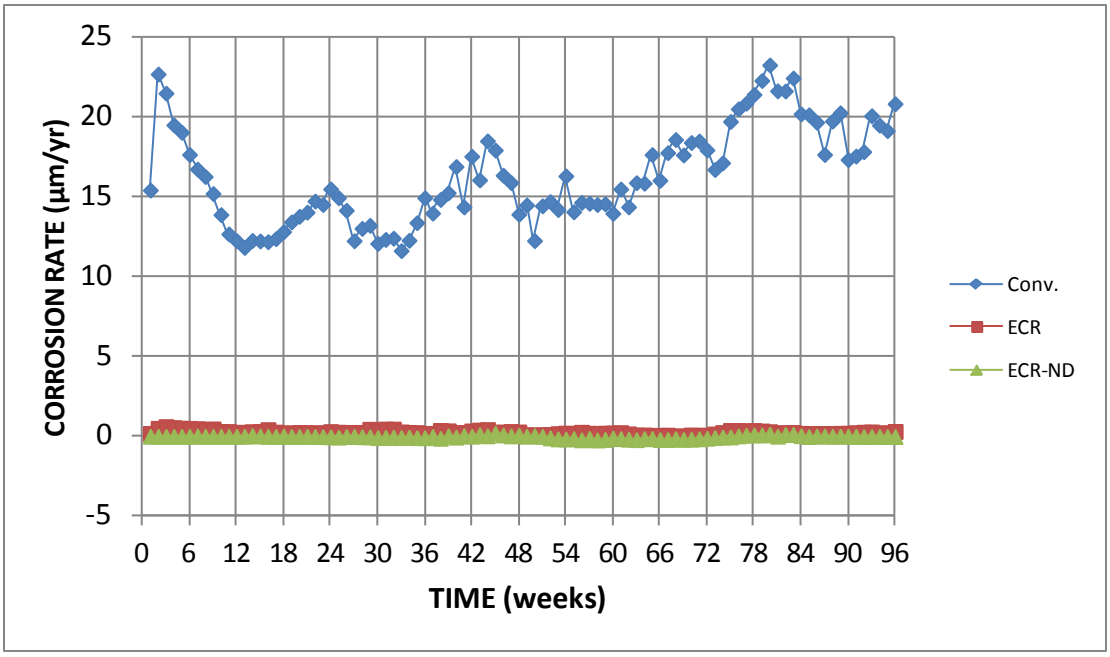

Figure 62a: Average corrosion rates of conventional, ECR, and undamaged ECR cracked beam specimens

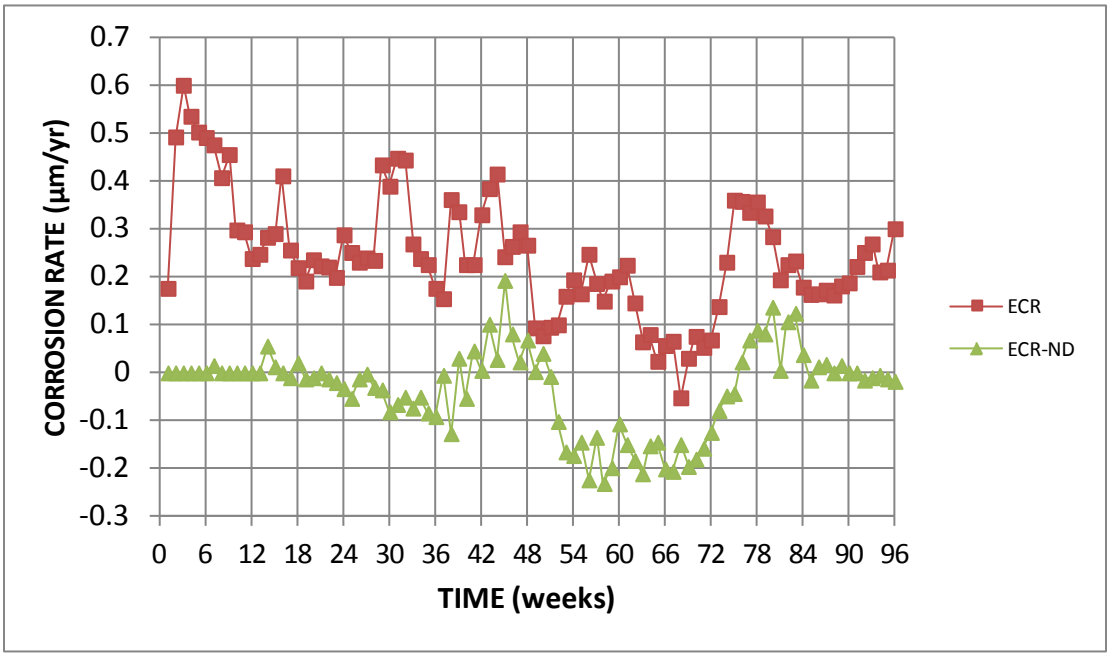

Figure 62b: Average corrosion rates of ECR and undamaged ECR cracked beam specimens (different scale)

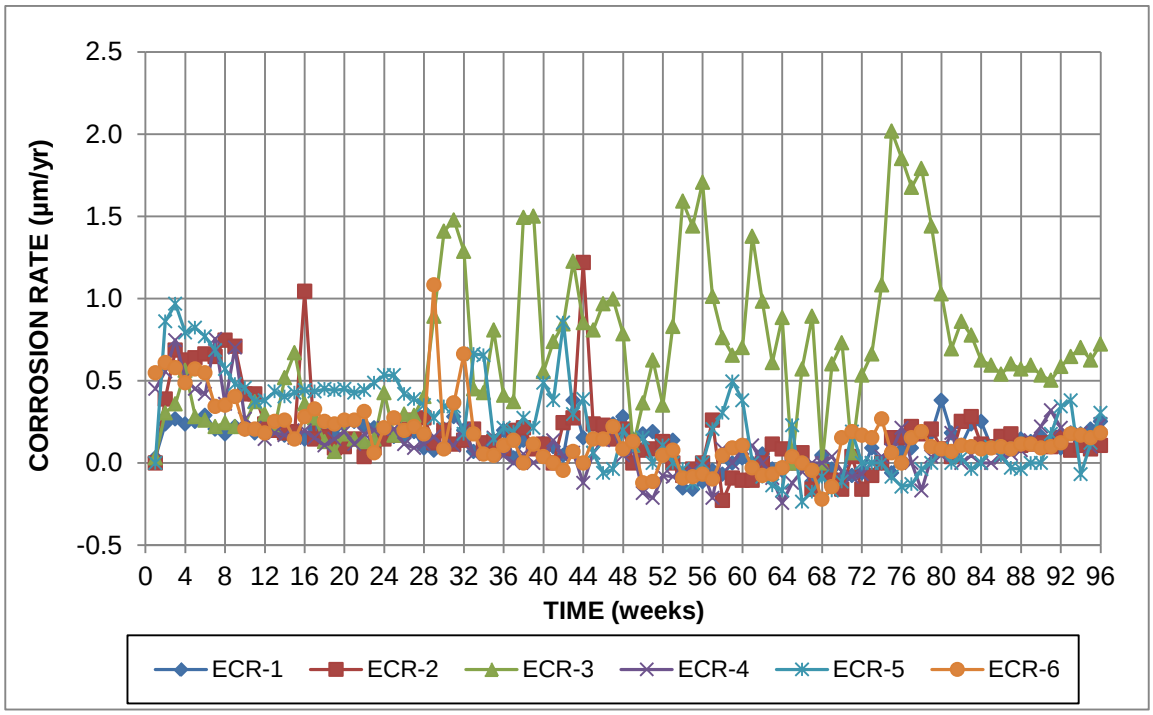

Figure 62c: Individual corrosion rates of ECR cracked beam specimens

4.2.4.2 2304 Stainless Steel

The average corrosion rates for the Southern Exposure specimens containing 2304 stainless steel are shown in Figure 63. The rates for the conventional, ECR, and ECR-ND specimens are also plotted for comparison.

The corrosion rate of the mixed Conv./2304 specimens was higher than that of the Conv. specimens suggesting galvanic corrosion. The specimens had average corrosion rates between 12 and 25 µm/yr once corrosion initiated. The mixed 2304/Conv. specimens exhibited an average corrosion rate around zero for most of the test with the exception of weeks 80-87 with average corrosion rates between 0.3 to 0.5 µm/yr (Figure 63b). As shown in Figure 63b, the average corrosion rates of the 2304 specimens are nearly equal to that of the ECR-ND specimens until week 84 when the 2304 average corrosion rate increased to approximately 0.1 µm/yr.

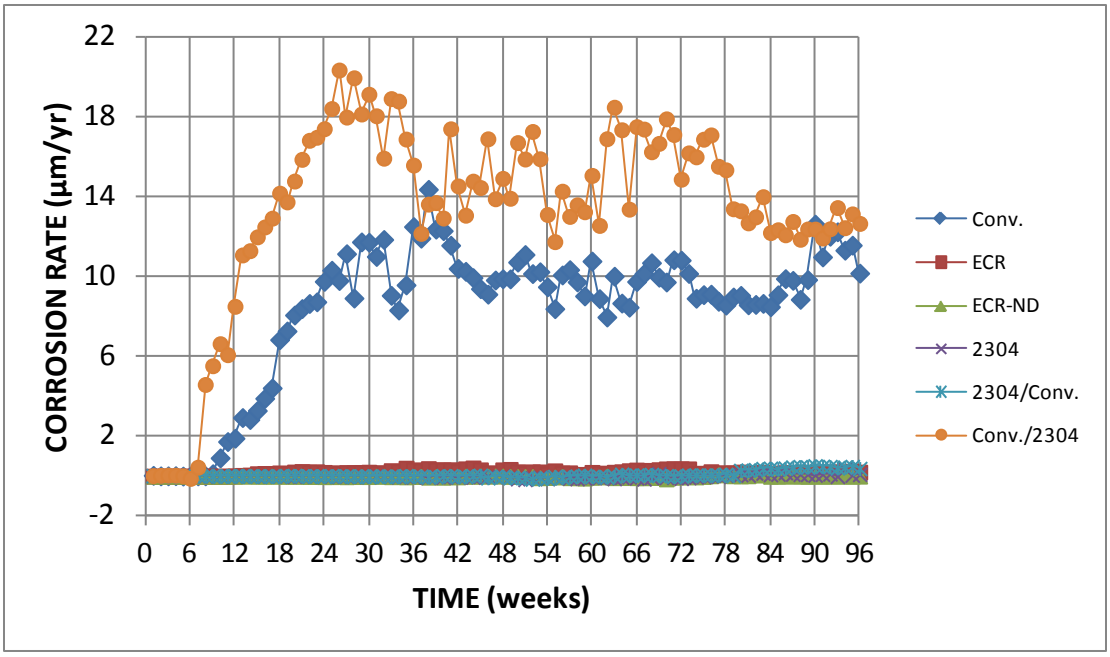

Figure 63a: Average corrosion rates of conventional, ECR, ECR-ND, 2304, mixed 2304/conventional, and mixed conventional/2304 Southern Exposure specimens

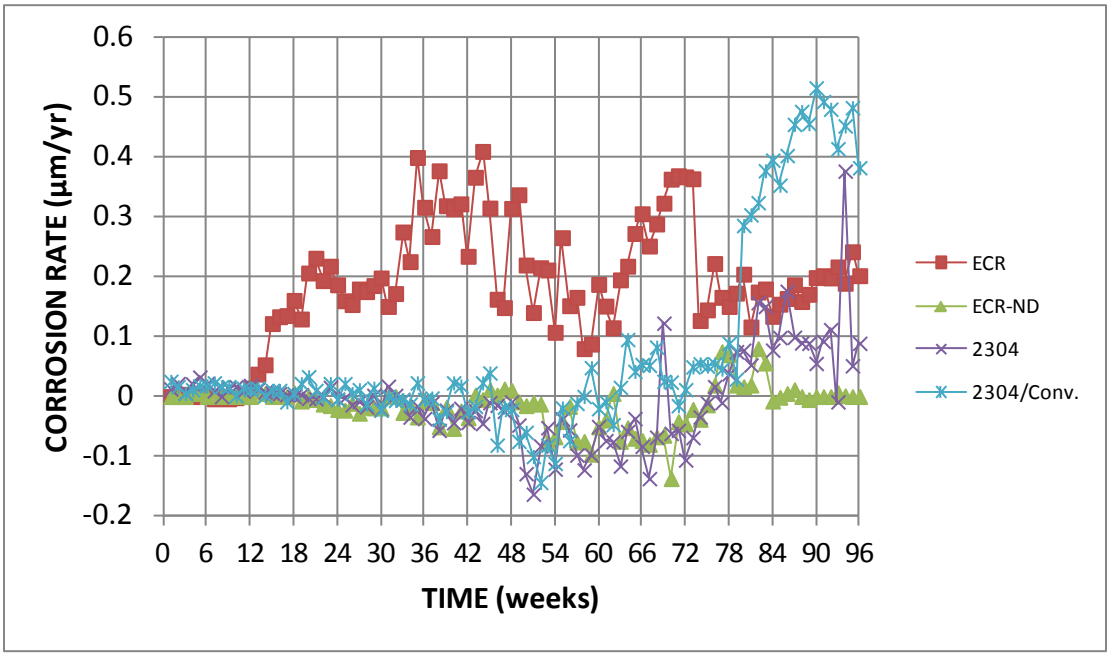

Figure 63b: Average corrosion rates of ECR, ECR-ND, 2304, and mixed 2304/conventional Southern Exposure specimens (different scale)

The individual corrosion rates for the Southern Exposure 2304 stainless steel specimens are shown in Figure 64. All specimens exhibited corrosion rates close to zero for most of the test. However, at week 75 specimen 2 started to exhibit increasingly higher corrosion rates, reaching a maximum of 1.17 µm/yr during the 96-week test. Specimen 3 initiated corrosion at week 96, just prior to autopsy. To gain additional data, the test for specimens 4, 5, and 6 were

extended past 96 weeks. Specimen 5 initiated corrosion at week 98 and has exceeded specimen 2 with a maximum corrosion rate of 3.65 µm/yr at week 114. Specimen 6 initiated corrosion at week 116 with a maximum corrosion rate of 1.53 µm/yr at week 119. Testing on specimens 4, 5, and 6 will continue through 144 weeks.

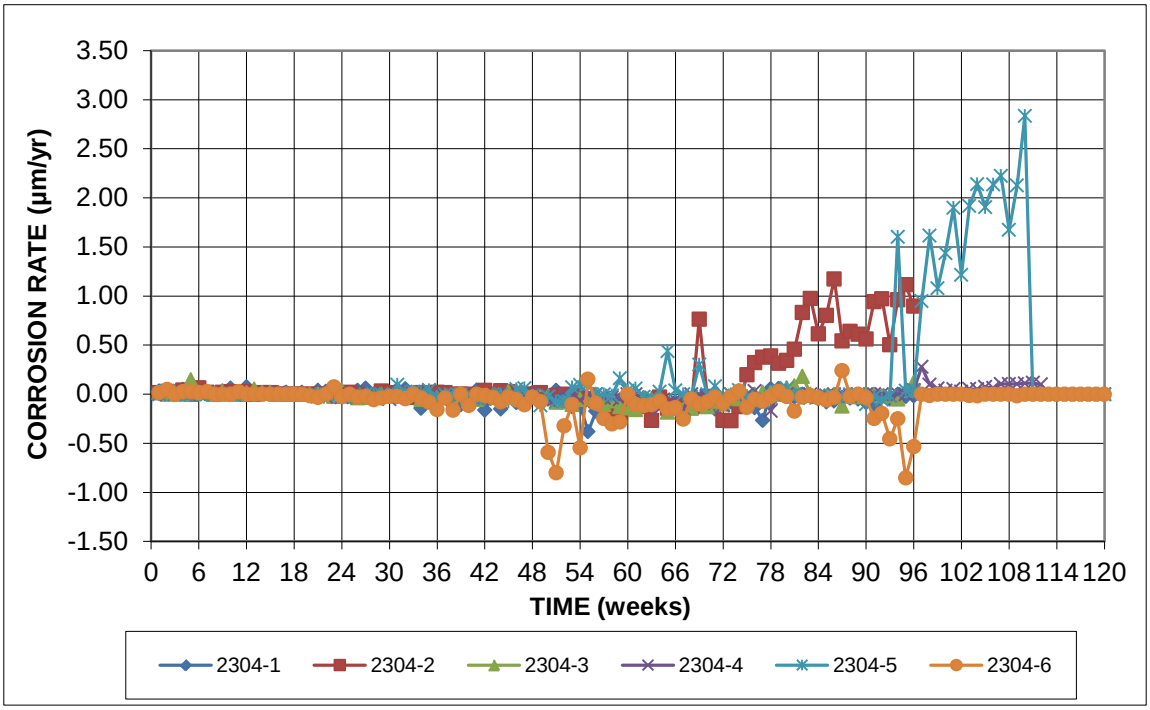

Figure 64: Individual corrosion rates for 2304 stainless steel Southern Exposure specimens

Specimens 2, 3, 5, and 6 initiated corrosion at weeks 75, 96, 98, and 116, respectively. Figures 65a and 65b show specimen 2 after autopsy. Both the top and bottom bars show signs of corrosion near the ends. Specimens 4, 5, and 6 are still undergoing testing and have not been autopsied.

Figure 65a: Top bars of specimen SE-2304-2 after autopsy showing signs of corrosion near the end of the bar

Figure 65b: Bottom bars of specimen SE-2304-2 after autopsy showing signs of corrosion near the end of the bar

The average corrosion rates of the cracked beam specimens containing 2304 stainless steel are shown in Figure 66. ASTM A955 stipulates that for a stainless steel to pass this test, the average corrosion rate must not exceed 0.20 µm/yr through 75 weeks. As can be seen in Figure 66b, the average corrosion rate for the cracked beam 2304 stainless steel specimens exceeded the limit at weeks 4, 37-39, 44-46, and 52 through the end of the test. At the end of the test, the average corrosion rate reached a maximum value of 3.16 µm/yr.

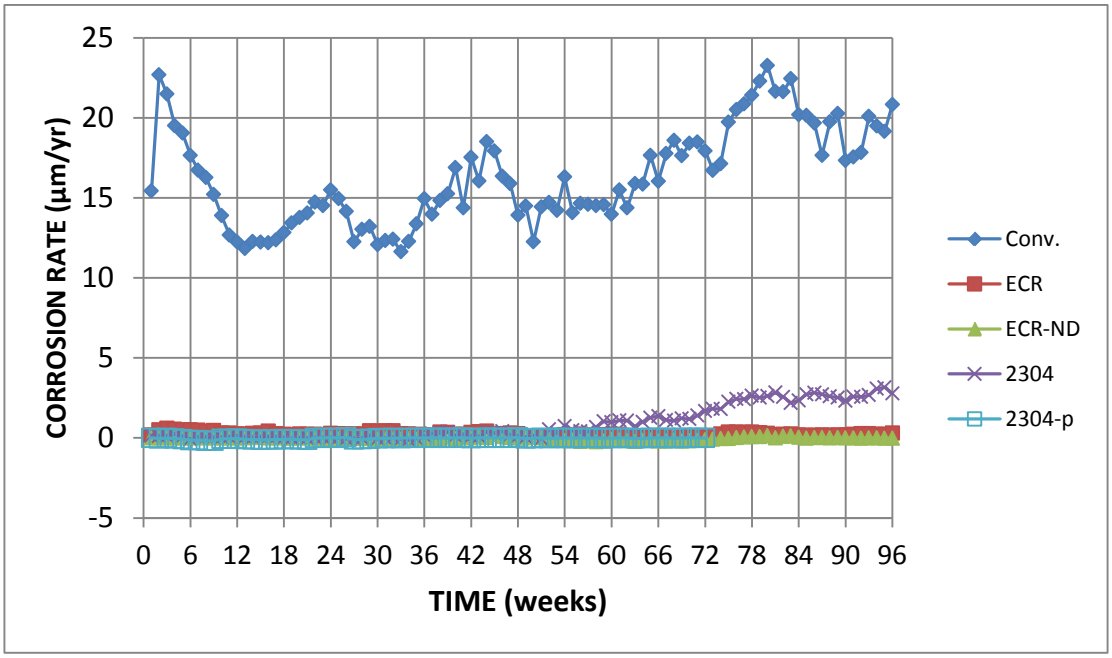

Figure 66a: Average corrosion rate (µm/yr) of cracked beam specimens containing conventional, ECR with ten holes in the coating, undamaged ECR, and 2304 stainless steel

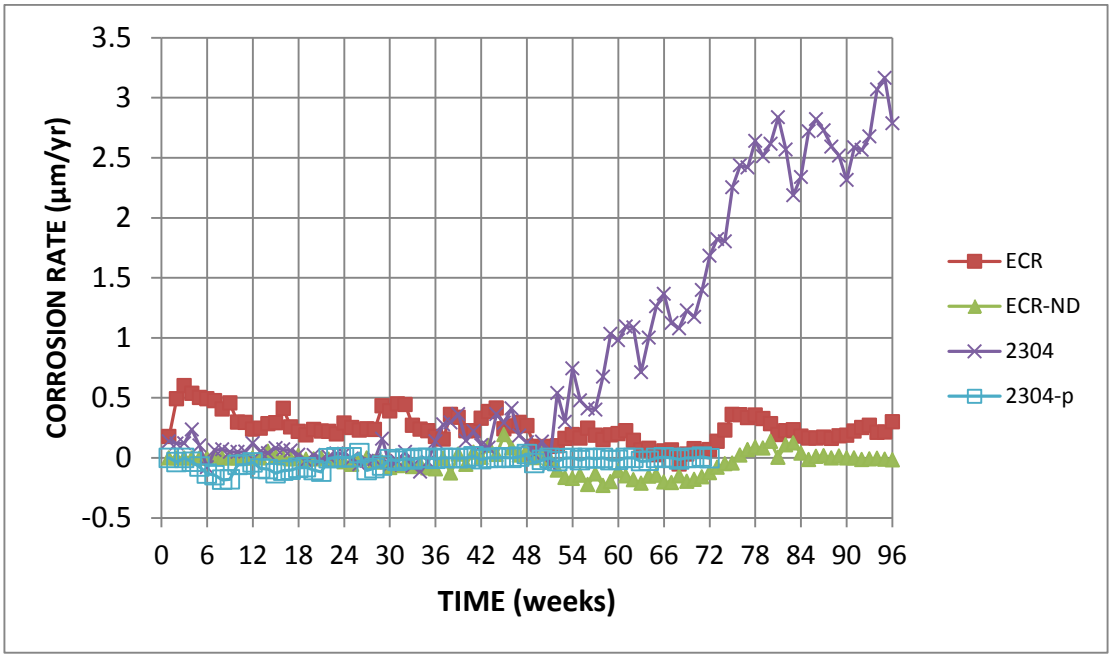

Figure 66b: Average corrosion rate (µm/yr) of cracked beam specimens containing conventional, ECR with ten holes in the coating, undamaged ECR, and 2304 stainless steel (different scale)

In addition to the limit on average corrosion rate, ASTM A955 specifies that individual stainless steel cracked beam specimens must have corrosion rates no greater than 0.5 µm/yr through 75 weeks. The individual corrosion rates for the cracked beam specimens with 2304 stainless steel are shown in Figure 67. As can be seen, all six of the 2304 specimens exceeded the maximum allowable corrosion rate of 0.5 µm/yr one or more times during the first 75 weeks

of the test. Five of the specimens continued to exhibit a corrosion rate of 0.5 µm/yr or higher after week 75. Specimen 2304-1 exhibited corrosion rates exceeding 0.5 µm/yr during weeks 4, 5, 7, 8, 12, 15, 17, and 52-96 while specimen 2304-2 exhibited rates exceeding 0.5 µm/yr during weeks 4, 5, 29, 36-48, 50-51, 66-67, 70, and 72-96. Specimen 2304-3 exhibited a rate above 0.5 µm/yr during weeks 38, 39, 41, 44-46, and 90-96. Specimen 2304-4 exhibited a rate above 0.5 µm/yr during weeks 57-62, 64-71, and 73-96. Specimen 2304-5 exhibited a rate above 0.5 µm/yr during weeks 52-96, and Specimen 2304-6 exhibited a rate above 0.5 µm/yr during weeks 75-96.

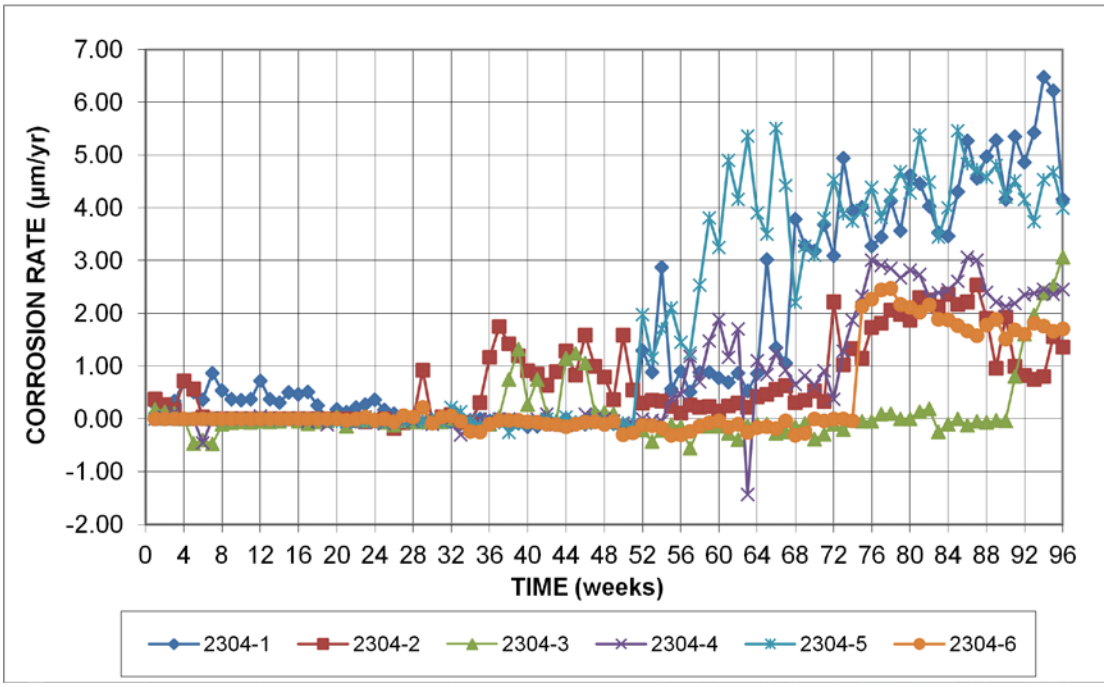

Figure 67: Individual corrosion rates (µm/yr) based on total area for cracked beam specimens with 2304 reinforcement

Due to both the mottled appearance and the poor performance of the 2304 stainless steel, the 2304 stainless steel was repickled and a new set of cracked beam tests was initiated. This test is in week 72 of the 96 week test. These cracked beam tests will not be completed by the end of the project, but they demonstrate the importance of properly pickling stainless steel reinforcement. Figure 68 shows the corrosion rates for the tests to date. The repickled 2304 specimens are exhibiting lower corrosion rates than the as-received 2304 specimens at the same age. All corrosion rates are below 0.20 µm/yr, which is well within the limit set by ASTM A955.

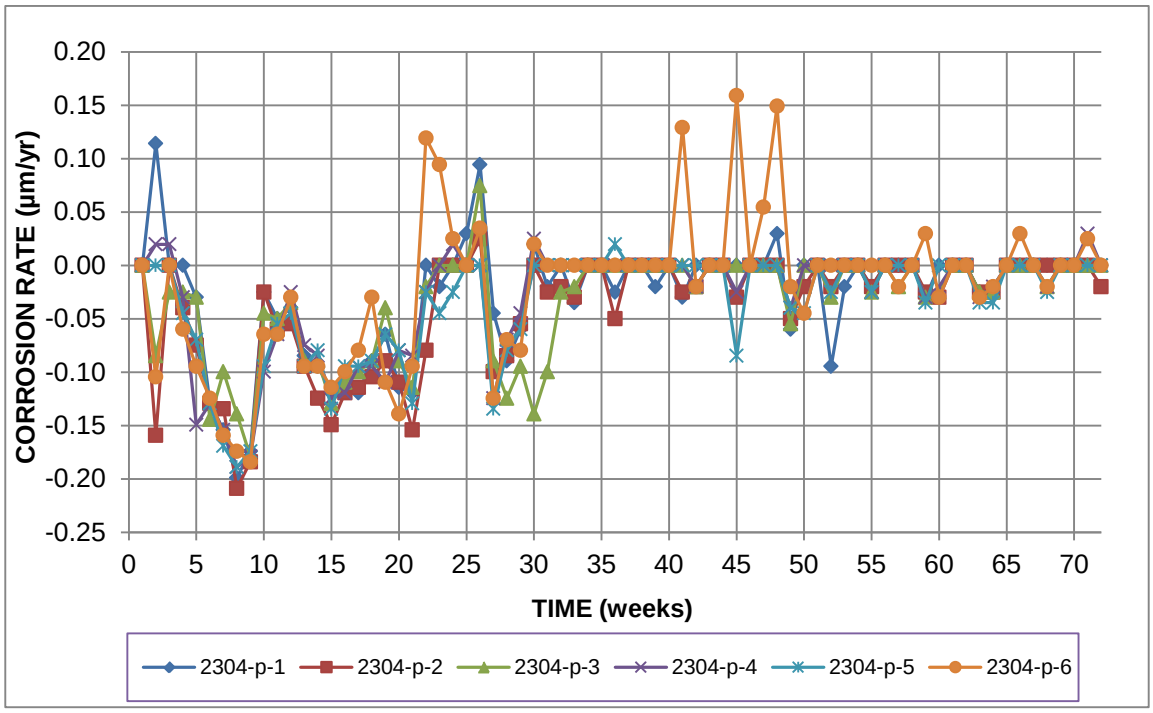

Figure 68: Individual corrosion rates (µm/yr) based on total area for cracked beam specimens with repickled 2304 duplex stainless steel reinforcement

To assess the potential for galvanic effects, specimens containing mats of both conventional and 2304 stainless steel reinforcement were tested. The 2304 stainless steel used in the mixed tests was tested in the as-received condition. Three specimens were tested with 2304 stainless steel as the anode and conventional reinforcement as the cathode, and three specimens were tested with conventional reinforcement as the anode and 2304 stainless steel as the cathode.

The average corrosion rates for these six specimens are shown in Figure 69a and 69b, with Conv. and 2304 averages shown for comparison. Individual corrosion rates are shown in Figures 69c and 69d. As shown in Figure 69a, the average corrosion rate of the Conv./2304 specimens is higher than that of conventional reinforcement alone, suggesting that galvanic corrosion may have played a role in the corrosion performance of the specimens. As shown in Figure 69b, the 2304/Conv. specimens had corrosion rates that were generally similar to those of the 2304 specimens for much of the test. The lack of an accelerated corrosion rate on the specimens with 2304 stainless steel as the anode suggests that there is not a galvanic corrosion effect altering the performance of the stainless steel. The 2304/Conv. specimens did show a greater corrosion rate than 2304 alone after week 80. Both SE-2304/Conv.-2 and SE-2304/Conv.-3 initiated corrosion, with specimen 2 reaching corrosion rates up to 1.20 µm/yr (Figure 69d)

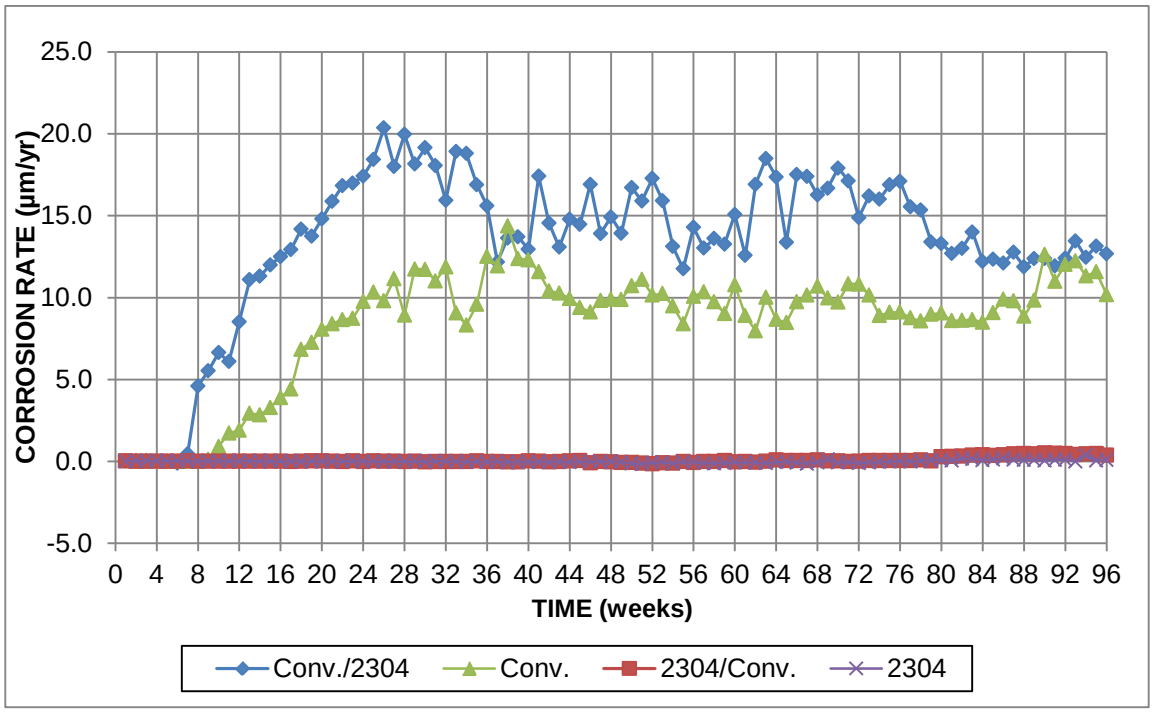

Figure 69a: Average corrosion rates of conventional/2304 stainless steel (anode/cathode) Southern Exposure specimens

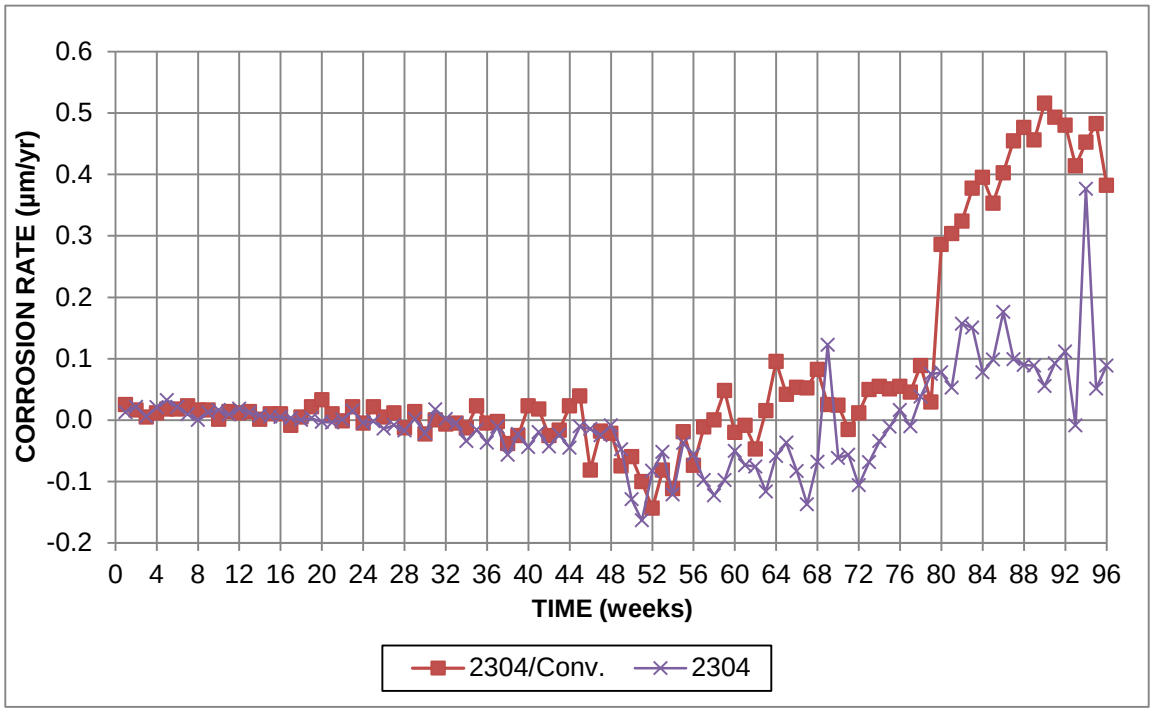

Figure 69b: Average corrosion rates of 2304/conventional (anode/cathode) Southern Exposure specimens

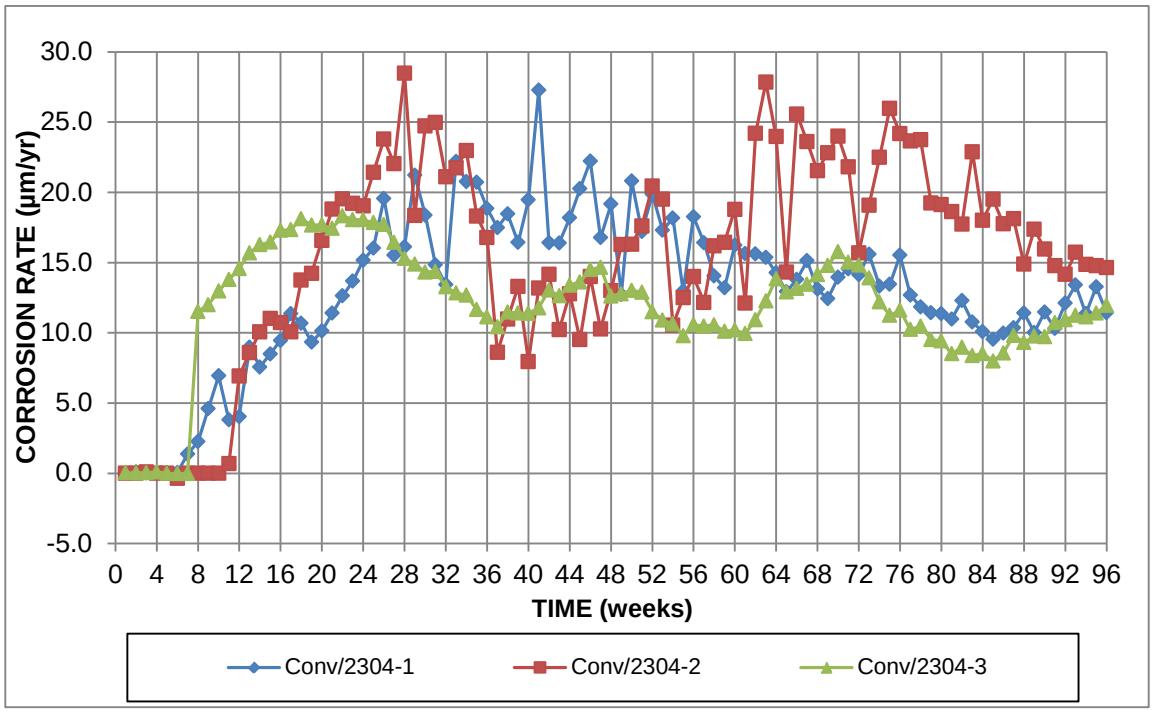

Figure 69c: Individual corrosion rates of conventional/2304 stainless steel (anode/cathode) Southern Exposure specimens

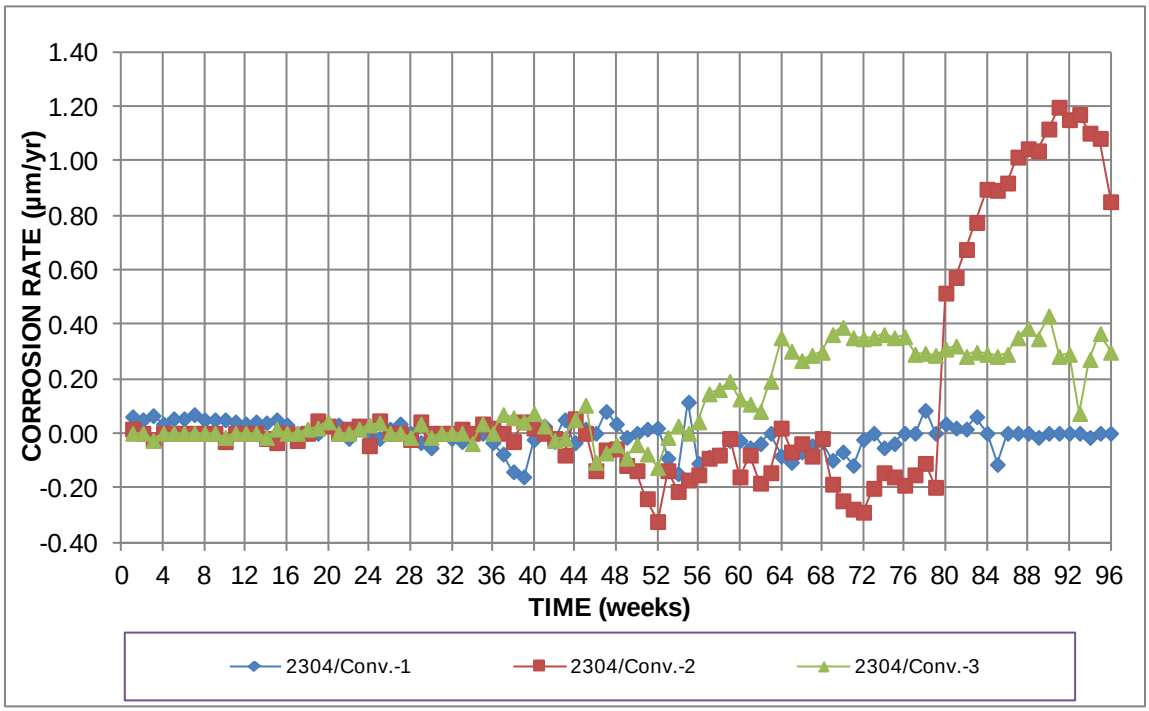

Figure 69d: Individual corrosion rates of 2304 stainless steel/conventional (anode/cathode) Southern Exposure specimens

Corrosion products were seen near the ends of the top bars of two of the SE-2304/Conv. specimens (Figure 70). Corrosion products were also seen on one SE-2304/Conv specimen on

the conventional bars near the ends as shown in Figure 71. One specimen with conventional bars as the anode (SE-Conv/2304-1) showed corrosion near the end of the 2304 cathode bars, as shown in Figure 72. Corrosion products were also observed on cathode bars of specimen SE-Conv/2304-2 (Figure 73), indicating that salt may have reached the bar via the electrical connection.

Figure 70: Corrosion product on 2304 stainless steel anode bar in 2304/Conv. Southern Exposure specimen 2 after autopsy

Figure 71: Corrosion on conventional cathode bar in 2304/Conv. Southern Exposure specimen 1 after autopsy

Figure 72: Cathode of 2304 stainless steel, mixed conventional/2304 steel Southern Exposure specimen 1 after autopsy

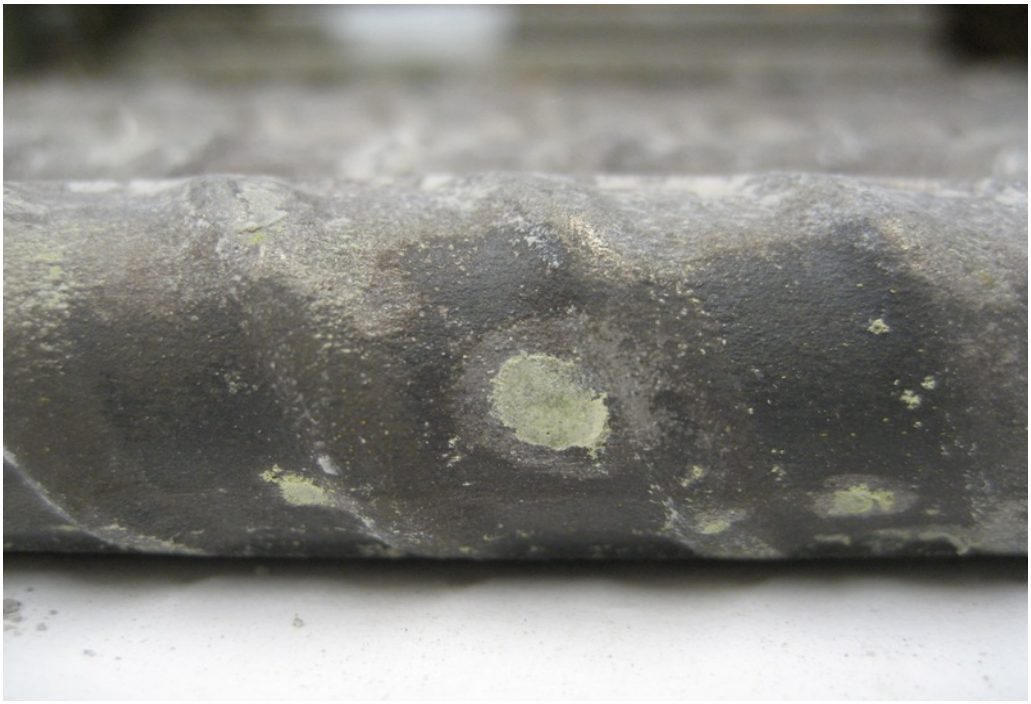

Figure 73: Corrosion product on 2304 stainless steel cathode bar in mixed Conv./2304 Southern Exposure specimen 2 after autopsy

4.2.4.3 NX-SCR™ stainless steel clad reinforcement

The average corrosion rates for the specimens containing NX-SCR™ stainless steel clad reinforcement (SSClad) are shown in Figures 74a and 74b. The results for the control specimens, conventional, ECR, and ECR-ND, are also shown for comparison.

The mixed Conv./SSClad specimens exhibited an average corrosion rate is similar to that of conventional steel.

Some SSClad bars (SSClad-4h) had conventional steel exposed at the holes drilled through the cladding. These specimens exhibited average corrosion rates between 0.1 and 0.5 µm/yr for the majority of the test (Figure 74b). During weeks 50-59 the average corrosion rate increased and reached a maximum of approximately 2 µm/yr. With the exception of these weeks, the average corrosion rate experienced by the SSClad specimens was similar to that of the ECR average corrosion rate.

The average corrosion rates of the undamaged and bent stainless steel clad specimens fluctuated around zero for the duration of the test. This seemingly "negative" corrosion has been discussed previously.

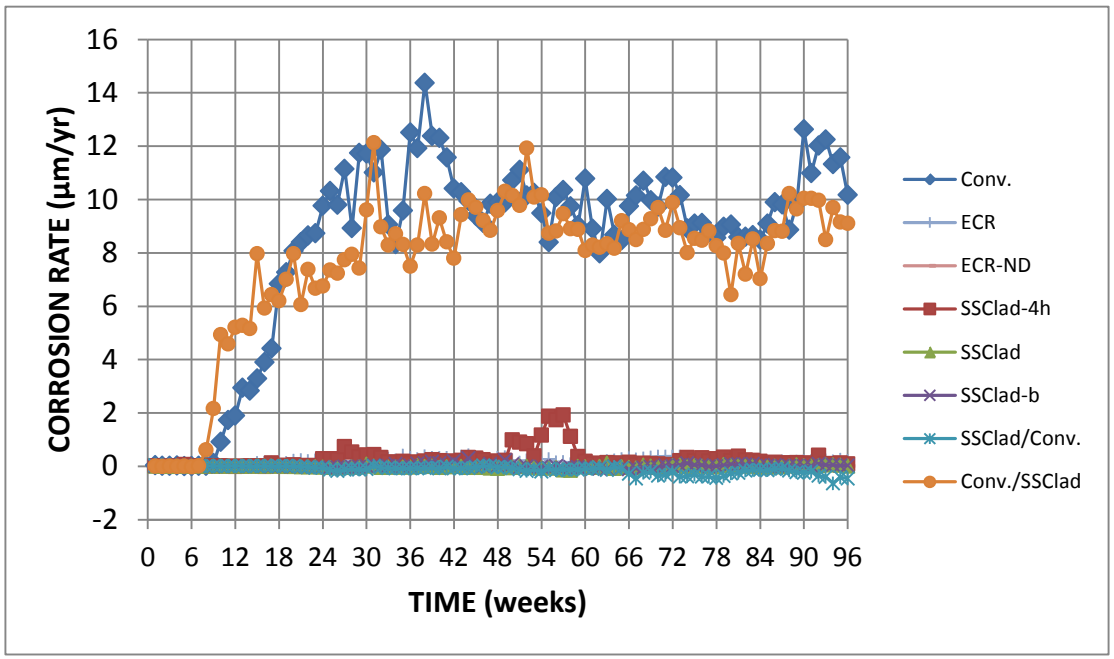

Figure 74a: Average corrosion rate of conventional, ECR, undamaged ECR, stainless steel clad, stainless steel clad with four holes through the cladding, bent stainless steel clad, mixed stainless steel clad/conventional, and mixed conventional/stainless steel clad Southern Exposure specimens

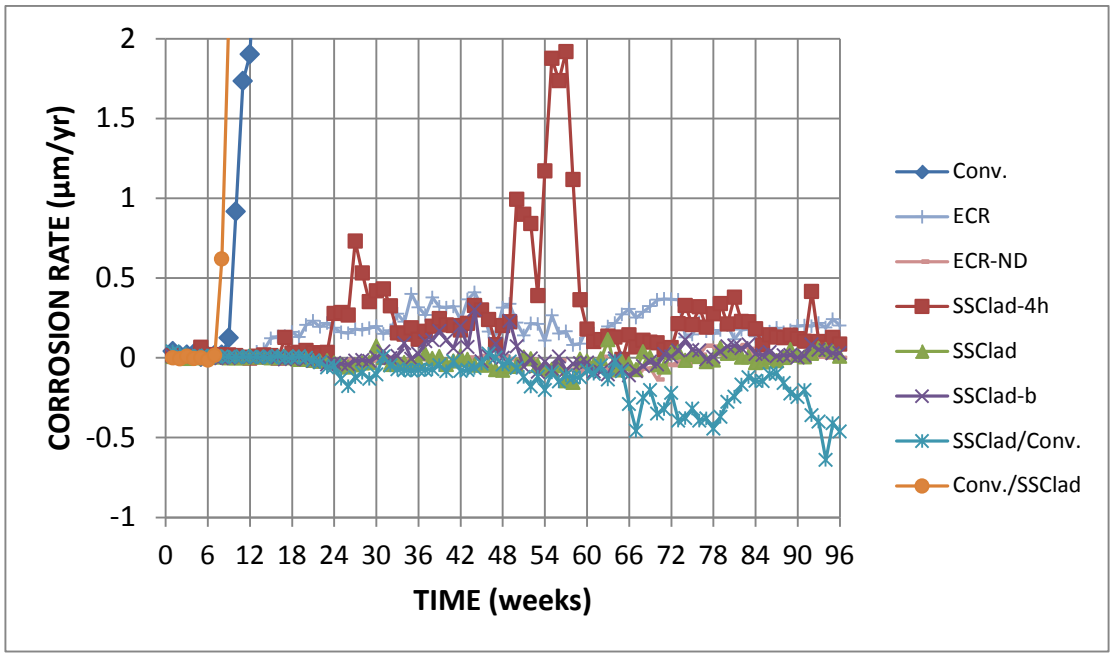

Figure 74b: Average corrosion rate of conventional, ECR, undamaged ECR, stainless steel clad, stainless steel clad with four holes through the cladding, bent stainless steel clad, mixed stainless steel clad/conventional, and mixed conventional/stainless steel clad Southern Exposure specimens (different scale)

Figure 75 shows the average corrosion rate for the cracked beam specimens containing stainless steel clad reinforcement. Plots for the control specimens are added for comparison. As discussed earlier, ASTM A955 that the average corrosion rate of stainless steel reinforcement must not exceed 0.20 µm/yr. The average corrosion rate for the SSClad specimens exceeded the 0.2 µm/yr limit during weeks 62-63 but remained below the limit for the remainder of the test. This failure is due to the corrosion of a single specimen (SSClad-1), discussed next.

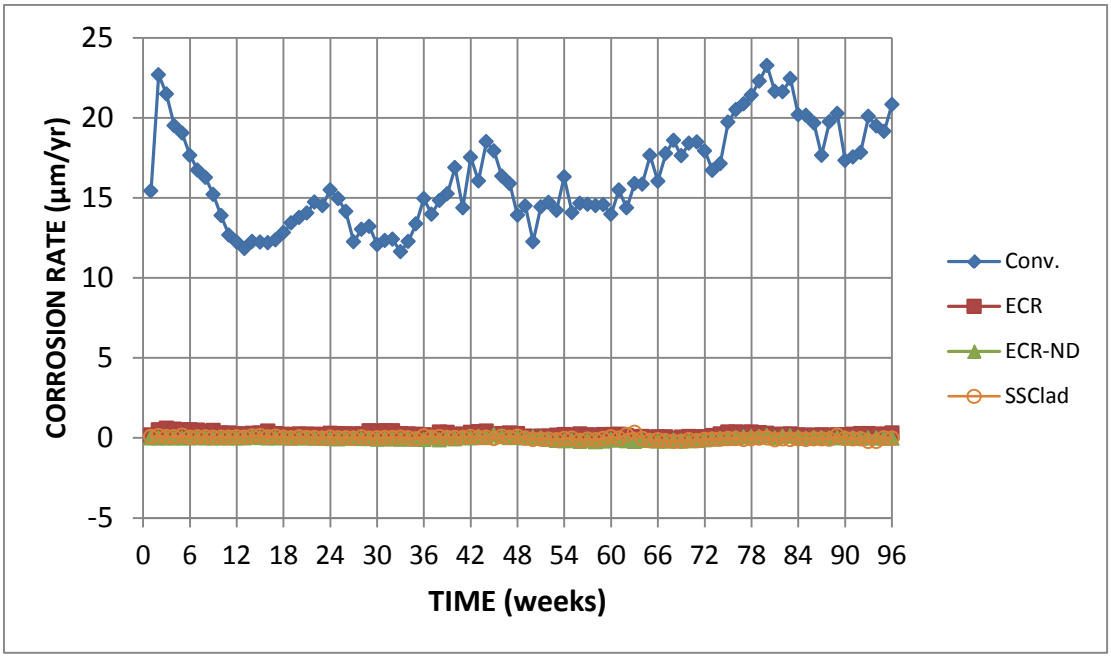

Figure 75a: Average corrosion rate of cracked beam specimens containing conventional reinforcement, epoxy coated reinforcement, undamaged epoxy coated reinforcement, and undamaged stainless steel clad reinforcement

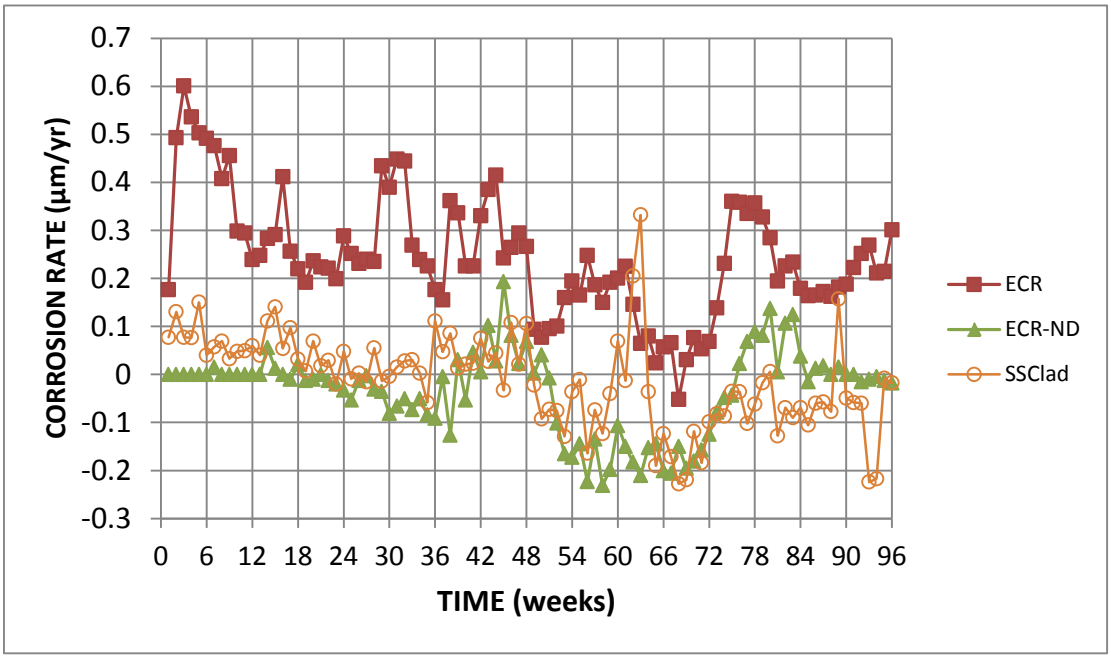

Figure 75b: Average corrosion rate of cracked beam specimens containing conventional reinforcement, epoxy coated reinforcement, undamaged epoxy coated reinforcement, and undamaged stainless steel clad reinforcement (different scale)

The corrosion rates for the individual cracked beam specimens with stainless steel clad reinforcement are shown in Figure 76. Specimen SSClad-1 exhibited a corrosion rate greater

than 0.5 µm/yr during weeks 5, 15, and 61-63. SSClad-2 had a corrosion rate exceeding 0.5 µm/yr during week 48, as did specimen SSClad-3 during weeks 36 and 37 and specimen 6 at week 89. Specimen SSClad-4 had shown corrosion rates exceeding 0.5 µm/yr during weeks 27 through 30. However, upon investigation and replacement of the anode electrical connection at the terminal box at week 31, corrosion rates for specimen SSClad-4 dropped to values near zero, and the rates exhibited during weeks 27-30 should be considered invalid. Other specimens in this series had generally lower corrosion rates throughout testing, although Specimen SSClad-1 had a significant increase in corrosion rate during weeks 61-63. The connections were checked and no damage was detected. Upon completion of the test, the specimen was disconnected and autopsied. Corrosion products were found on the ribs (Figure 77a) and at the end of the specimen (Figure 77b). Corrosion products were also observed on the ends of specimens 4 and 6, suggesting some of the spikes in corrosion rate were from corrosion at the electrical connection. However, the corrosion products on the ribs of specimen 1 lie in a groove introduced during rolling, which served as an initiation site for corrosion. This suggests the cladding may be susceptible to corrosion if not rolled or cleaned properly, and the bars in the as-received condition do not pass ASTM A955.

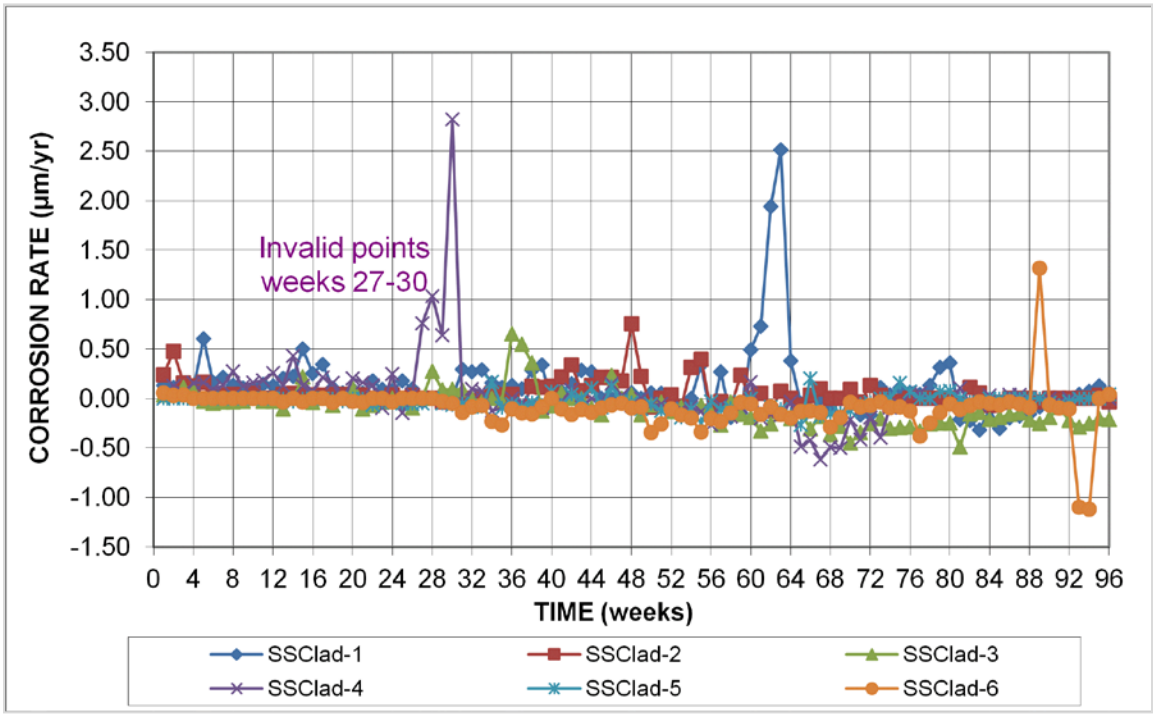

Figure 76: Individual corrosion rates (µm/yr) based on total area for cracked beam stainless steel clad reinforcement

Figure 77a: CB-SSClad-1 top bar upon completion of test showing corrosion on deformations

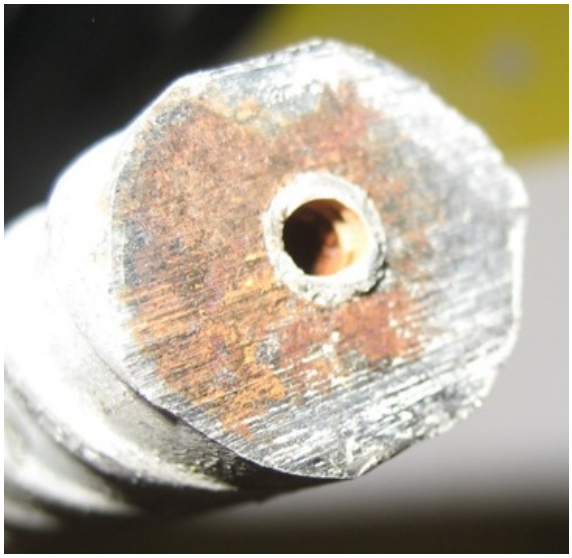

Figure 77b: Corrosion at the end of specimen CB-SSClad-1 upon completion of test

The average corrosion rate for the Southern Exposure specimens containing stainless steel clad bars with four holes in the cladding is shown in Figure 78a; individual rates are shown in Figure 78b. As shown in Figure 78a, these specimens had similar corrosion rates to specimens containing epoxy-coated bars with holes through the coating, with the exception of a jump in corrosion rate for stainless steel clad bars with four holes in the coating during weeks 24 through 32 and weeks 50 through 58. These jumps were due to the accelerated corrosion of either one or two specimens SSClad-4h-3 had an increase in corrosion rate during weeks 24 through 32 and again during weeks 50 through 58, reaching corrosion rates of over 8 µm/yr. Specimen SSClad-4h-6 experienced a spike in corrosion rate at week 40 and continued to display an increased corrosion rate for the duration of the test reaching 5.73 µm/yr at week 58. All specimens had significant corrosion products at the holes, as discussed in the Autopsy section (Figures 97a-97e). In comparison, no individual ECR specimen experienced a corrosion rate above 2.02 µm/yr (Figure 62c).

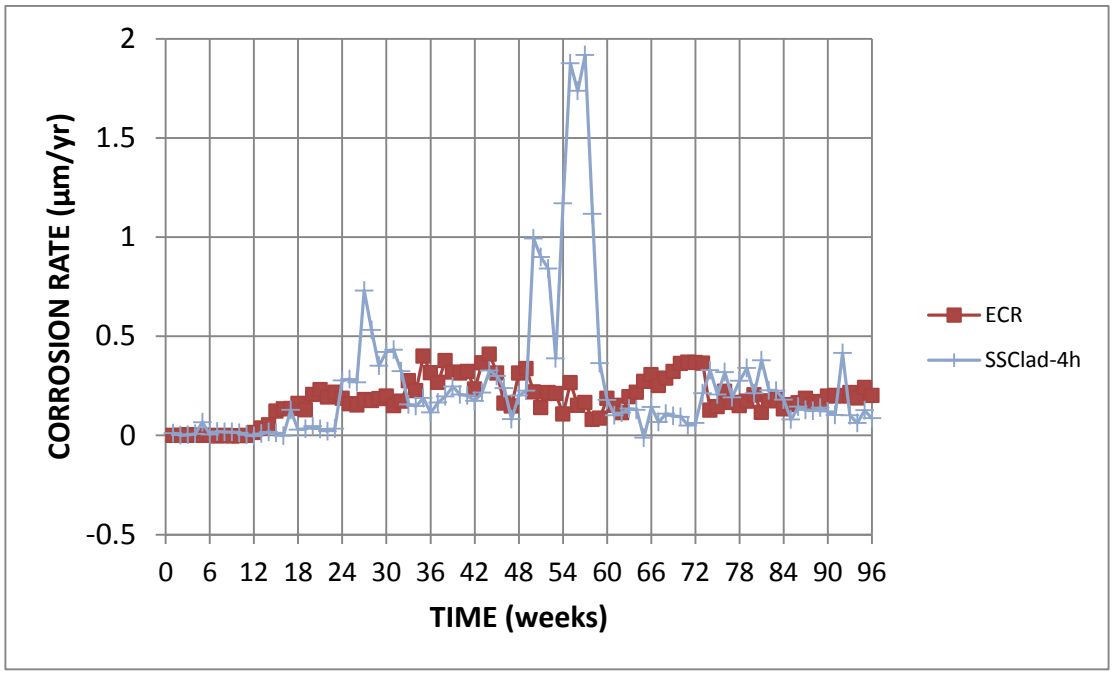

Figure 78a: Average corrosion rates for Southern Exposure specimens containing NX-SCR™ stainless steel clad bar with four holes through the cladding and ECR

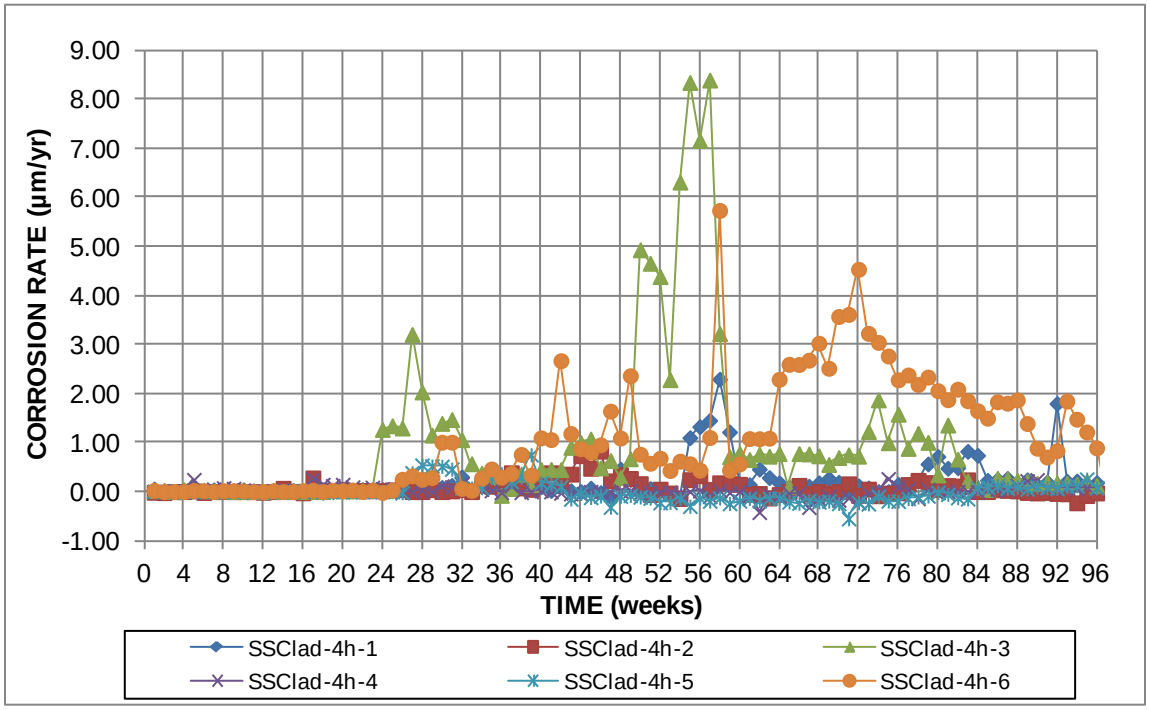

Figure 78b: Individual corrosion rates for Southern Exposure specimens containing NX-SCR™ stainless steel clad bar with four holes through the cladding

The corrosion rates for the individual bent NX-SCR™ stainless steel clad (SSClad) Southern Exposure specimens are shown in Figure 79. For most specimens, the individual corrosion rates remained near zero. However, specimens SSClad-b-2 and SSClad-b-3 initiated corrosion at weeks 36 and 71, respectively. The highest corrosion rate was experienced by SSClad-b-2, reaching 2 µm/yr at week 44. Although no visible penetration of the cladding was noted at the time of bending, the transverse ribs were visibly flattened by the rolling pin, and both specimens exhibited corrosion products at the flattened regions (Figure 80a), suggesting that the cladding was penetrated or torn during the bending operation. Other specimens did not initiate corrosion; however, the potential for damage indicates clad reinforcement should be fabricated using the same precautions used for ECR. Corrosion products were also observed on the end of the conventional core of one cathode bar of SSClad-b-2 (Figure 80b). This would tend to slightly decrease the measured macrocell corrosion rate of the specimen.

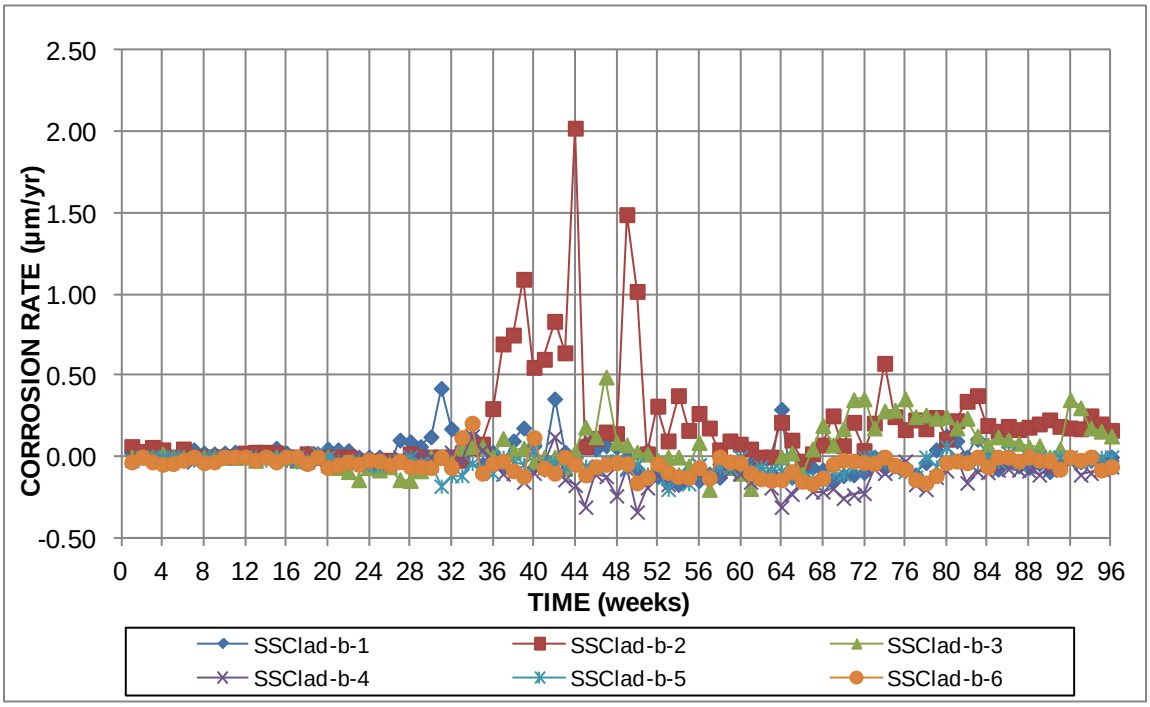

Figure 79: Individual corrosion rates of bent NX-SCR™ stainless steel clad Southern Exposure specimens

Figure 80a: Corrosion staining on SSClad-b-2 upon autopsy, bent NX-SCR^{TM} stainless steel clad bar (close-up)

Figure 80b: Corrosion on end of SE-SSClad-b-2 cathode bar

The average corrosion rates for the Conv./SSClad and SSClad/Conv. Southern Exposure specimens are shown in Figures 81a and 81b, respectively. The corrosion rates for individual specimens are shown in Figures 82a and 82b. As shown in Figures 81a, the specimens with conventional bars as the anode performed much like the Conv. specimens, with corrosion rates around 10 µm/yr. This suggests no galvanic effects for conventional reinforcement when paired with stainless steel clad bars. Mixed specimens with stainless steel clad bars as an anode (Figure 81b) performed similarly to specimens with clad bars as anode and cathode through week 64. The negative corrosion rate observed after week 64 suggests salt has reached the conventional steel bars in the cathode, causing them to corrode. This does not indicate a galvanic corrosion problem with the stainless steel clad bars. All individual corrosion rates (Figure 82b) remained approximately zero or negative with the exception of SSClad/Conv.-1 during weeks 64-69. No individual corrosion rate exceeded 1.25 µm/yr.

Autopsy results show no signs of corrosion on the anode bars of this specimen, suggesting minor corrosion at an electrical connection may have been the source of this corrosion.

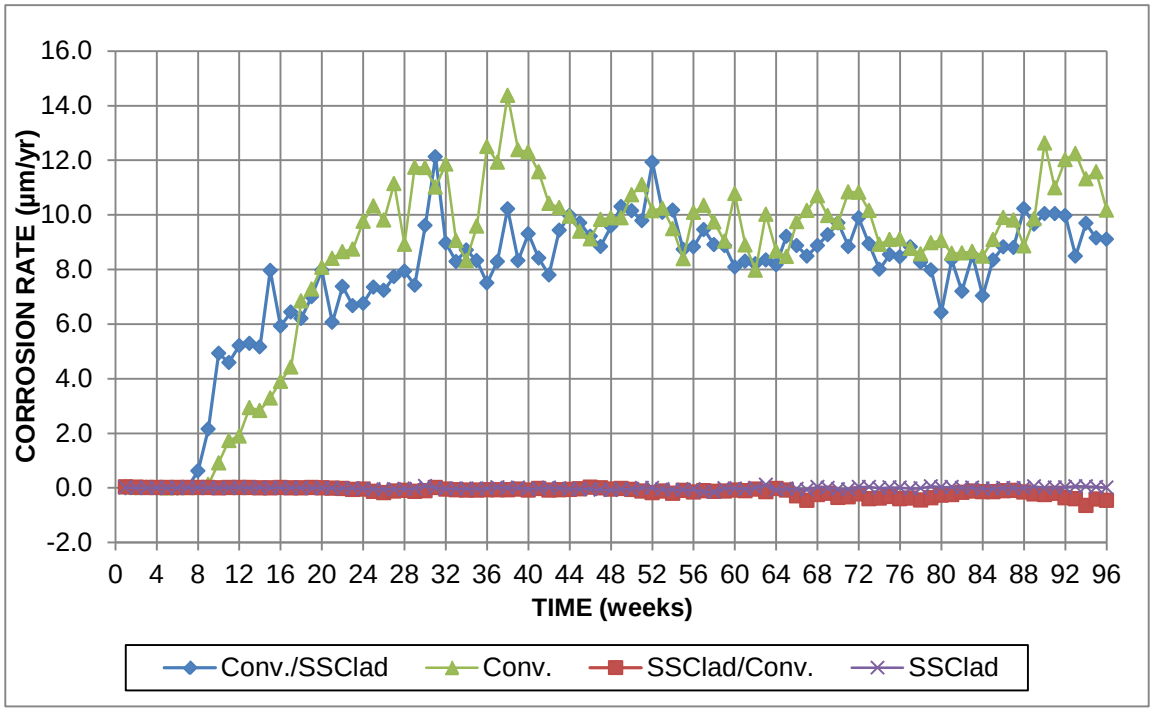

Figure 81a: Average corrosion rates of mixed Conv./NX-SCR™ stainless steel clad Southern Exposure specimens

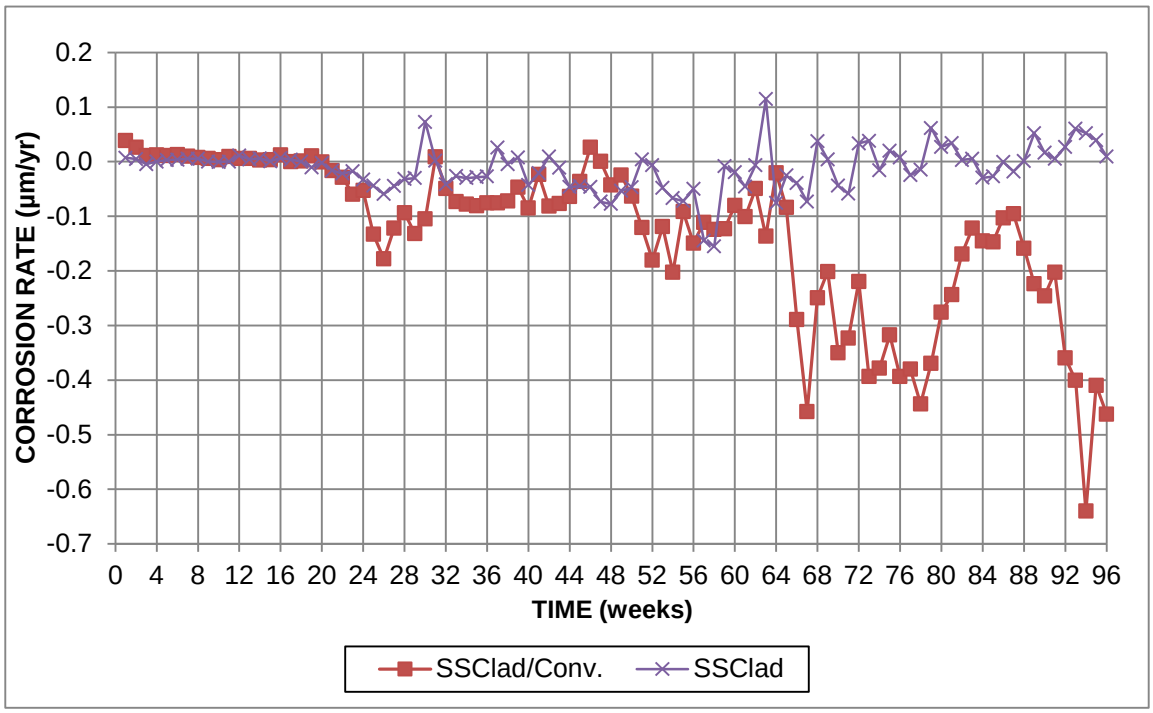

Figure 81b: Average corrosion rates of mixed NX-SCR™ stainless steel clad/Conv. Southern Exposure specimens

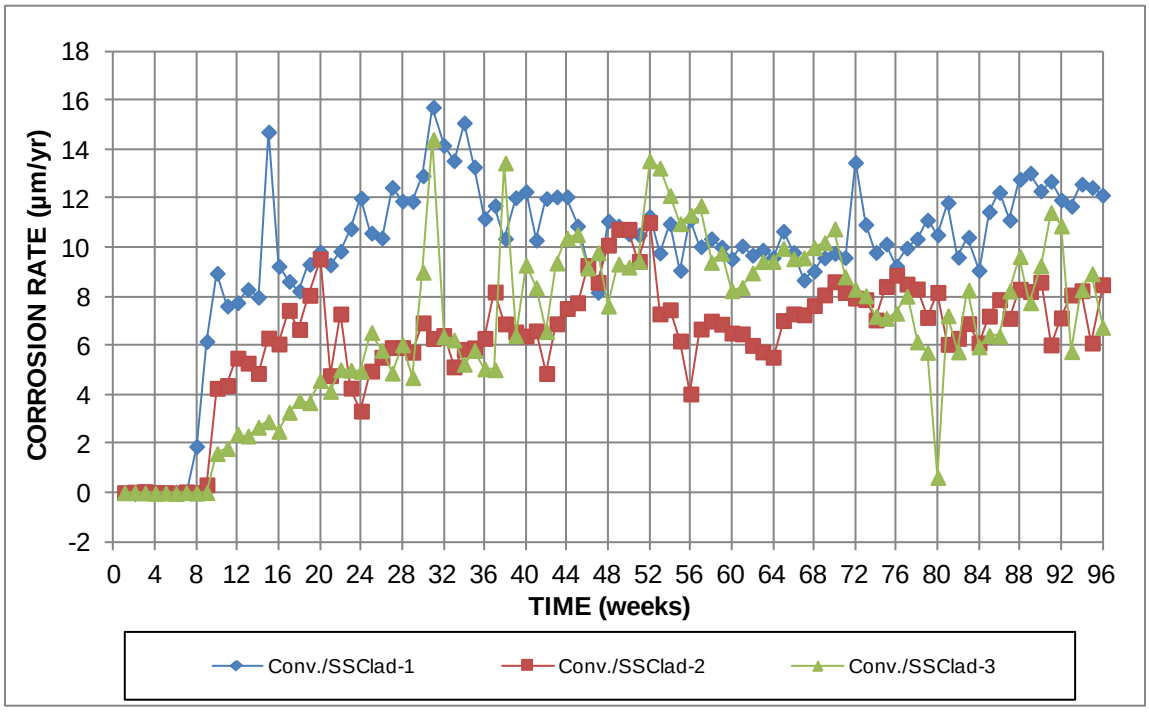

Figure 82a: Individual corrosion rates of mixed Conv./NX-SCR™ stainless steel clad (anode/cathode) Southern Exposure specimens

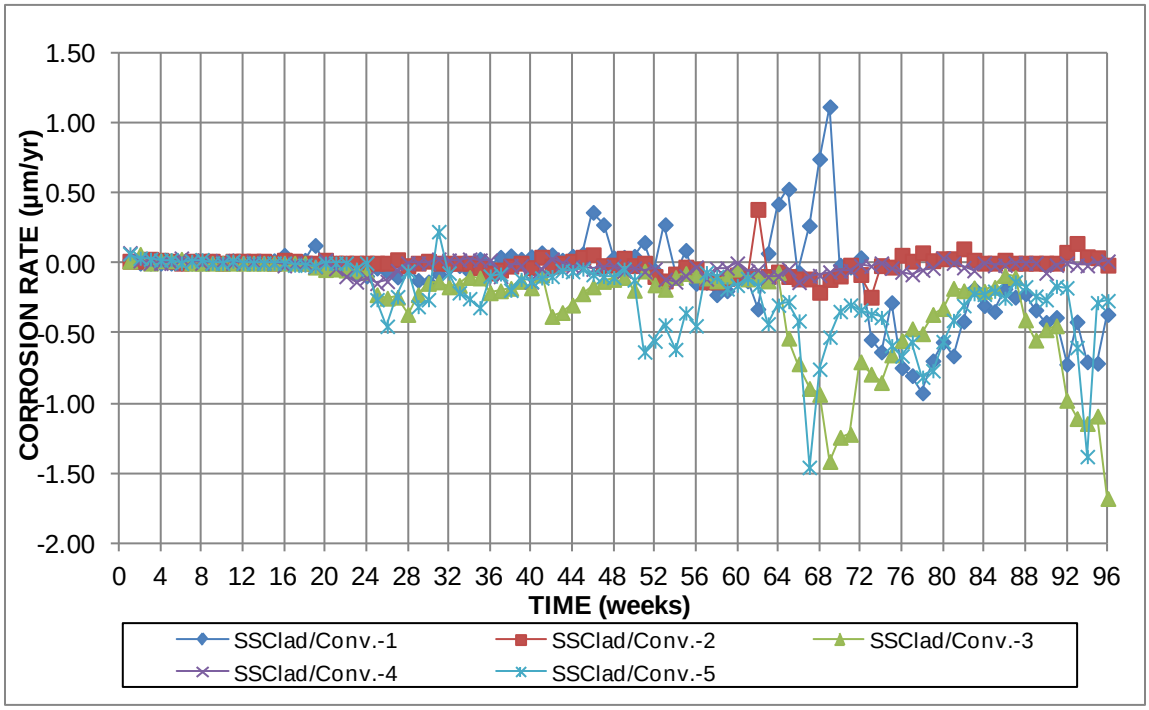

Figure 82b: Individual corrosion rate of mixed NX-SCR™ stainless steel clad/Conv. (anode/cathode) Southern Exposure specimens

4.2.5 Linear Polarization Resistance (LPR) Results

Individual and average total corrosion losses at 96 weeks, as measured by linear polarization resistance (LPR), for the Southern Exposure and cracked beam specimens are shown in Tables 11a and 11b, respectively.

The Southern Exposure specimens with conventional reinforcement had an average LPR corrosion loss of 16.6 µm (Table 11a). The Conv./SSClad specimens (conventional steel at the anode) exhibited 33 percent higher losses at 96 weeks, 22.2 µm, while the Conv./2304 specimens had 51 percent higher losses, 25.1 µm. The ECR specimens exhibited an average LPR loss of 1.05 µm. No significant losses were observed on undamaged ECR.

Among specimens with 2304 stainless steel at the anode, the mixed 2304/conv. specimens exhibited the greatest losses, 8.11 µm, followed by the 2304 specimens at 7.33 µm. Among specimens with NX-SCR^{TM} stainless steel clad bars as the anode, the specimens with holes in the cladding (SSClad-4h) had the greatest losses, averaging 2.43 µm. The SSClad-b, SSClad/Conv., and undamaged SSClad bars exhibited similar average losses, 2.17 µm, 2.24 µm, and 2.14 µm, respectively. Specimen SSClad/Conv.-1, the only SSClad/Conv. specimen to exhibit a positive macrocell corrosion rate during testing, also had the greatest total loss of the SSClad/Conv. specimens, 2.62 µm, although the loss was not significantly greater than the average for these specimens.

Table 11a: Total (LPR) Corrosion Losses (µm) at 96 Weeks for Southern Exposure Specimens

System[a]	Specimen						Average	Standard Deviation
	1	2	3	4	5	6		
Conv.	12.8	16.2	19.8	14.1	20.5	16.2	16.6	3.06
ECR	0.472	0.607	3.02	0.755	0.837	0.594	1.05	0.973
ECR-ND	0.013	0.022	0.004	-	-	-	0.013	0.009
2304	6.94	6.33	8.14	6.51	8.16	7.88	7.33	0.832
2304/Conv.	6.19	9.02	9.11	-	-	-	8.11	1.66
Conv./2304	18.8	23.0	33.6	-	-	-	25.1	7.65
SSClad-4h	2.09	2.38	2.93	1.98	2.60	2.61	2.43	0.355
SSClad	2.86	2.13	2.91	1.64	1.16	2.13	2.14	0.683
SSClad-b	2.68	1.80	1.35	1.23	2.69	3.26	2.17	0.827
SSClad/Conv.	2.62	2.50	2.34	2.29	1.47	-	2.24	0.452
Conv./SSClad	29.0	21.8	15.8	-	-	-	22.2	6.65

[a] Conv. = conventional reinforcement, ECR = epoxy-coated reinforcement with ten 1/8-in. diameter holes through the epoxy, ECR-ND= undamaged ECR, 2304 = 2304 stainless steel, SSClad-4d = stainless steel clad reinforcement with four 1/8-in. diameter holes through the cladding, SSClad = undamaged stainless steel clad reinforcement, SSClad-b = bent stainless steel clad reinforcement.

For mixed specimens, the reinforcement on the top mat is listed first.

"-" = No specimen cast in this batch.

The cracked beam specimens with conventional reinforcement exhibited an average LPR corrosion loss of 56.4 µm (Table 11b), over three times greater than the average loss observed in uncracked concrete (Table 11a). Specimens epoxy-coated bars with and without

holes in the epoxy exhibited average LPR losses of 3.71 µm and 0.093 µm, also over three times greater than the losses observed in uncracked concrete.

The stainless steel and stainless steel clad specimens also saw greater corrosion losses in cracked concrete, but not to the extent observed in the control specimens. Specimens with 2304 stainless steel exhibited a loss of 10.9 µm, and specimens with NX-SCR™ stainless steel clad bars exhibited an average loss of 2.50 µm.

Table 11b: Total (LPR) Corrosion Losses (µm) at 96 Weeks for Cracked Beam Specimens

System[a]	Specimen						Average	Standard Deviation
	1	2	3	4	5	6		
Conv.	70.7	71.3	41.6	47.8	60.1	46.8	56.4	12.8
ECR	5.76	2.08	1.32	6.41	2.67	4.03	3.71	2.05
ECR-ND	0.001	0.102	0.180	-	-	-	0.094	0.090
2304	8.77	11.1	9.19	12.4	12.3	11.7	10.9	1.58
SSClad	1.81	3.08	4.69	2.55	1.83	1.02	2.50	1.28

[a] Conv. = conventional reinforcement, ECR = epoxy-coated reinforcement with ten 1/8-in. diameter holes through the epoxy, ECR-ND= undamaged ECR, 2304 = 2304 stainless steel, SSClad = undamaged stainless steel clad reinforcement.

"-" = No specimen cast in this batch.

A comparison between macrocell and total corrosion losses for the Southern Exposure specimens is shown in Figures 83a and 83b. The results for the cracked beam specimens are shown in Figures 84a and 84b. All systems in this study show average total corrosion losses greater than macrocell losses. In the Southern Exposure test, the total losses are on average 1.12 times greater than the macrocell losses when considering all specimens (Figure 83a); removing specimens with conventional reinforcement results in a ratio of total loss to macrocell loss of 3.67 (Figure 83b). For the cracked beam test, the ratios of total to macrocell loss is 1.89 and 6.77 with (Figure 84a) and without (Figure 84b) specimens containing conventional reinforcement. This suggests that ECR and stainless steel bars see a greater percentage of local corrosion than conventional reinforcement; a result also observed in the rapid macrocell test. Also of note is that Southern Exposure specimens containing 2304 stainless steel in the as-received condition exhibited low macrocell losses, but relatively high total losses. This mirrors results seen in the rapid macrocell test.

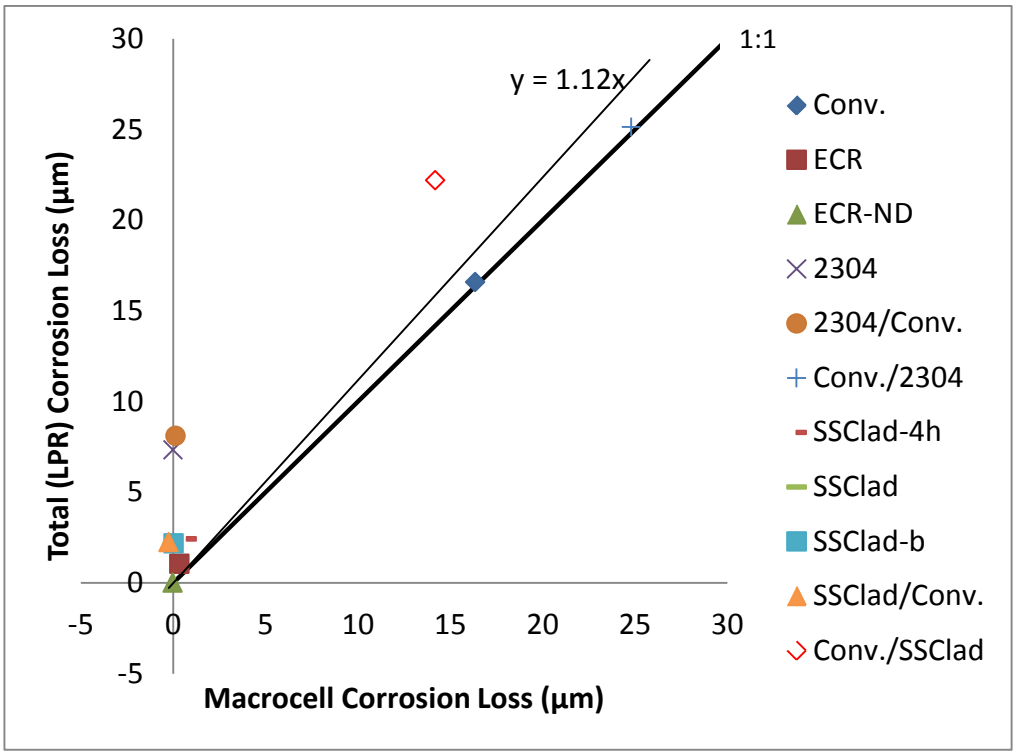

Figure 83a: Southern Exposure test-comparison between corrosion loss (µm) from macrocell and total corrosion loss readings

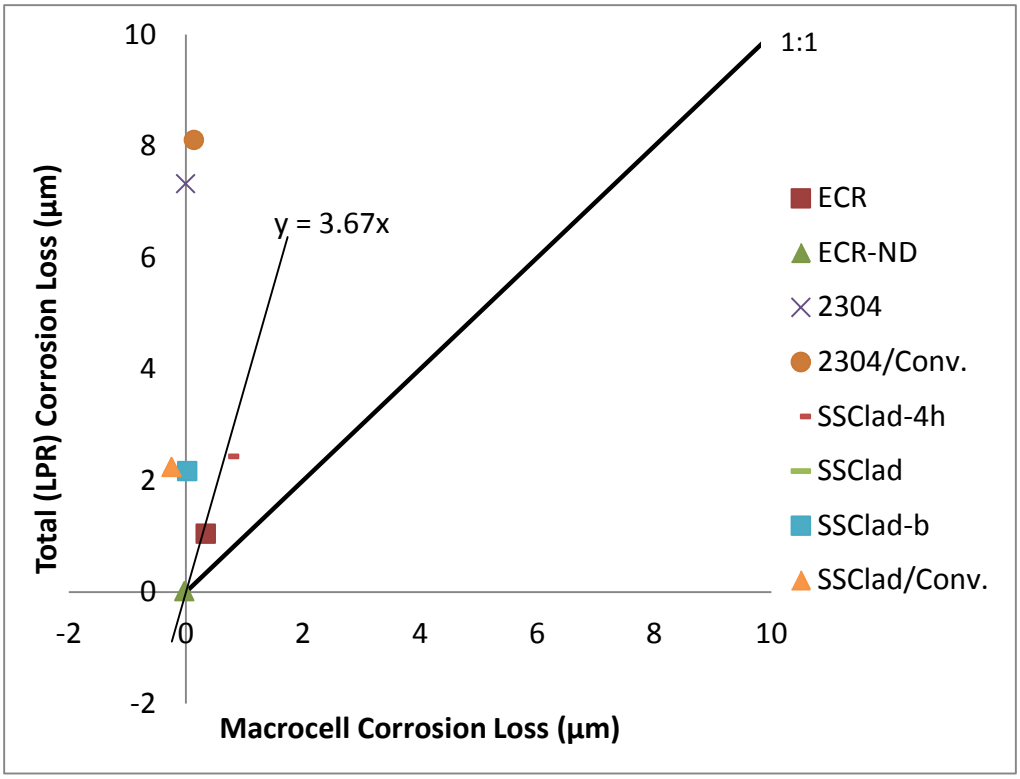

Figure 83b: Southern Exposure test-comparison between corrosion loss (µm) from macrocell and total corrosion loss readings

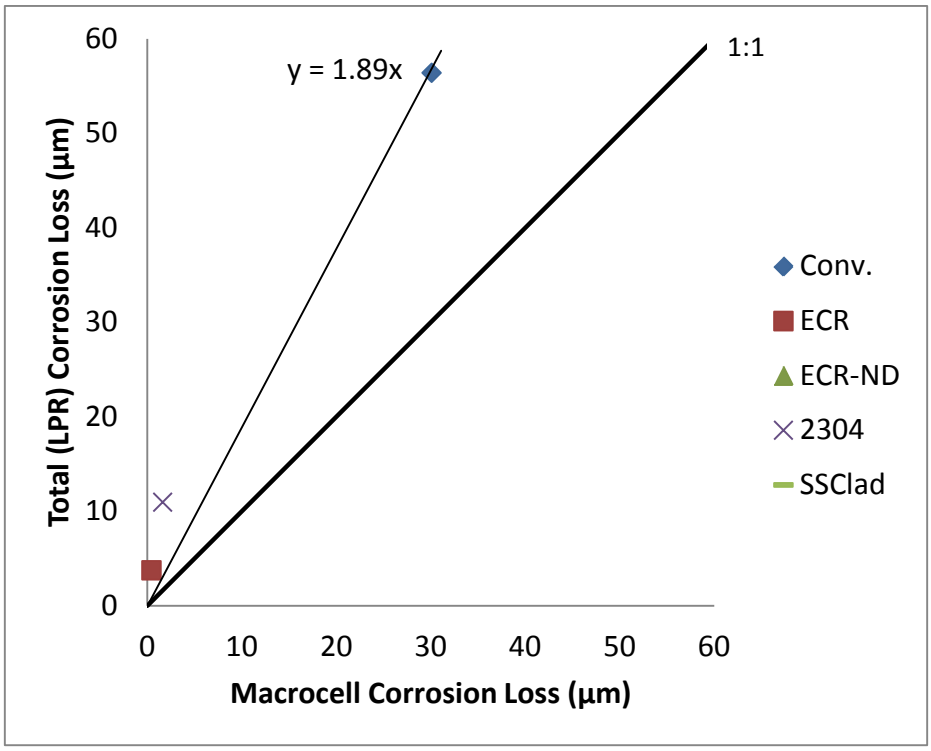

Figure 84a: Cracked beam test-comparison between corrosion loss (µm) from macrocell and total corrosion loss readings

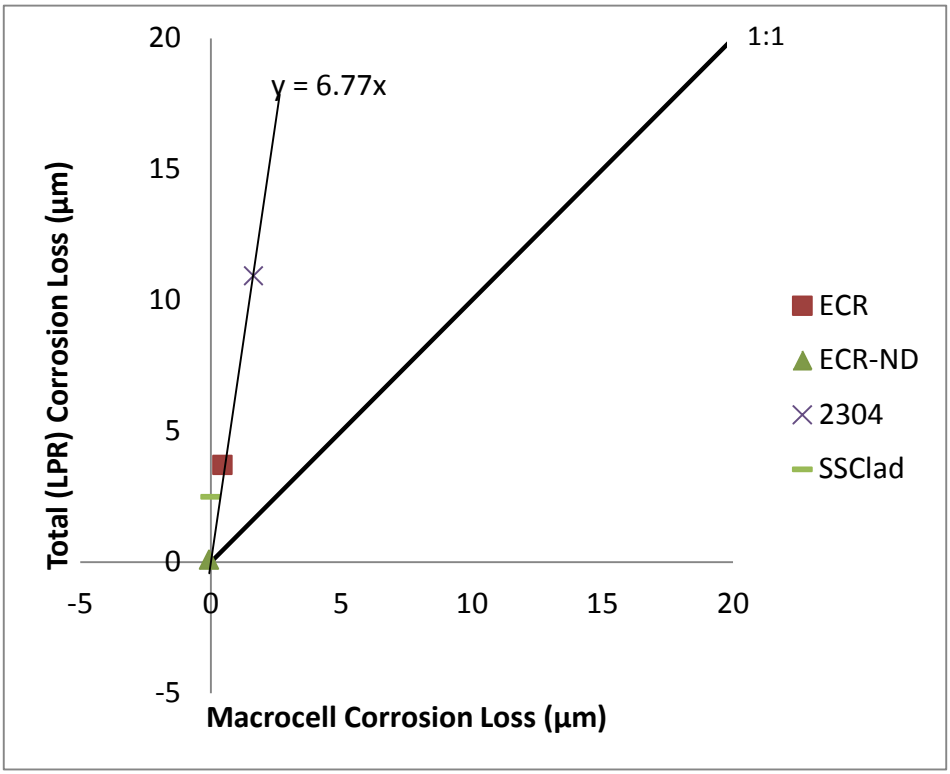

Figure 84b: Cracked beam test-comparison between corrosion loss (µm) from macrocell and total corrosion loss readings

4.2.6 Critical chloride threshold measured using Southern Exposure specimens

At the time of corrosion initiation, Southern Exposure specimens are sampled for chloride content. Tables 12a-h give the individual and average chloride contents and ages at corrosion initiation. Table 12a shows the results for the specimens with conventional bars. The average time to initiation for the Conv. specimens was 12.5 weeks at an average chloride content of 1.78 lb/yd^3 with a standard deviation of 1.45 lb/yd^3. Initiation ages ranged from 9 to 18 weeks. Average chloride contents for individual specimens ranged from 1.14 to 2.78 lb/yd^3. Table 12b shows results for the mixed Conv./2304 specimens. The average time to initiation was 8.0 weeks with an average chloride content of 1.76 lb/yd^3 and a standard deviation of 1.34 lb/yd^3. Initiation ages ranged between 5 and 11 weeks, and the average chloride contents for individual specimens ranged from 0.88 to 2.42 lb/yd^3. Table 12c shows results for the mixed Conv./SSClad specimens. The average time to initiation was 9.3 weeks with an average chloride content of 1.59 lb/yd^3 and standard deviation of 1.45 lb/yd^3. The individual ages of initiation for these specimens are between 8 and 10 weeks. The chloride contents for individual specimens ranged from 1.10 to 2.13 lb/yd^3. Previous studies conducted at KU (Darwin et al. 2009, Draper et al. 2009, O'Reilly et al. 2011) have shown average chloride contents for specimens containing conventional reinforcement between 1.63, and 1.81 lb/yd^3, similar to the values observed in this study.

Table 12a: Chloride contents at corrosion initiation for specimens with conventional reinforcement

Specimen	Initiation Age (weeks)	Chloride Content (lb/yd^3)						Average	Standard Deviation
		1	2	3	4	5	6		
Conv.-1	16	3.91	2.78	2.02	0.63	0.57	4.82	2.45	1.80
Conv.-2	18	1.69	0.50	2.59	1.64	0.44	1.14	1.33	1.41
Conv.-3	10	1.01	1.70	1.39	1.14	0.88	0.76	1.15	0.60
Conv.-4	10	3.03	0.44	2.33	0.38	1.58	2.02	1.53	1.02
		2.59	0.63	2.02	0.32				
Conv.-5	9	1.45	3.41	2.02	0.57	0.76	0.44	1.44	1.13
Conv.-6	12	6.43	0.32	1.27	5.43	2.78	0.44	2.78	2.04
Average	12.5							**1.78**	**1.45**

Table 12b: Chloride contents at corrosion initiation for specimens with conventional (top) and 2304 (bottom) reinforcement

Specimen	Initiation Age (weeks)	Chloride Content (lb/yd^3)						Average	Standard Deviation
		1	2	3	4	5	6		
Conv./2304-1	5	0.99	0.74	0.52	1.54	1.14	0.35	0.88	0.43
Conv./2304-2	11	5.11	2.08	1.45	1.15	1.01	1.14	1.99	1.58
Conv./2304-3	8	1.14	3.09	2.02	4.04	0.63	3.60	2.42	1.38
Average	8.0							**1.76**	**1.34**

Table 12c: Chloride contents at corrosion initiation for specimens with conventional (top) and stainless steel clad (bottom) reinforcement

Specimen	Initiation Age (weeks)	Chloride Content (lb/yd^3)						Average	Standard Deviation
		1	2	3	4	5	6		
Conv./SSClad-1	8	0.99	0.74	1.17	1.54	1.14	1.05	1.10	0.26
Conv./SSClad-2	10	3.03	0.44	2.33	0.38	1.58	2.02	1.53	1.02
		3.91	0.63	0.69	0.50				
Conv./SSClad-3	10	4.04	0.50	0.63	0.19	6.25	0.25	2.13	2.28
		2.59	0.63	2.02	0.32				
Average	9.3							**1.59**	**1.45**

The specimens containing coated reinforcement exhibited longer times to initiation and higher chloride contents at initiation than the specimens containing conventional steel. Table 12d shows the results for the epoxy-coated reinforcement. These specimens had initiation ages between 13 and 26 weeks with an average of 16.5 weeks. The average chloride content was 4.59 lb/yd^3 with a standard deviation of 3.11 lb/yd^3. The average chloride contents for individual specimens ranged from 2.14 to 7.98 lb/yd^3. The specimens with stainless steel cladding with four holes through the cladding had initiation ages between 17 and 48 weeks with an average initiation age of 26.7 weeks, as shown in Table 12e. The average chloride content was 7.62 lb/yd^3 with a standard deviation of 4.52 lb/yd^3. The average chloride contents for individual specimens ranged from 3.56 to 11.76 lb/yd^3. The average chloride contents at corrosion initiation for the ECR and SSClad-4h specimens were higher than for the Conv. specimens. The higher threshold of these specimens is in all likelihood due to the non-uniform chloride content in the concrete and the low probability that a region of locally high chloride content will specifically coincide with a point on the bar where the coating or cladding is penetrated. In previous studies (O'Reilly et al. 2011, Draper et al. 2009), epoxy-coated reinforcement with penetrations through the coating has shown average chloride thresholds between 7.30 and 10.3 lb/yd^3, about twice the average value observed in this study; however, the earlier studies also included ECR with a smaller exposed area.

Table 12f gives the results for the two SSClad-b specimens for which corrosion initiated. The initiation ages are 35 and 46 weeks with an average of 40.5 weeks. The average chloride content is 15.0 lb/yd^3 with a standard deviation of 5.82 lb/yd^3.

Table 12g gives the results for the 2304 specimens that have initiated corrosion. The average age at initiation is 99.8 weeks and the average chloride content is 20.5 lb/yd^3 with a standard deviation of 4.22 lb/yd^3. The average chloride content for the 2304/Conv. specimens for which corrosion has initiated is given in Table 12h. The average age at initiation is 75 weeks and the average chloride content is 20.5 lb/yd^3 with a standard deviation of 4.71 lb/yd^3., essentially the same as for the "all" 2304 specimens.

Table 12d: Chloride contents at corrosion initiation for specimens with epoxy-coated reinforcement

Specimen	Initiation Age (weeks)	Chloride Content (lb/yd^3)						Average	Standard Deviation
		1	2	3	4	5	6		
ECR-1	26	5.83	6.69	12.5	8.20	7.89	6.75	7.98	2.38
ECR-2	12	4.82	2.14	5.11	1.45	1.14	3.15	2.97	1.70
ECR-3	14	1.26	5.49	6.50	5.39	2.50	3.22	4.06	2.04
ECR-4	20	6.24	15.3	3.56	4.23	5.75	3.11	6.37	4.56
ECR-5	13	1.39	1.64	0.57	2.02	2.84	4.42	2.14	1.34
ECR-6	14	2.75	6.67	3.37	1.26	5.24	4.98	4.05	1.95
Average	16.5							**4.59**	**3.11**

Table 12e: Chloride contents at corrosion initiation for specimens containing stainless steel clad reinforcement with four drilled holes through the cladding

Specimen	Initiation Age (weeks)	Chloride Content (lb/yd^3)						Average	Standard Deviation
		1	2	3	4	5	6		
SSClad-4h-1	48	18.0	21.1	14.6	13.4	8.80	11.2	8.44	2.91
SSClad-4h-2	35	6.12	5.55	10.0	7.07	7.44	8.83	8.02	1.53
SSClad-4h-3	24	3.03	4.04	6.44	9.78	9.97	8.16	6.90	2.92
SSClad-4h-4	17	1.03	2.90	3.03	14.57	4.03	1.89	4.57	5.00
SSClad-4h-5	26	10.09 9.15	9.72 10.03	9.15 10.79	10.96 9.34	11.80	9.65	10.07	0.87
SSClad-4h-6	27	14.19 12.24	14.70 12.87	9.34 11.80	13.75 12.87	9.34	6.50	11.76	2.60
SSClad-4h-7	10	4.54 6.06	2.14 4.73	3.34 6.12	3.66 1.45	1.58	1.96	3.56	1.77
Average	26.7							**7.62**	**4.52**

Table 12f: Chloride contents at corrosion initiation for specimens with bent stainless steel clad reinforcement

Specimen	Initiation Age (weeks)	Chloride Content (lb/yd^3)						Average	Standard Deviation
		1	2	3	4	5	6		
SSClad-b-2	35	9.53	12.11	11.36	19.68	13.25	16.72	14.0	2.89
SSClad-b-3	46	23.70	24.80	26.20	20.40	17.10	24.60	16.0	2.79
Average	40.5							**15.0**	**5.82**

Table 12g: Chloride contents for 2304 stainless steel specimens that have initiated corrosion

Specimen	Initiation Age (weeks)	Chloride Content (lb/yd^3)						Average	Standard Deviation
		1	2	3	4	5	6		
2304-2	89	13.12	11.67	16.65	12.74	13.25	19.94	14.56	3.12
2304-3	96	20.46	13.77	18.85	18.66	21.25	28.45	20.99	4.11
			26.74	20.10	20.80	20.78			
2304-5	98	24.44	24.32	30.81	20.73	22.09	26.43	24.69	5.30
			30.92	14.19	28.23				
2304-6	116	28.96	24.79	26.81	23.03	21.88	22.21	21.87	4.35
			17.85	15.14	21.01	17.03			
Average	99.8							**20.53**	**4.22**

Table 12h: Chloride contents for 2304 stainless steel (top) and Conv. (bottom) specimen that has initiated corrosion

Specimen	Initiation Age (weeks)	Chloride Content (lb/yd^3)						Average	Standard Deviation
		1	2	3	4	5	6		
2304/Conv-2	81	17.61	13.82	21.11	22.94	31.30	18.60	22.01	5.54
			27.13	23.59					
2304/Conv.-3	69	19.37	23.34	18.61	17.85	14.45	20.33	18.99	2.93
Average	75.0							**20.50**	**4.71**

4.2.7 Autopsy

Upon completion of the 96-week bench-scale tests, all specimens were autopsied, using the following procedure:

1. Specimens are disconnected and rinsed with deionized water.
2. All Southern Exposure specimens are drilled for chloride content.
3. The electrical connection of each specimen is closely examined for signs of corrosion.
4. Photographs are taken of each specimen.
5. The reinforcing steel is removed from the concrete by use of a sledgehammer.
6. Photographs are taken of all reinforcing steel specimens.
7. Where applicable, photographs of staining of the concrete are taken.
8. In the case of ECR and ECR-ND specimens, disbondment tests are performed on each bar.

The disbondment test is performed at three holes on ECR bars, and two randomly chosen locations on ECR-ND bars as described in Section 4.1.4. For plotting purposes, bars with total disbondment are assigned a disbonded area of 1.05 in.^{2}, which corresponds to the area of a rectangle extending 0.5 in. from the initial hole in the longitudinal direction and to the longitudinal ribs on either side of the hole. Three sites on each bar being evaluated are subjected to disbondment tests, two of which are on the upper surface of the bar as it was oriented in the specimen and one on the underside of the bar.

The values of the disbonded area for each of the ECR specimens with penetrations in the coating are shown in Figures 85a for the Southern Exposure specimens and 85b for the cracked beam specimens. As can be seen, all of the top bars in both tests experienced total disbondment. The bottom bars experienced less disbondment and, for the case of specimens SE-ECR-2 and CB-ECR-2, no disbondment was experienced on the bottom bars. The

disbonded areas on the bottom bars for the cracked beam specimens were higher than those for the Southern Exposure specimens. No disbondment was measured for the ECR-ND specimens.

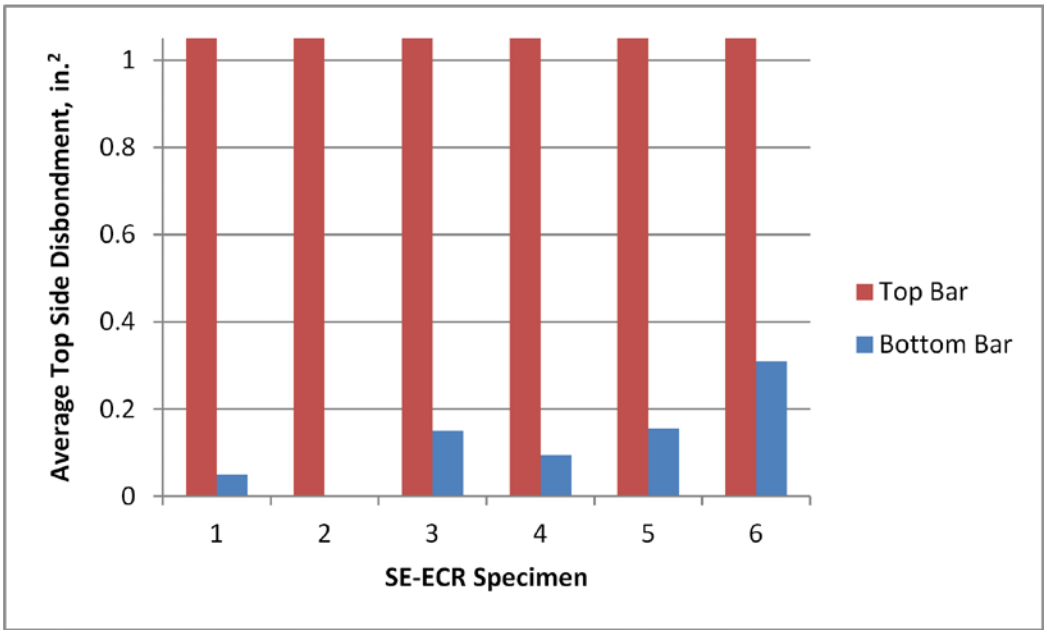

Figure 85a: Average disbondment for Southern Exposure ECR Specimens with penetrations in coating

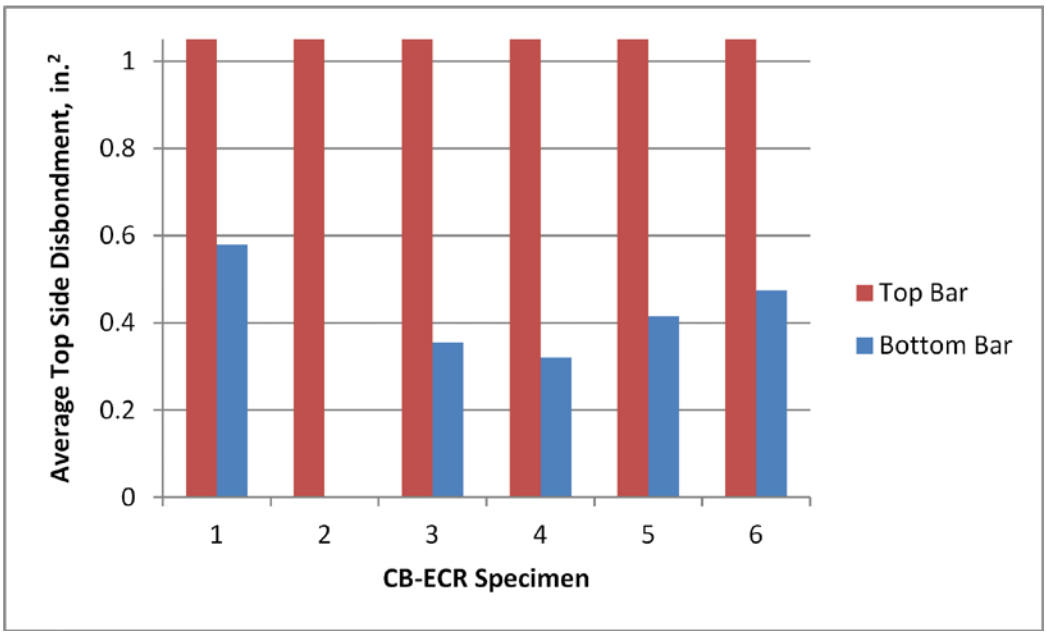

Figure 85b: Average disbondment for cracked beam ECR Specimens with penetrations in coating

Each specimen was photographed upon completion of the bench-scale tests. The photographs in Figures 86 through 101 are representative of typical specimens. Where corrosion products and staining are shown in the figures, these effects were observed for all specimens in a set.

Figures 86a and 86b show a typical Southern Exposure specimen containing conventional reinforcement (Conv.) upon completion of the test. The photograph in Figure 86a, taken before autopsy, shows staining on the outer surface of the specimen. Figure 86b, taken after autopsy, shows the two top bars with significant corrosion product along the length of the bars.

Figure 86a: Staining on outside of Southern Exposure specimen 5 with conventional steel in the top mat

Figure 86b: Bars from Southern Exposure specimen 2 containing conventional reinforcement after autopsy

Figures 87a and 87b show a typical cracked beam specimen containing conventional reinforcement (Conv.) before and after autopsy, respectively. As with the Southern Exposure specimen shown in Figure 86, the top bar exhibits significant corrosion along the length of the bar.

Figure 87a: Staining of cracked beam specimen 1 containing conventional reinforcement

Figure 87b: Bars from cracked beam specimen 1 containing conventional reinforcement after autopsy

A Southern Exposure specimen with conventional steel as the anode and 2304 stainless steel as the cathode is shown in Figures 88 and 89. Figure 88a shows staining on the top surface of the specimen as well as cracking caused by the corrosion of the top bars. Figures

88b and 88c show the bars after being removed from the concrete. It can be seen that the top (conventional) bars show significant corrosion products. One Conv./2304 specimen also exhibited staining on the stainless steel cathode bar, as shown in Figure 89.

Figure 88a: Staining on Southern Exposure specimen 3 containing mixed Conv./2304 (anode/cathode)

Figure 88b: Bars from Southern Exposure specimen 3 containing conventional reinforcement as the anode and 2304 stainless steel as the cathode after autopsy

Figure 88c: Close up of conventional top bar in Southern Exposure specimen 3 containing conventional reinforcement as the anode and 2304 stainless steel as the cathode after autopsy

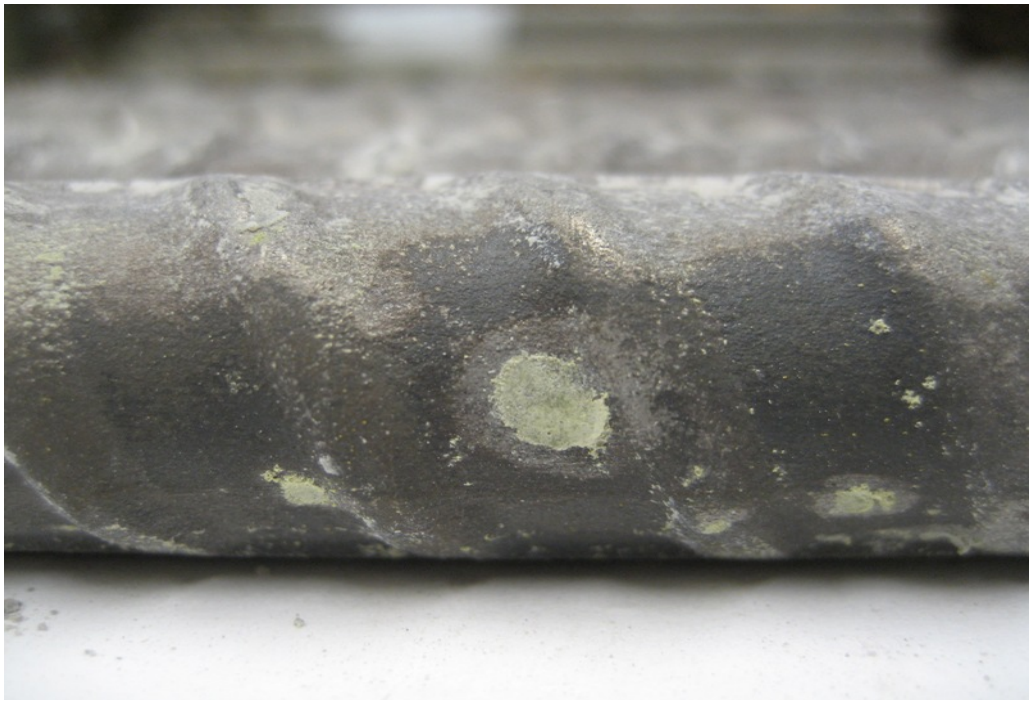

Figure 89: Corrosion product on 2304 stainless steel cathode bar in mixed Conv./2304 Southern Exposure specimen 2 after autopsy-not typical of all specimens

Figure 90 shows a typical Southern Exposure specimen with conventional steel as the anode and stainless steel clad reinforcement as the cathode after autopsy. As with all other specimens containing conventional steel in the top mat, the top bars exhibit significant corrosion products along the length of the beam.

Figure 90: Bars from Southern exposure specimen 1 containing conventional reinforcement as the anode and stainless steel clad reinforcement as the cathode after autopsy

Figure 91: Staining on inside of Southern Exposure specimen 3 containing epoxy-coated reinforcement with penetrations in the epoxy.

Figure 91 shows staining on the inside of a Southern Exposure specimen containing ECR. Figure 92 shows total disbondment of the top bar.

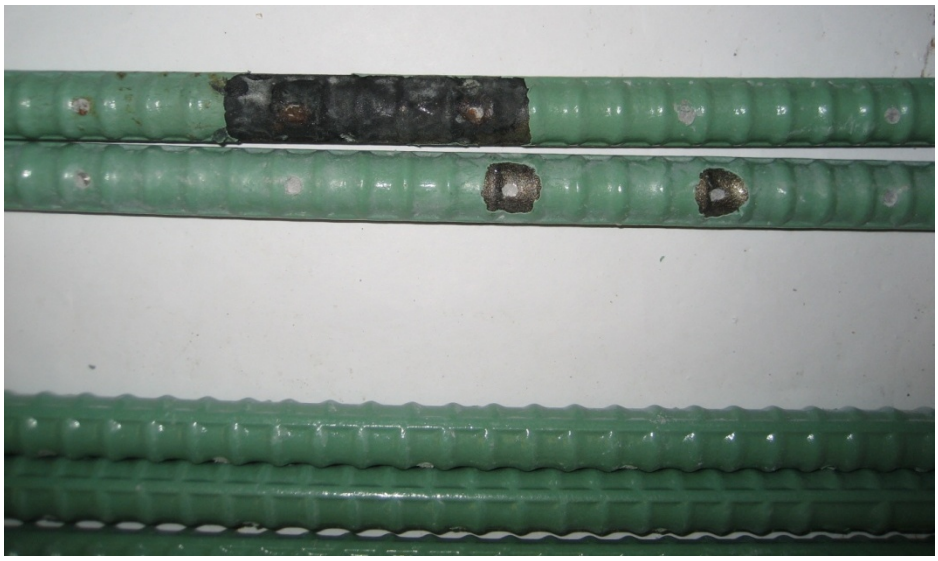

Figure 92: Bars from Southern Exposure specimen 6 containing epoxy coated reinforcement with penetrations in the epoxy after autopsy, showing total disbondment in top mat

Figure 93 shows staining both in the crack of a 2304 cracked beam specimen (Figure 93a) and also on the inside of the specimen after autopsy (Figure 93b).

Figure 93a: Staining in the crack of cracked beam specimen 5 containing 2304 stainless steel

Figure 93b: Staining on inside of cracked beam specimen 1 containing 2304 stainless steel

Corrosion products can be seen on the top bar of a 2304 cracked beam specimen (Figure 94a). There is evidence of corrosion at the end as well as in the middle of the bar (Figures 94b and 93c).

Figure 94a: Bars from cracked beam specimen 1 containing 2304 stainless steel after autopsy

Figure 94b: Top bar from cracked beam specimen 1 containing 2304 stainless steel after autopsy, showing corrosion product on top bar (close up)

Figure 94c: Top bar from cracked beam specimen 2 containing 2304 stainless steel after autopsy, showing corrosion product near the end of the top bar (close up)

There were also corrosion products on the end of one top bar in a Southern Exposure 2304 specimen as shown in Figure 95.

Figure 95: Bars from Southern Exposure specimen 2 containing 2304 stainless steel after autopsy

Figure 96 shows bars from a Southern Exposure specimen with 2304 stainless steel as the anode and conventional steel as the cathode after autopsy. Two of the three specimens showed corrosion near the end of the top bar.

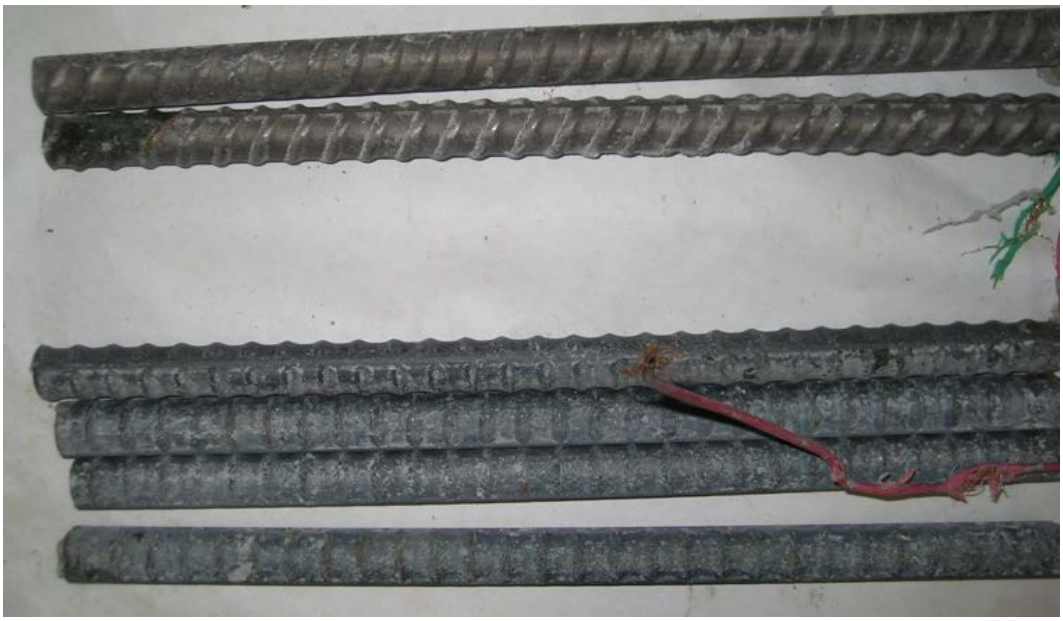

Figure 96: Bars from Southern exposure specimen 2 containing 2304 stainless steel as the anode and conventional steel as the cathode after autopsy

Figure 97 shows bars from a typical SSClad specimen with four holes through the cladding after autopsy. There are corrosion products at some of the holes on the top bars as well as slight corrosion products in the holes on the bottom bars (Figure 97c). There were also corrosion products observed on the exposed ends of the both the top and bottom bars. A cut

through one of the holes in the cladding showed a moderate degree of pitting corrosion spreading beyond the diameter of the hole (Figure 97e).

Figure 97a: Bars from Southern Exposure specimen 5 containing stainless steel clad reinforcement with four holes through the cladding after autopsy

Figure 97b: Top Bars from Southern Exposure specimen 5 containing stainless steel clad reinforcement with holes through the cladding after autopsy, showing corrosion at damage site on top bars (close up)

Figure 97c: Bottom bars from Southern Exposure specimen 5 containing stainless steel clad reinforcement with four holes through the cladding after autopsy, showing corrosion at damage site on bottom bars (close up)

Figure 97d: Bars from Southern Exposure specimen 5 containing stainless steel clad reinforcement with four holes through the cladding after autopsy, showing corrosion at ends of top and bottom bars (close up)

Figure 97e: Bars from Southern Exposure specimen 5 containing stainless steel clad reinforcement with four holes through the cladding after autopsy, showing extent of corrosion underneath the hole

Bars from a typical Southern Exposure specimen with undamaged stainless steel clad reinforcement are shown in Figure 98. There was no observed corrosion of the stainless steel. However, there were some corrosion products at the ends of the underlying conventional steel core (Figure 98b), highlighting the importance of protecting the cut ends of the bars.

Figure 98a: Bars from Southern Exposure specimen 5 containing undamaged stainless steel clad reinforcement after autopsy

Figure 98b: Bars from Southern Exposure specimen 4 containing undamaged stainless steel clad reinforcement after autopsy, showing corrosion at ends of top and bottom bars (close up)

Figure 99: Bars from cracked beam specimen 6 containing undamaged stainless steel clad reinforcement after autopsy

Figure 99 shows bars from a cracked beam specimen containing undamaged stainless steel clad reinforcement after autopsy. There was no observed corrosion.

Figure 100 shows bars from a Southern Exposure specimen containing bent SSClad reinforcement after autopsy. As discussed earlier, bars from two specimens displayed corrosion products near the bend (Figure 80a). The rest of the specimens showed no signs of corrosion. However, because of the potential for damage, it is recommended that the SSClad bars be

protected during the bending process in a manner similar to that for epoxy coated reinforcement.

Figure 100: Bars from Southern Exposure specimen 5 containing bent stainless steel clad reinforcement after autopsy

Bars from a Southern Exposure specimen containing stainless steel clad reinforcement as the anode and conventional steel as the cathode are shown in Figure 101. Significant corrosion products were seen on one conventional bottom bar (Figure 101b). There were also corrosion products at the ends of the SSClad bars (Figure 101c).

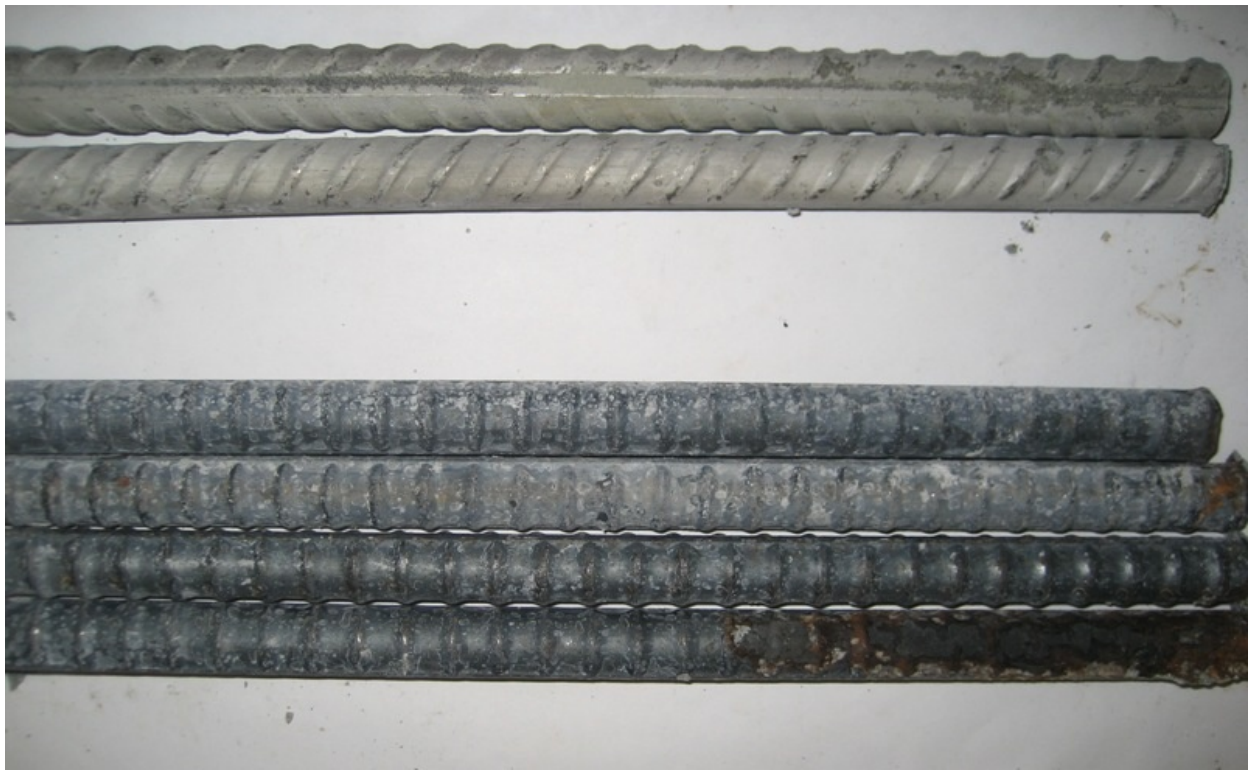

Figure 101a: Bars from a Southern Exposure specimen 3 containing stainless steel clad reinforcement as the anode and conventional steel as the cathode after autopsy

Figure 101b: Bottom bars from Southern Exposure specimen 3 containing stainless steel clad reinforcement as the anode and conventional steel as the cathode after autopsy

Figure 101c: Top bars from Southern Exposure specimen 2 containing stainless steel clad reinforcement as the anode and conventional steel as the cathode after autopsy, showing corrosion of at ends of top bars (close up)

4.2.8 End of life chloride analysis

The average chloride contents for all the Southern Exposure specimens at 96 weeks are presented in Table 13, along with the standard deviation of the individual chloride samples. Average chloride contents range between 17.6 lb/yd^3 for the undamaged SSClad specimens and 26.2 lb/yd^3 for the Conv./SSClad specimens. The procedure for sampling and testing for chloride content is the same as that discussed earlier for chloride content at corrosion initiation. The averages in the table are based upon six specimens with 10 samples from each specimen with the exception of the mixed specimens for which there were three specimens, each with 10 samples. It was found that the average of the ten samples from one 2304 specimen (2304-2) was much lower than other samples from the same batch of concrete. Therefore, it was decided that an error occurred during the sampling or testing of those samples, and they were subsequently discarded. Thus, the 2304 average is based upon only five specimens, each with 10 samples. Chloride content results for individual specimens at initiation and end of life are included in Appendix C.

Table 13: Average Chloride Contents (lb/yd^3) for all Southern Exposure Specimens at 96 weeks

System[a]	Specimen Chloride Content, lb/yd^3						Average	Standard Deviation
	1	2	3	4	5	6		
Conv.	20.5	13.2	23.2	26.4	20.1	27.7	21.8	5.77
ECR	19.5	22.5	26.3	26.6	25.8	24.9	24.3	4.92
2304	15.3	11.7*	21.0	24.4	22.6	21.9	21.0	4.99
2304/Conv.	19.5	-	30.4	-	25.4	-	25.1	5.87
Conv./2304	-	27.1	-	17.8	-	25.2	23.4	8.03
SSClad-4h	12.8	13.8	14.5	20.4	18.3	25.4	17.5	5.43
SSClad	17.1	24.5	19.7	17.7	13.8	15.0	18.0	4.91
SSClad-b	18.7	30.3	21.3	21.7	24.6	22.9	23.3	5.74
SSClad/Conv	-	16.8	18.2	25.1	23.1	21.3	20.9	5.57
Conv./SSClad	25.6	-	26.6	-	21.7	-	24.6	4.28

[a] Conv. = conventional reinforcement, ECR = epoxy-coated reinforcement with ten 1/8-in. diameter holes through the epoxy, ECR-ND= undamaged ECR, 2304 = 2304 stainless steel, SSClad-4d = stainless steel clad reinforcement with four 1/8-in. diameter holes through the cladding, SSClad = undamaged stainless steel clad reinforcement, SSClad-b = bent stainless steel clad reinforcement.
*Not included in average

Figure 102 shows the average chloride contents in a bar graph with error bars showing the maximum and minimum individual sample chloride contents. It can be seen that the scatter of the individual chloride samples is large. This is due mostly to the non-homogenous nature of concrete. Each sample was collected from a different site in the concrete specimen. Since the chlorides cannot penetrate through the aggregate, some sites have higher levels of chlorides than others.

To determine the statistical significance of the differences in chloride concentrations at 96, a two-tailed Student's T-test is used. The student's T-test is a method of statistical analysis that compares the means and variances of two data sets to determine the probability, α, that any differences in mean values could have arisen by chance; that is, the differences in the mean values for two data sets are due to natural variability not differences in behavior. Values of α greater than 0.10 are often used as an indication that the measured values are similar. No differences were observed between the average chloride contents of specimens with $\alpha > 0.10$. Therefore, the differences in chloride contents are considered to be due to random variation and the average of all specimen chloride data at 96 weeks, 21.6 lb/yd^3, can be taken as representative of the specimens.

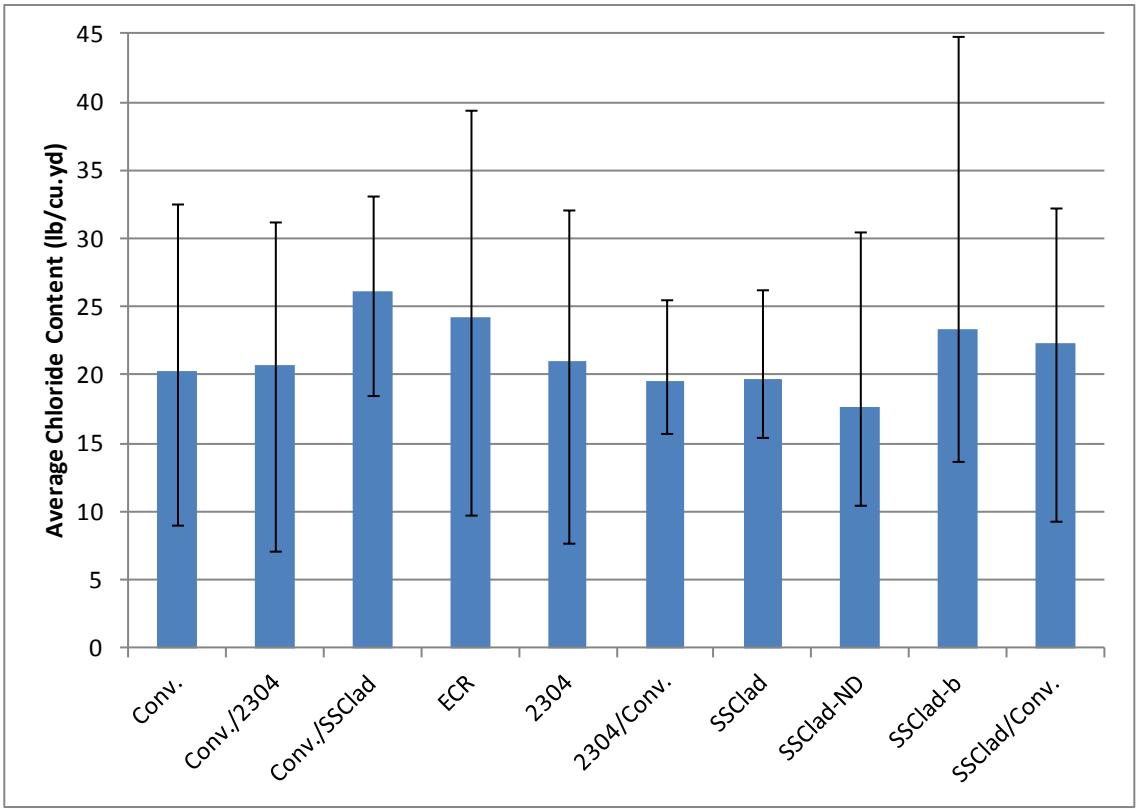

Figure 102: Average Chloride Content at 96 weeks for all specimen types with error bars showing maximum and minimum individual sample chloride contents

5. LIFE EXPECTANCY AND COST EFFECTIVENESS

5.1 LIFE EXPECTANCY

The life expectancy of a bridge deck is based on an estimate of the time to first repair, which is combined with the time between repairs to establish the present cost of a deck over a its design life (Darwin et.al. 2011). In many cases, the time to first repair is estimated based on experience. For example, the South Dakota Department of Transportation (SDDOT) has estimated that the time to first repair for bridge decks containing conventional steel is 10 years under harsh environmental conditions and 25 years in arid conditions (Darwin et.al 2002). The latter value matches the time to first repair estimated by the Kansas Department of Transportation (KDOT). In 2001, the time to first repair for bridge decks containing ECR was estimated to be 35 and 40 years by KDOT and SDDOT, respectively. The estimate for decks with ECR was based on the fact that, as of the year 2000, no bridge decks containing ECR had required repair due to corrosion-induced damage since its first use in the late 1970s (Kepler et.al 2000). Other estimates of time to first repair use models that are based on the time required for chloride ions to diffuse through uncracked concrete. Models of this type usually include a preselected time for the corrosion products to cause the concrete to crack following corrosion initiation. Diffusion-based models have two key drawbacks. They do not account for the role played by cracks in the concrete in allowing rapid penetration of chlorides to the level of the reinforcing steel, and the preselected time for the corrosion products to cause the concrete to crack is not based on actual corrosion rates. Because surveys of bridge decks with ages ranging from several months to over 20 years demonstrate that reinforced concrete bridge decks exhibit significant cracking parallel to and directly above the reinforcing bars, the estimates of time to first repair are based principally on corrosion in the presence of cracks.

The procedures used in the current analysis are based on field and laboratory evidence addressing corrosion initiation and propagation in cracked concrete, combined with experience with deck repair. Using this approach, the time to first repair depends on (1) the time required for the chloride content of the concrete to reach the critical chloride initiation threshold for the system, (2) the time required after initiation for corrosion products to cause cracking and spalling of the concrete cover, and (3) the time between first cracking and the time that the repair is made. Although the cracked beam tests on the repickled 2304 steel (2304p) are not complete, its excellent performance of these specimens to date along with its performance in the rapid macrocell test strongly suggests that properly pickled 2304 will perform in a superior manner. Therefore, 2304p reinforcement is considered along with conventional, epoxy-coated, 2304 (as-delivered), and stainless steel clad bars in the analyses presented in this chapter.

5.1.1 Time to Corrosion Initiation

The time to corrosion initiation is estimated based on chloride contents measured at crack locations on bridge decks in Kansas and the CCCT (critical chloride corrosion threshold) based on water-soluble chloride content for each type of reinforcing steel, as previously discussed in section 4.2.6. The chloride contents in bridge decks are based on work by Lindquist (2005) and Miller (2000). In those studies, chloride samples were obtained using a vacuum drill from bridge decks that were cast monolithically and with high-density conventional and silica fume overlays. The samples were obtained in increments of 0.75 in. to a depth of 3.75 in. both at and away from cracks in bridge decks, primarily in northeast Kansas. Figure 103 shows the relationship between the average chloride content at crack locations interpolated to a depth of 2.5 in., the cover typically specified for the top layer of reinforcement in bridge decks in Oklahoma, versus age for bridges with an average annual daily traffic (AADT) greater than 7,500 (relatively high traffic bridges). The 2.5-in. depth is based on the concrete clear cover indicated on standard plans provided by ODOT for a 40-foot clear roadway supported by 4

girders. This is less than the 3-in. clear cover specified by the Kansas Department of Transportation, which will be used for comparison. Figure 103 also demonstrates that the chloride content at cracks is independent of the type of deck.

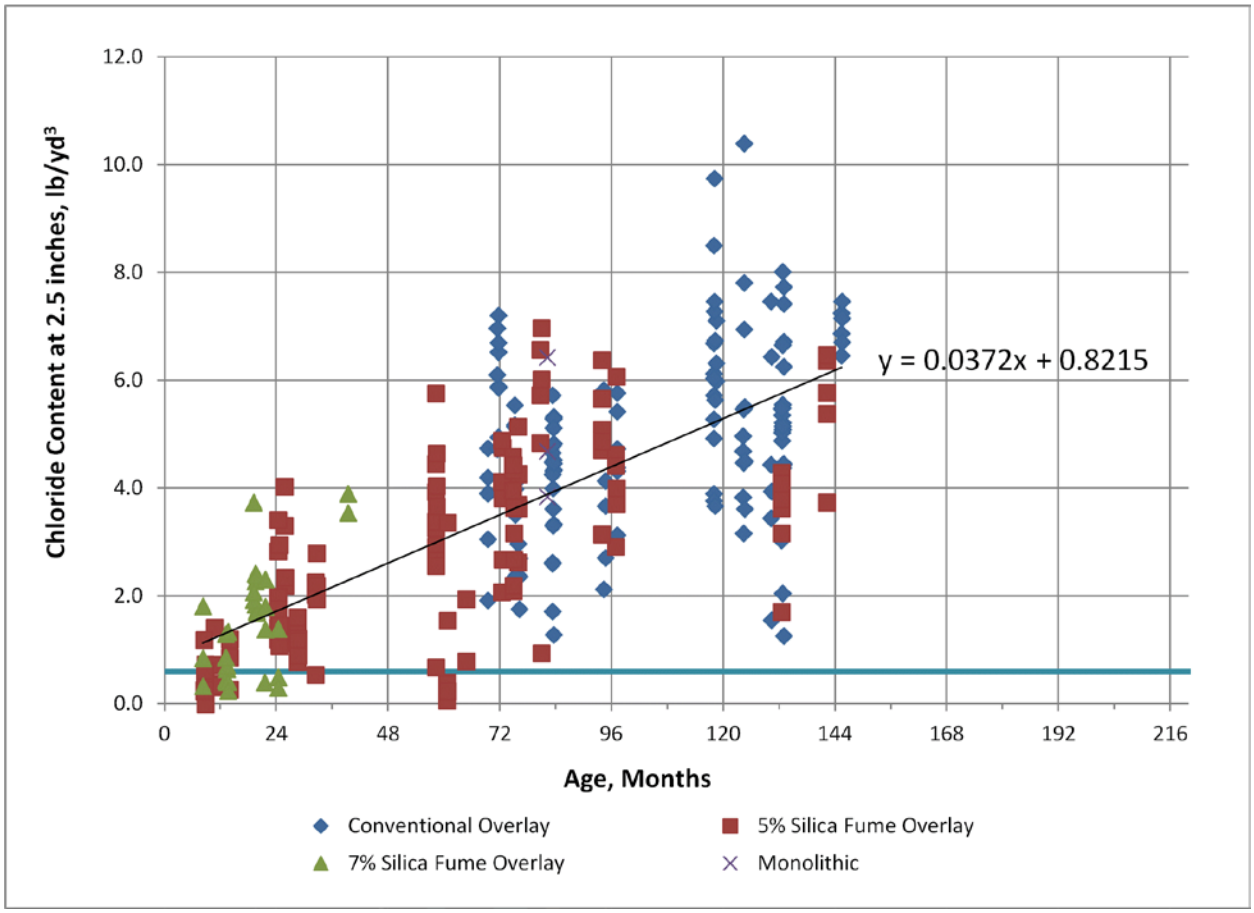

Figure 103: Chloride content taken at cracks interpolated at a depth of 2.5 in. versus age for bridges with an AADT greater than 7,500

Equation (4) expresses the average chloride content *C* as a function of time *T* for the relationship shown in Figure 103. Rearranging the equation gives the average time to reach a specific chloride content at a depth of 2.5 in. [Eq. (5)].

$$C = 0.0372T + 0.8215 \tag{4}$$

$$T = \frac{C - 0.8215}{0.0372} \tag{5}$$

Based on the work by Lindquist (2005) and Miller (2000), the equations for chloride content and time to reach a specific chloride content at a depth of 3.0 in are

$$C = 0.0315T + 0.7440 \tag{6}$$

$$T = \frac{C - 0.7440}{0.0315} \tag{7}$$

Table 14 gives the estimated times to corrosion initiation in bridge decks at depths of 2.5 in and 3.0 in. The corrosion thresholds shown in the table are based on the average chloride contents in Southern Exposure specimens at the time of corrosion initiation for conventional, 2304, and epoxy-coated reinforcement (Tables 12a and 12d). No Southern Exposure SSClad specimens initiated corrosion within the 96-week test; therefore, the time to corrosion initiation is calculated based on the average end-of-life chloride content (Table 13) and represents a lower bound on life expectancy. Southern Exposure specimens were not used for repickled 2304 (2304p), but the critical chloride threshold is assumed to be higher than that for the 2304 in the as-received condition because the cracked beam 2304p specimens did not initiate corrosion while the 2304 cracked beam specimens did.

Table 14: Estimated average times to corrosion initiation for configurations of reinforcing steel in bridge decks with 2.5 and 3.0-in. covers

Steel Designation[a]	Chloride Threshold, lb/yd^3	Age at Corrosion Initiation in Bridge Decks, yr (2.5-in. cover)	Age at Corrosion Initiation in Bridge Decks, yr (3.0-in. cover)
Conv.	1.78	2.1	2.7
ECR	4.59	8.4	10.2
2304	20.5	44	52
2304p	>20.5	>44	>52
SSClad	>21.6	>47	>55

[a] Conv. = conventional reinforcement, ECR = epoxy-coated reinforcement with ten 1/8-in. diameter holes through the epoxy, 2304 = 2304 stainless steel as received, 2304p = repickled 2304 stainless steel, SSClad = stainless steel clad reinforcement.

As shown in Table 14, the average age at corrosion initiation for conventional reinforcement at a depth of 2.5 in. is 2.1 years and at 3.0 in. is 2.7 years, compared with 2.2 years calculated by Darwin et. al. (2011). Epoxy-coated reinforcement has an age at corrosion initiation of 8.4 years at a depth of 2.5 in. and 10.2 years at a depth of 3.0 in. which is less than the 20 years estimated by Darwin et al. Darwin et al., however, examined epoxies with a range of exposed areas, all less than or equal to the area exposed for this study. 2304 stainless steel has an age at corrosion initiation at 44 years with a 2.5 in. cover and 52 years with a 3 in. cover. These values should be taken as minimums when 2304 stainless steel is properly pickled. SSClad reinforcement has an age at corrosion initiation greater than 47 years with 2.5 in. cover and greater than 55 years with 3 in. cover. Table 14 shows that using a higher cover can significantly increase the time to corrosion initiation, in this case by 18% or more for an increase in cover from 2.5 to 3.0 in.

5.1.2 Time to Cracking After Corrosion Initiation

The time required to generate enough corrosion products to crack concrete is a function of the total corrosion rate and the corrosion loss required to cause cracking. The latter is a function of the bar size and the concrete cover (Darwin et. al. 2011). Total corrosion rates will be covered first.

5.1.2.1 Corrosion Rates Based on Losses

The method for determining the average corrosion rate after initiation for a corrosion protection system proceeds as follows: Corrosion loss is obtained by integrating the corrosion rate of a specimen over time. The corrosion loss plots for cracked beam specimens with stainless steel clad bars are shown in Figure 104 and will be used to demonstrate the method for determining the average corrosion rate.

To determine the average corrosion rate from the corrosion loss plot (Figure 104a), the location at which the corrosion loss of each individual specimen or bar begins to increase steadily is determined and marked (Figure 104b). A line connecting the corrosion loss at corrosion initiation to the corrosion loss at the end of testing is drawn for each specimen (Figure 104c). The slope of this line is the average corrosion rate for each specimen. The average of the individual corrosion rates is taken as the average corrosion rate for the corrosion protection system.

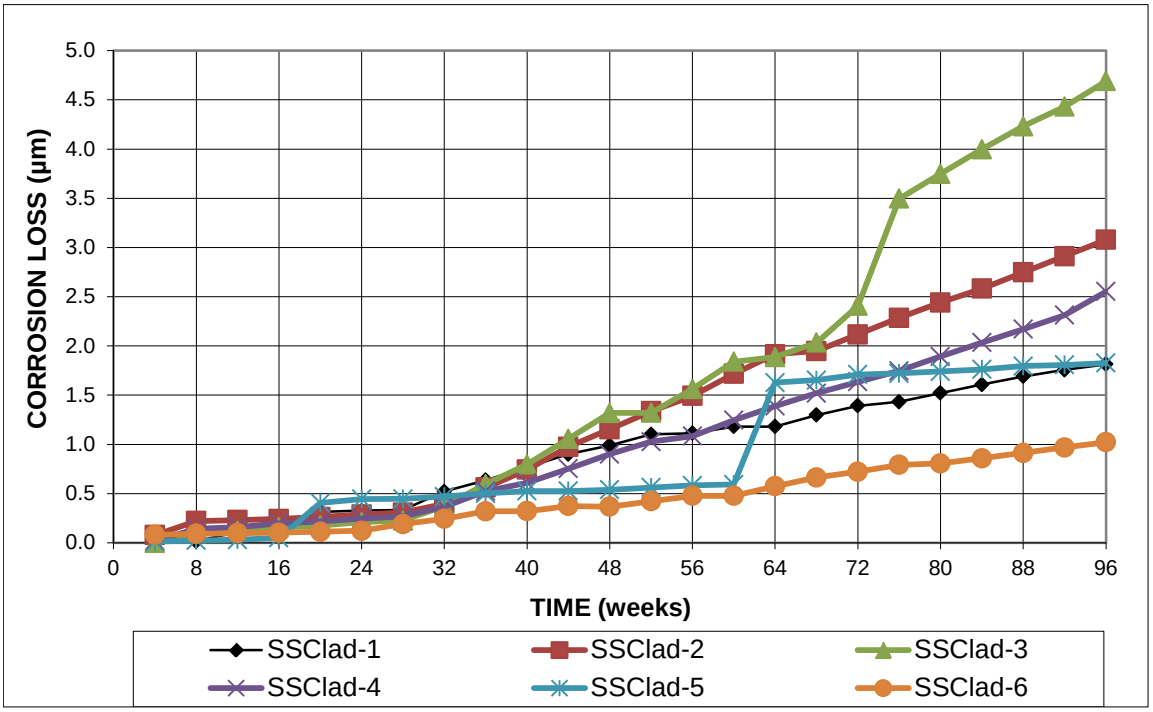

Figure 104a: Individual corrosion losses for cracked beam specimens with stainless steel clad reinforcement

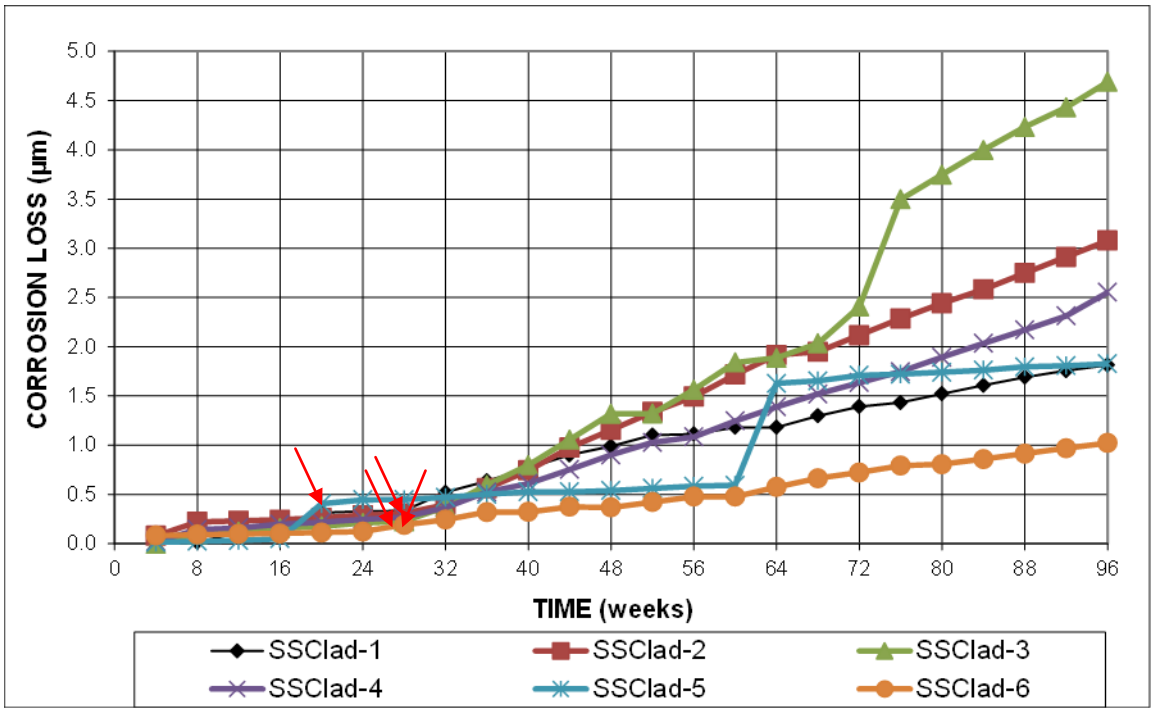

Figure 104b: Individual corrosion losses for cracked beam specimens with stainless steel clad reinforcement with corrosion initiation marked

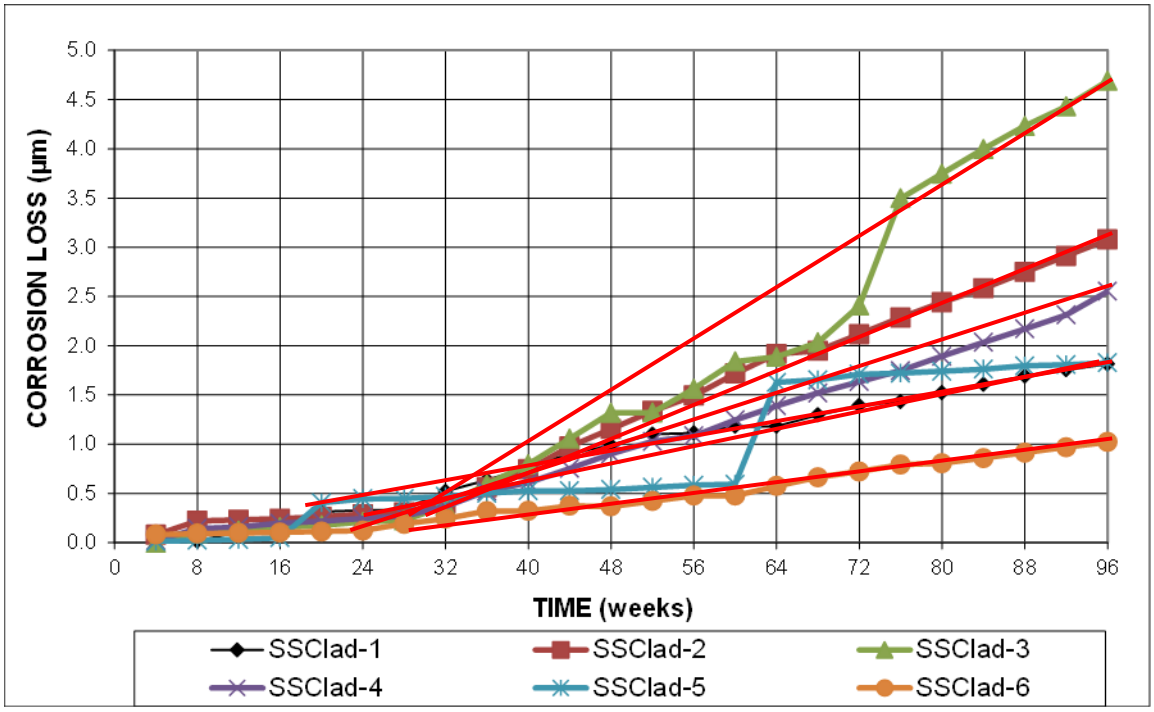

Figure 104c: Individual corrosion losses for cracked beam specimens with stainless steel clad reinforcement with lines connecting corrosion loss at initiation to corrosion loss at end of life

Because cracking is caused by total losses (rather than macrocell losses) and because the greatest corrosion occurs in bridge decks for bars at cracks, linear polarization resistance

(LPR) results for cracked beam specimens are used to determine life expectancy. The average LPR corrosion rates based on losses for cracked beam specimens are presented in Table 15. As discussed earlier, bridges tend to form cracks parallel to and directly above reinforcing steel; thus, the cracked beam corrosion rates will be used to determine life expectancy. Specimens with conventional reinforcement exhibited the greatest average corrosion rate, 30.5 µm/yr. Specimens with 2304 reinforcement and ECR with holes penetrating the epoxy (based on total area of the bar) exhibited corrosion rates of 8.23 µm/yr and 2.03 µm/yr, respectively. Undamaged ECR, repickled 2304 stainless steel, and clad stainless steel bars exhibited no measurable corrosion.

Table 15: Average corrosion rates based on losses for cracked beam specimens

System	Average Corrosion Rate, µm/yr	Standard Deviation
Conv.	30.5	6.95
ECR	2.03	1.08
ECR-ND	No Corrosion	
2304	8.23	1.40
2304p	No Corrosion	
SSClad	No Corrosion	

5.1.2.2 Equivalent Field Test Corrosion Rates

The accelerated nature of the laboratory corrosion tests result in corrosion rates greater than those observed in bridge decks. It is therefore necessary to convert the corrosion rates in the laboratory to those obtained in the field. The determination of effective field corrosion rates in this report is based on methods developed by Darwin et al. (2011) in which identical corrosion protection systems were tested in laboratory and field specimens to establish a correlation between laboratory and field test specimen performance. The field test specimens were 4-ft square sections of bridge deck with a reduced (1-in.) top cover that were exposed to the weather and de-icing salts, with the salt applied at the average rate for bridge decks in northeast Kansas. Darwin et. al. (2011) established the ratio of laboratory corrosion rate to field specimen corrosion rate, along with an additional factor to account for localized corrosion of the bar was applied. Field test specimens were not used in this study, so an estimate of corrosion rate based on bench-scale tests is needed. This is done using the ratio of field test to bench-scale macrocell corrosion rates determined by Darwin et. al. (2011) for conventional reinforcement in concrete with cracks above the reinforcement. Comparisons are made based on the corrosion rates in cracked concrete because bridge decks inevitably develop cracks over and parallel to the reinforcement due to settlement of plastic concrete and shrinkage of the hardened concrete.

Figure 105, taken from Darwin et al. (2011), compares the average macrocell corrosion rates after corrosion initiation based on total area for field test and cracked beam specimens containing conventional reinforcement in cracked concrete. The figure also shows error bars representing the maximum and minimum rates experienced by both types of specimens. Corrosion rates and losses for conventional reinforcement are consistently lower in field test specimens than in bench-scale specimens.

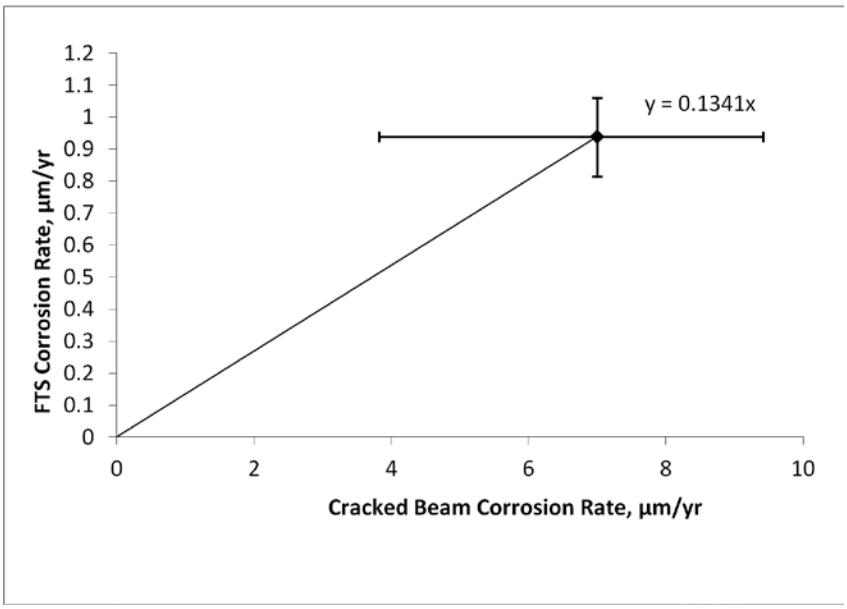

Figure 105: Comparison between average macrocell corrosion rates after corrosion initiation based on total area for cracked beam and field test specimens with conventional reinforcement in cracked concrete

As shown in Figure 105, the average macrocell corrosion rate in the field test specimens with cracks above the reinforcement equals 13.4 percent of the average rate in the cracked beam specimens. This value is used to convert the corrosion rates for the cracked beam specimens shown in Table 15 to the equivalent macrocell corrosion rates in field test specimens shown in Table 16. The stainless steel clad cracked beam specimens did not initiate corrosion over the duration of the test, and therefore, these bars are assigned a corrosion rate of zero. This point is further supported by the rapid macrocell test results, which show significantly higher corrosion rates for the as-received 2304 bars compared to SSClad bars and the 2304p bars, which are also assigned a corrosion rate of zero.

Table 16: Equivalent field test specimen macrocell corrosion rates, µm/yr

Steel Designation[a]	Cracked Beam Corrosion Rate	Equivalent FTS Corrosion Rate
Conv.	30.5	4.09
ECR	2.03	0..272
2304	8.23	1.10
2304p	-	-
SSClad	-	-

[a] Conv. = conventional reinforcement, ECR = epoxy-coated reinforcement with ten 1/8-in. diameter holes through the epoxy, 2304 = 2304 stainless steel as-received, 2304p = repickled 2304 stainless steel, SSClad = stainless steel clad reinforcement,

For ECR, the corrosion rates and losses in this report have been expressed in terms of the entire surface area of the bar. This, however, is not the case – a majority of the corrosion is limited to the sites on the bar where the coating is penetrated. Therefore, it is necessary to convert the ECR corrosion rates to an equivalent "exposed area" corrosion rate by multiplying by the ratio of the surface area of the bar to the area of intentional damage on the bar, 192. The corrosion rates for the bare bar systems also assume the entire area of steel is corroding. Autopsy results from field test specimens, however, indicated that corrosion covers only about 40 percent of the total area for bars in cracked concrete (Darwin et al. 2011). Because corrosion only occurs on limited regions of the bar, the corrosion rates for bare bars in cracked concrete are multiplied by 2.5 to obtain a macrocell corrosion rate based on effective area undergoing corrosion loss for these systems. The converted corrosion rates for both uncoated and coated bars are listed in Table 17.

Table 17: Equivalent field test specimen corrosion rates based on effective area, μm/yr

Steel Designation[a]	FTS Corrosion Rate (Total Area)	FTS Corrosion Rate (Effective Area)
Conv.	4.09	10.2[b]
ECR	0.272	52.2[c]
2304	1.10	2.75[b]
2304p	-	-
SSClad	-	-

FTS = Field test specimen

[a] Conv. = conventional reinforcement, ECR = epoxy-coated reinforcement, 2304 = 2304 stainless steel

[b] Assuming corrosion products form over 40 percent of the bar surface

[c] Based on exposed area

5.1.3 Corrosion Loss to Cause Concrete Cracking

Based on work done by Darwin et. al (2011), the corrosion loss in μm required to cause the formation of cracks (often described as delamination cracks) in concrete can be expressed as

$$x_{crit} = 13.5\left(\frac{C^{2-A_f}}{D^{0.38}L_f^{\ 0.1}A_f^{\ 0.6}} + 0.6\right)\times 3^{A_f-1} \qquad (8)$$

where
x_{crit} = corrosion loss at crack initiation, μm
C = cover, in.
D = bar diameter, in.
L_f = fractional length of bar corroding, $L_{corroding}/L_{bar}$
A_f = fractional surface area of bar corroding, $A_{corroding}/A_{bar}$

For a No. 5 uncoated conventional steel bar with a concrete cover of 2.5 in. $L_f = A_f = 0.4$ (since 40% of the surface area corrodes in field specimens), the value of x_{crit} is 72 μm. For the

same bar with 3.0 in. cover, x_{crit} is 94 µm. For a No. 5 epoxy-coated bar with a damage pattern equal to that used for the field test specimens (1/8-in. diameter holes spaced at 4.9 in. on each side of the bar), the fractional length of exposed bar L_f is 0.024, the fractional area of exposed bar A_f is 0.0023, and the value of x_{crit} is 1826 µm. For the same bar with 3.0 in. cover the value of x_{crit} is 2627 µm. For the purposes of the analysis, the bars in bridge decks are assumed to have the same damage pattern as the bars in the field tests.

5.1.4 Propagation Time

The time from corrosion initiation to initial cracking of the concrete cover caused by expansive corrosion products (propagation time) for each system is found by taking the corrosion losses required to crack concrete, calculated above, and dividing by the estimated total corrosion rates listed in Table 17. The estimated times to first cracking after corrosion initiation are presented in Table 18. Conventional reinforcement has a time to cracking of 7.0 years with 2.5 in. of cover and 9.2 years with 3 in. of cover. Epoxy-coated reinforcement has a time to cracking of 35 years with 2.5 in. of cover and 50 years with 3.0 in. of cover. 2304 stainless steel has a time to cracking of 26 years with 2.5 in. of cover and 34 years with 3.0 in. of cover. Like the effect of additional cover on the time to corrosion initiation (shown in Table 14), additional cover increases the time between corrosion initiation and the formation of delamination cracks in the concrete. Table 18 shows that using 3.0 in. of cover instead of 2.5 in. of cover will increase the time to cracked concrete by 2.2 years for conventional reinforcement, 8.3 years for 2304 stainless steel reinforcement, and 15 years for ECR. This is in addition to the increased time to corrosion initiation shown in Table 14.

Table 18: Estimated times to formation of initial delamination cracks after corrosion initiation (propagation time), yrs

Steel Designation[a]	Time to Cracked Concrete 2.5 in. Cover	Time to Cracked Concrete 3.0 in. Cover
Conv.	7.0	9.2
ECR	35	50
2304	26	34

[a] Conv. = conventional reinforcement, ECR = epoxy-coated reinforcement with ten 1/8-in. diameter holes through the epoxy, 2304 = 2304 stainless steel.

5.1.5 Time to First Repair

The time to first repair for each system is found by combining the time to corrosion initiation, the time to initial delamination cracking of the concrete after corrosion initiation, and the time from first cracking to the time when the deck is repaired. The latter period is based on the observation that a bridge deck does not undergo full repair when the first crack forms. Rather, the bridge typically undergoes a series of short-term temporary repairs first. To account for this period, a 10-year delay between first cracking and repair is assumed based on the experience of KDOT. Tables 19a and 19b show the total estimated times from construction to first repair for each system with 2.5. and 3.0-in covers, respectively. With a 2.5-in. cover, conventional reinforcement has a time to first repair of 19 years compared to values 53.4 years for epoxy-coated reinforcement and 80 years for 2304 stainless steel. With 3.0 in. of cover, the

times to first repair increase to 21.9 years for conventional reinforcement, 70 years for epoxy-coated reinforcement, and 96 years for 2304 stainless steel. Repickled 2304 and stainless steel clad reinforcement are expected to have times to first repair greater than 100 years.

Table 19a: Time to first repair based on corrosion rate in cracked concrete with 2.5 in. of cover, yrs

Steel Designation[a]	Time to Initiation	Time from Initiation to Cracking	Time from Cracking to Repair	Expected Time to First Repair
Conv.	2.1	7.0	10	19
ECR	8.4	35	10	53
2304	44	26	10	80.0
2304p	> 44	-	10	> 100*
SSClad	> 47	-	10	> 100*

Table 19b: Time to first repair based on corrosion rate in cracked concrete with 3.0 in. of cover, yrs

Steel Designation[a]	Time to Initiation	Time from Initiation to Cracking	Time from Cracking to Repair	Expected Time to First Repair
Conv.	2.7	9.2	10	22
ECR	10	50	10	70
2304	52	34	10	96
2304p	> 44	-	10	> 100*
SSClad	> 47	-	10	> 100*

[a] Conv. = conventional reinforcement, ECR = epoxy-coated reinforcement with ten 1/8-in. diameter holes through the epoxy, 2304 = 2304 stainless steel as received, 2304p = repickled 2304 stainless steel, SSClad = stainless steel clad reinforcement

*Assumed, since specimen did not corrode.

5.2 COST EFFECTIVENESS

Seventy-five and 100-year economic lives are used to compare the costs associated with the different types of reinforcing steel for a typical bridge deck. A 150-ft-long, 42.2-ft-wide, 8-in.-thick bridge deck with concrete cover of 2.5 in. is used in the analysis. Costs include those for initial construction and repair over the design life. With the exception of the reinforcing steel costs, which were obtained from the manufacturers, costs are based on winning bids for new construction in 2012 and full-deck replacements in Oklahoma from 2006 through 2012. Specific project costs used to calculate averages are included in Appendix E. User costs are not included in the analysis.

5.2.1 Initial cost

In most cases the material costs for reinforcement used in this analysis are provided by the material suppliers; the exception is the cost of stainless steel clad reinforcement, which was obtained from a study published by the Michigan Department of Transportation (Kahl 2012) because the manufacturer is no longer in business. The base cost for conventional reinforcement is $0.35/lb, ECR has a base cost of $0.99/lb, and 2304 stainless steel has a base

cost of \$2.40/lb. Stainless steel clad reinforcement has a base cost of \$1.77/lb. A placement cost of \$0.52/lb is used for all reinforcement. A steel reinforcement density of 246 lb/yd^3 is used, based on the average quantity of steel used in 15 bridge decks constructed in Oklahoma in 2012. An 8-in.-thick bridge deck requires 54.7 lb /yd^2 of steel based on the surface area of deck, as shown in Eq. (9).

$$\frac{246\,\text{lb}}{\text{yd}^3} \times \frac{8}{36}\,\text{yd} = 54.7\,\text{lb / yd}^2 \tag{9}$$

Using the required reinforcement per unit surface area determined using Eq. (9), the reinforcement costs for each system are calculated, as shown in Eq. (10) through (13).

Conventional reinforcement:

$$\frac{\$0.35 + \$0.52}{\text{lb}} \times 54.7\,\frac{\text{lb}}{\text{yd}^2} = \$47.59 / \text{yd}^2 \tag{10}$$

ECR:

$$\frac{\$0.99 + \$0.52}{\text{lb}} \times 54.7\,\frac{\text{lb}}{\text{yd}^2} = \$82.60 / \text{yd}^2 \tag{11}$$

2304 Stainless steel:

$$\frac{\$2.40 + \$0.52}{\text{lb}} \times 54.7\,\frac{\text{lb}}{\text{yd}^2} = \$159.72 / \text{yd}^2 \tag{12}$$

Stainless Steel Clad Reinforcement:

$$\frac{\$1.76 + \$0.52}{\text{lb}} \times 54.7\,\frac{\text{lb}}{\text{yd}^2} = \$124.72 / \text{yd}^2 \tag{13}$$

The base in-place cost of concrete used in this study is \$518.40/yd^3 based on costs for new bridge decks let in 2012 in Oklahoma. Assuming an 8-in.-thick bridge deck, 0.222 yd^3 of concrete are required per 1 yd^2 surface area of deck. Concrete cost is calculated using Eq. (14).

$$\frac{\$518.40}{\text{yd}^3} \times 0.222\,\text{yd} = \$115.18 / \text{yd}^2 \tag{14}$$

The total initial cost, i.e. the sum of reinforcement and concrete costs, for each system is shown in Table 20. A deck with conventional reinforcement has the lowest initial cost at \$162.77/yd^2 of bridge deck. A deck containing 2304 stainless steel has the highest initial cost at \$362.42/yd^2. Properly pickled 2304 stainless steel has the same initial cost as poorly pickled stainless steel.

Table 20: Total in-place cost for new deck construction, $/yd^2

Steel Designation	Reinforcement Cost	Concrete Cost	Total Cost
Conv.	$47.59	$115.18	$162.77
ECR	$82.60	$115.18	$197.78
2304	$159.72	$115.18	$274.90
2304p	$159.72	$115.18	$274.90
SSClad	$124.72	$115.18	$239.90

5.2.2 Repair Costs

Repair costs for the bridge deck are based on full deck replacement costs in Oklahoma from 2006 to 2012. Full deck replacement is chosen because it is the most commonly used means of repair in Oklahoma. Current data include repair of bridge decks with conventional reinforcement only because bridge decks constructed in Oklahoma since the late 1970s have been constructed using ECR and have not needed repair as of the date of this report. It is estimated that repair costs of bridge decks with ECR will be similar to those for decks with conventional reinforcement.

A typical full-deck repair project includes costs for concrete, reinforcing steel, bridge rail replacement or repair, approach guard rail modifications, approach pavement work, mobilization, traffic control, and removal of the existing deck. Minor bid items such as erosion control, replacing bearing pads, and clearing and grubbing, though typical, are not included in this analysis. Table 21 shows a summary of repair costs per square yard of deck, excluding the cost of reinforcing steel. Equation (15) gives the calculations for the bridge rail modification cost. The calculation for the approach guard rail is given by Eq. (16).

Table 21: Deck replacement costs for bridge decks in Oklahoma excluding reinforcement costs

Item	Unit	Unit Cost[a]	Cost per yd^2
Concrete	per yd^2	$168.10	$168.10
Concrete bridge rail	per linear ft	$80.81	$63.83
Guardrail	Lump sum	$10,940.92	$15.59
Approach pavement work	Lump sum	$50,182.98	$71.49
Mobilization	Lump sum	$51,234.90	$72.98
Traffic control	Lump sum	$44,877.64	$63.93
Remove bridge existing deck	Lump sum	$75,011.36	$106.85
Total repair costs			$562.77

[a] Costs were obtained from winning bids on full deck replacement projects in Oklahoma from 2006 through 2012

Concrete Bridge Rail:

$$\frac{\$81.81}{\text{ft}} \times 150\,\text{ft} \times \frac{2\,\text{sides}}{\text{bridge}} \times \frac{1}{42.2\,\text{ft bridge width}} \times \frac{\text{yd}^2}{9\,\text{ft}^2} = \$63.83 / \text{yd}^2 \quad (15)$$

Guardrail:

$$\frac{\$10{,}941}{\text{project}} \times \frac{\text{deck area}}{703\,\text{yd}^2} = \$15.59 / \text{yd}^2 \quad (16)$$

The total repair cost is the sum of the reinforcement cost and the other repair costs (Table 21). Table 22 shows the deck replacement costs per square yard of bridge deck. Conventionally reinforced decks have a total replacement cost of $610.36/yd^2, which is much greater than the $162.77/yd^2 initial cost. The same is true of decks containing epoxy coated reinforcement and 2304 stainless steel, which have replacement costs of $645.37/yd^2 and $722.49/yd^2, respectively, and are also much greater than the respective initial costs of $197.78 and $274.90 /yd^2.

Table 22: Total deck replacement costs with conventional and epoxy coated reinforcement, $/yd^2

Steel Designation	Reinforcement Cost	Other Repair Costs	Total Cost
Conv.	$47.59	$562.77	$610.36
ECR	$82.60	$562.77	$645.37
2304	$159.72	$562.77	$722.49

The time between repairs is calculated based on the assumption that the full deck will be replaced using the same reinforcement type so that corrosion would proceed as it would with new construction. Therefore, the time from first repair to the subsequent repair is assumed to be the same as the time to first repair. This contrasts with a common practice of the Kansas DOT to repair bridge decks using a partial depth repair, exposing the top mat of reinforcement and applying a high-density silica fume overlay, which has been found to provide 25 years before the next repair is needed for a conventionally reinforced bridge deck.

5.2.3 Present Value

The total life cycle cost of each type of reinforcement is calculated using the time to first repair for systems in cracked concrete listed in Table 19. Cost effectiveness is based on the initial cost of the deck and the present value of future repair costs. The present value is calculated as shown Eq. (17), where *P* is the present value, *F* is the future cost of a repair, *i* is the discount rate, and n is the time to repair.

$$P = F\left(1+i\right)^{-n} \quad (17)$$

For this study, discount rates of 2, 4, and 6 percent are used. A value of 2 percent is used for most of the discussion that follows because state governments typically use lower rather than higher discount rates. Tables 23 and 24 show the estimated costs over 75 and 100-year design lives.

For a 75-year design life, the deck with conventional reinforcement must be replaced three times and the deck with ECR must be replaced once. The decks with 2304 stainless steel and stainless steel clad reinforcement do not require replacement.

Table 23: Total costs ($/yd^2) over 75-year design life for types of reinforcement using time to first repair based on corrosion rates in cracked concrete

Steel Designation	Initial Cost, $/yd^2	Time to Repair, years			Repair Cost, $/yd^2	Present Cost, $/yd^2		
		1	2	3		i=2%	i=4%	i=6%
Conv.	163	19.6	39.2	58.8	610	1048	638	440
ECR	198	53.4	-	-	645	422	277	227
2304	275	-	-	-	-	275	275	275
2304p	275	-	-	-	-	275	275	275
SSClad	240	-	-	-	-	240	240	240

Because it requires three repairs and has the lowest time to first repair, conventional reinforcement has the highest present cost, $1048/yd^2 at a 2 percent discount rate. ECR is significantly more cost effective, $422/yd^2 than conventional reinforcement because it only requires one replacement during a 75-year design life, despite having a higher initial cost. 2304 stainless steel reinforcement has a significantly higher initial cost at $275 compared to ECR at $198, but at a 2 percent discount rate, the present cost is lower ($275 compared with $422) because it does not require replacement during a 75-year life. Stainless steel clad reinforcement appears to be the most cost-effective steel with a present cost of $240/yd^2, although this type of reinforcement is not currently available.

Table 24 shows the estimated costs over a 100-year design life using the time to first repair based on the corrosion rate in cracked concrete. Under this scenario the conventionally reinforced deck must repaired five times, the deck containing epoxy-coated reinforcement must be replaced once, and the 2304 stainless steel reinforced deck must be replaced once. Decks constructed with properly pickled 2304 and stainless steel clad reinforcement do not require replacement. Compared with a 75-year design life, the conventionally reinforced deck and the deck containing poorly-pickled 2304 reinforcement have higher present costs at $1265 and $423/yd^2, respectively because each requires one or more replacements. The present cost of a deck reinforced with ECR remains at $422/yd^2 for a 100-year design life, less than the deck reinforced with poorly-pickled 2304 . Present costs for properly pickled 2304 and stainless steel clad reinforced decks do not increase from a 75-year design life because replacements are not needed.

Table 24: Total costs ($/yd^2) over 100-year design life for types of reinforcement using time to first repair based on corrosion rates in cracked concrete

Steel Designation	Initial Cost, $/yd^2	Time to Repair, years					Repair Cost, $/yd^2	Present Cost, $/yd^2		
		1	2	3	4	5		i=2%	i=4%	i=6%
Conv.	163	19.6	39.2	58.8	78.4	98	610	1265	679	448
ECR	198	53.4	-	-	-	-	645	422	277	227
2304	275	80	-	-	-	-	722	423	306	282
2304p	275	-	-	-	-	-	-	275	275	275
SSClad	240	-	-	-	-	-	-	240	240	240

5.3. DISCUSSION

Conventional reinforcement had the lowest initial cost of the types of reinforcement in this study. The low chloride threshold and high corrosion rate, however, result in the early replacement of the bridge deck. A bridge with conventional reinforcement will need to be replaced many times over the 75 or 100 year design life, resulting in the highest life cycle cost of all the types of reinforcement in this study.

Epoxy-coated reinforcement also has a low initial cost, and needs repair far less frequently than conventional reinforcement-only once over a 100 year design life. ECR and poorly pickled 2304 have nearly identical costs over a 100-year design life.

The performance of 2304 stainless steel reinforcement was hindered somewhat by poor surface finish of the bars in the as-received condition. This problem is not unique to 2304 steel. When not properly pickled, many stainless steels perform significantly worse than pickled stainless steels in terms of corrosion resistance (Balma et al. 2002). The 2304 stainless steel evaluated in this study performed well even in the poorly-pickled condition. However, near the end of the cracked beam test, the 2304 reinforcement showed significant increases in corrosion rate, which could significantly reduce the time to first repair if continued. Long-term field specimens are needed to evaluate the performance of poorly pickled reinforcement. Until such results are available, it is important to ensure stainless steel is properly pickled to ensure a long design life. Specifications for stainless steel reinforcing bars should include wording to the effect that “the bars shall be pickled to a bright or uniformly light finish.”

Stainless steel clad reinforcement performed very well in terms of corrosion resistance and life cycle cost; however, its benefits are mitigated by several factors. Although stainless steel clad reinforcement exhibited low overall corrosion rates, many individual cracked beam specimens had corrosion rates exceeding the ASTM A955 limits. This raises concerns about the long-term performance of these bars. The life expectancy of stainless steel clad reinforcement is based on the performance of straight bars. As observed earlier, bending stainless steel clad reinforcement can in some cases introduce defects in the coating that allow corrosion to occur much earlier than would otherwise be expected. Care should be taken when fabricating stainless steel clad bars to avoid damaging the coating. It is also important to protect the cut ends of a stainless steel clad bar with a cap. Failure to do so will significantly shorten the time to first repair. The supplier of stainless steel clad reinforcement used in this study has declared bankruptcy, and the bars are not currently available. Bars produced in a similar manner should perform in a similar manner; if another stainless steel is used as a cladding, that steel should be evaluated for suitability before being used in a bridge deck.

It is worth considering methods of lowering life cycle cost other than changing the reinforcement in the deck. The cost of a full deck replacement is very high-much higher than the

initial cost of the deck. As a result, any repair drives the life cycle cost up. Other repair methods, such as partial deck replacements, have shown satisfactory performance at a much lower cost (Darwin et al. 2011). Switching to partial deck replacement, especially on decks with ECR, could significantly lower the life cycle cost of a deck.

Another means of lowering life cycle cost is to increase the clear cover to the reinforcement from 2.5 inches to 3 inches. As noted above, this has the dual benefit of increasing the time to corrosion initiation and increasing the amount of corrosion loss required to crack concrete, resulting in an extra 12.6 years before first repair for ECR and an extra 18.9 years before first repair for poorly-pickled 2304 stainless steel.

Mixing stainless steel and conventional reinforcement will reduce initial cost. No galvanic effects were observed on stainless steel clad reinforcement, and no or minor effects were observed on 2304 during testing., Conventional reinforcement, however, did exhibit an increase rate in corrosion rate when paired with these steels. Since chlorides will eventually reach the bottom mat of conventional steel in a bridge decks, a deck with a bottom mat of conventional steel will see accelerated corrosion on the bottom mat, as has been observed on decks with epoxy-coated reinforcement in the top mat and conventional steel in the bottom mat. Because a partial deck replacement is not an option for repairing the bottom mat of steel, the entire deck will need to be replaced when this occurs. Therefore, the use of conventional reinforcement in the bottom mat and stainless steel in the top mat is not recommended as a cost-saving measure.

6. SUMMARY AND CONCLUSIONS

6.1 SUMMARY

The corrosion resistance of 2304 stainless steel reinforcement and NX-SCR™ stainless steel clad reinforcement was evaluated and compared to conventional and epoxy-coated reinforcement (ECR). 2304 stainless steel was tested in both the as-received condition, having a dark mottled finish suggesting a problem with the pickling process, and repickled to a bright shiny finish. Specimens were evaluated using rapid macrocell, Southern Exposure, and cracked beam tests. ECR and stainless steel clad specimens were evaluated with the coating with no intentional damage and with the coating or cladding penetrated. ECR with the coating penetrated is used to represent ECR that has undergone damage during construction. Clad bars were also bent to evaluate the corrosion resistance of the cladding after fabrication.

Bars were tested for corrosion loss and corrosion initiation. The critical chloride corrosion threshold for each system was established, as was an average corrosion rate after initiation. Results obtained from bench-scale specimens are used to estimate cost effectiveness for each system under a 75-year and 100-year service life.

6.2 CONCLUSIONS

The following conclusions are based on the research presented in this report.

1. Epoxy-coated reinforcement and NX-SCR™ stainless steel clad bars with and without intentional penetrations in the coating, as well as 2304 stainless steel in the as-received and repickled conditions exhibit a significant increase in corrosion resistance and critical chloride corrosion threshold compared to conventional steel, with undamaged epoxy-coated specimens exhibiting the lowest corrosion rate.
2. In the as-received condition, 2304 stainless steel did not satisfy the requirements for either test method in ASTM A955. While 2304 stainless steel in the macrocell test did exhibit an average corrosion rate below 0.25 µm/yr, the corrosion rate of individual specimens exceeded 0.50 µm/yr. In the cracked beam test, both the individual and average corrosion rates of 2304 in the as-received condition exceeded the corrosion rate limits of ASTM A955.
3. The repickled 2304 stainless steel satisfied the requirements of ASTM A955, with an average corrosion rate not exceeding 0.25 µm/yr and the corrosion rate of the individual specimens not exceeding 0.50 µm/yr for the macrocell test. Through 72 weeks, all cracked beam repickled 2304 specimens are within the limits set by ASTM A955.
4. The undamaged, capped NX-SCR™ stainless steel clad bars satisfied the requirements of the rapid macrocell test in ASTM A955. However, some cracked beam specimens containing NX-SCR™ stainless steel clad bars exceeded the ASTM A955 requirements for maximum allowable corrosion rate, suggesting the cladding needs to be improved to ensure sufficient corrosion performance. While bent NX-SCR™ bars showed acceptable performance on average, isolated corrosion was observed on some individual specimens. Corrosion will occur at the cut end of an uncapped stainless steel clad bar if not protected.
5. In the rapid macrocell test, 2304 stainless steel showed a slightly increased corrosion rate when paired with a conventional steel cathode compared to specimens with a 2304 stainless steel cathode, suggesting possible galvanic corrosion effects. No such effect,

however, was noted for 2304 paired with a conventional steel cathode in the Southern Exposure tests. No galvanic corrosion effect was noted for stainless steel clad reinforcement in any test.

6. Rapid macrocell and Southern Exposure specimens with conventional reinforcement as top bars and 2304 stainless steel reinforcement as bottom bars show greater average corrosion rates and losses than conventional reinforcement alone, although no significant difference was observed in the critical chloride corrosion threshold. Similar specimens with stainless steel clad reinforcement as bottom bars showed no increase in corrosion rate.
7. Conventional steel has the shortest time to first repair, 19 years, and is the least cost-effective, at $\$1265/yd^2$ over a 100-year design life based on a 2 percent discount rate. 2304 stainless steel in the as-received condition (80 years to first repair) is the next most costly, at $\$423/yd^2$. ECR with penetrations through the epoxy, which is typical of ECR in practice (53 years to first repair), is more cost effective, at $\$422/yd^2$. Correctly pickled 2304 stainless steel does not require repair over 100 years and is the second most cost effective, at $\$275/yd^2$. Stainless steel clad reinforcement is the most cost-effective reinforcement in this study ($\$240/yd^2$); however, it is not currently available, and its failure to pass ASTM A955 calls its long-term performance into question.

6.3 RECOMMENDATIONS

1. Conventional reinforcement is not a cost-effective material for bridge decks exposed to chlorides and should not be used in those environments.

2. Stainless steel clad reinforcement is a cost effective reinforcement in bridge decks; however, it should be handled in a manner similar to ECR during fabrication to minimize damage to the cladding, and any cut ends should be sealed with a protective cap.

3. Specifications for stainless steel reinforcement should require that the steel “shall be pickled to a bright or uniformly light finish” to ensure acceptable performance.

4. Any stainless steel clad reinforcement should be evaluated for corrosion resistance before use; it may represent a cost-effective solution if test performance is acceptable.

5. Increasing the cover over the top mat of steel and considering partial-deck replacements, where applicable, are methods that should be considered to decrease life cycle costs.

REFERENCES

AASHTO T 260-97, 2005. “Standard Method of Test for Sampling and Testing for Chloride Ion in concrete and Concrete Raw Materials,” Standard Specifications for Transportation Materials and Methods of Sampling and Testing, AASHTO. pp. T 260-1 – T 260-10.

ASTM A775, 2007, “Epoxy-Coated Steel Reinforcing Bars (ASTM A775/A775M-07b),” ASTM International, West Conshohocken, PA, 11 pp.

ASTM A955, 2012, “Standard Specification for Plain and Deformed Stainless-Steel Bars for Concrete Reinforcement (ASTM A955/A955M-12),” ASTM International, West Conshohocken, PA, 11 pp.

ASTM C876, 2009, “Standard Test Method for Corrosion Potentials of Uncoated Reinforcing Steel in Concrete,” ASTM International, West Conshohocken, PA, 7 pp.

Balma, J., Darwin, D., Browning, J. P., and Locke, C. E., 2005. “Evaluation of Corrosion Protection Systems and Corrosion Testing Methods for Reinforcing Steel in Concrete,” *SM Report* No. 76, University of Kansas Center for Research, Inc., Lawrence, Kansas, 517 pp.

Cady, P. D., and Gannon, E. J., 1992. “Condition Evaluation of Concrete Bridges Relative to Reinforcement in Concrete”, SHRP-S/FR-92-103, Vol. 1, State of the Art of Mixing Methods, Strategic Highway Research Program, National Research Council, Washington, D.C., 70 pp.

Clemeña, G. G., 2002. “Testing of Selected Metallic Reinforcing Bars for Extending the Service Life of Future Concrete Bridges: Summary of Conclusions and Recommendations,” VTRC 03-R7, Virginia Transportation Research Council, Charlottesville, Virginia, 8 pp.

Cross, W. M., Duke E. F., Kellar, J. J., Han, K. N., and Johnston, D., 2001. “Stainless Steel Clad Rebar in Bridge Decks,” *Report* No. SD2000-04-F, South Dakota Department of Transportation Report, , 55 pp.

Darwin, D., Locke, C. E,, Balma, J., Kahrs, J. T., 1999. “Evaluation of Stainless Steel Clad Reinforcing Bars,” *SL Report* 99-3, University of Kansas Center for Research, Inc., Lawrence, Kansas, 17 pp.

Darwin, D., Browning, J., Nguyen, T. V., and Locke, C. E., 2002 “Mechanical and Corrosion Properties of a High-Strength, High Chromium Reinforcing Steel for Concrete”, *Report* No. SD2001-05-F, South Dakota Department of Transportation.

Darwin, D., Browning, J., Nguyen, T. V., and Locke, C. E., 2007. “Evaluation of Metallized Stainless Steel Clad Reinforcement,” *Report* No. SD2002-16-F, South Dakota Department of Transportation, , 156 pp.

Darwin, D., Browning, J.P., O’Reilly, M., Xing, L. and Ji, J., 2009, “Critical Chloride Corrosion Threshold of Galvanized Reinforcing Bars,” *ACI Materials Journal*, Vol. 106, No. 2, March/April 2009, 8 pp.

Darwin, D., Browning, J., O’Reilly, M., Locke, C. E., and Virmani, Y. P., 2011. “Multiple Corrosion Protection Systems for Reinforced Concrete Bridge Components,” *Publication* No. FHWA-HRT-11-060, Federal Highway Administration, November 2011, 255 pp.

Draper, J., Darwin, D., Browning, J., Locke, C. E., 2009. “Evaluation of Multiple Corrosion Protection Systems for Reinforced Concrete Bridge Decks,” *SM Report No. 96,* University of Kansas Center for Research, Inc., Lawrence, Kansas, December 2009, 429 pp.

Fliz, J., Akshey, S., Li, D., Kyo, Y., Sabol, S., Pickering, H., and Osseo-Asare, K., 1992. “Condition Evaluation of Concrete Bridges Relative to Reinforcement Corrosion – Volume 2 – Method for Measuring the Corrosion Rate of Steel in Concrete,” Strategic Highway Research Program.

Hartt W. H., Powers, R. G., Marino, F. P., Paredes, M., Simmons, R., Yu, H., Himiob, R., and Virmani, Y. P., 2009. “Corrosion Resistant Alloys for Reinforced Concrete,” *Publication No. FHWA-HRT-09-020,* Federal Highway Administration, April 2009, 146 pp.

Ji, J., Darwin, D., and Browning, J., 2005. “Corrosion Resistance of Duplex Stainless Steels and MMFX Microcomposite Steel for Reinforced Concrete Bridge Decks,” *SM Report* No. 80, University of Kansas Center for Research, Inc., Lawrence, KS, 453 pp.

Jones, D. A., 1992. *Principles and Prevention of Corrosion,* Macmillan Publishing Company, New York, 568 pp.

Kahl, S., 2012. “Stainless and Stainless-Clad Reinforcement for Highway Bridge Use,” Michigan Department of Transportation Operations Field Services Division, Lansing, Michigan, 26 pp

Kahrs, J. T., Darwin, D., and Locke, C. E., 2001. “Evaluation of Corrosion Resistance of Type 304 Stainless Steel Clad Reinforcing Bars,” *SM Report* No. 65, University of Kansas Center for Research, Inc., Lawrence, Kansas, 76 pp

Kepler, J. L., Darwin, D., and Locke, C.E., 2000. “Evaluation of Corrosion Protection Methods for Reinforced Concrete Highway Structures”, *SM Report* No. 58, University of Kansas Center for Research, Lawrence, KS.

Lindquist, W. D., Darwin, D., and Browning, J., 2005. “Cracking and Chloride Contents in Reinforced Concrete Bridge Decks,” *SM Report* No. 78, University of Kansas Center for Research, Lawrence, KS.

Lindquist, W. D., Darwin, D., Browning, J., and Miller, G.G., 2006. “Effect of Cracking on Chloride Content in Concrete Bridge Decks,” *ACI Materials Journal*, American Concrete Institute, Farmington Hills, MI., Vol. 103, No. 6, pp. 467–473,

Locke, C., 1985. “Corrosion of Steel in Portland Cement Concrete: Fundamental Studies,” *ASTM Special Technical Publication, Corrosion Effect of Stray Currents and the Techniques for Evaluating Corrosion of Rebars in Concrete,* pp. 5-14.

Manning, D., 1996. “Corrosion Performance of Epoxy-Coated Reinforcing Steel: North American Experience,” *Construction and Building Materials*, Vol. 10, No. 5, Jul. pp. 349-365.

McDonald, D. B., Pfeifer, D. W., and Sherman, M. R., 1998. “Corrosion Evaluation of Epoxy-Coated, Metallic-Clad and Solid Metallic Reinforcing Bars in Concrete,” *Publication* No. FHWA-RD-98-153, Federal Highway Administration, McLean, VA, December., 127 pp.

Miller, G. G. and Darwin, D., 2000. “Performance and Constructability of Silica Fume Bridge Deck Overlays”, *SM Report* No. 57, University of Kansas Center for Research, Lawrence, KS, 423 pp.

O'Reilly, M., Sturgeon, W. J., Darwin, D., and Browning, J., 2010. "Rapid Macrocell Tests of LDX 2101® Stainless Steel Bars," *SL Report* 10-2, University of Kansas Center for Research, Inc., Lawrence, Kansas,, 42 pp.

O’Reilly, M., Darwin, D., Browning, J., and Locke, C. E., 2011. “Evaluation of Multiple Corrosion Protected Systems for Reinforced Concrete Systems” *SM Report* No. 100, University of Kansas Center for Research, Inc., Lawrence, Kansas, January 2011, 535 pp.

Sagues, A., Powers, R., and Kessler, R., 1994. “Corrosion Processes and Field Performance of Epoxy-Coated Reinforcing Steel in Marine Substructures,” *NACE Conference-Corrosion ’94.* Paper No. 299, 15 pp.

Scully, J. R. and Hurley, M. F., 2007. “Investigation of the Corrosion Propagation Characteristics of New Metallic Reinforcing Bars,” *Final Report*, VTRC 07-CR9, Virginia Transportation Research Council, Charlottesville, Virginia, 58.pp.

Smith, J. and Virmani, P., 1996. “Performance of Epoxy-Coated Rebars in Bridge Decks,” *Report* No. FHWA-RD-96-092, Federal Highway Administration, Washington, D.C.

Sturgeon, W. J., O'Reilly, M., Darwin, D., and Browning, J., 2010a. "Rapid Macorcell Tests of Endurament® 32 Stainless Steel Bars," *SL Report 10-5*, University of Kansas Center for Research, Inc., Lawerence, Kansas, November 2010. 17 pp.

Sturgeon, W. J., O'Reilly, M., Darwin, D., and Browning, J., 2010b. “Rapid Macrocell Tests of ASTM A775, A615, and A1035 Reinforcing Bars” *SL Report* 10-4, University of Kansas Center for Research, Inc., Lawrence, Kansas, November 2010, 46 pp.

Sturgeon, W. J., O'Reilly, M., Darwin, D., and Browning, J., 2011. "Rapid Macorcell Tests of Endurament® 33, Endurament® 316LN, and Endurament® 2205 Stainless Steel Bars," *SL Report 11-1*, University of Kansas Center for Research, Inc., Lawerence, Kansas, January 2011. 24 pp.

Yunovich, M., Thompson, N. G., Balvanyos, T., and Lave, L., 2002. “Highway Bridges,” Appendix D, *Corrosion Cost and Preventive Strategies in the United States*, by G. H. Koch, M. PO. H. Broongers, N. G. Thompson, Y. P. Virmani, and J. H. Payer, *Report No*. FHWA-RD-01-156, Federal Highway Administration, McLean, Virginia, March, 773 pp.

APPENDIX A

CORROSION RATE, LOSS, AND POTENTIALS OF LABORATORY SPECIMENS

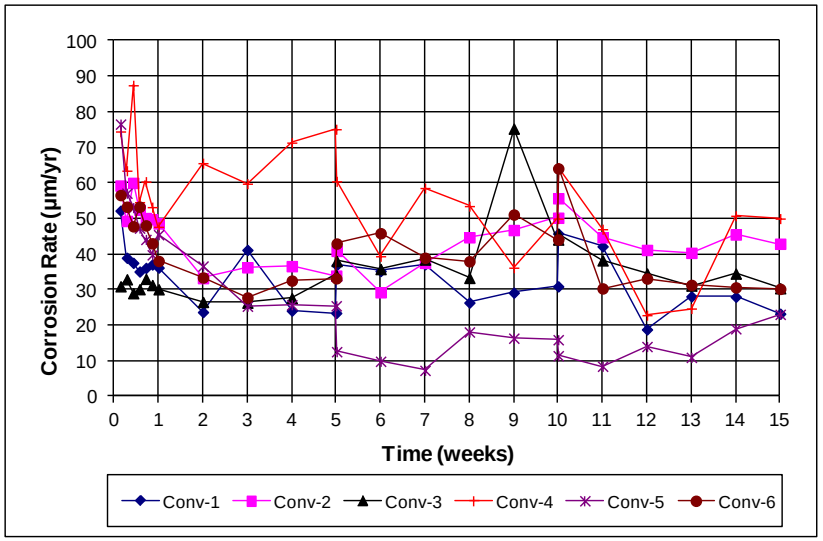

(a)

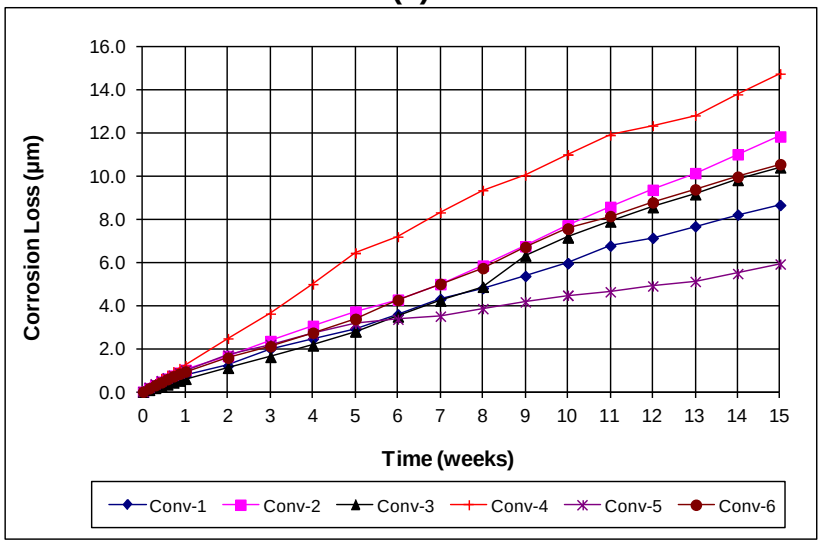

(b)

Figure A.1: (a) Corrosion rate and (b) total corrosion losses for conventional macrocell specimens

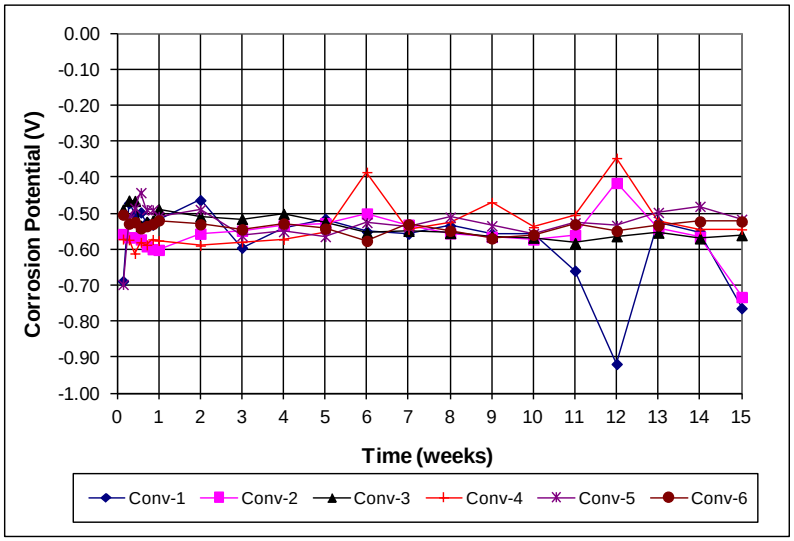

(a)

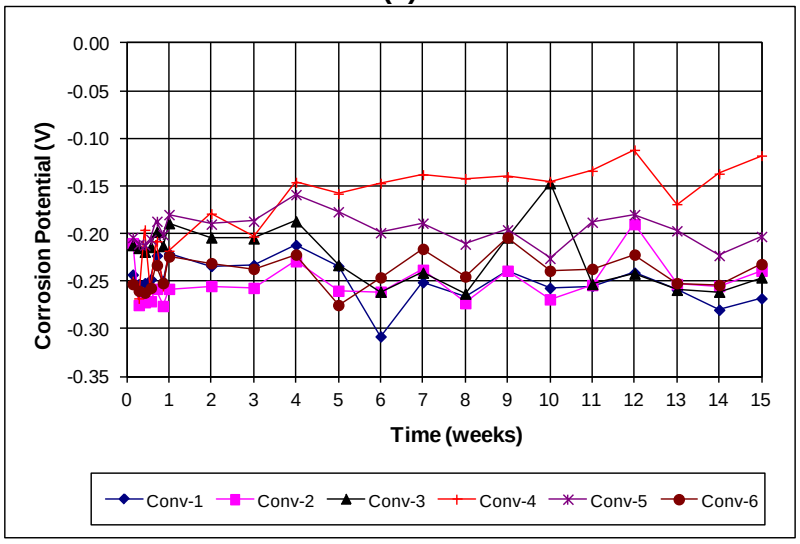

(b)

Figure A.2: (a) Top mat corrosion potentials and (b) bottom mat corrosion potentials for conventional macrocell specimens

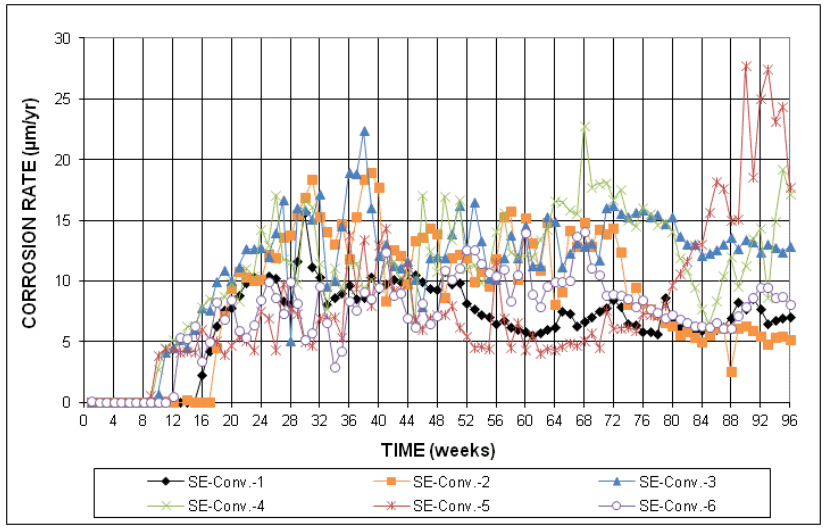

(a)

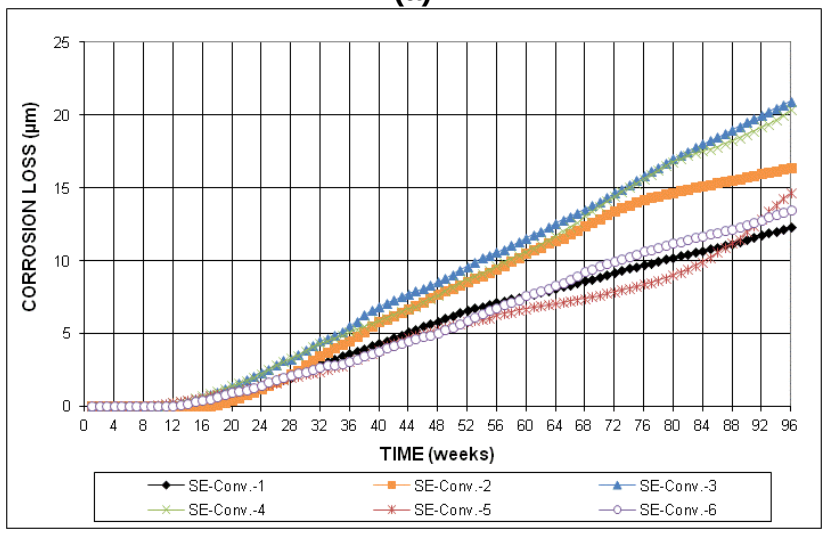

(b)

Figure A.3: (a) Corrosion rate and (b) total corrosion losses for conventional Southern Exposure specimens

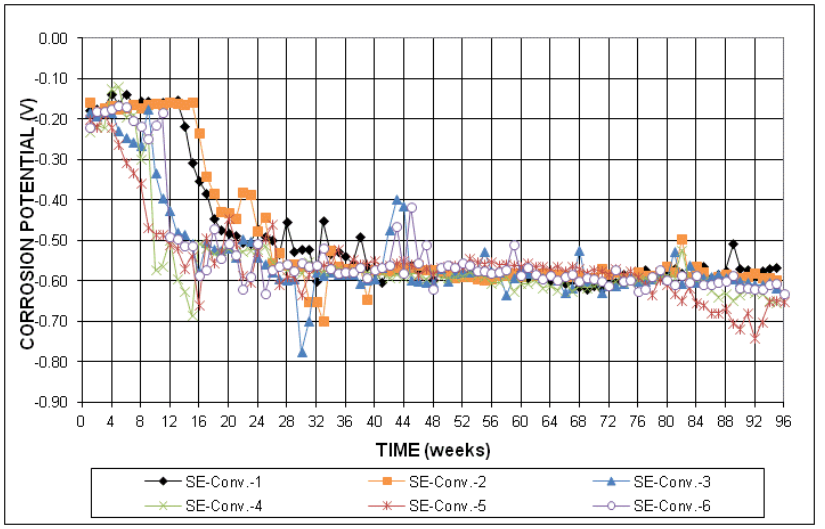

(a)

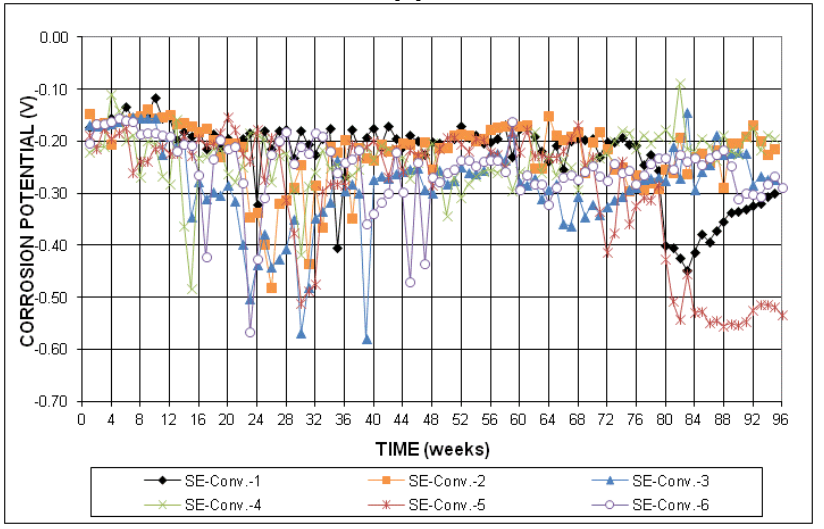

(b)

Figure A.4: (a) Top mat corrosion potentials and (b) bottom mat corrosion potentials for conventional Southern Exposure specimens

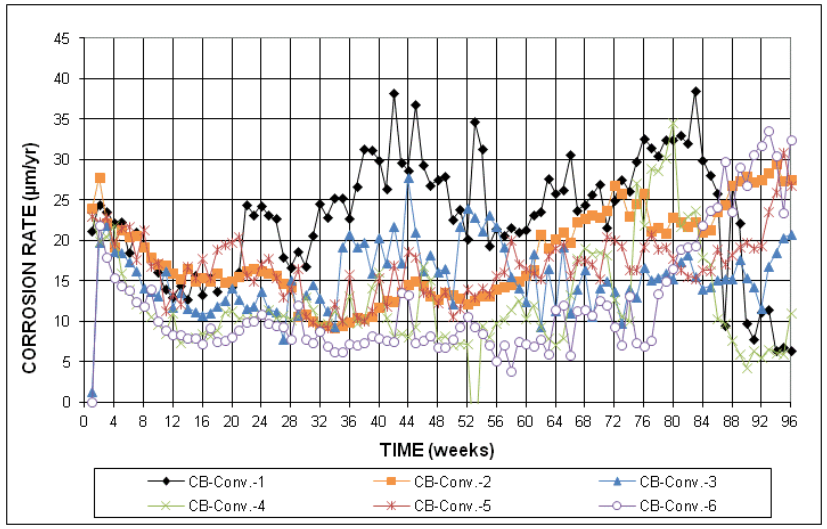

(a)

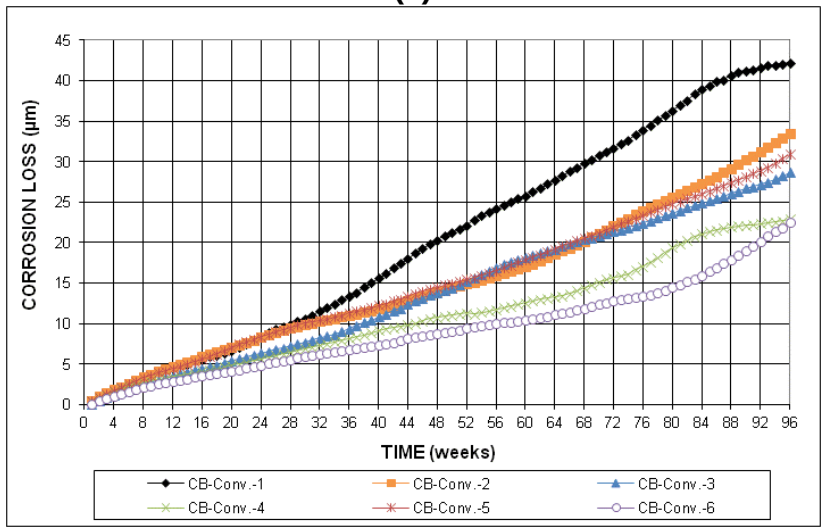

(b)

Figure A.5: (a) Corrosion rate and (b) total corrosion losses for conventional cracked beam specimens

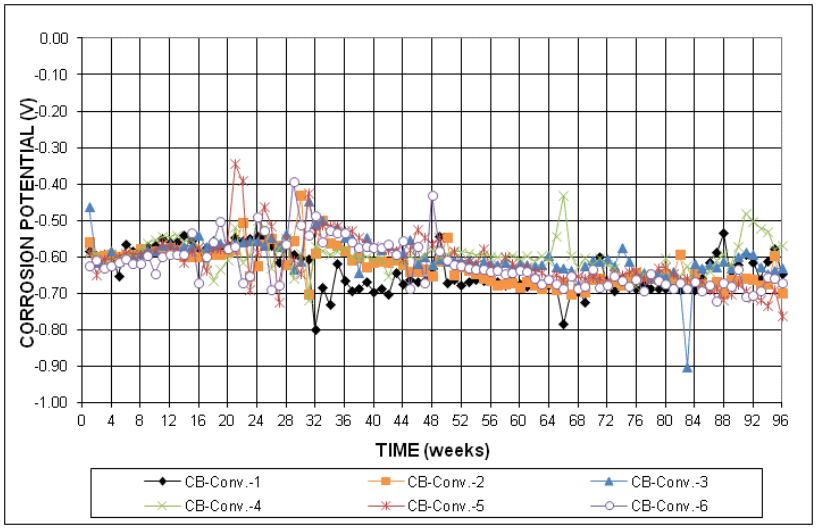

(a)

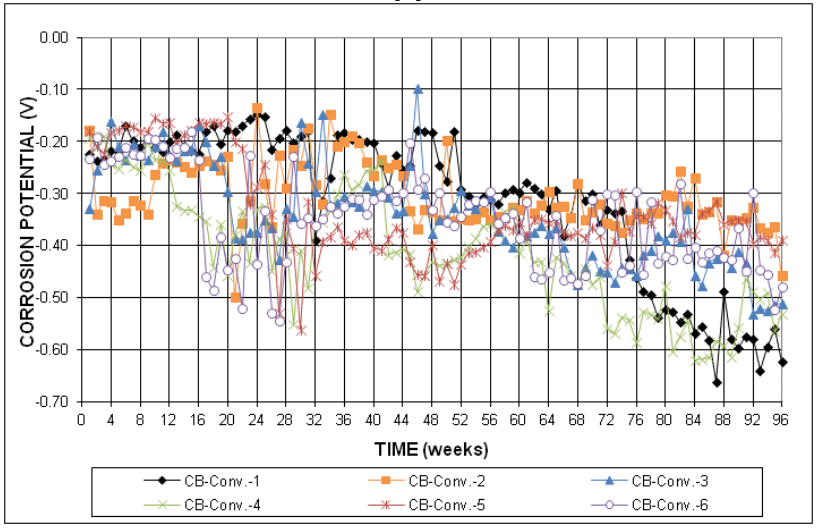

(b)

Figure A.6: (a) Top mat corrosion potentials and (b) bottom mat corrosion potentials for conventional cracked beam specimens

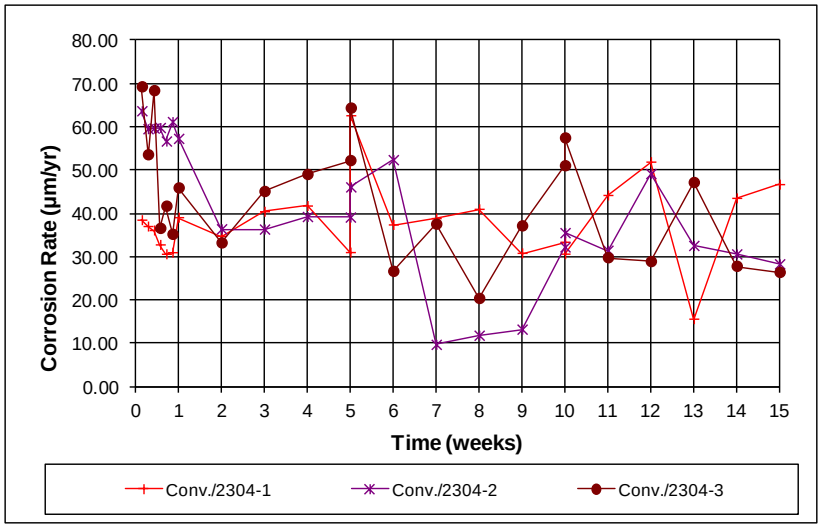

(a)

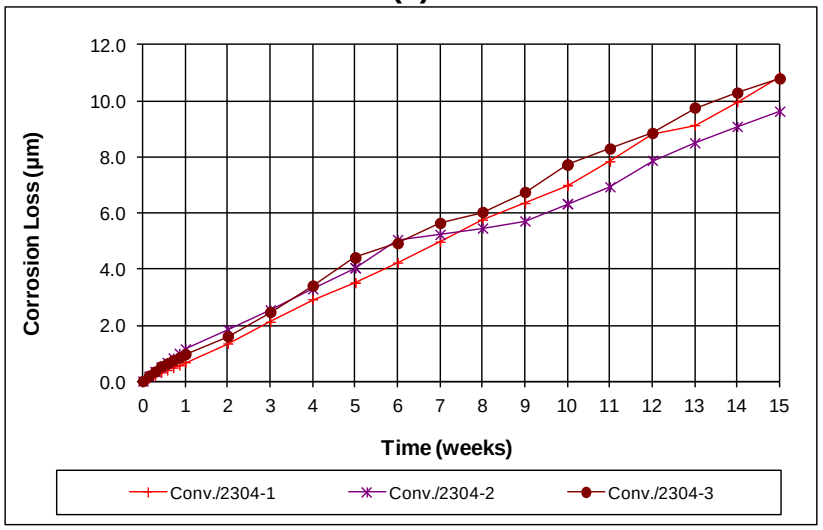

(b)

Figure A.7: (a) Corrosion rate and (b) total corrosion losses for conventional (anode) with 2304 stainless steel (cathode) macrocell specimens

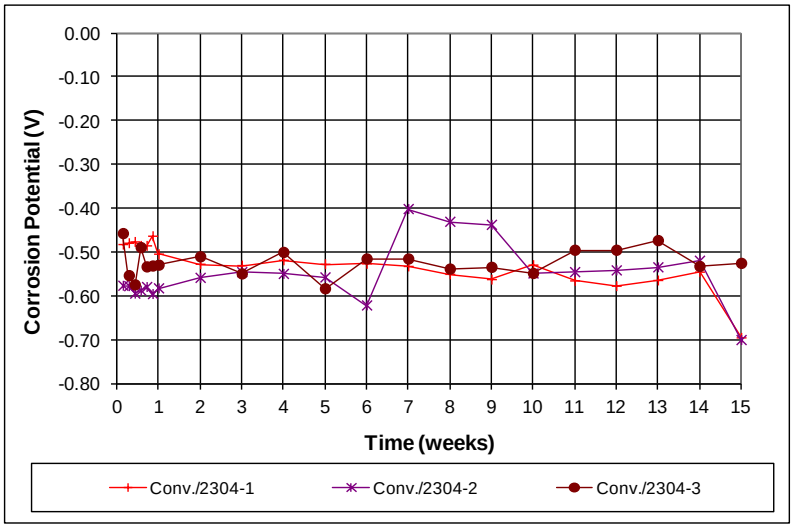

(a)

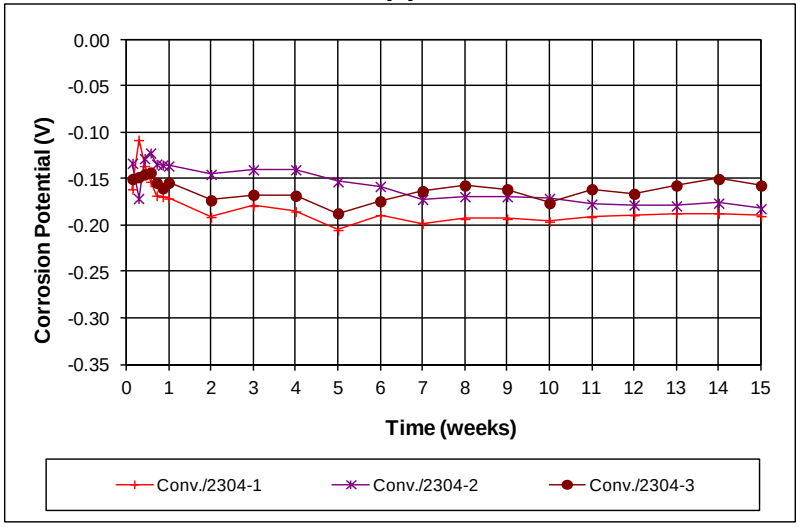

(b)

Figure A.8: (a) Top mat corrosion potentials and (b) bottom mat corrosion potentials for conventional (anode) with 2304 stainless steel (cathode) macrocell specimens

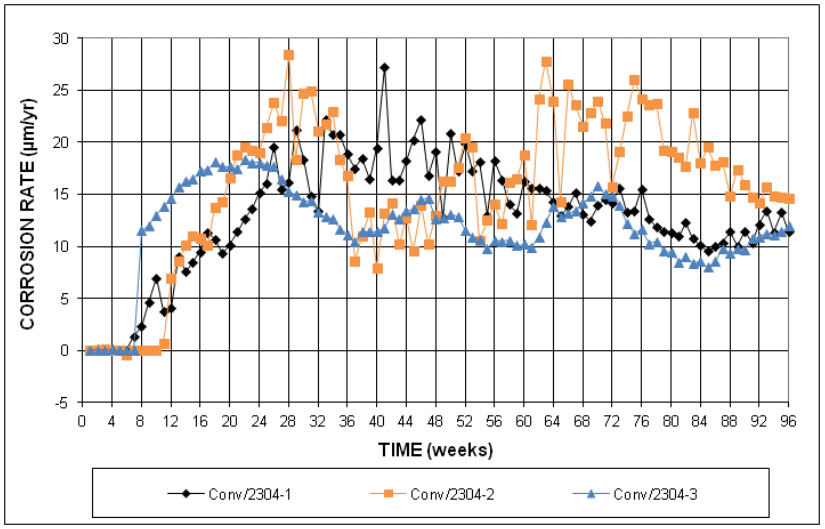

(a)

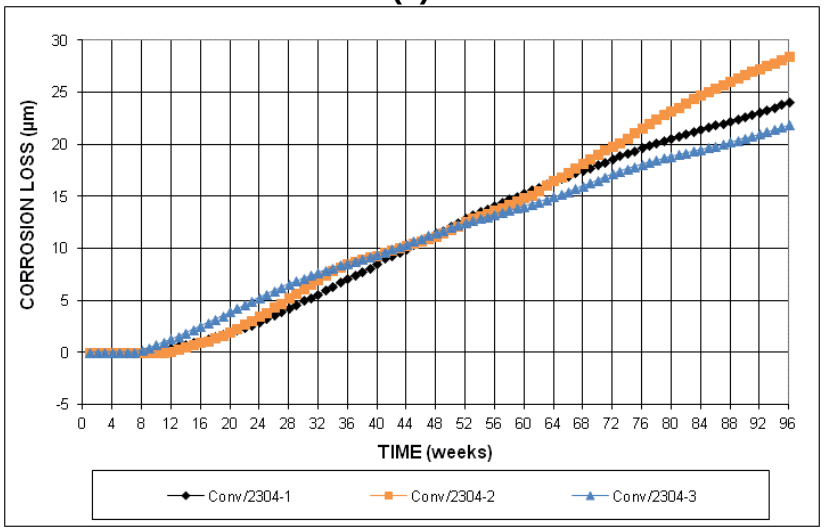

(b)

Figure A.9: (a) Corrosion rate and (b) total corrosion losses for conventional (anode) with 2304 stainless steel (cathode) Southern Exposure specimens

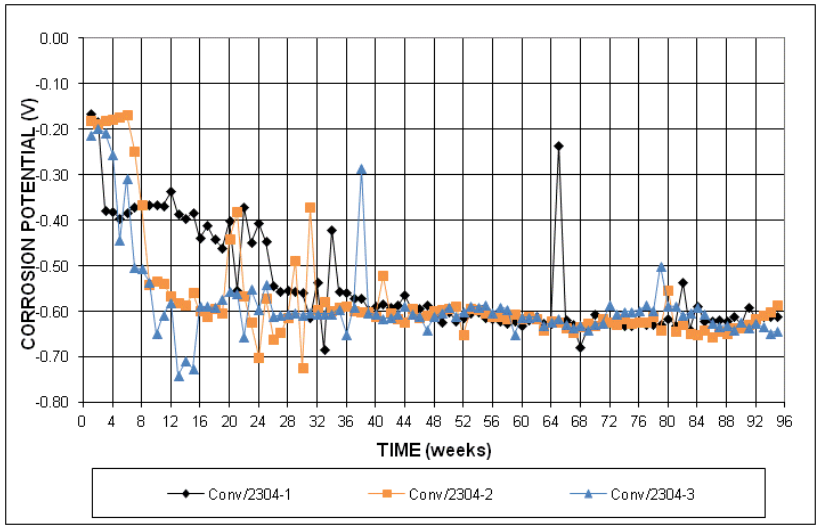

(a)

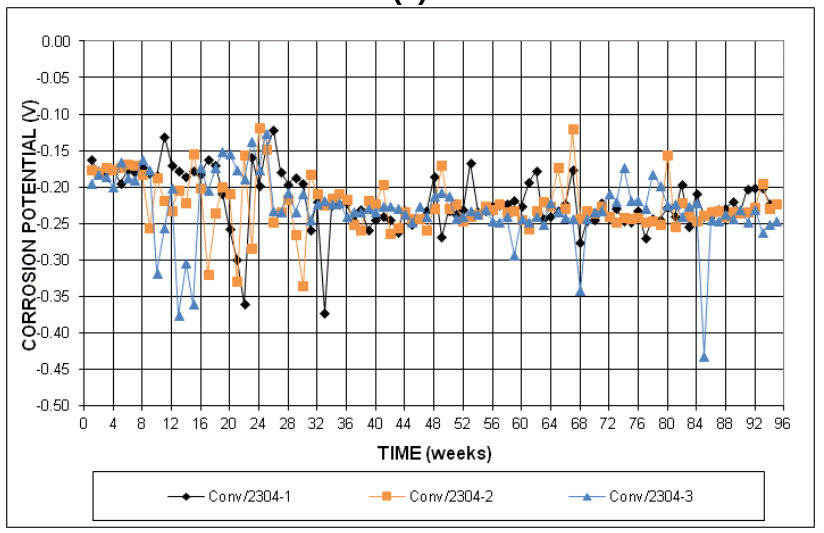

(b)

Figure A.10: (a) Top mat corrosion potentials and (b) bottom mat corrosion potentials for conventional (anode) with 2304 stainless steel (cathode) Southern Exposure specimens

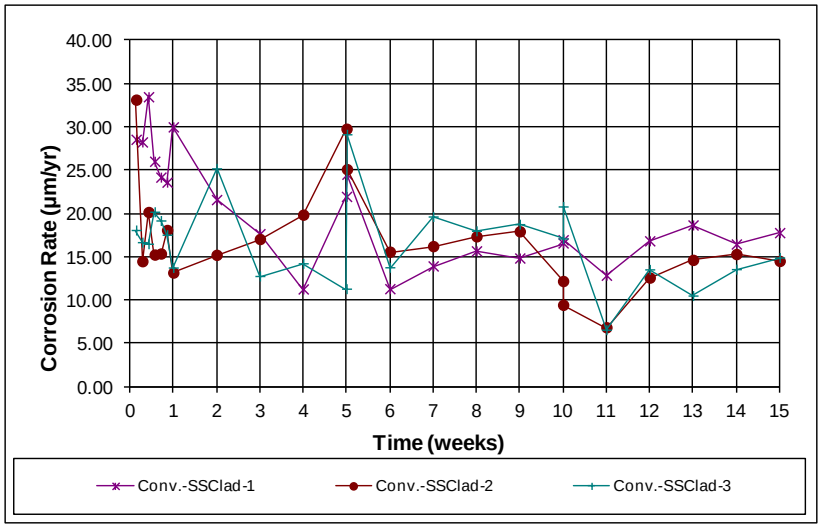

(a)

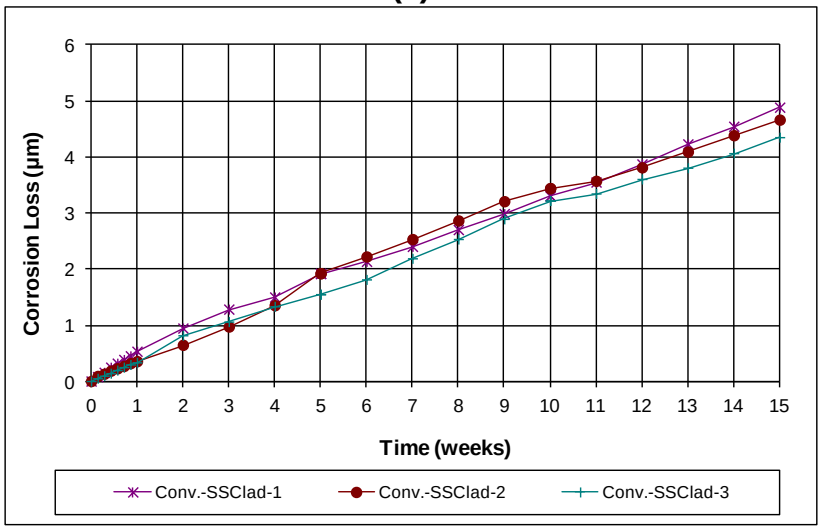

(b)

Figure A.11: (a) Corrosion rate and (b) total corrosion losses for conventional (anode) with SSClad (cathode) macrocell specimens

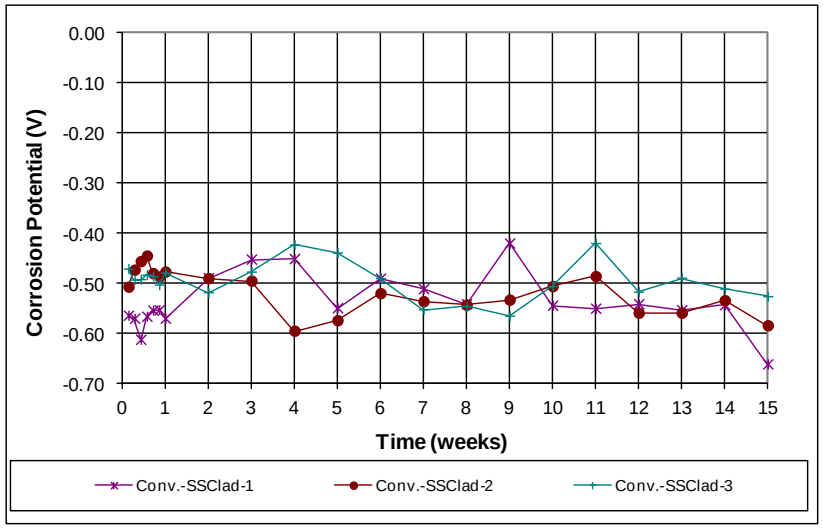

(a)

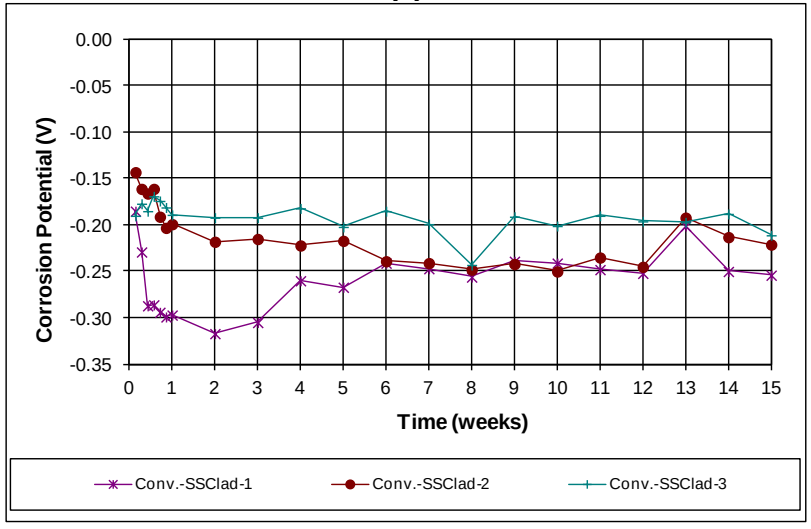

(b)

Figure A.12: (a) Top mat corrosion potentials and (b) bottom mat corrosion potentials for conventional (anode) with SSClad (cathode) macrocell specimens

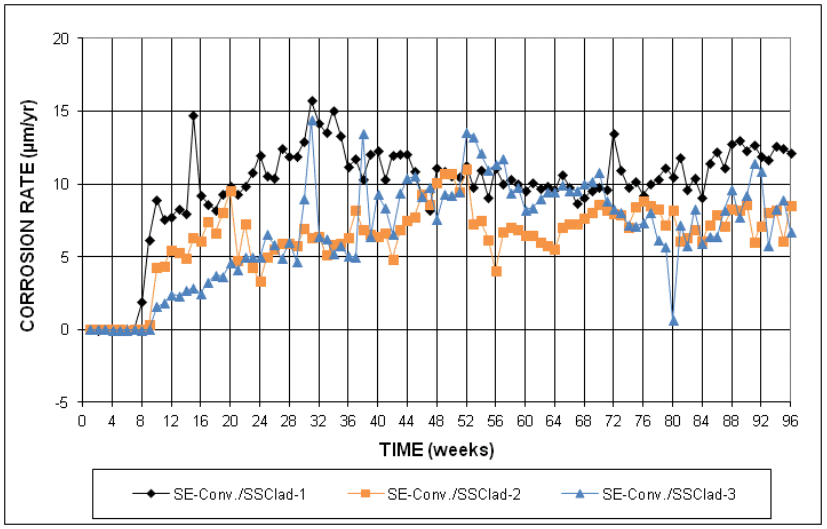

(a)

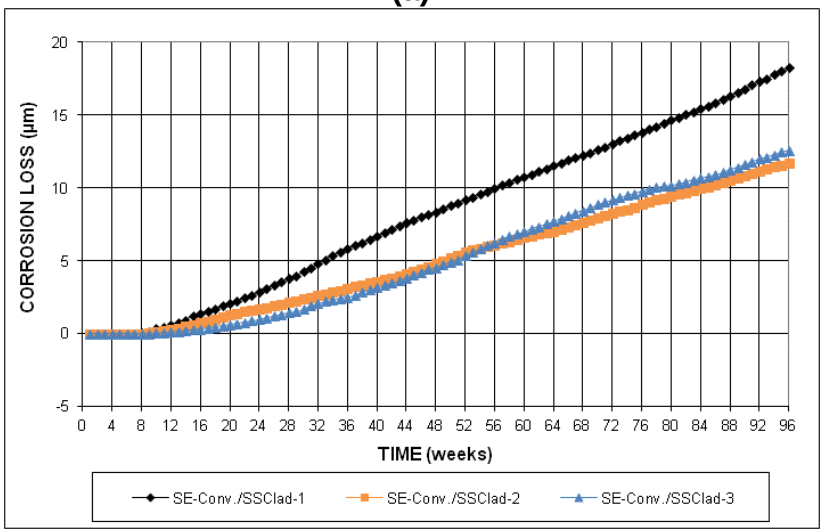

(b)

Figure A.13: (a) Corrosion rate and (b) total corrosion losses for conventional (anode) with SSClad (cathode) Sothern Exposure specimens

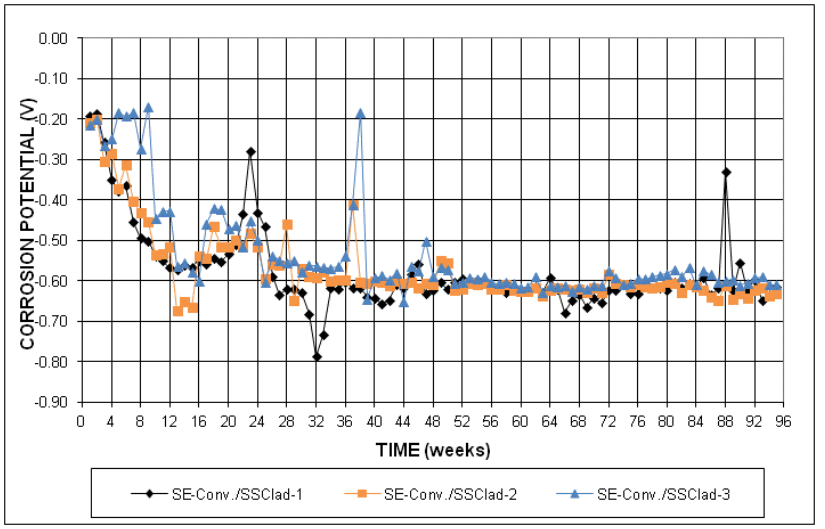

(a)

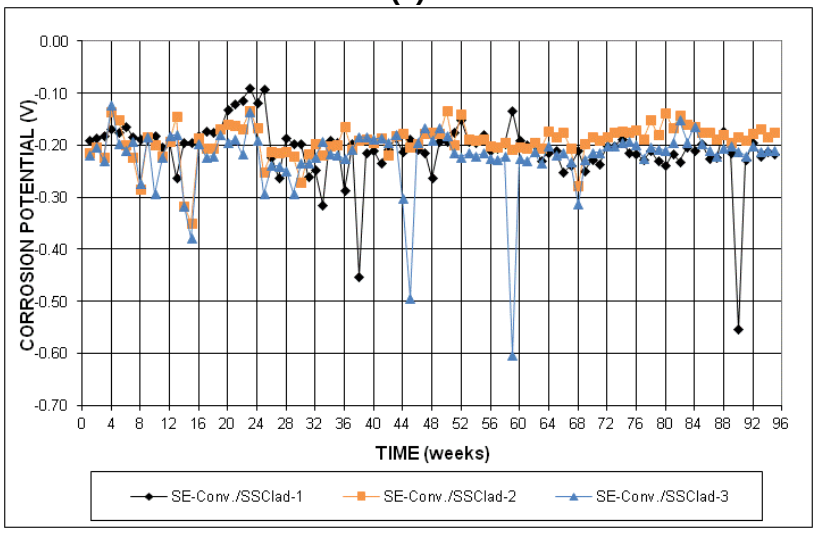

(b)

Figure A.14: (a) Top mat corrosion potentials and (b) bottom mat corrosion potentials for conventional (anode) with SSClad (cathode) Southern Exposure specimens

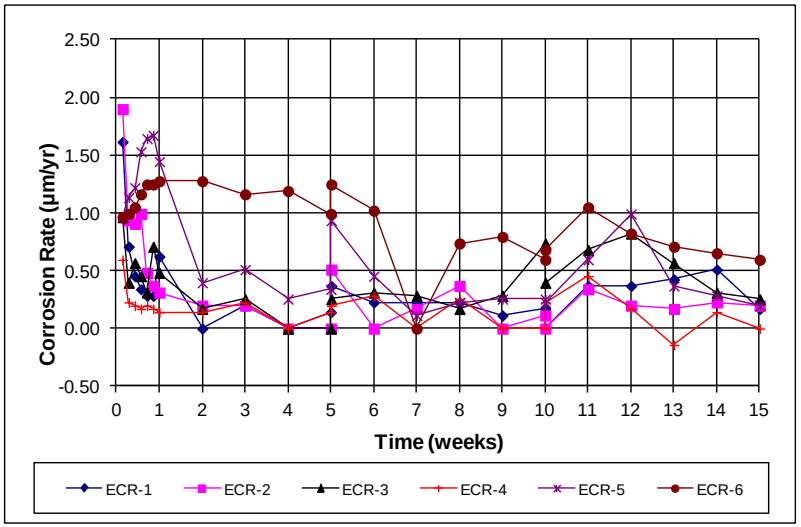

(a)

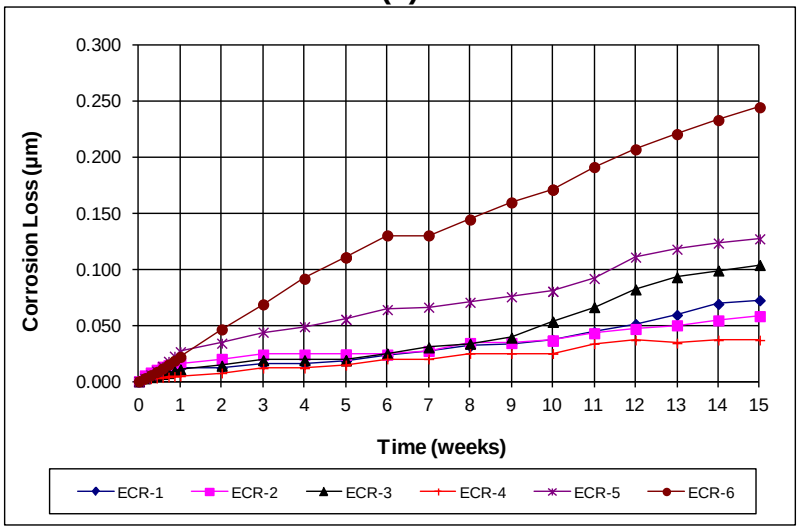

(b)

Figure A.15: (a) Corrosion rate and (b) total corrosion losses for ECR macrocell specimens

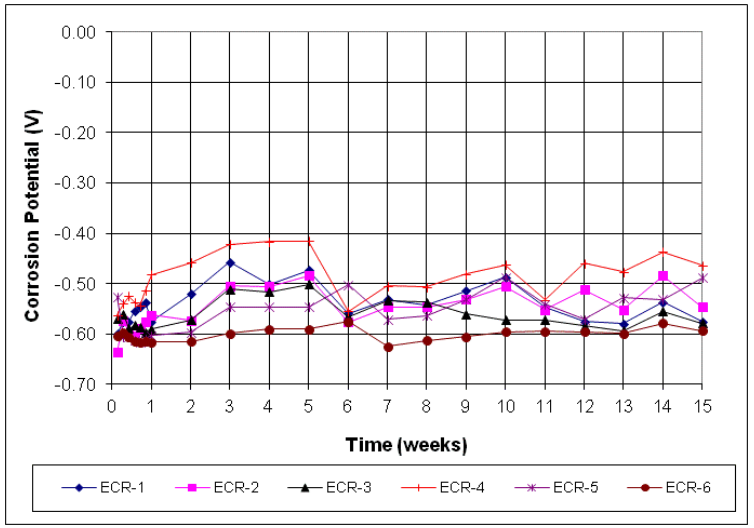

(a)

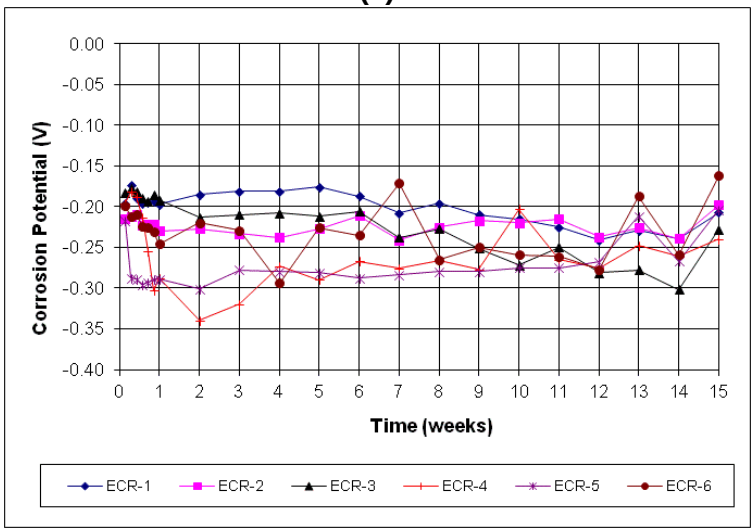

(b)

Figure A.16: (a) Top mat corrosion potentials and (b) bottom mat corrosion potentials for ECR macrocell specimens

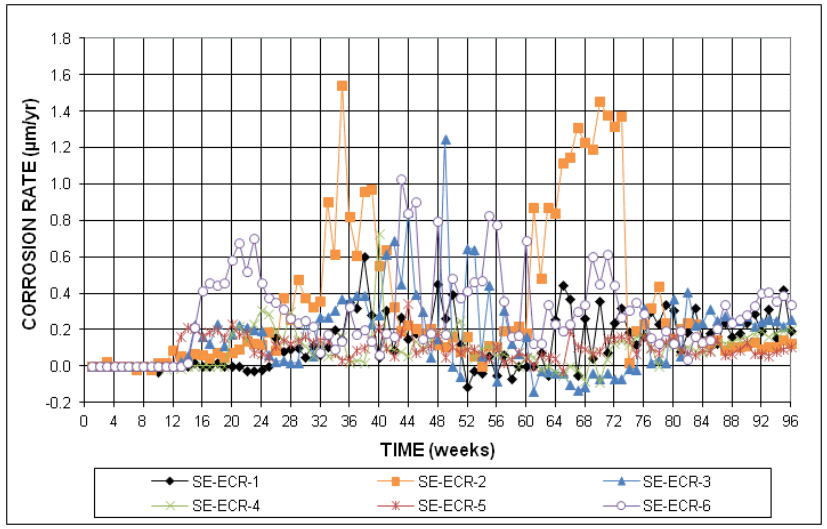

(a)

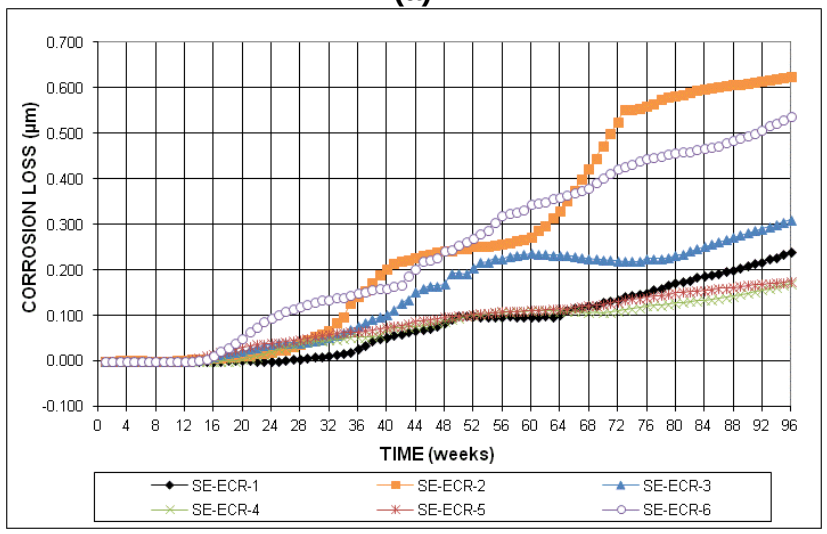

(b)

Figure A.17: (a) Corrosion rate and (b) total corrosion losses based on total area for ECR Southern Exposure specimens

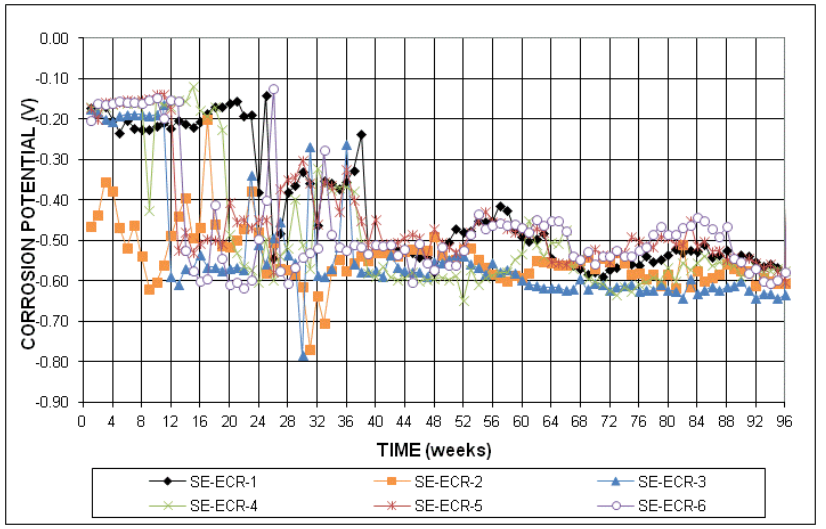

(a)

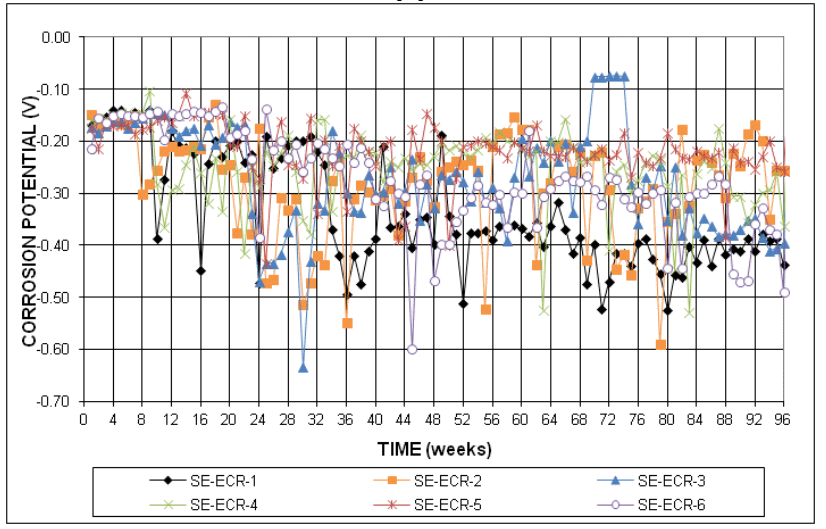

(b)

Figure A.18: (a) Top mat corrosion potentials and (b) bottom mat corrosion potentials ECR Southern Exposure specimens

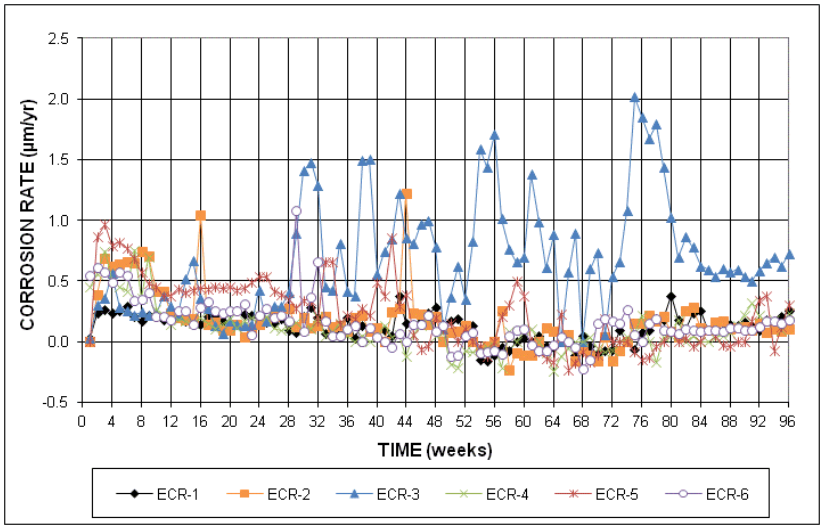

(a)

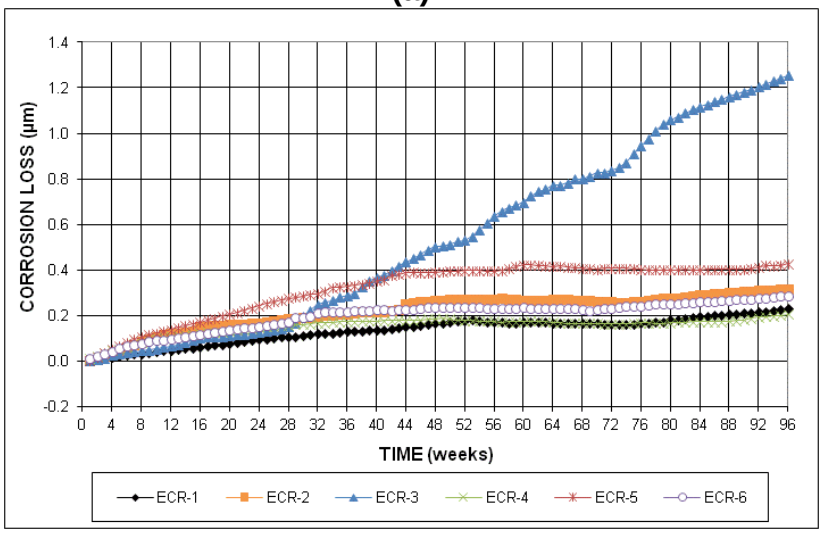

(b)

Figure A.19: (a) Corrosion rate and (b) total corrosion losses based on total area for ECR cracked beam specimens

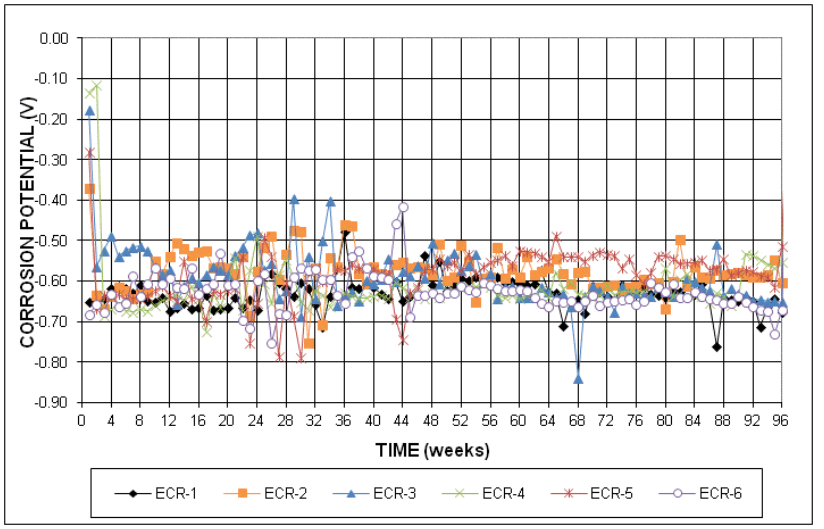

(a)

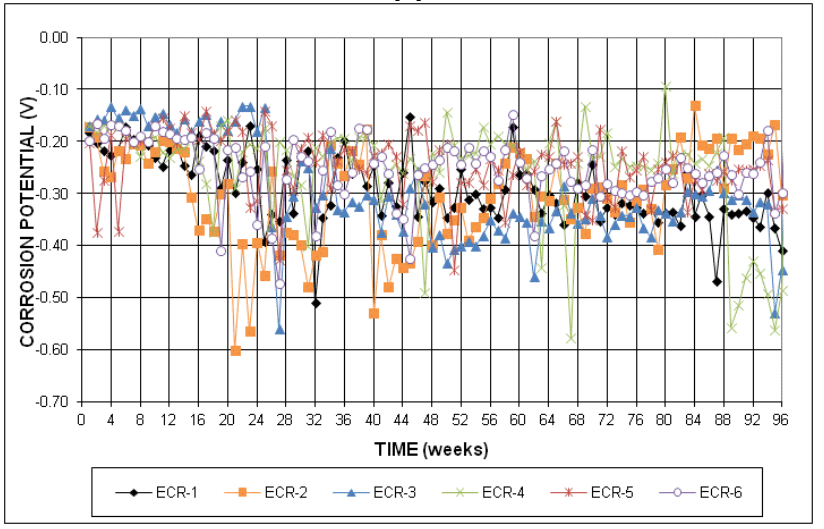

(b)

Figure A.20: (a) Top mat corrosion potentials and (b) bottom mat corrosion potentials for ECR cracked beam specimens

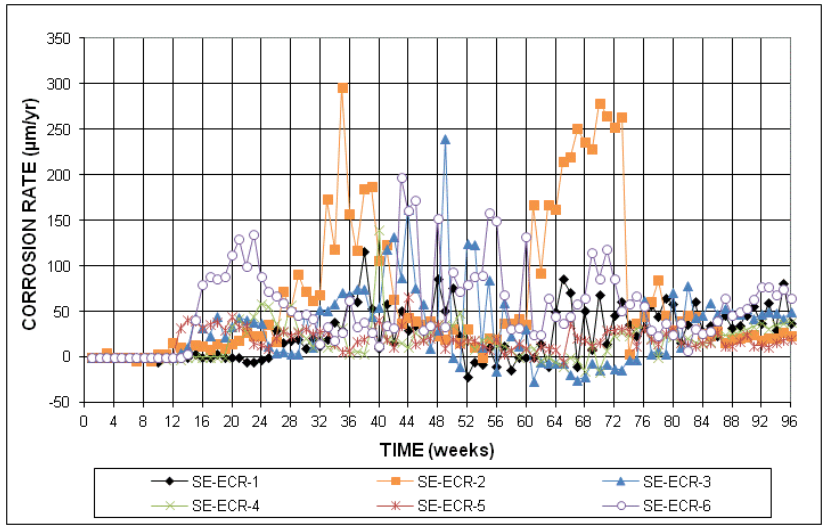

(a)

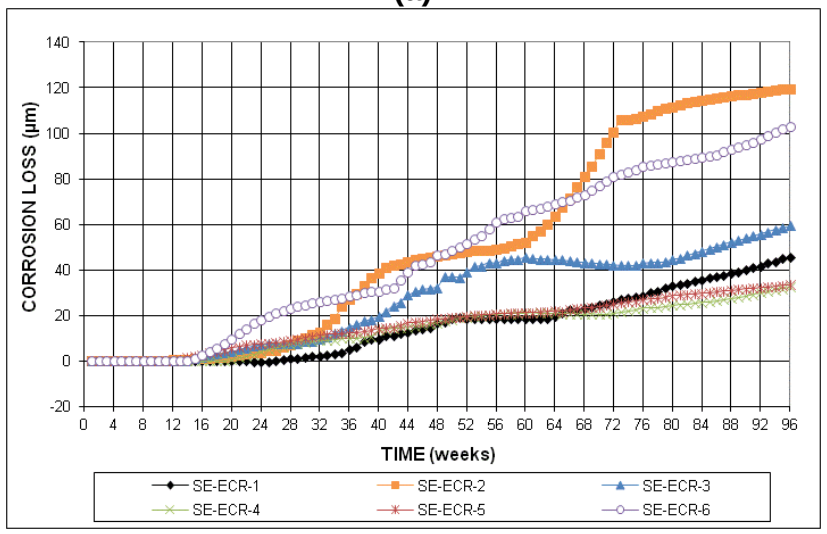

(b)

Figure A.21: (a) Corrosion rate and (b) total corrosion losses based on exposed area for ECR Southern Exposure specimens

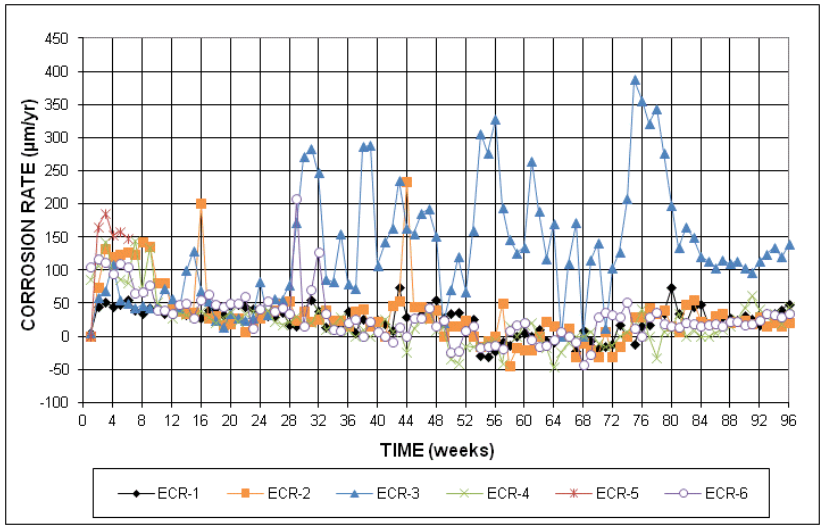

(a)

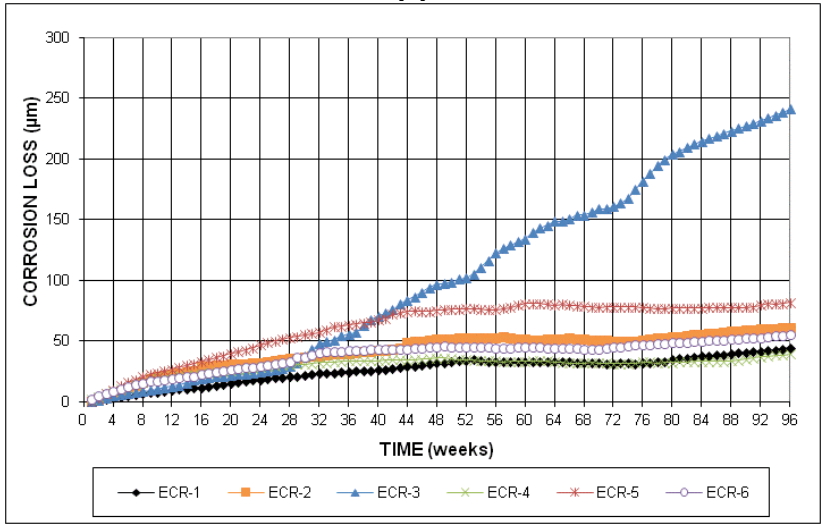

(b)

Figure A.22: (a) Corrosion rate and (b) total corrosion losses based on exposed area for ECR cracked beam specimens

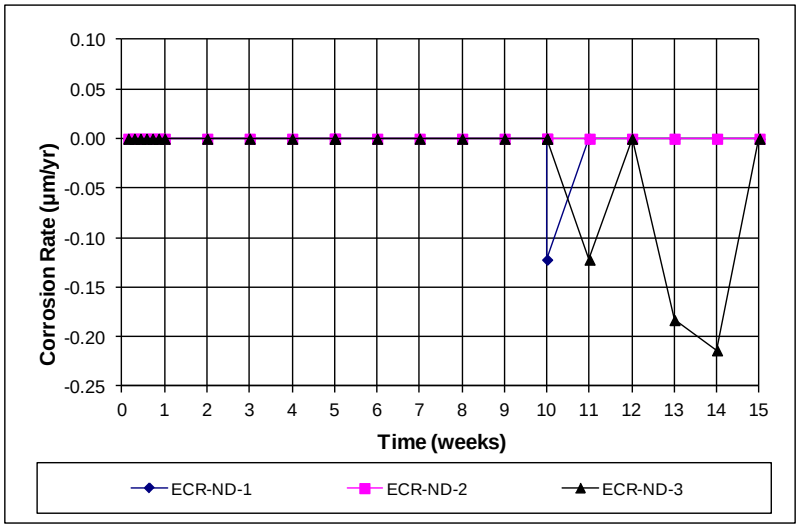

(a)

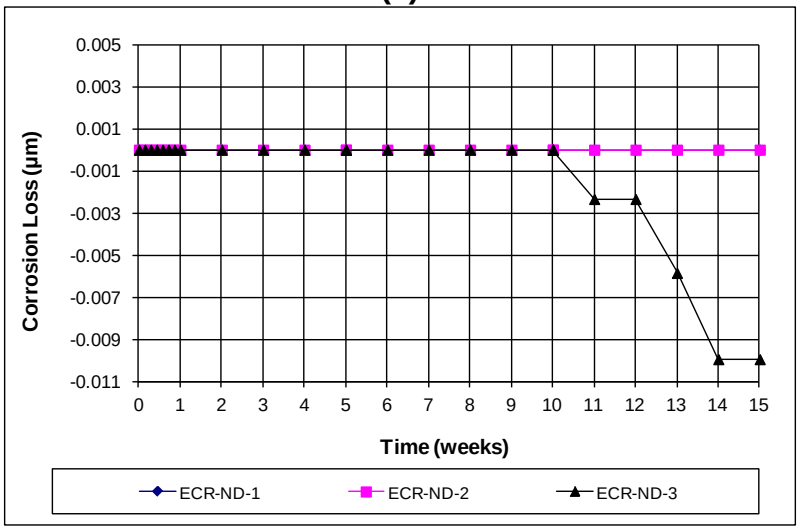

(b)

Figure A.23: (a) Corrosion rate and (b) total corrosion losses for undamaged ECR macrocell specimens

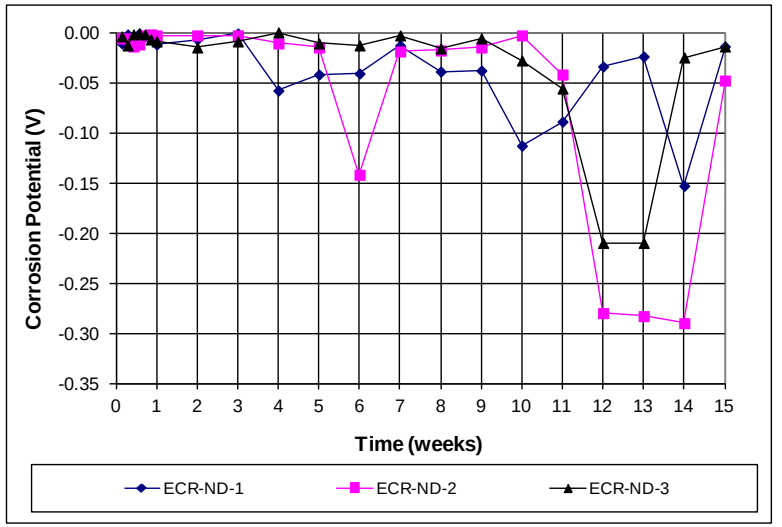

(a)

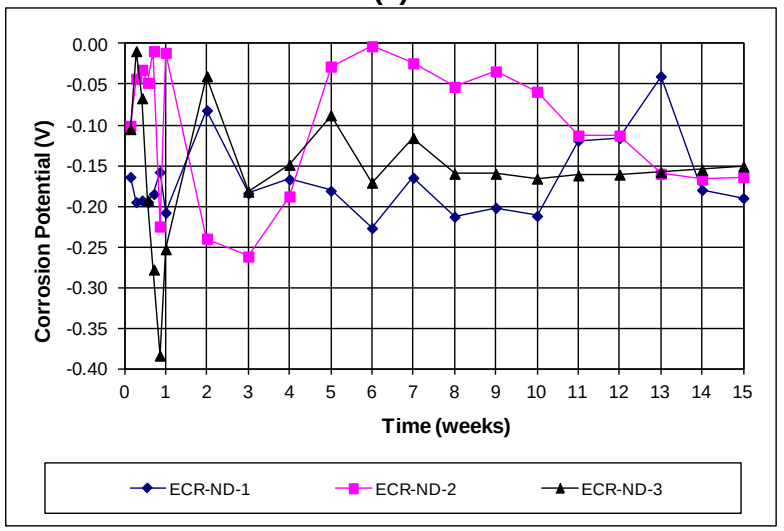

(b)

Figure A.24: (a) Top mat corrosion potentials and (b) bottom mat corrosion potentials for undamaged ECR macrocell specimens

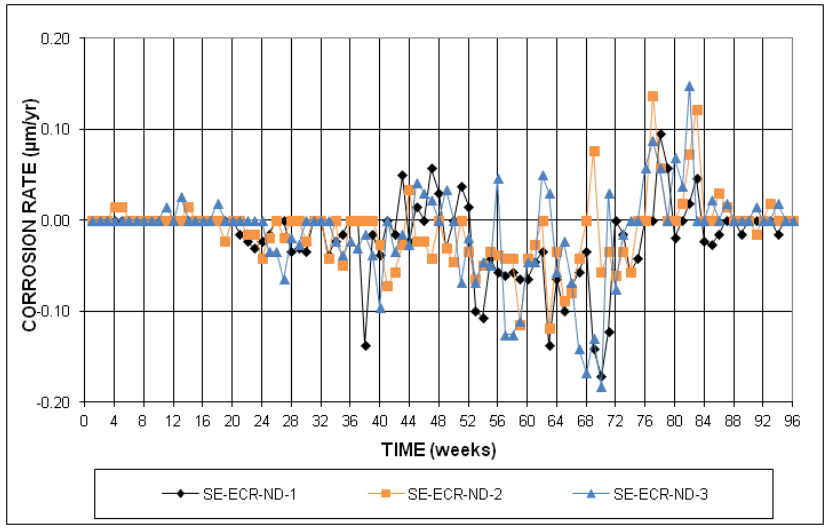

(a)

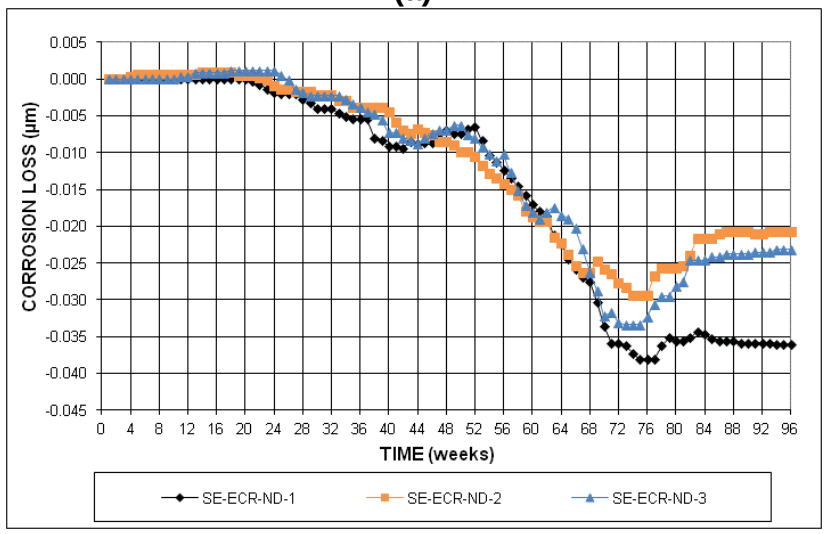

(b)

Figure A.25: (a) Corrosion rate and (b) total corrosion losses for undamaged ECR Southern Exposure specimens

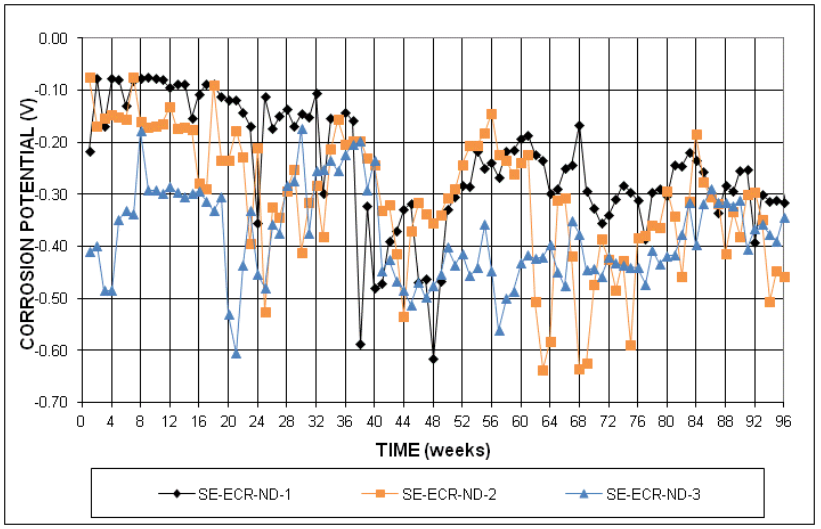

(a)

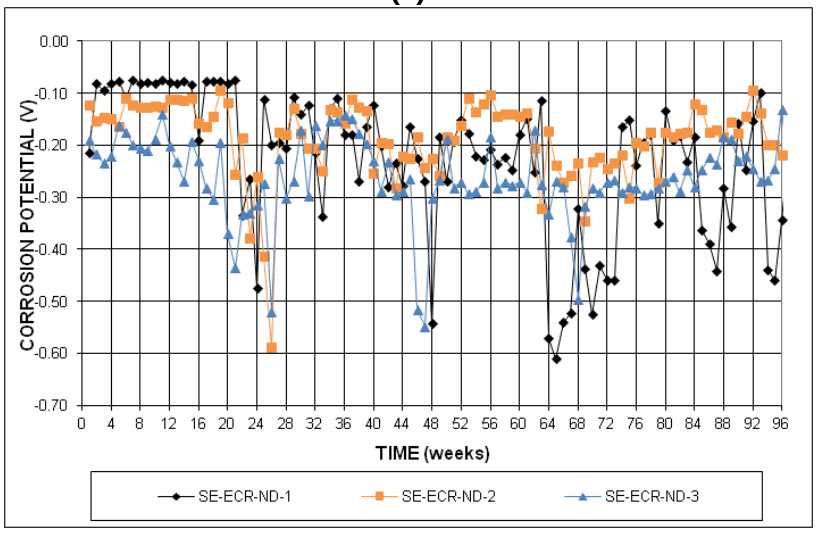

(b)

Figure A.26: (a) Top mat corrosion potentials and (b) bottom mat corrosion potentials for undamaged ECR Southern Exposure specimens

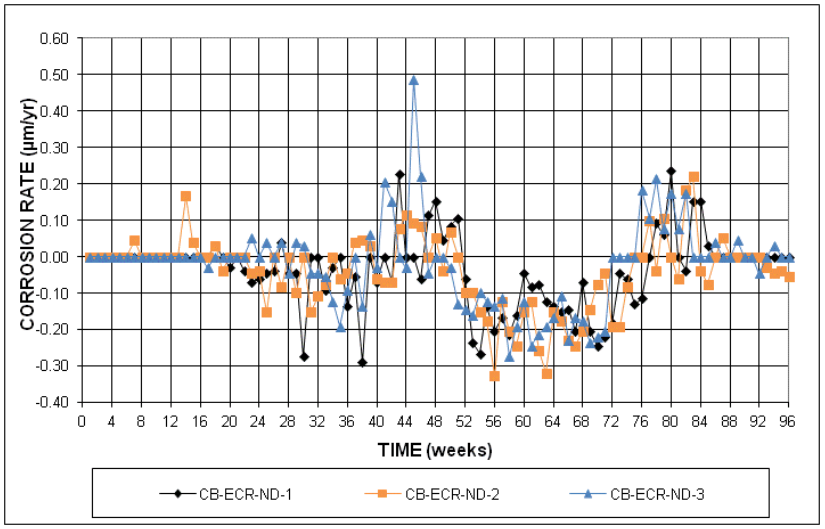

(a)

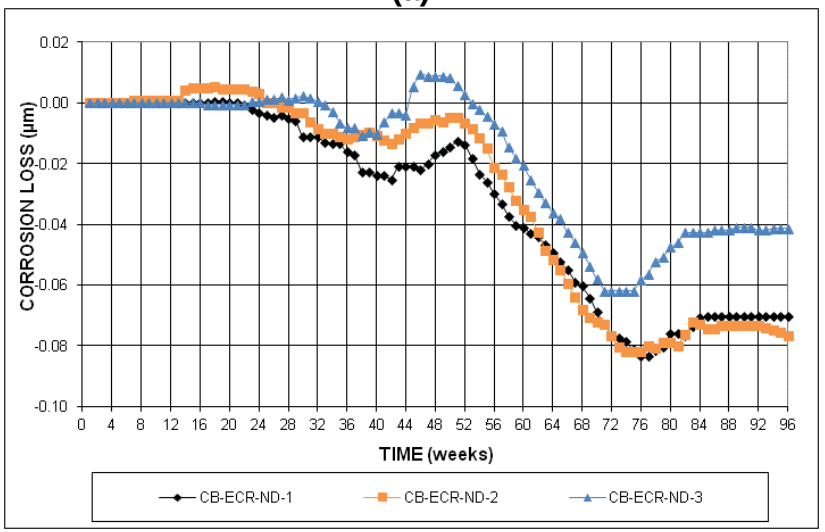

(b)

Figure A.27: (a) Corrosion rate and (b) total corrosion losses for undamaged ECR cracked beam specimens

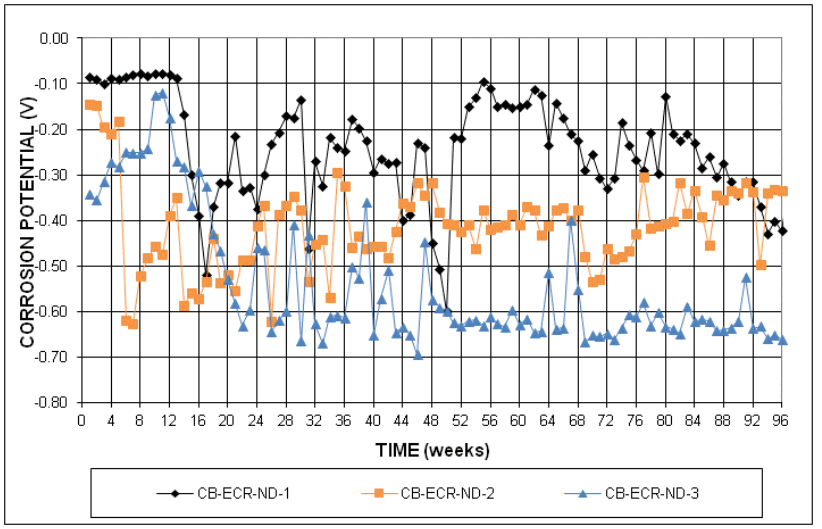

(a)

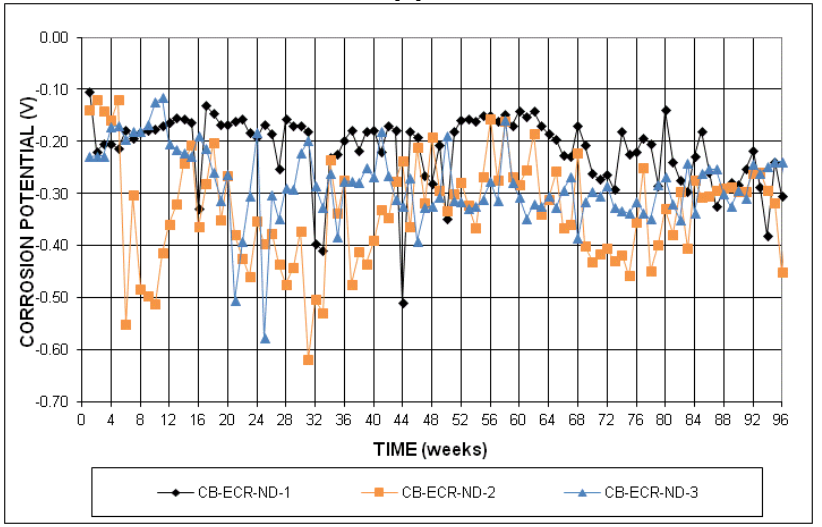

(b)

Figure A.28: (a) Top mat corrosion potentials and (b) bottom mat corrosion potentials for undamaged ECR cracked beam specimens

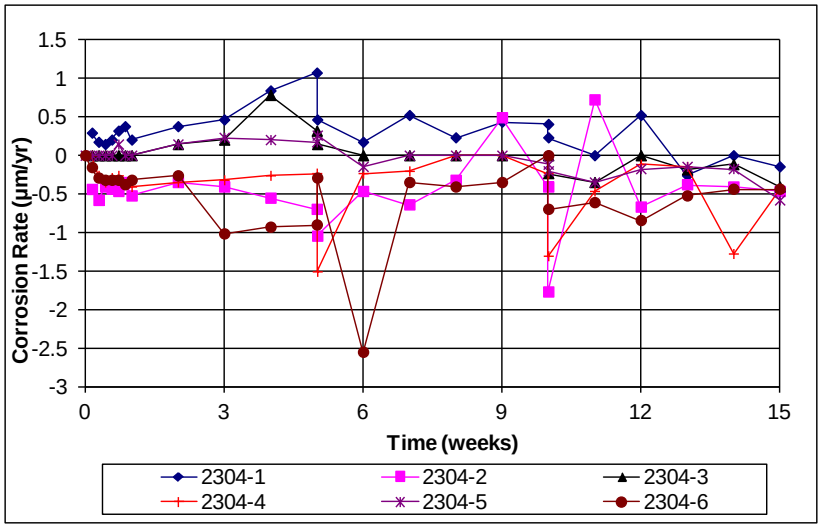

(a)

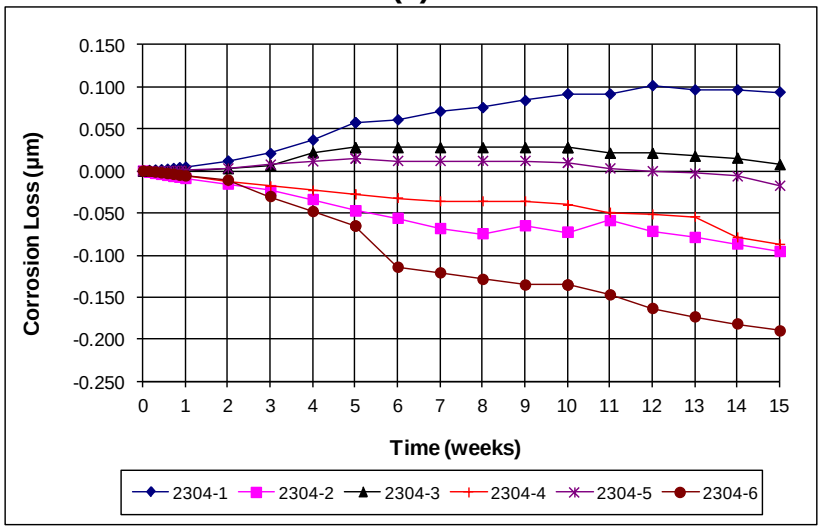

(b)

Figure A.29: (a) Corrosion rate and (b) total corrosion losses for 2304 stainless steel macrocell specimens

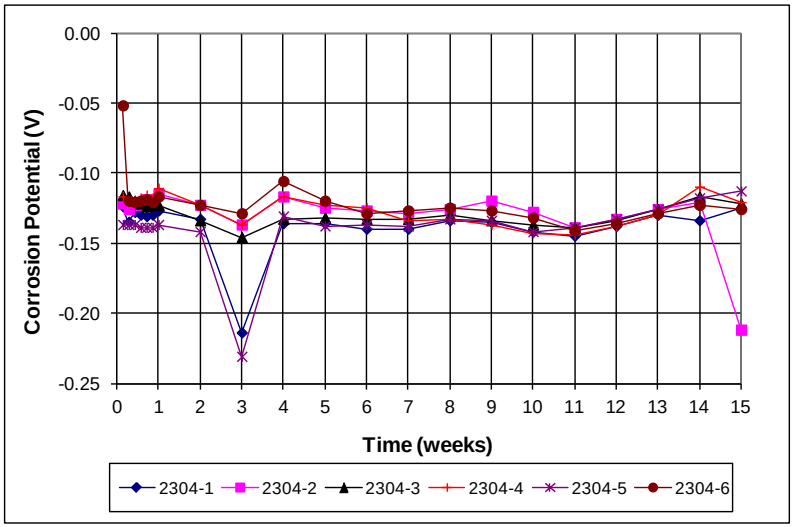

(a)

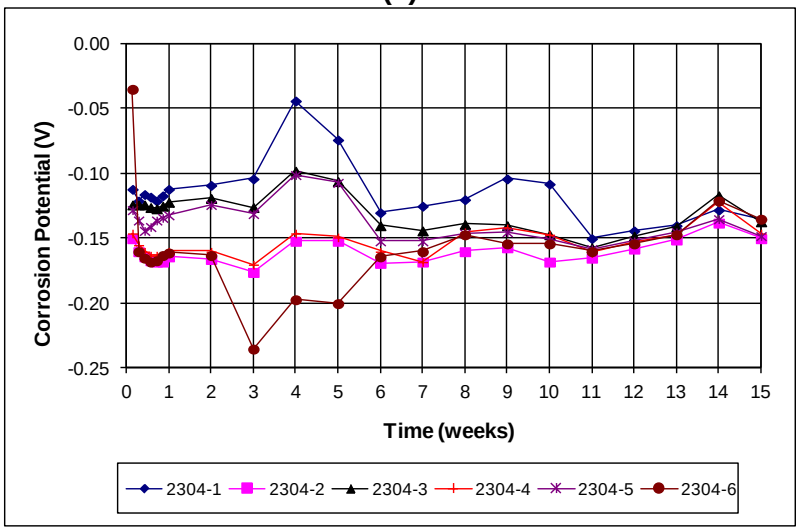

(b)

Figure A.30: (a) Top mat corrosion potentials and (b) bottom mat corrosion potentials for 2304 stainless steel macrocell specimens

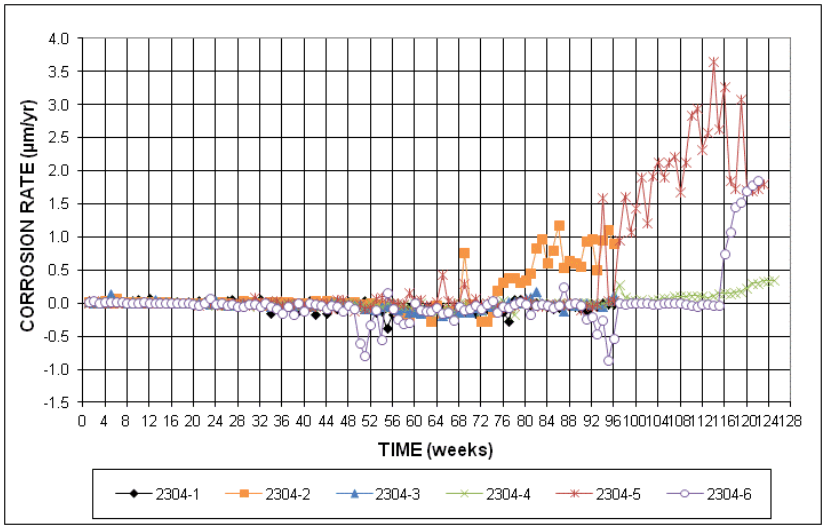

(a)

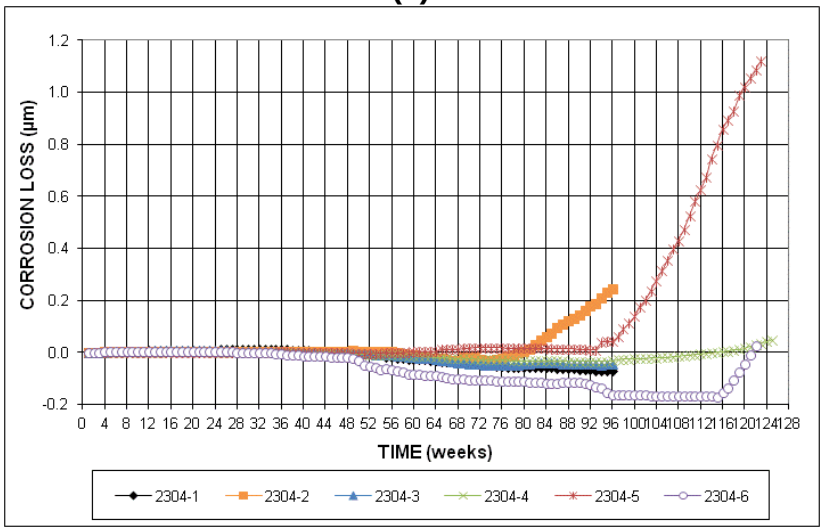

(b)

Figure A.31: (a) Corrosion rate and (b) total corrosion losses for 2304 stainless steel Southern Exposure specimens

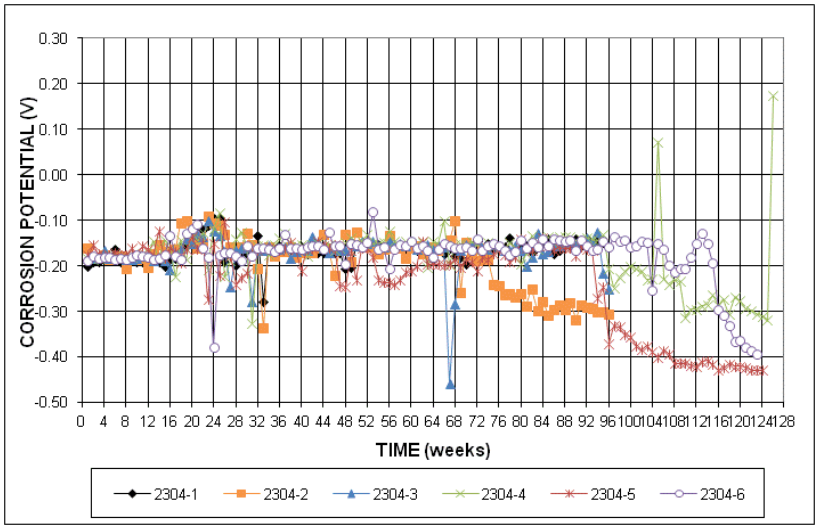

(a)

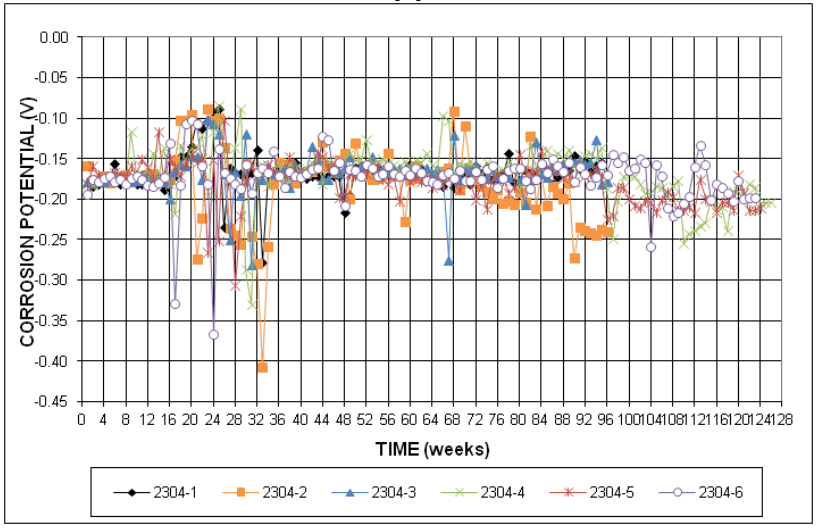

(b)

Figure A.32: (a) Top mat corrosion potentials and (b) bottom mat corrosion potentials for 2304 stainless steel Southern Exposure specimens

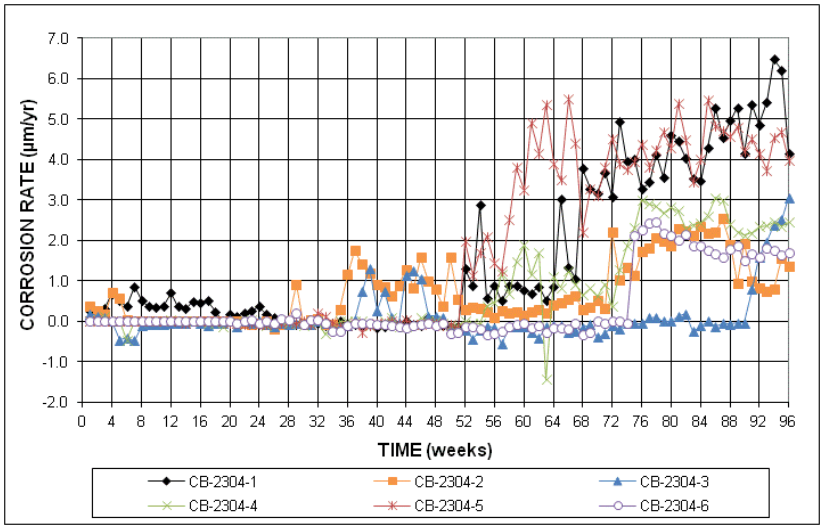

(a)

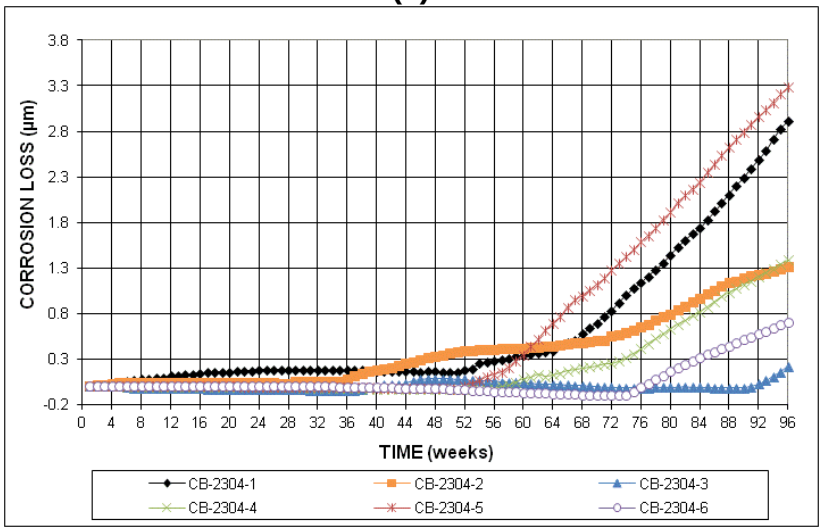

(b)

Figure A.33: (a) Corrosion rate and (b) total corrosion losses for 2304 stainless steel cracked beam specimens

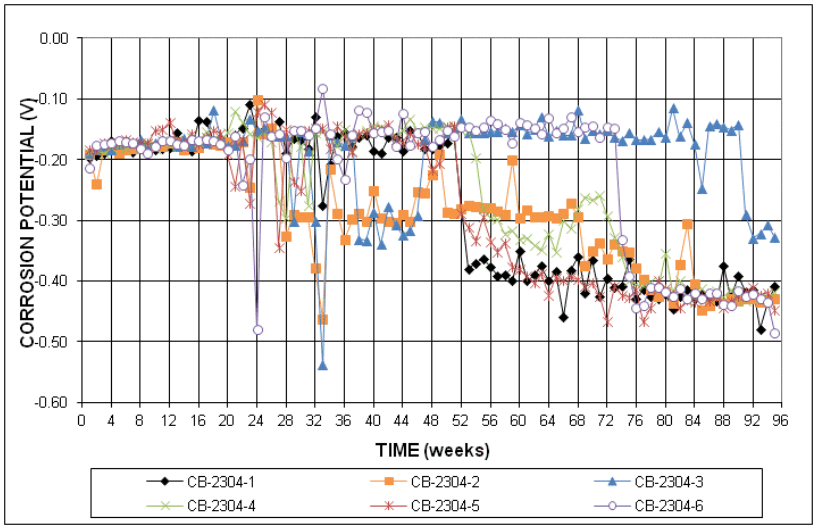

(a)

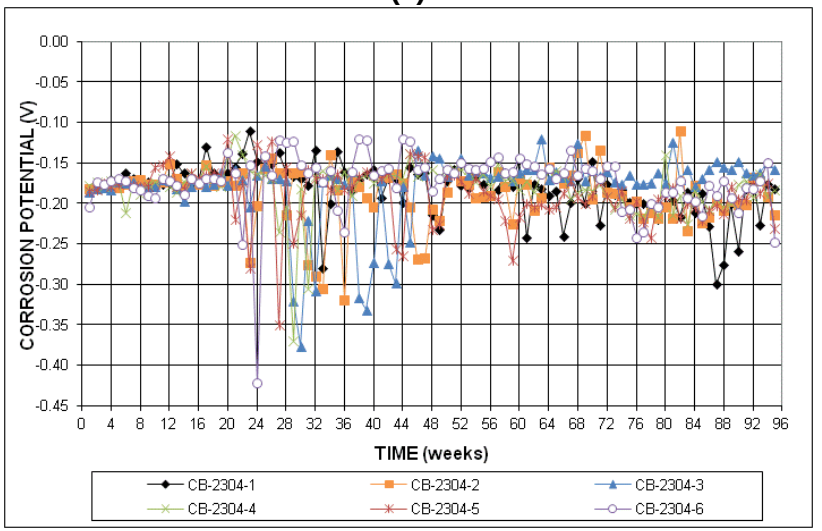

(b)

Figure A.34: (a) Top mat corrosion potentials and (b) bottom mat corrosion potentials for 2304 stainless steel cracked beam specimens

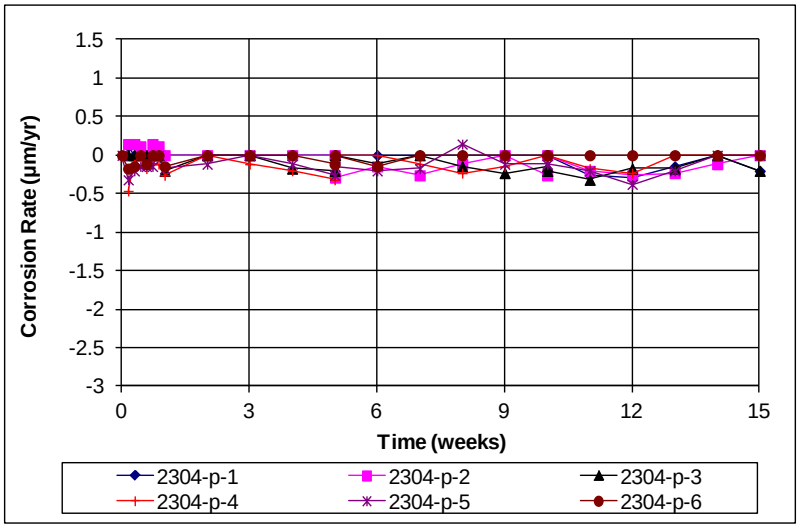

(a)

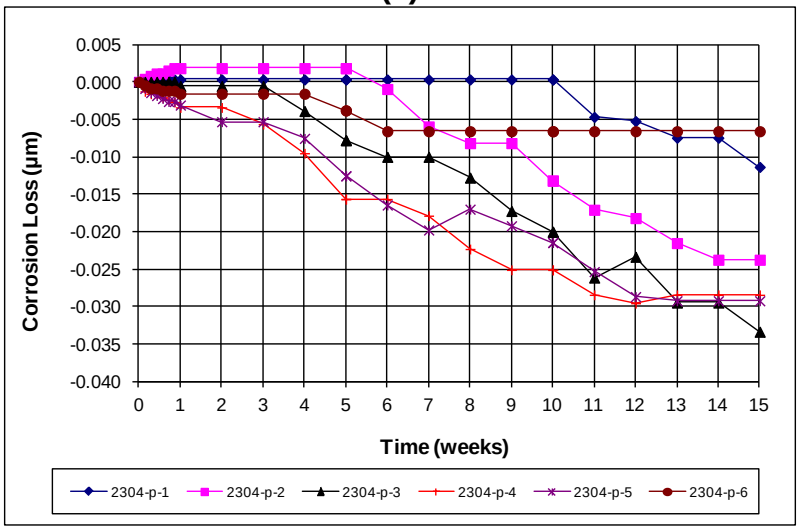

(b)

Figure A.35: (a) Corrosion rate and (b) total corrosion losses for repickled 2304 stainless steel macrocell specimens

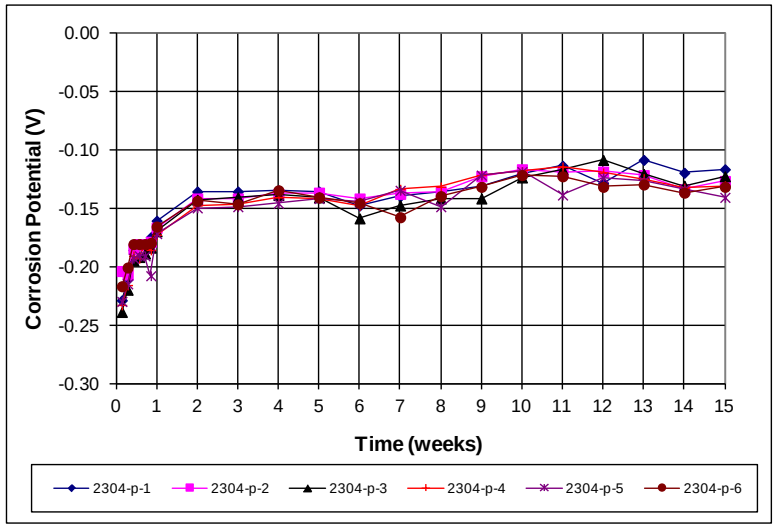

(a)

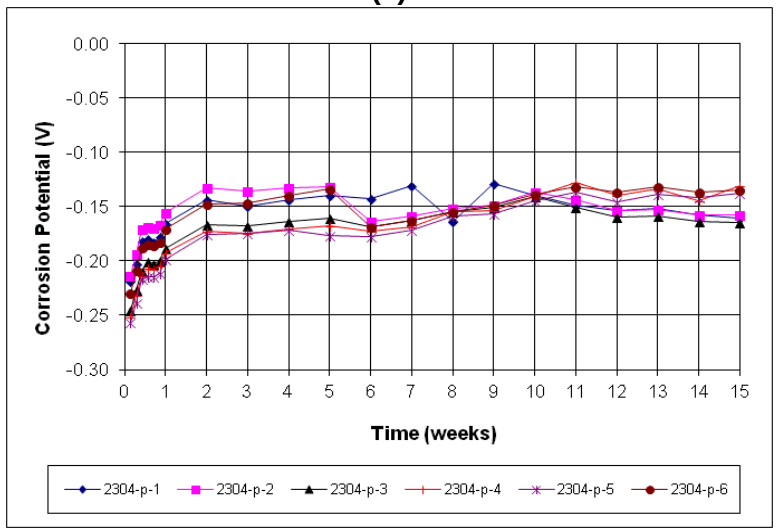

(b)

Figure A.36: (a) Top mat corrosion potentials and (b) bottom mat corrosion potentials for repickled 2304 stainless steel macrocell specimens

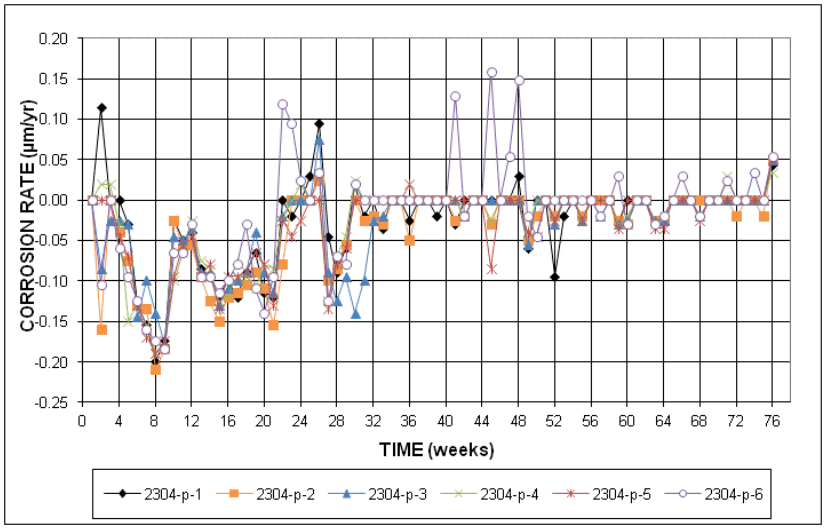

(a)

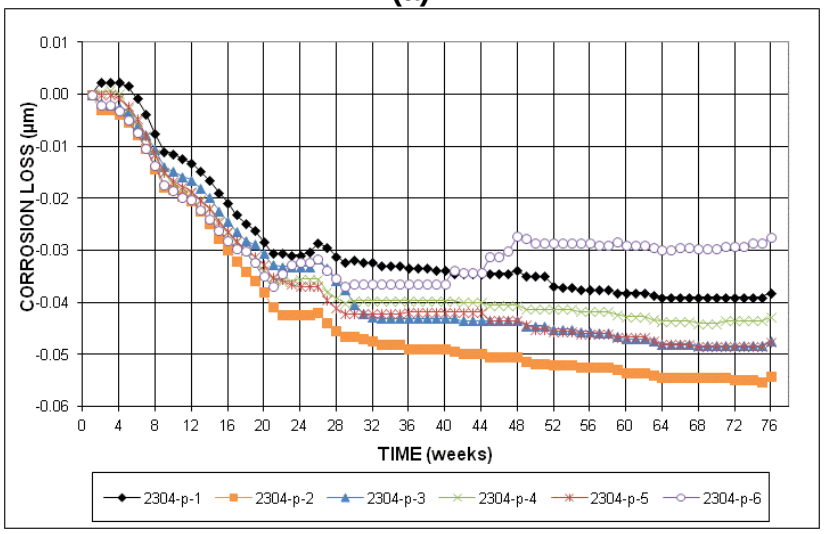

(b)

Figure A.37: (a) Corrosion rate and (b) total corrosion losses for repickled 2304 stainless steel cracked beam specimens

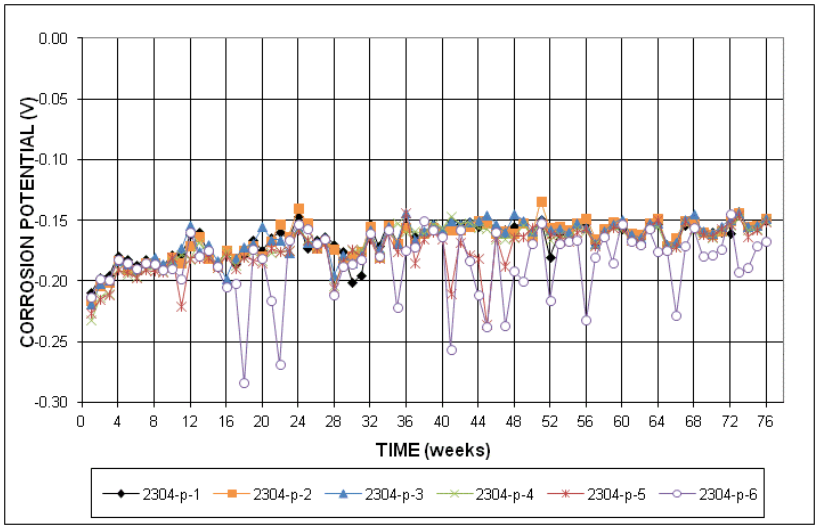

(a)

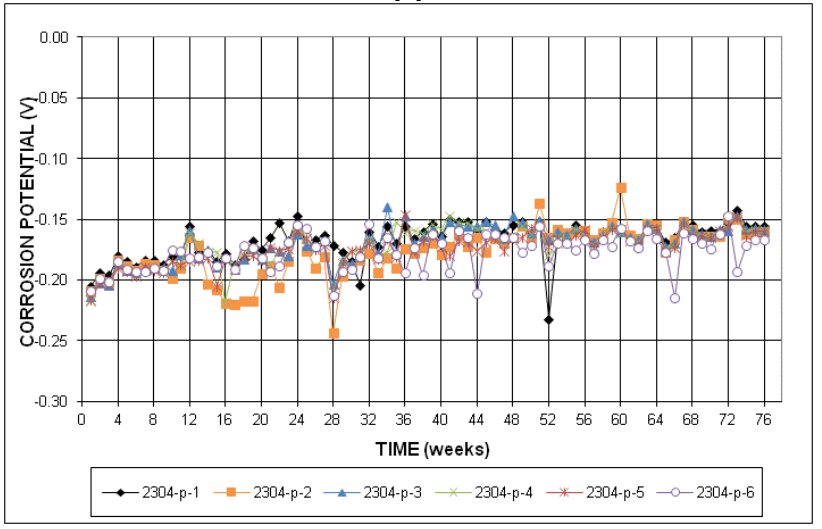

(b)

Figure A.38: (a) Top mat corrosion potentials and (b) bottom mat corrosion potentials for repickled 2304 stainless steel cracked beam specimens

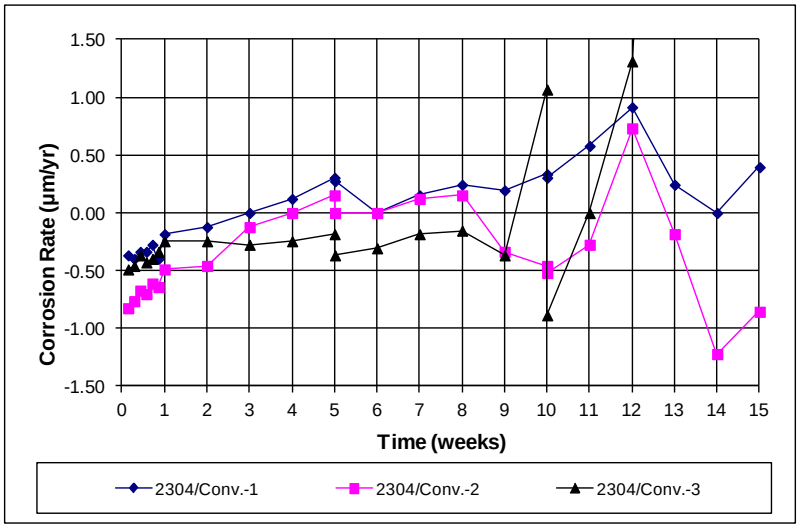

(a)

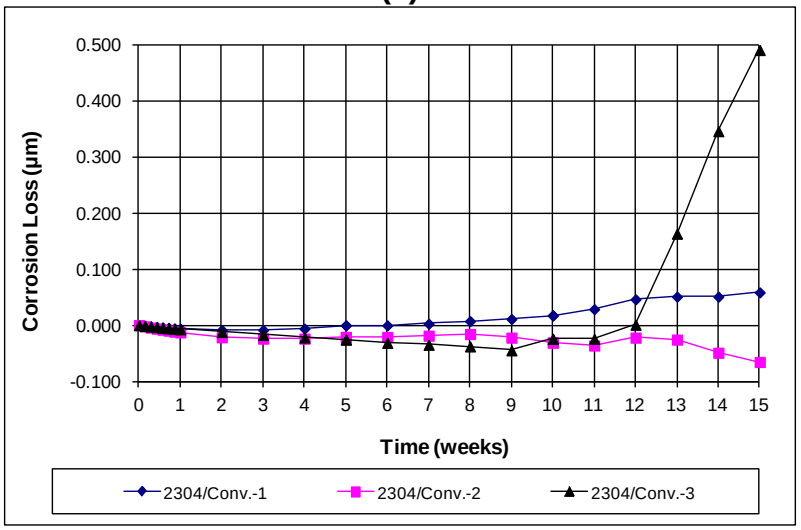

(b)

Figure A.39: (a) Corrosion rate and (b) total corrosion losses for 2304 stainless steel (anode) and conventional (cathode) macrocell specimens

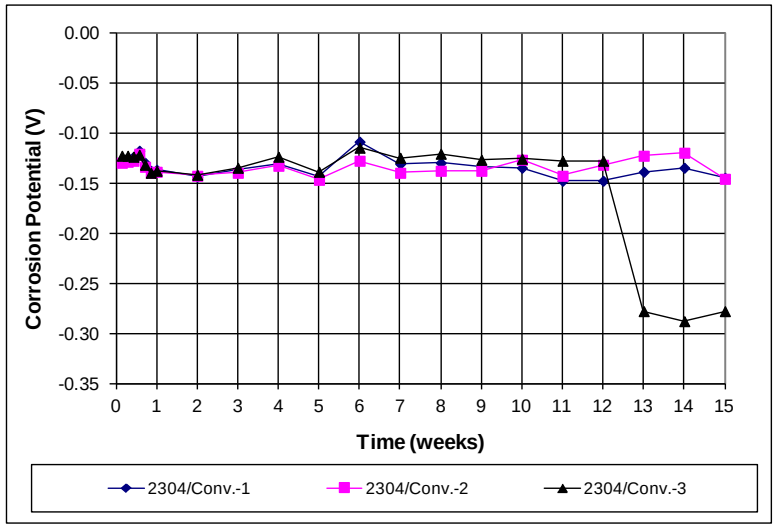

(a)

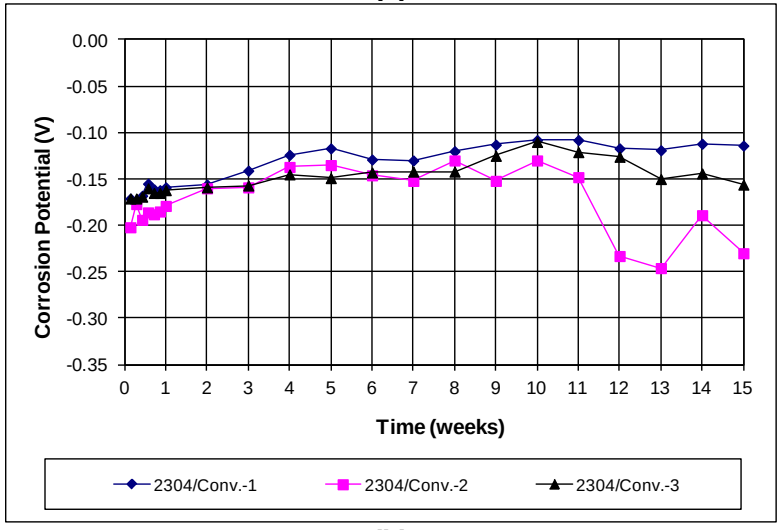

(b)

Figure A.40: (a) Top mat corrosion potentials and (b) bottom mat corrosion potentials for 2304 stainless steel (anode) and conventional (cathode) macrocell specimens

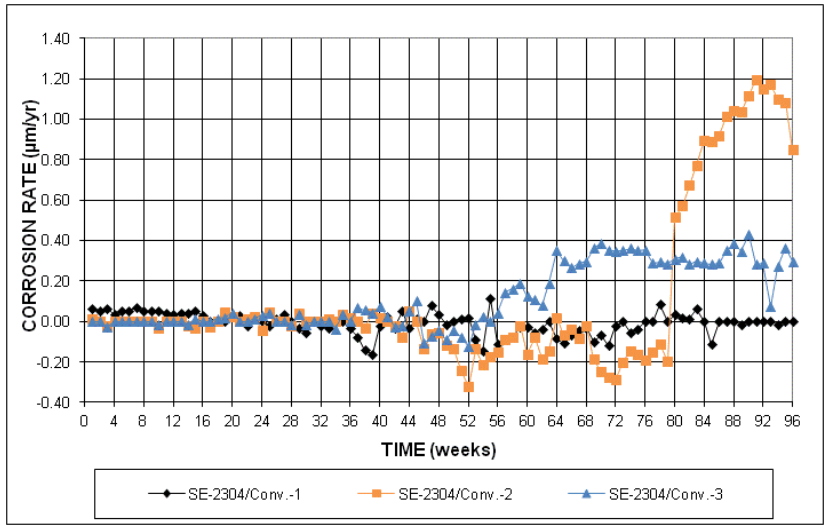

(a)

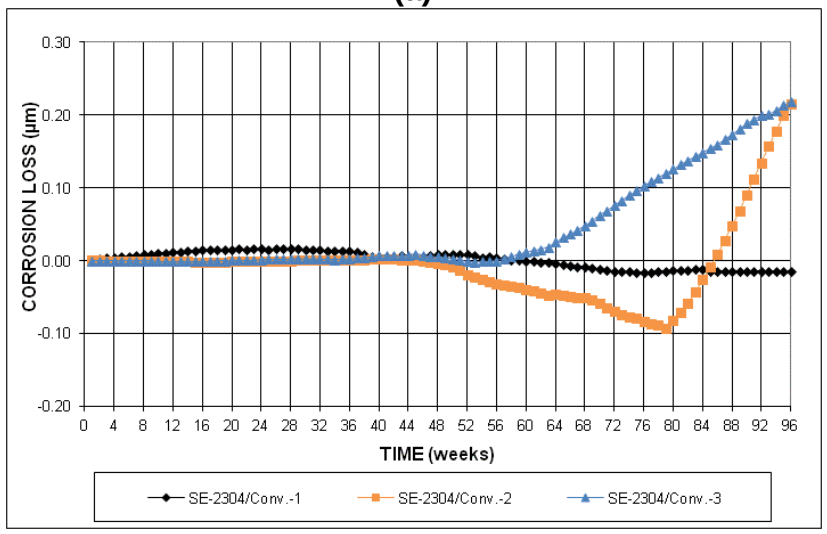

(b)

Figure A.41: (a) Corrosion rate and (b) total corrosion losses for 2304 stainless steel (anode) and conventional (cathode) Southern Exposure specimens

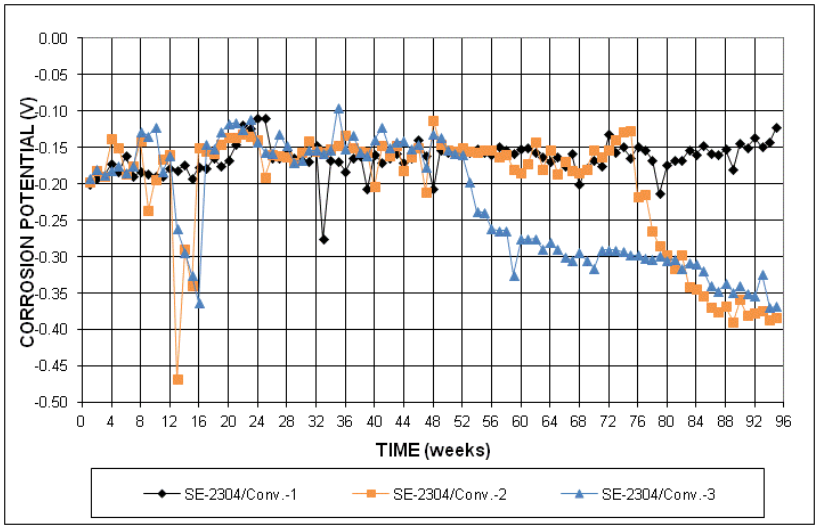

(a)

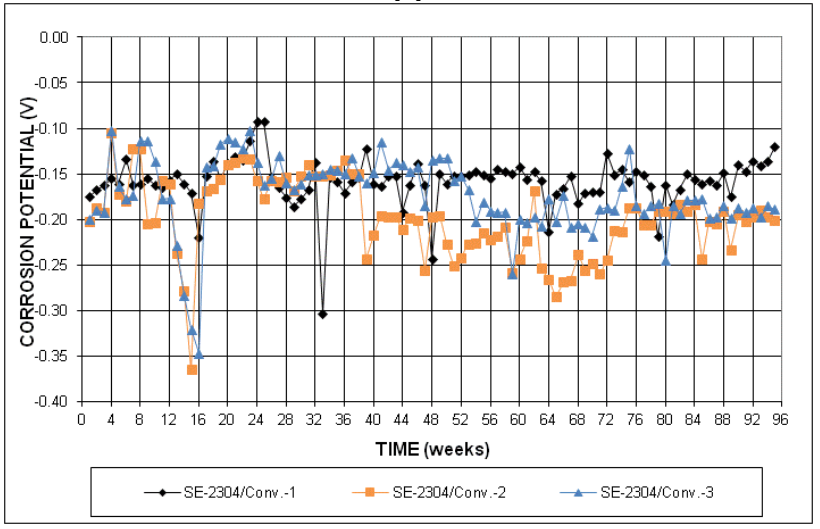

(b)

Figure A.42: (a) Top mat corrosion potentials and (b) bottom mat corrosion potentials for 2304 stainless steel (anode) and conventional (cathode) Southern Exposure specimens

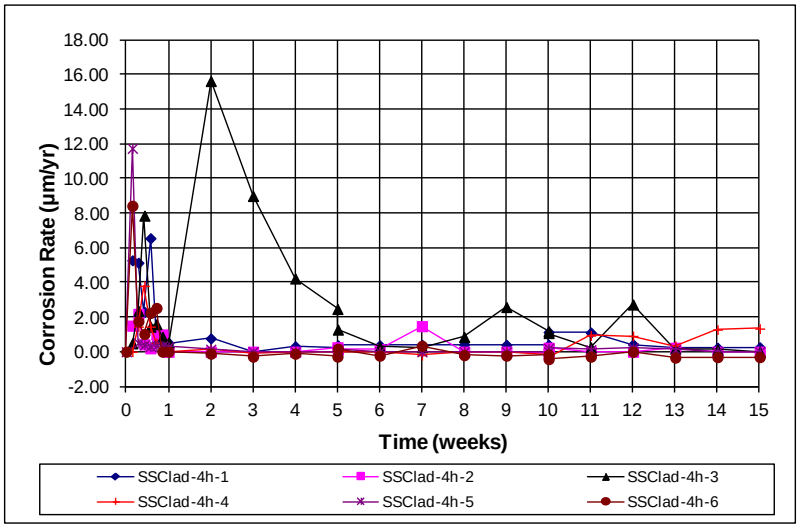

(a)

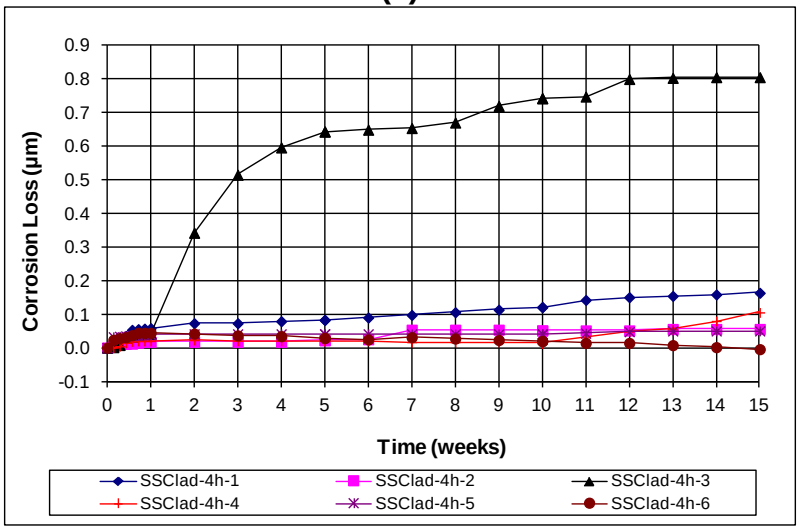

(b)

Figure A.43: (a) Corrosion rate and (b) total corrosion losses for SSClad with four holes macrocell specimens

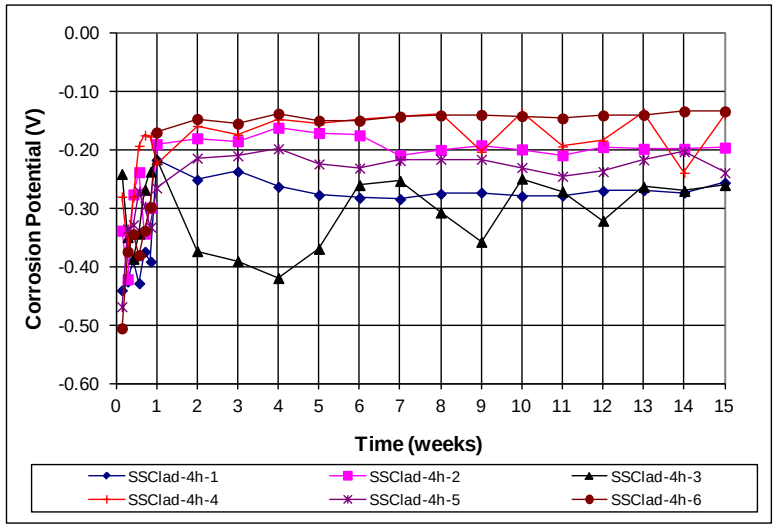

(a)

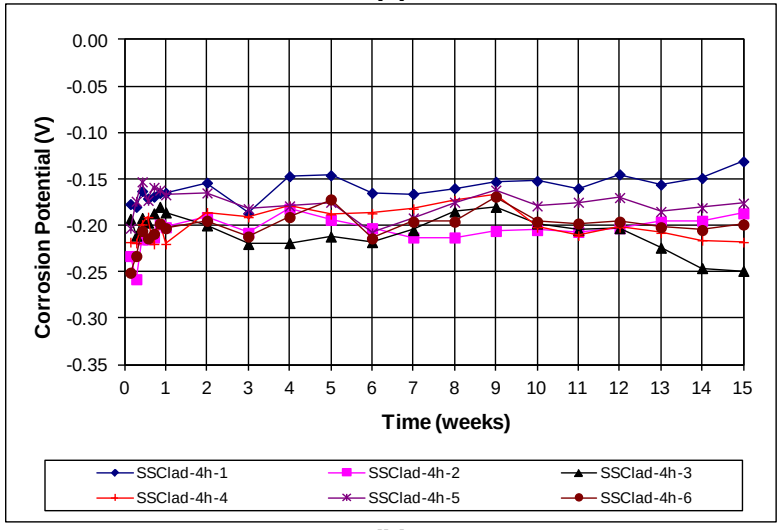

(b)

Figure A.44: (a) Top mat corrosion potentials and (b) bottom mat corrosion potentials for SSClad with four holes macrocell specimens

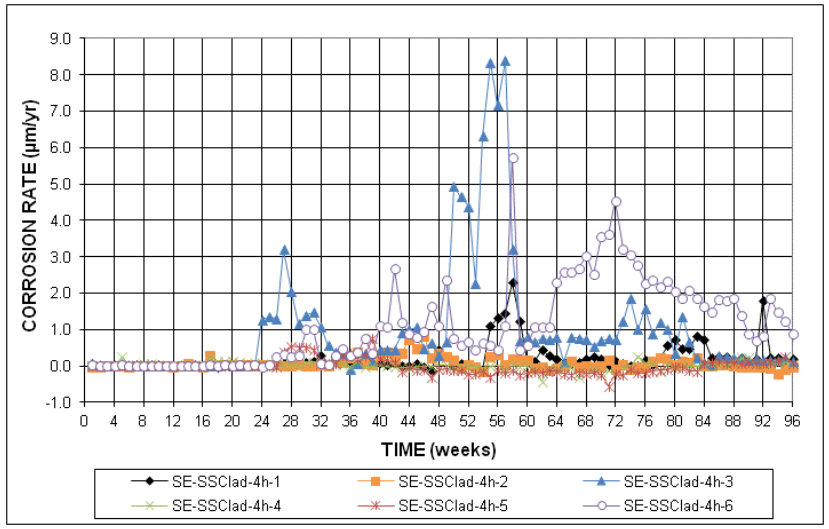

(a)

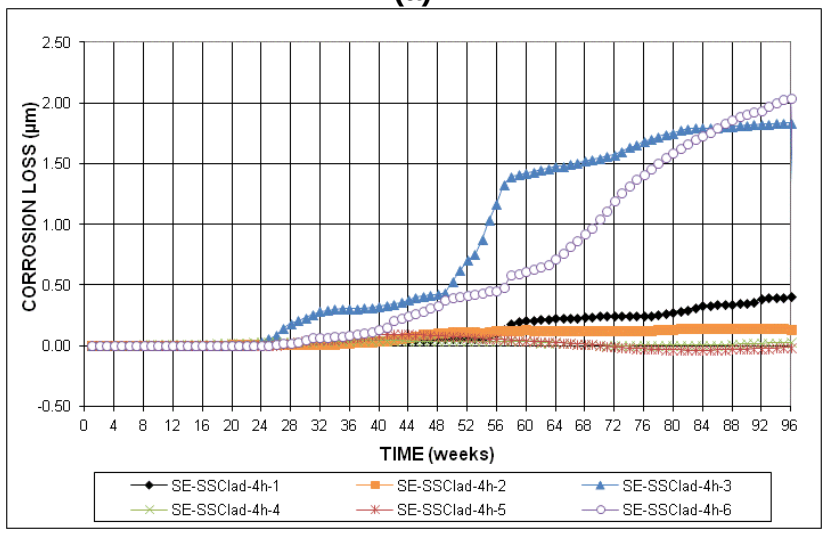

(b)

Figure A.45: (a) Corrosion rate and (b) total corrosion losses based on total area for SSClad with four holes Southern Exposure specimens

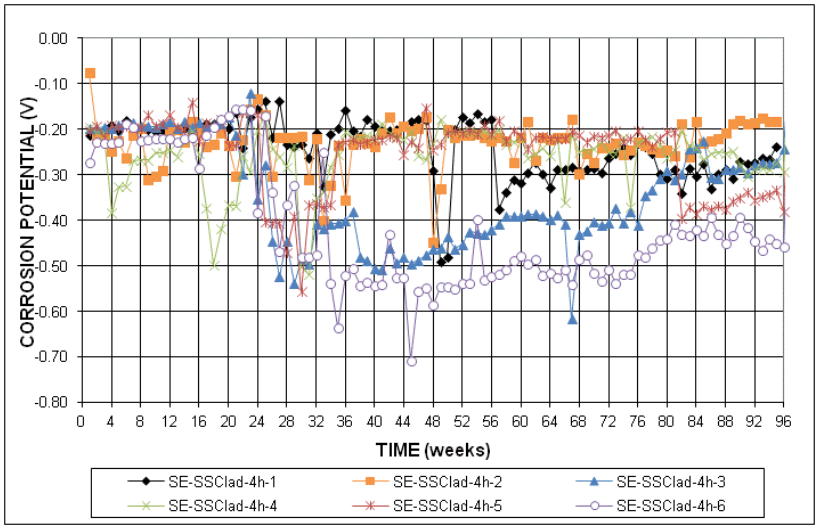

(a)

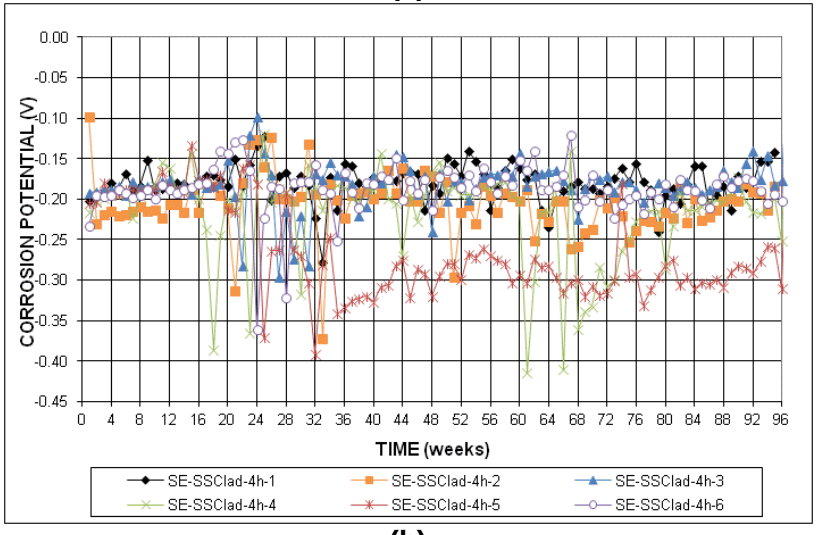

(b)

Figure A.46: (a) Top mat corrosion potentials and (b) bottom mat corrosion potentials for SSClad with four holes Southern Exposure specimens

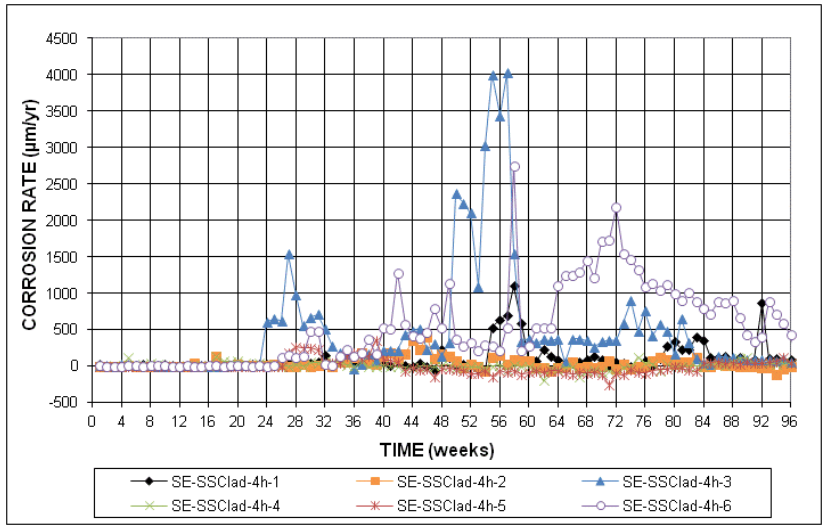

(a)

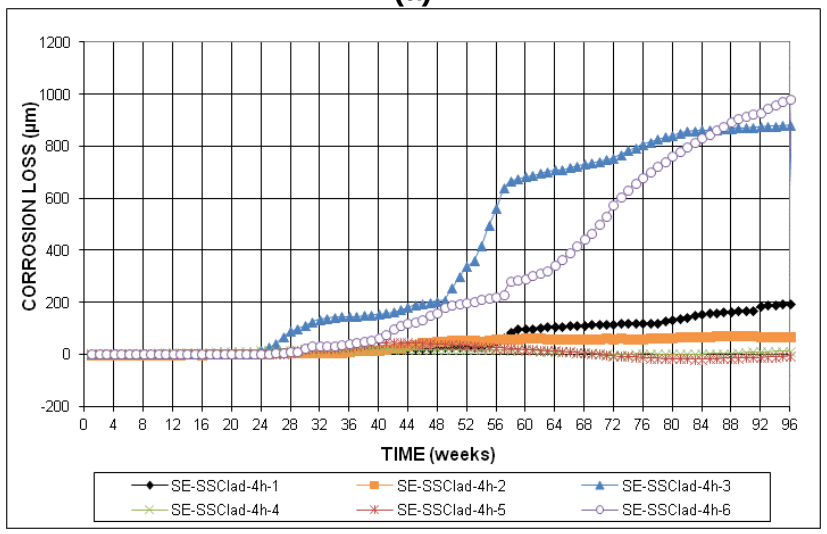

(b)

Figure A.47: (a) Corrosion rate and (b) total corrosion losses based on exposed area for SSClad with four holes Southern Exposure specimens

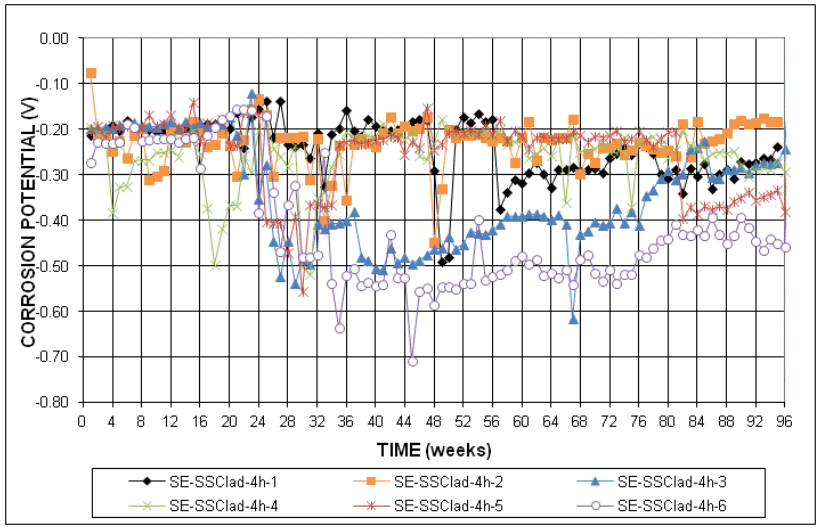

(a)

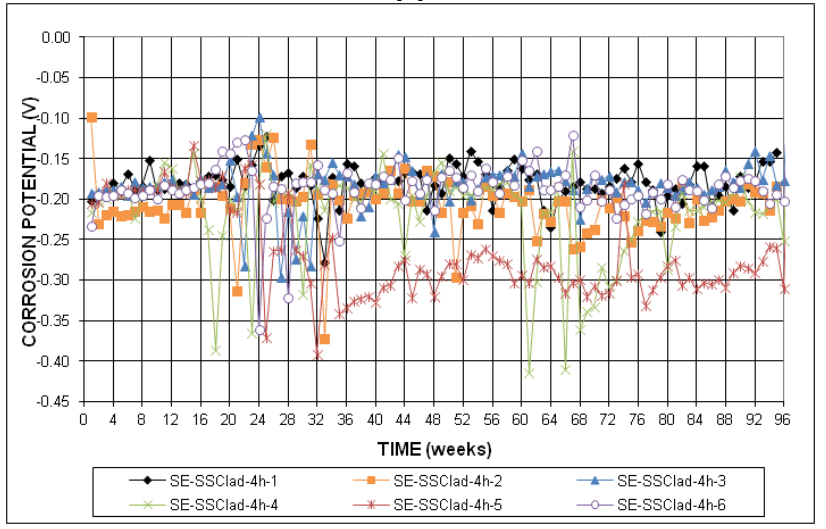

(b)

Figure A.48: (a) Top mat corrosion potentials and (b) bottom mat corrosion potentials for SSClad with four holes Southern Exposure specimens

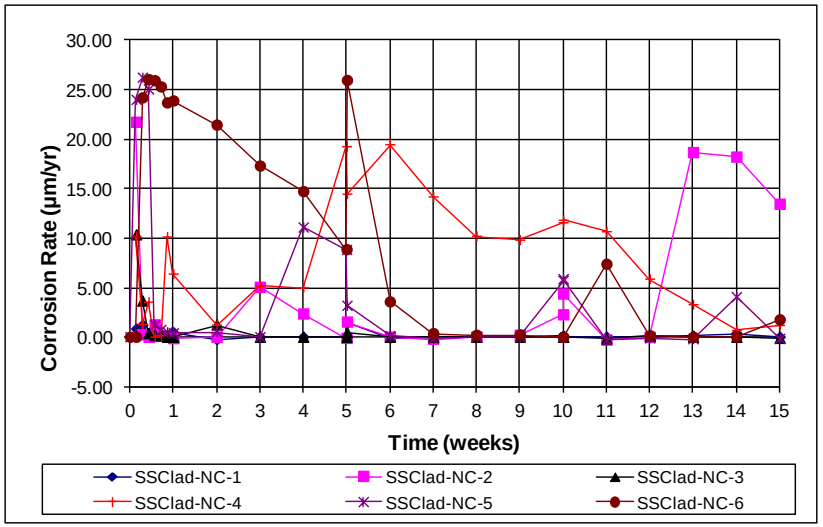

(a)

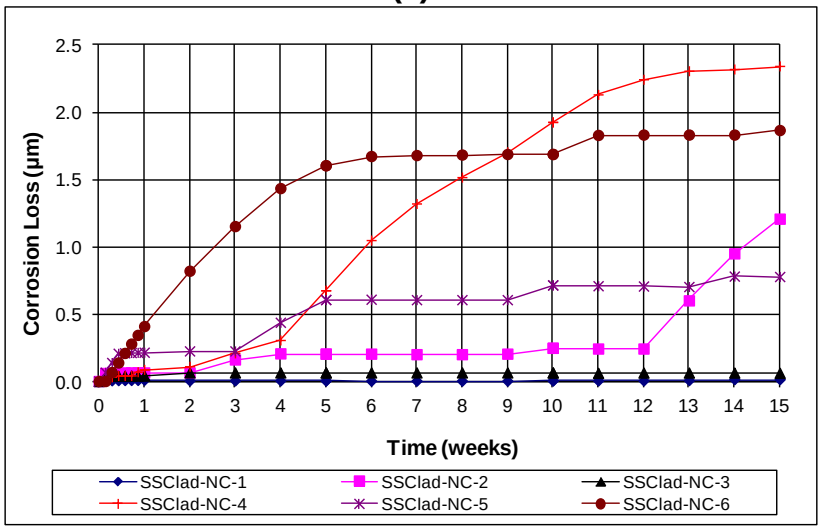

(b)

Figure A.49: (a) Corrosion rate and (b) total corrosion losses for SSClad without a cap macrocell specimens

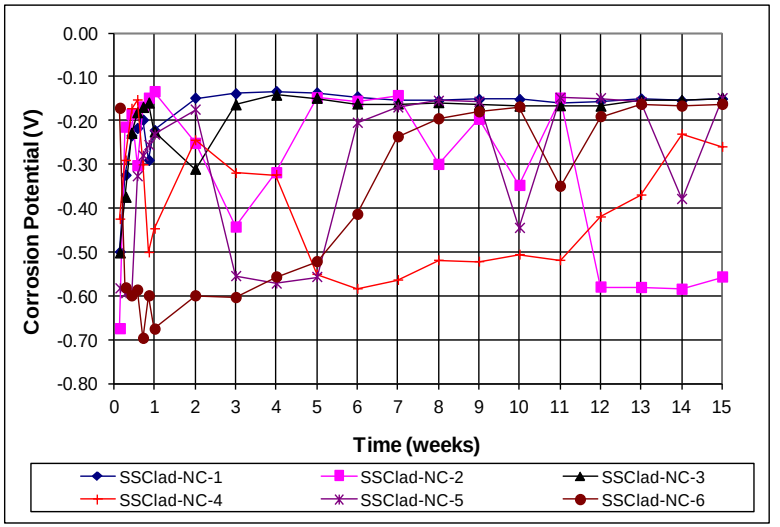

(a)

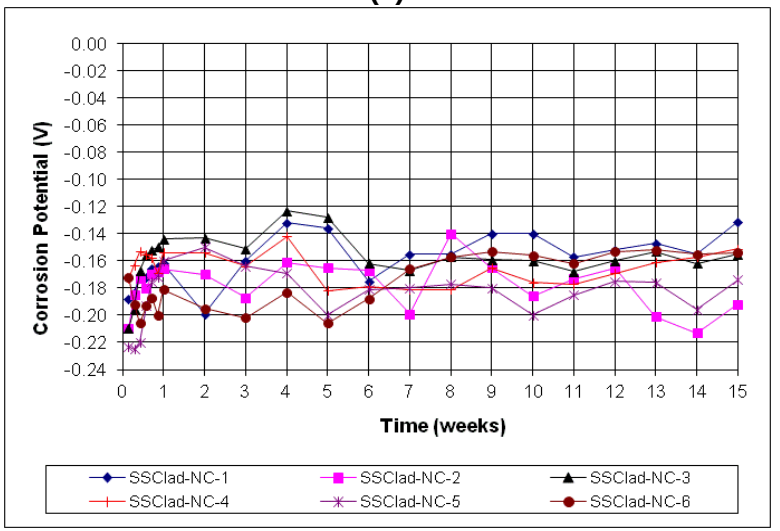

(b)

Figure A.50: (a) Top mat corrosion potentials and (b) bottom mat corrosion potentials for SSClad without a cap macrocell specimens

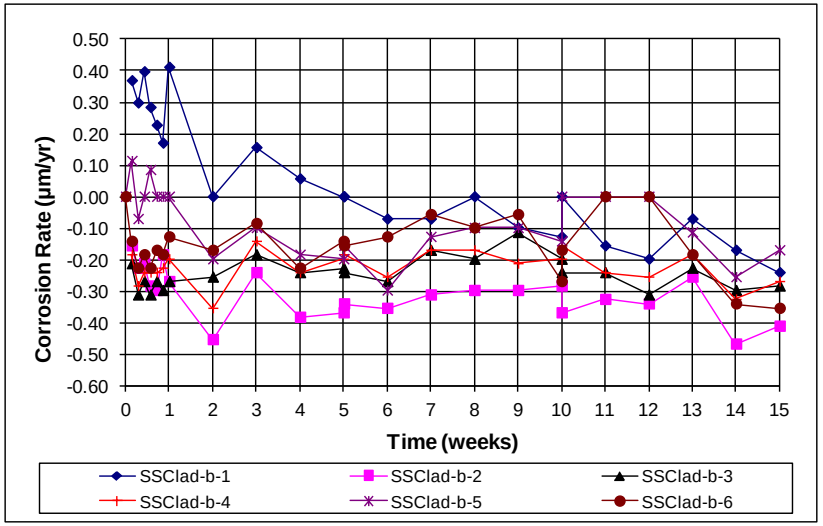

(a)

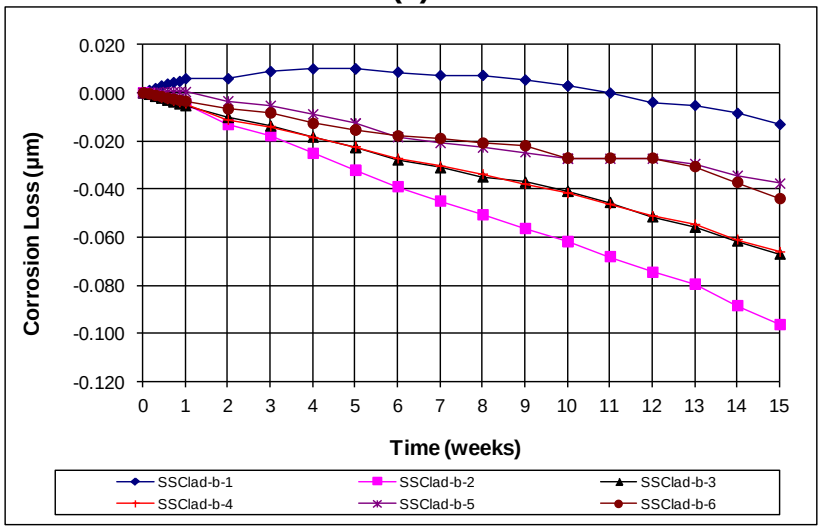

(b)

Figure A.51: (a) Corrosion rate and (b) total corrosion losses for bent SSClad macrocell specimens

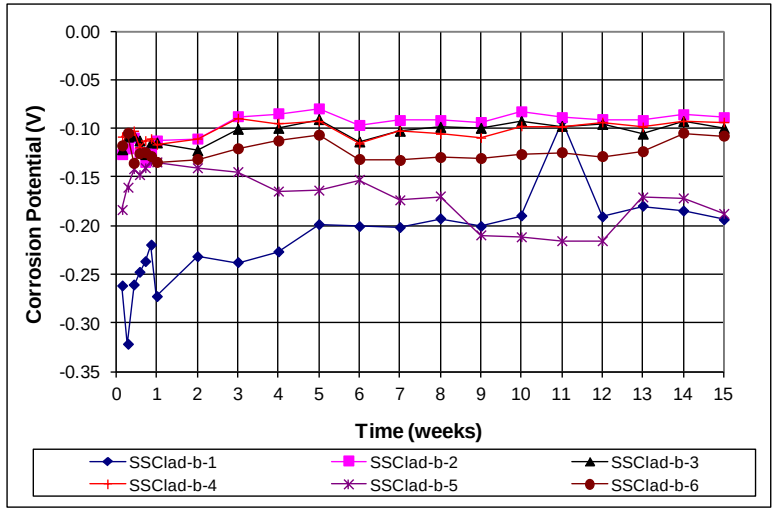

(a)

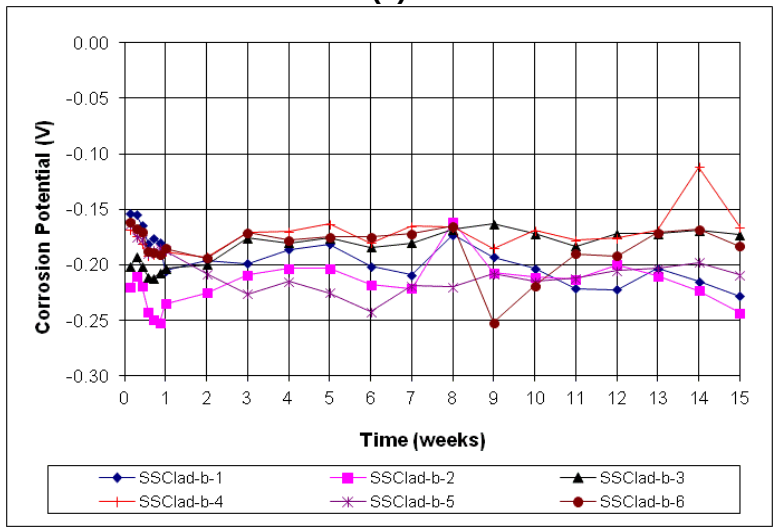

(b)

Figure A.52: (a) Top mat corrosion potentials and (b) bottom mat corrosion potentials for bent SSClad macrocell specimens

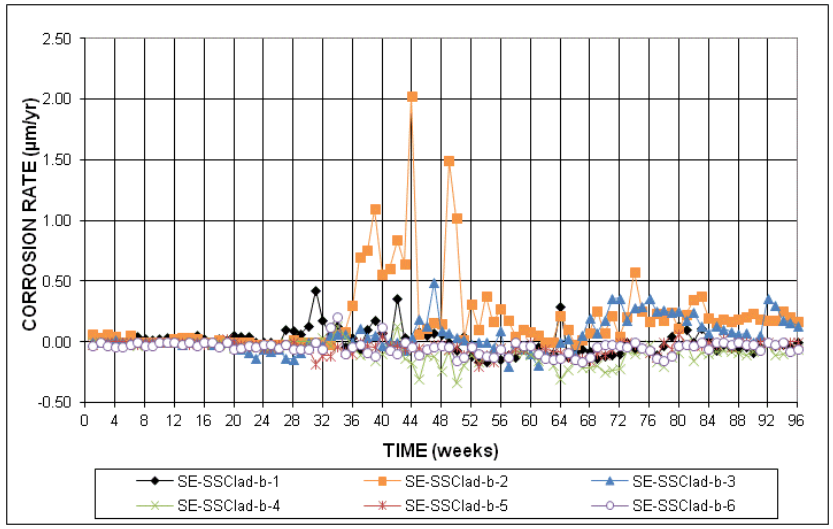

(a)

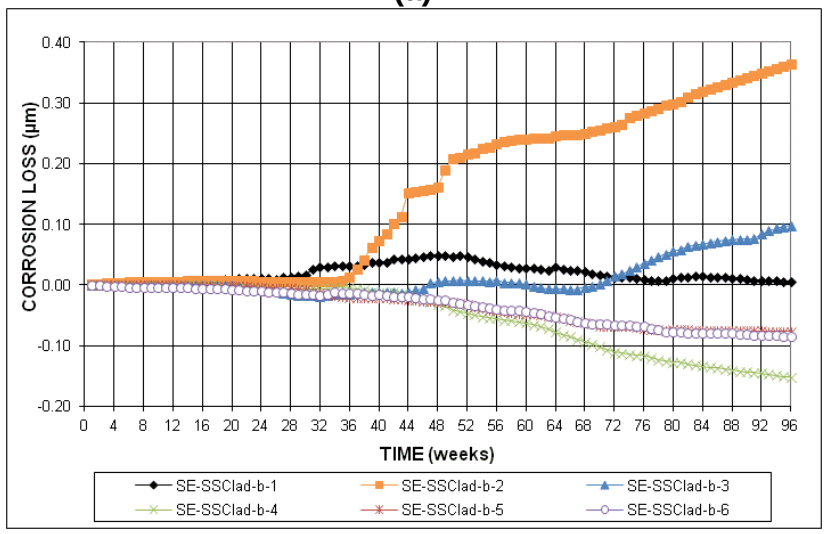

(b)

Figure A.53: (a) Corrosion rate and (b) total corrosion losses for bent SSClad Southern Exposure specimens

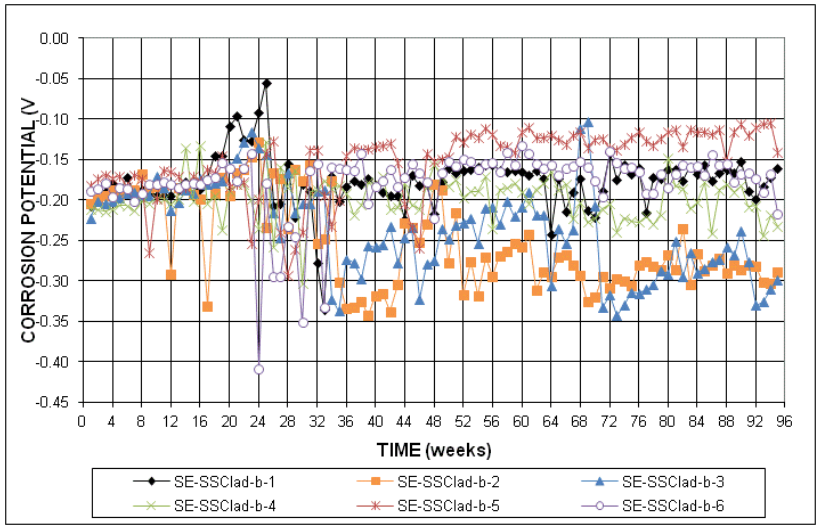

(a)

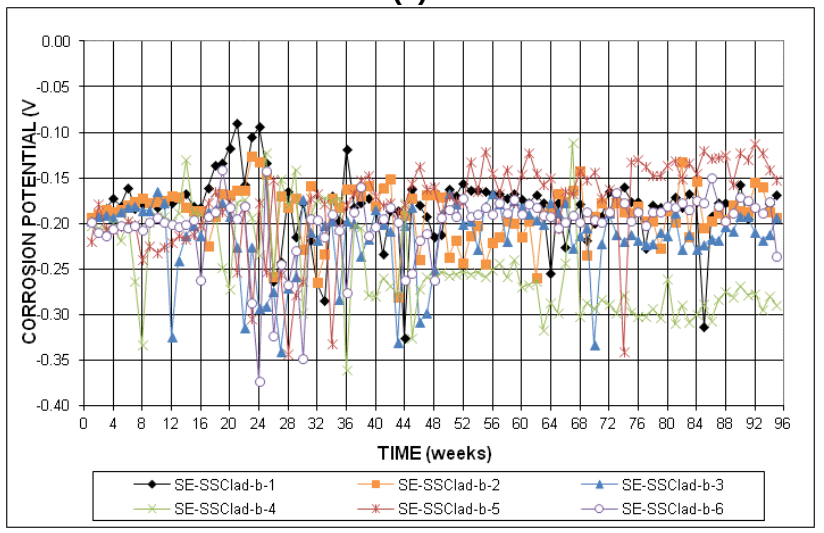

(b)

Figure A.54: (a) Top mat corrosion potentials and (b) bottom mat corrosion potentials for bent SSClad Southern Exposure specimens

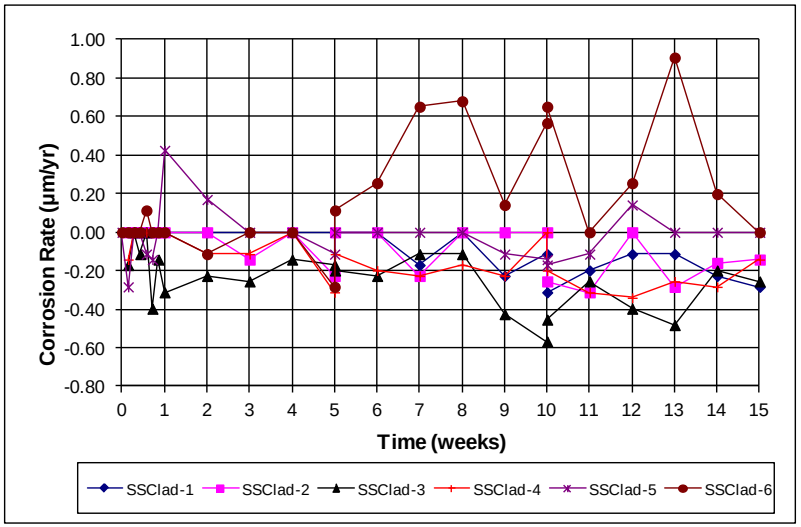

(a)

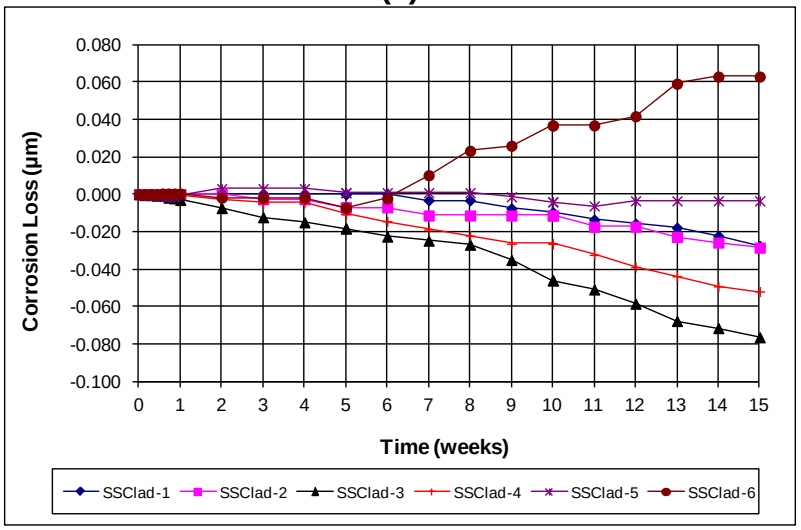

(b)

Figure A.55: (a) Corrosion rate and (b) total corrosion losses for undamaged SSClad macrocell specimens

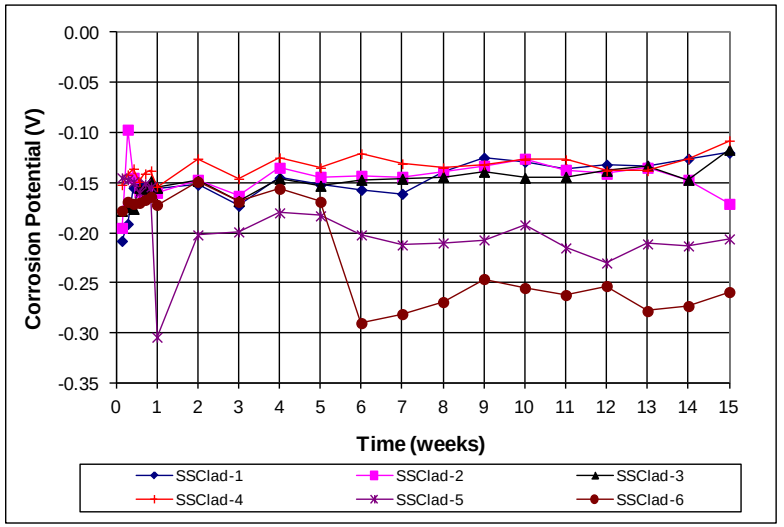

(a)

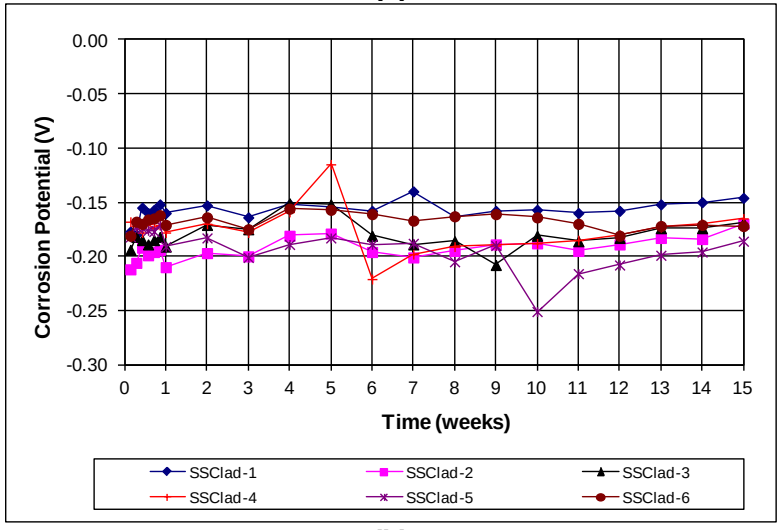

(b)

Figure A.56: (a) Top mat corrosion potentials and (b) bottom mat corrosion potentials for undamaged SSClad macrocell specimens

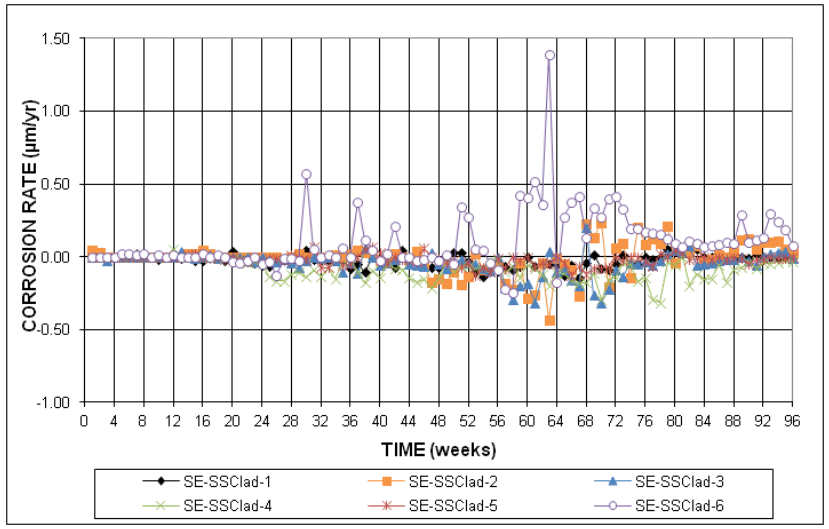

(a)

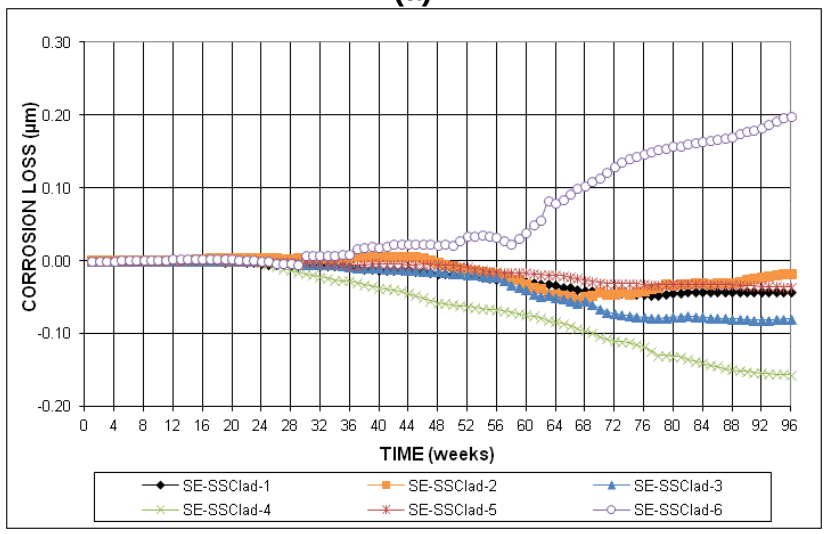

(b)

Figure A.57: (a) Corrosion rate and (b) total corrosion losses for undamaged SSClad Southern Exposure specimens

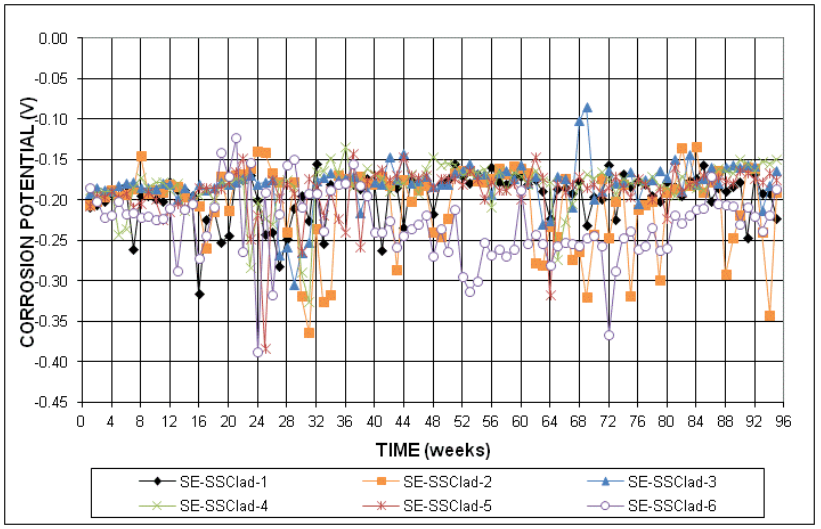

(a)

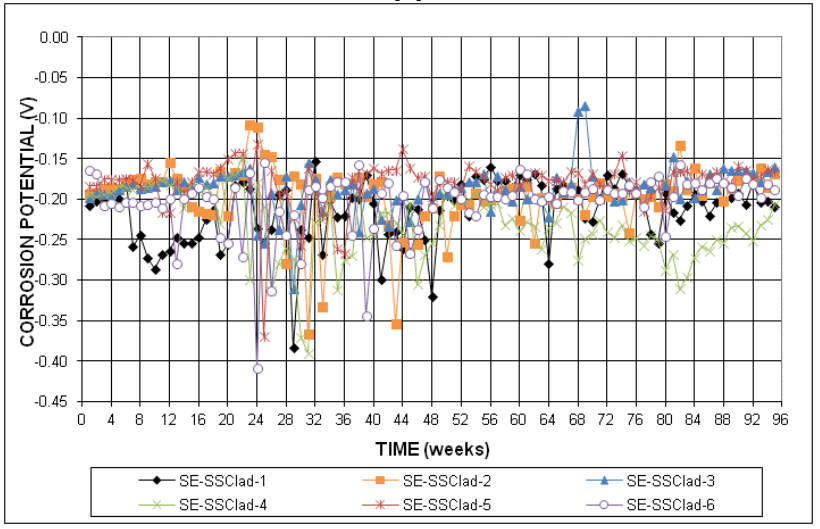

(b)

Figure A.58: (a) Top mat corrosion potentials and (b) bottom mat corrosion potentials for undamaged SSClad Southern Exposure specimens

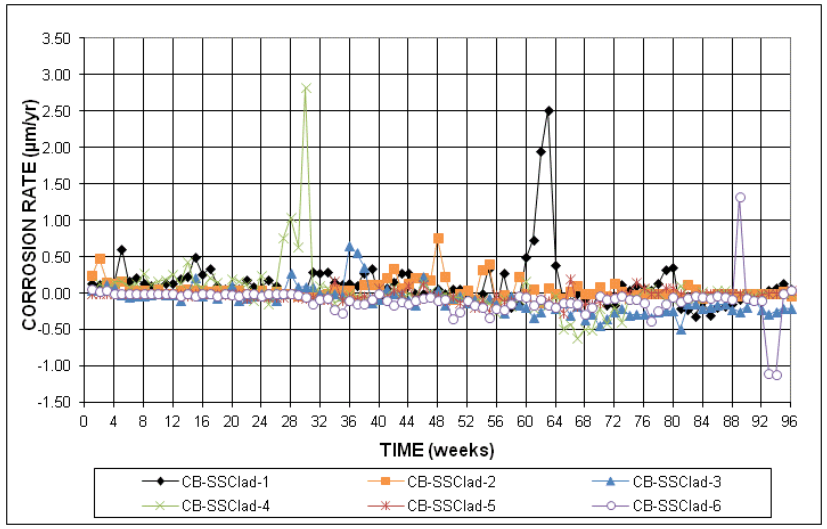

(a)

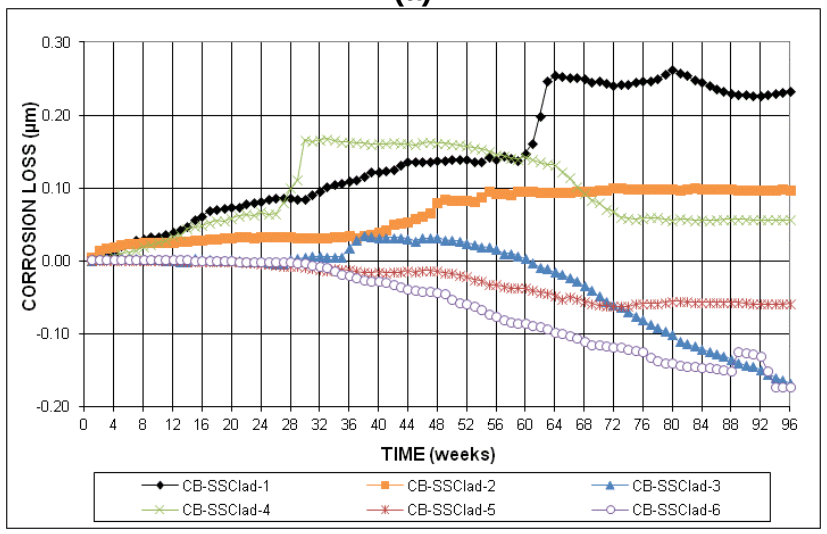

(b)

Figure A.59: (a) Corrosion rate and (b) total corrosion losses for undamaged SSClad cracked beam specimens

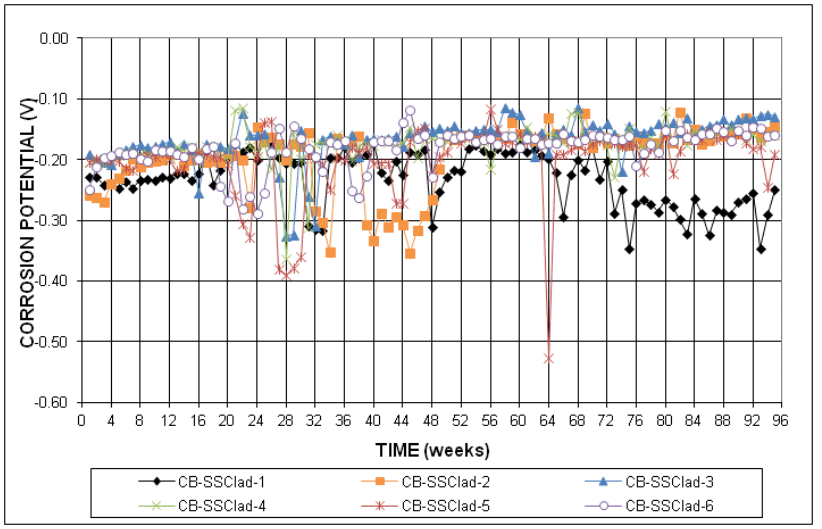

(a)

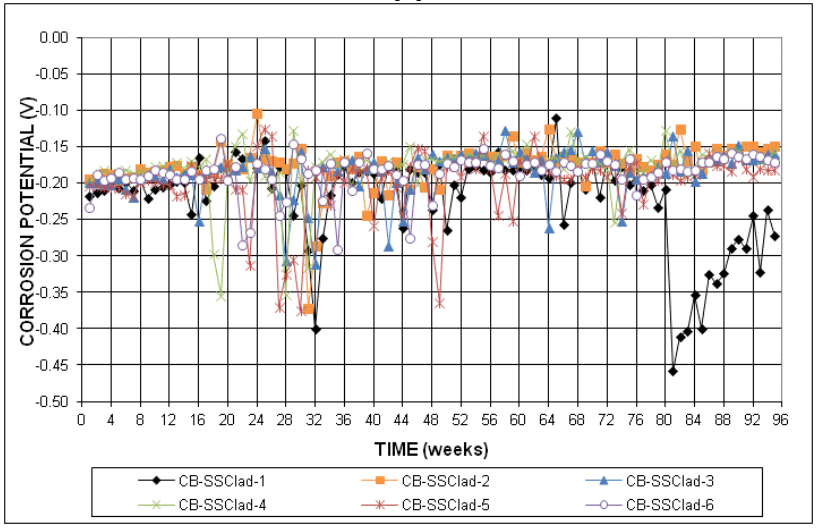

(b)

Figure A.60: (a) Top mat corrosion potentials and (b) bottom mat corrosion potentials for undamaged SSClad cracked beam specimens

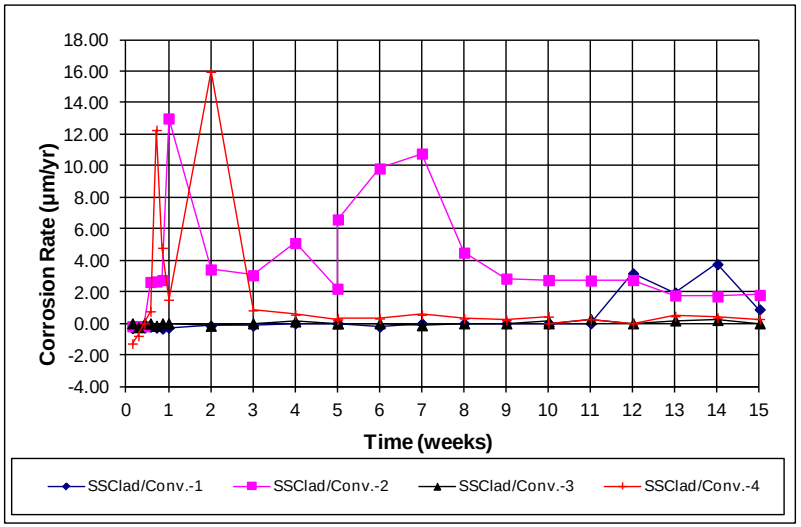

(a)

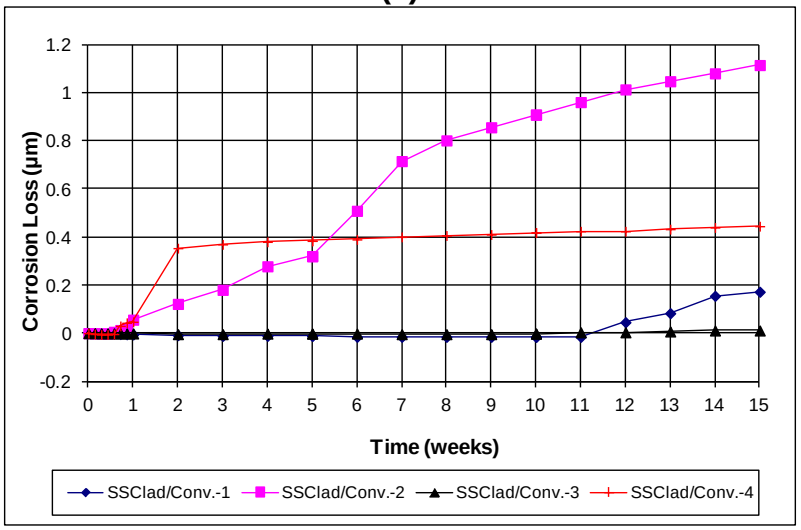

(b)

Figure A.61: (a) Corrosion rate and (b) total corrosion losses for SSClad (anode) and conventional (cathode) macrocell specimens

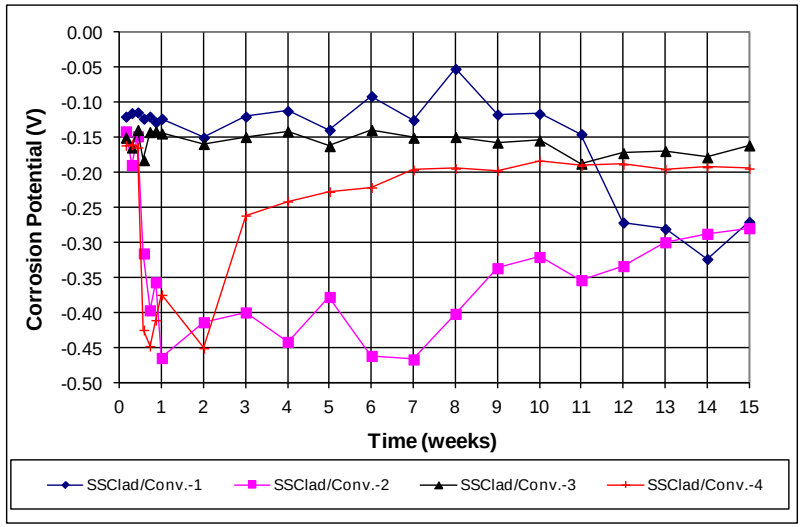

(a)

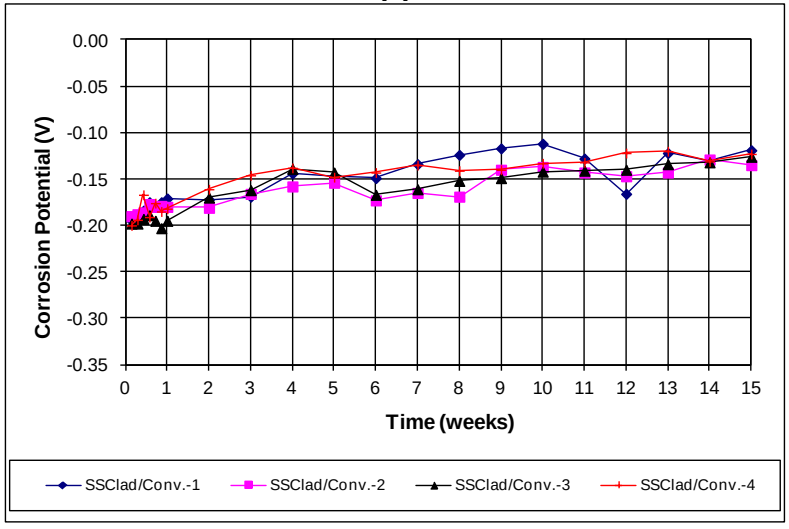

(b)

Figure A.62: (a) Top mat corrosion potentials and (b) bottom mat corrosion potentials for SSClad (anode) and conventional (cathode) macrocell specimens

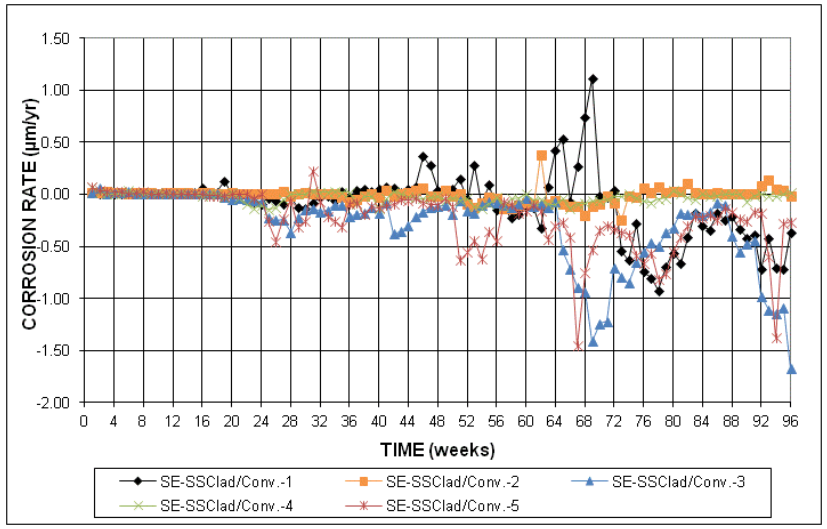

(a)

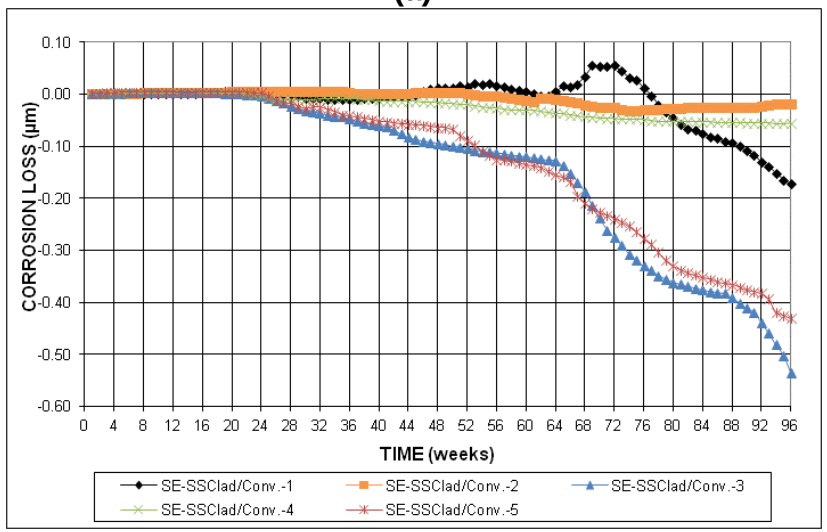

(b)

Figure A.63: (a) Corrosion rate and (b) total corrosion losses for SSClad (anode) and conventional (cathode) Southern Exposure specimens

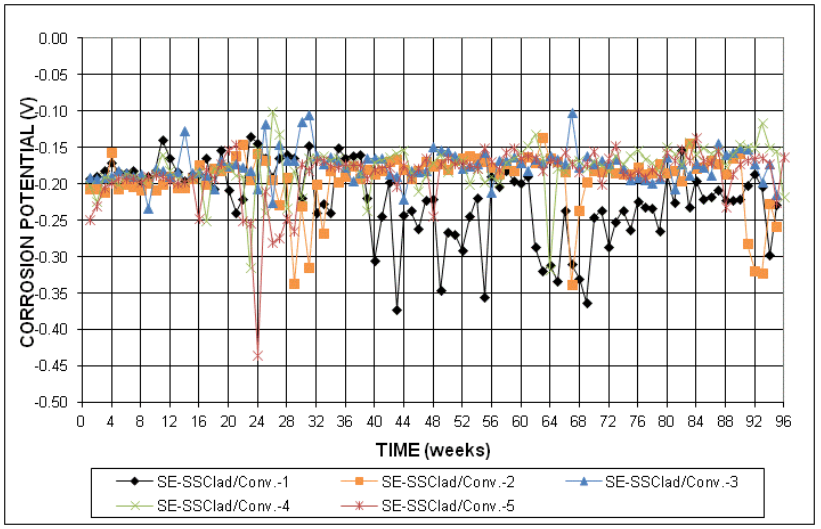

(a)

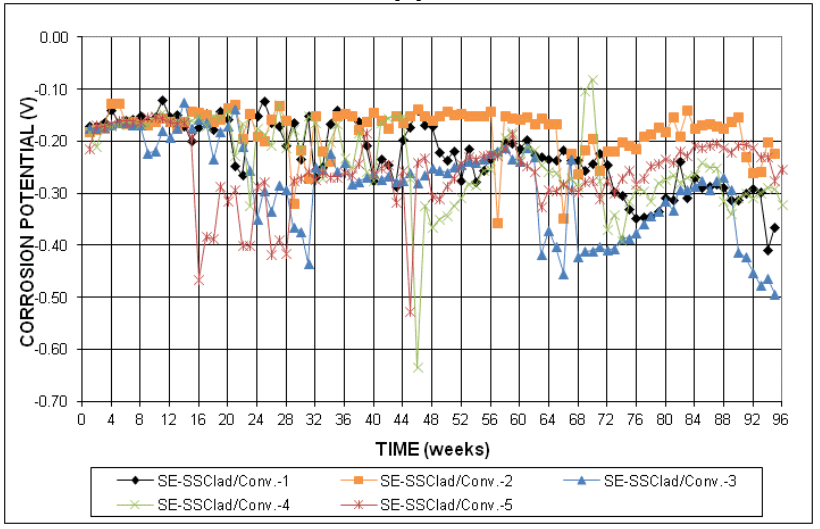

(b)

Figure A.64: (a) Top mat corrosion potentials and (b) bottom mat corrosion potentials for SSClad (anode) and conventional (cathode) Southern Exposure specimens

APPENDIX B

MAT-TO-MAT RESISTANCE OF BENCH-SCALE SPECIMENS

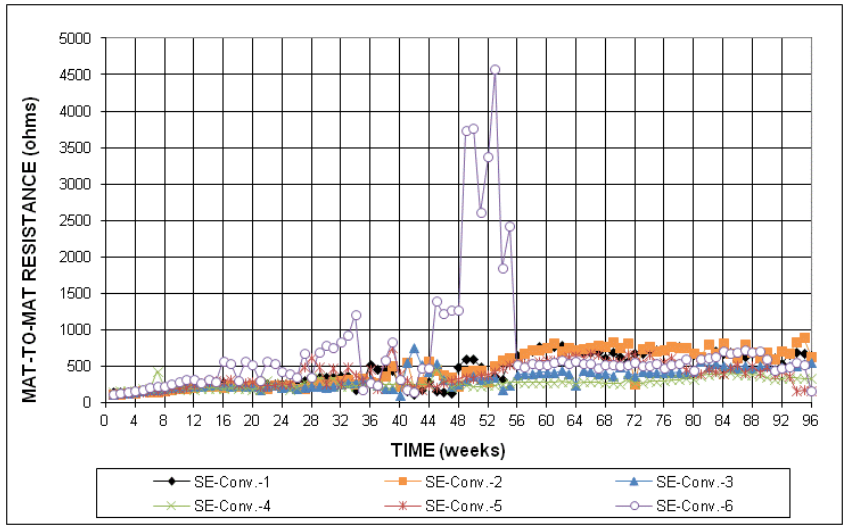

Figure B.1: Mat-to mat resistance for Southern Exposure specimens containing Conventional steel

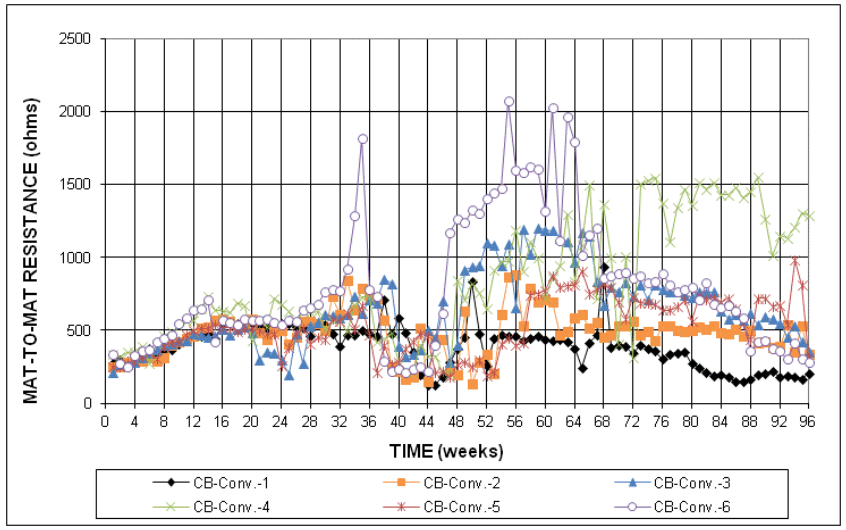

Figure B.2: Mat-to-mat resistance for cracked beam specimens containing conventional steel

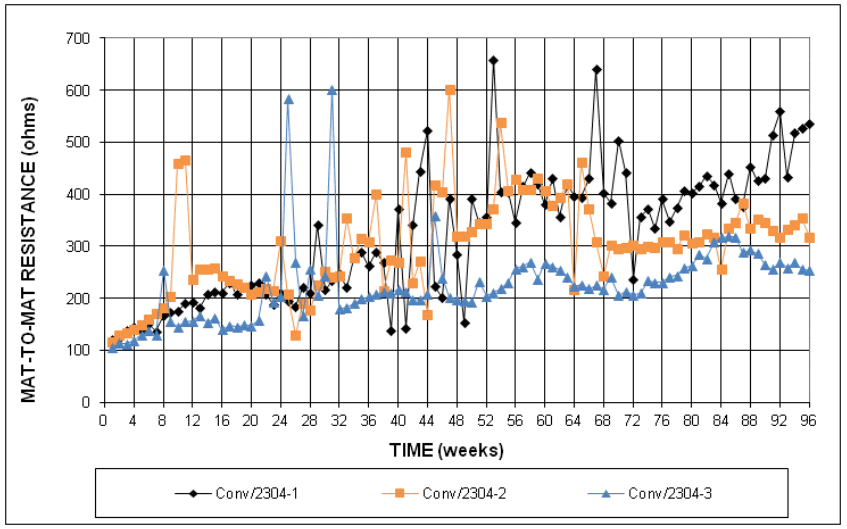

Figure B.3: Mat-to-mat resistance for Southern Exposure specimens containing Conventional (anode) and 2304 stainless steel (cathode)

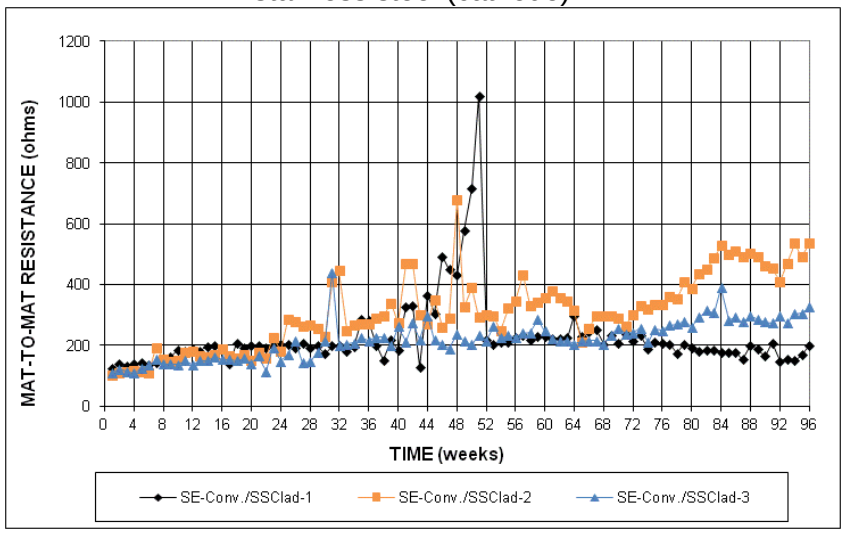

Figure B.4: Mat-to mat resistance for Southern Exposure specimens containing Conventional (anode) and SSClad (cathode)

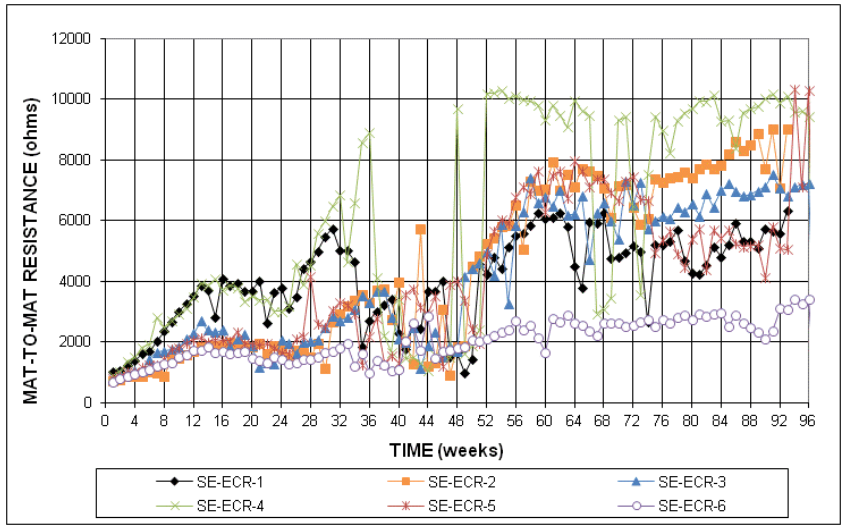

Figure B.5: Mat-to mat resistance for Southern Exposure specimens containing ECR

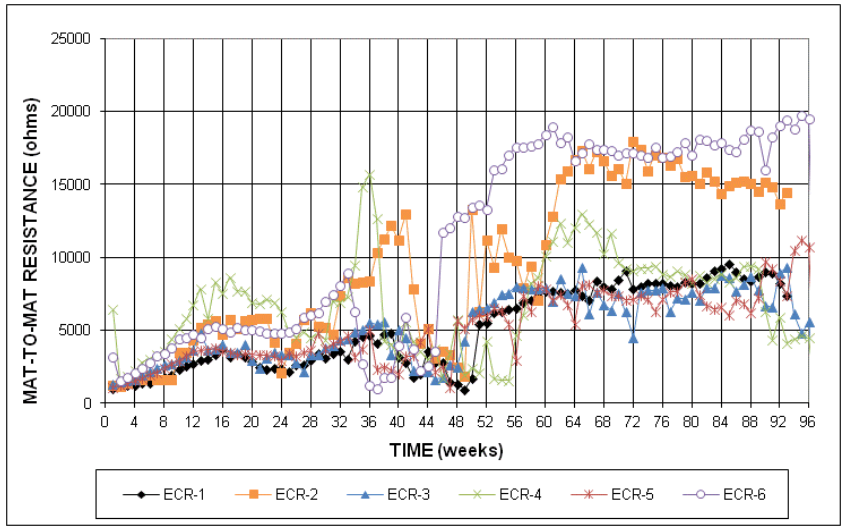

Figure B.6: Mat-to-mat resistance for cracked beam specimens containing ECR

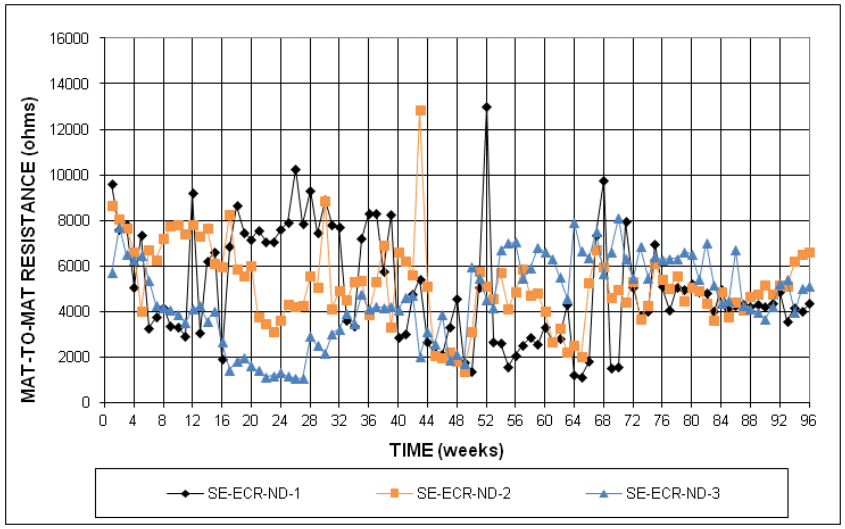

Figure B.7: Mat-to-mat resistance for Southern Exposure specimens containing undamaged ECR

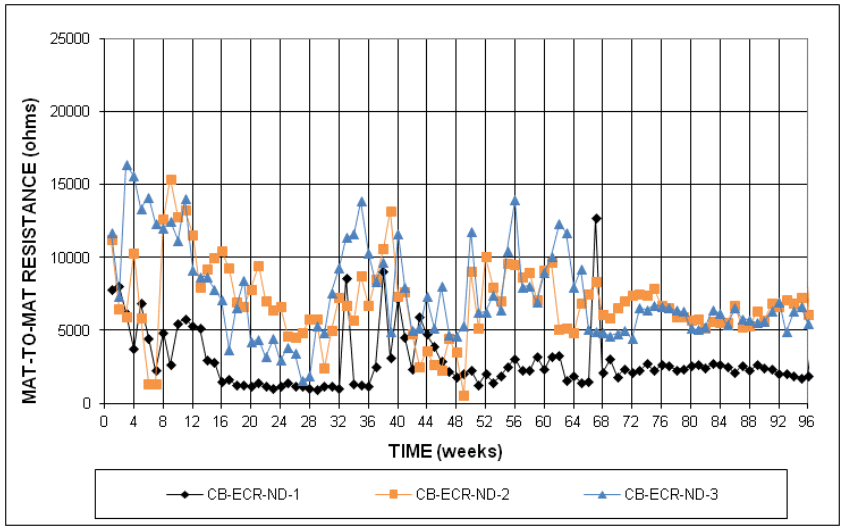

Figure B.8: Mat-to mat resistance for cracked beam specimens containing undamaged ECR

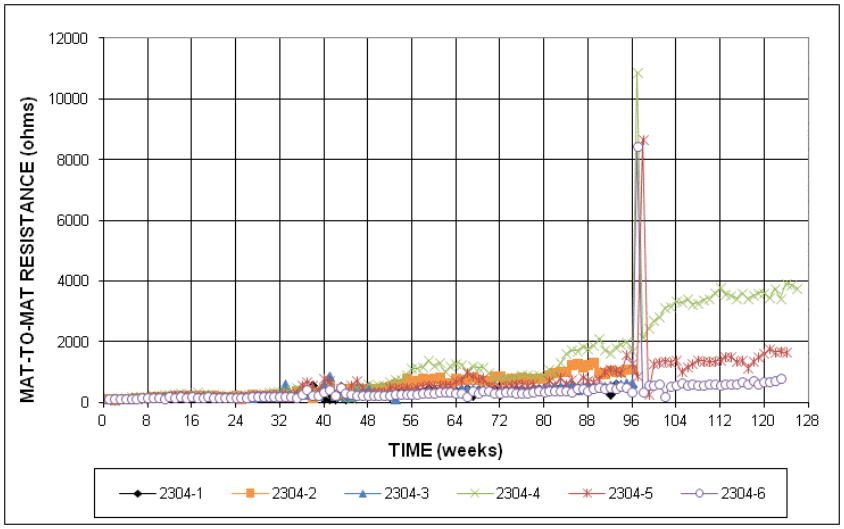

Figure B.9: Mat-to mat resistance for Southern Exposure specimens containing 2304 stainless steel

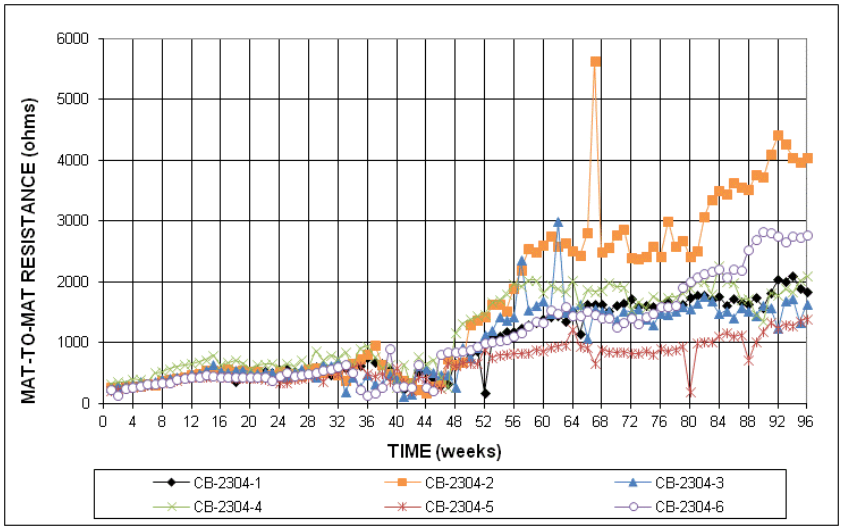

Figure B.10: Mat-to-mat resistance for cracked beam specimens containing 2304 stainless steel

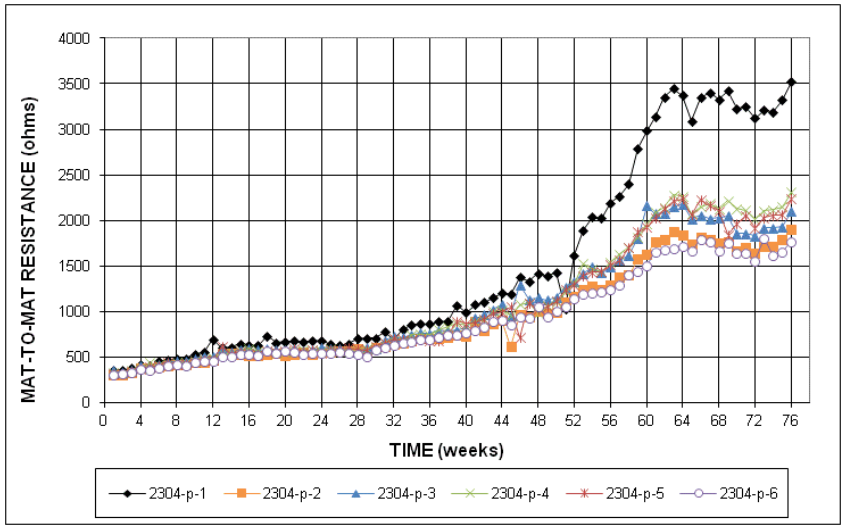

Figure B.11: Mat-to-mat resistance for cracked beam specimens containing repickled 2304 stainless steel

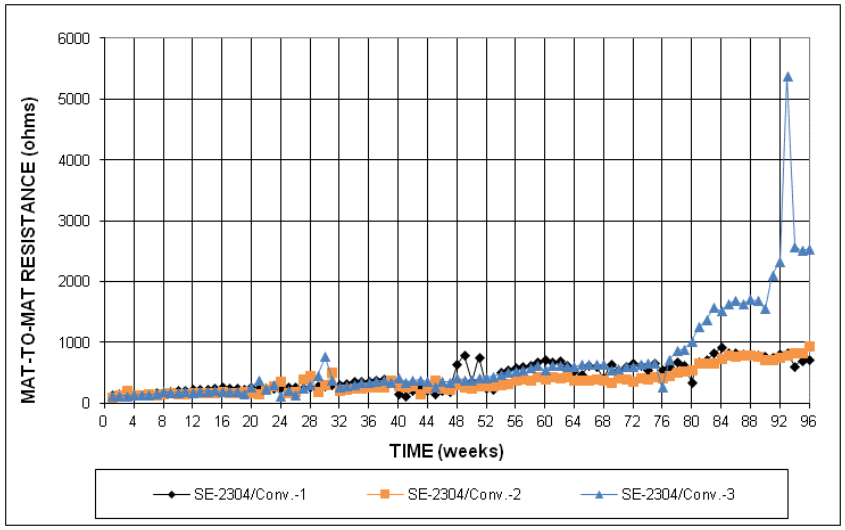

Figure B.12: Mat-to mat resistance for Southern Exposure specimens containing 2304 stainless steel (anode) and Conventional steel (cathode)

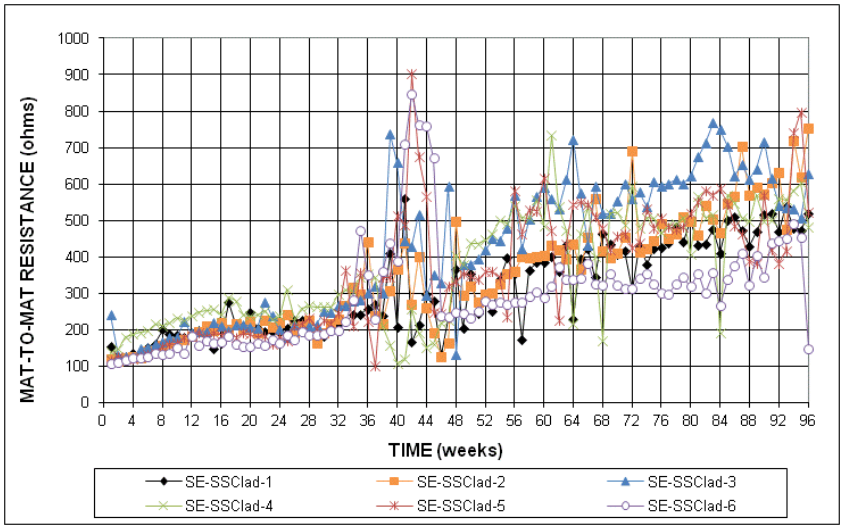

Figure B.13: Mat-to mat resistance for Southern Exposure specimens containing undamaged SSCIad

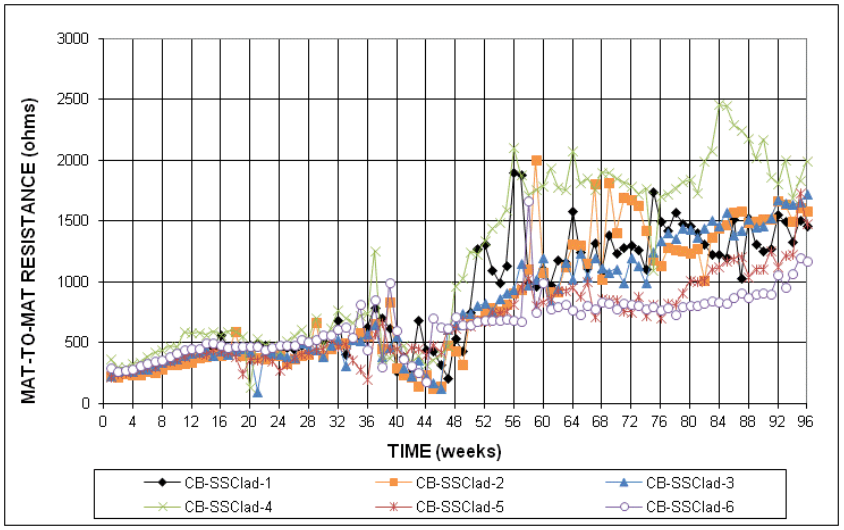

Figure B.14: Mat-to-mat resistance for cracked beam specimens containing undamaged SSCIad

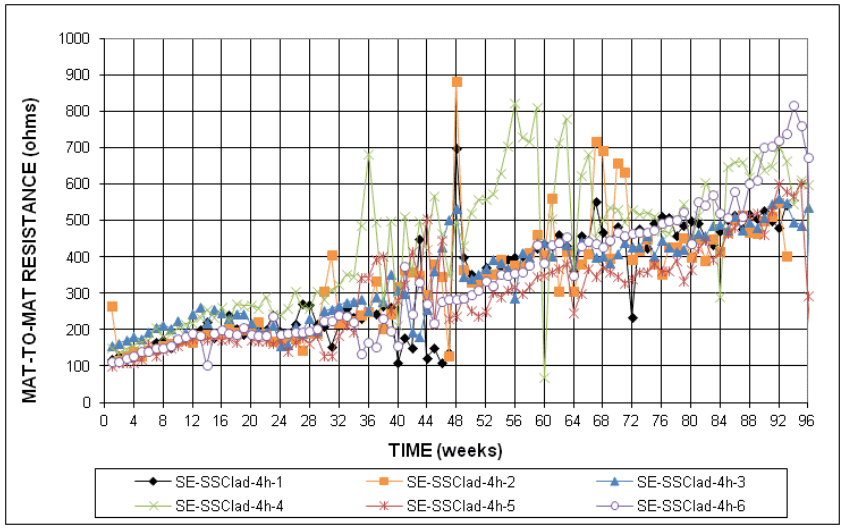

Figure B.15: Mat-to-mat resistance for Southern Exposure specimens containing SSCIad with four holes

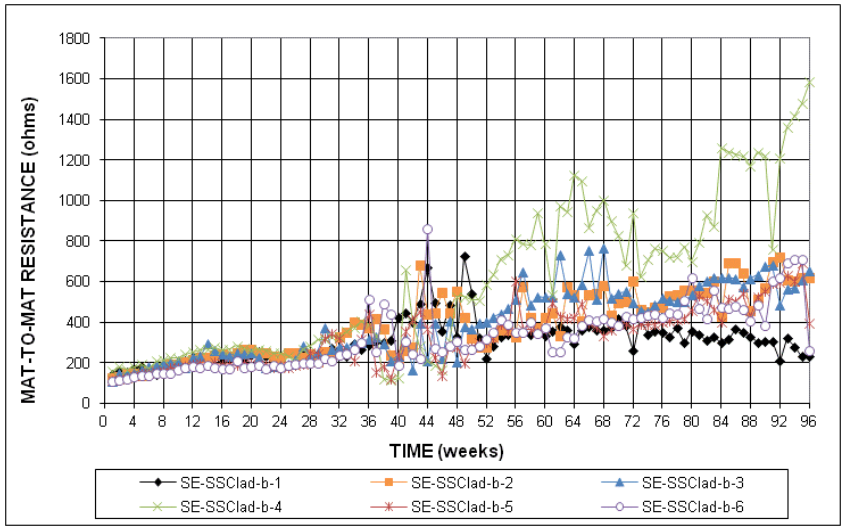

Figure B.16: Mat-to mat resistance for Southern Exposure specimens containing bent SSCIad

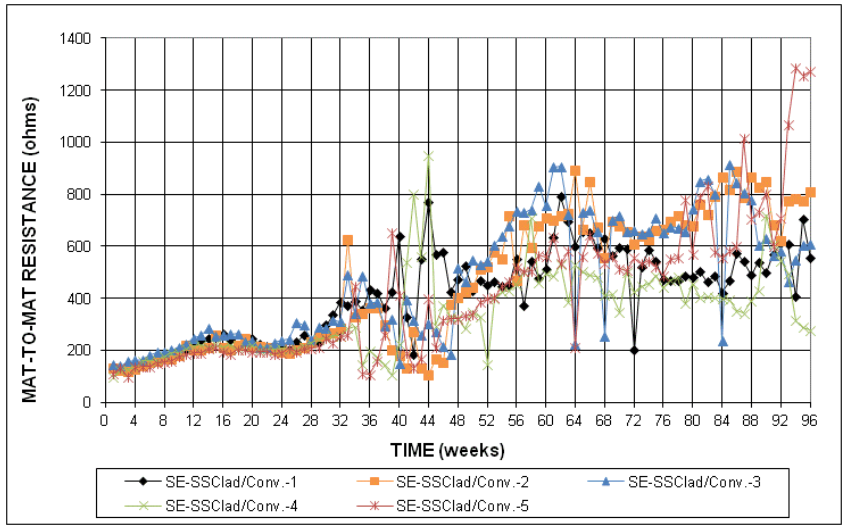

Figure B.17: Mat-to mat resistance for Southern Exposure specimens containing SSClad (anode) and Conventional (cathode)

APPENDIX C

CHLORIDE CONCENTRATION DATA

Table C.1: Chloride concentration data for Conventional specimens at 96 weeks

Specimen	Chloride Content (lb/yd^3)										Average	Standard Deviation
	1	2	3	4	5	6	7	8	9	10		
Conv-1												
Conv-2	20.29	11.62	11.89	12.68	12.47	15.50	10.60	13.21	14.43	9.08	13.18	3.09
Conv-3												
Conv-4												
Conv-5	17.97	15.33	19.37	20.82	15.77	23.28	19.81	24.04	18.15	26.24	20.08	3.56
Conv-6	28.01	25.05	29.59	24.04	24.22	26.75	30.34	28.77	28.14	32.59	27.75	2.78
Average											**20.33**	**6.78**

Table C.2: Chloride concentration data for Conventional (anode) and 2304 stainless steel (cathode) specimens at 96 weeks

Specimen	Chloride Content (lb/yd^3)										Average	Standard Deviation
	1	2	3	4	5	6	7	8	9	10		
Conv/2304-1	14.26	11.55	12.30	13.13	14.26	-	7.09	12.68	13.37	10.54	12.13	2.24
Conv/2304-2	22.39	21.83	19.37	25.05	24.67	17.29	22.52	22.19	17.92	18.67	21.19	2.73
Conv/2304-3	22.27	22.99	31.24	25.65	31.13	29.94	30.80	24.97	26.20	25.94	27.11	3.40
Conv/2304-4	20.06	21.85	18.17	24.48	15.96	12.43	14.51	17.02	15.39	18.23	17.81	3.59
Conv/2304-5	22.77	21.51	27.58	26.87	23.48	29.52	-	-	-	-	25.29	3.15
Conv/2304-1r	34.57	34.95	35.64	-	32.74	23.09	26.87	38.95	45.27	36.44	34.28	6.44
Average											**22.97**	**8.03**

Table C.3: Chloride concentration data for Conventional (anode) and SSClad (cathode) specimens at 96 weeks

Specimen	Chloride Content (lb/yd^3)										Average	Standard Deviation
	1	2	3	4	5	6	7	8	9	10		
Conv/SSClad-1	26.67	28.88	18.48	28.94	27.05	23.45	24.88	25.53	20.57	33.10	25.75	4.25
Conv/SSClad-2	26.24	32.07	20.88	25.61	28.39	22.27	22.27	30.68	29.05	28.89	26.64	3.83
Conv/SSClad-3	22.36	20.18	22.40	20.35	23.32	25.11	28.07	16.65	17.92	20.94	21.73	3.34
Average											**24.71**	**4.28**

Table C.4: Chloride concentration data for ECR specimens at 96 weeks

Specimen	Chloride Content (lb/yd^3)										Average	Standard Deviation
	1	2	3	4	5	6	7	8	9	10		
ECR-1	27.63	24.79	20.19	20.27	15.58	9.72	16.28	17.14	15.99	27.55	19.51	5.77
ECR-2	19.43	18.36	20.17	19.68	23.99	21.41	19.83	33.17	24.46	24.23	22.47	4.36
ECR-3	29.84	28.10	26.81	33.44	26.04	26.29	23.02	26.05	19.18	24.67	26.34	3.82
ECR-4	24.41	26.56	18.72	28.14	29.90	23.33	23.09	39.37	31.37	21.12	26.60	5.95
ECR-5	26.00	23.87	29.68	28.16	23.97	25.93	24.34	22.80	28.17	24.94	25.79	2.24
ECR-6	24.63	27.95	27.60	28.78	21.03	-	24.69	22.19	24.30	22.97	24.90	2.70
Average											**24.27**	**4.92**

Table C.5: Chloride concentration data for 2304 stainless steel at 96 weeks

Specimen	Chloride Content (lb/yd^3)										Average	Standard Deviation
	1	2	3	4	5	6	7	8	9	10		
2304-1	11.61	11.48	12.11	15.91	16.59	17.21	19.06	15.88	16.06	17.28	15.32	2.65
~~2304-2~~	~~14.01~~	~~9.27~~	~~10.70~~	~~11.22~~	~~7.70~~	~~11.57~~	~~10.65~~	~~14.70~~	~~12.69~~	~~14.02~~	~~11.65~~	~~2.23~~
2304-3	20.46	13.77	18.85	18.66	21.25	28.45	26.74	20.10	20.80	20.78	20.99	4.11
2304-4	30.54	24.16	18.71	19.71	26.54	32.17	22.77	26.75	21.18	21.89	24.44	4.50
2304-5	26.33	28.06	17.38	14.64	22.39	23.71	23.77	26.77	17.37	25.34	22.57	4.58
2304-6	22.39	21.01	23.72	21.26	19.39	21.69	12.55	26.22	28.32	22.31	21.89	4.20
Average											**21.04**	**4.99**

- Specimen 2 was found to be an outlier likely due to error during the chloride testing

Table C.6: Chloride concentration data for 2304 stainless steel (anode) and Conventional (cathode) at 96 weeks

Specimen	Chloride Content (lb/yd^3)										Average	Standard Deviation
	1	2	3	4	5	6	7	8	9	10		
2304/Conv.-1	14.33	16.70	19.28	17.43	15.74	25.59	20.09	23.03	23.28	20.35	19.58	3.62
2304/Conv.-2	26.34	28.42	24.98	27.76	30.34	32.17	35.09	33.77	37.46	27.82	30.42	4.08
2304/Conv.-3	20.94	22.90	33.31	26.31	26.69	25.49	23.15	30.34	21.13	23.40	25.37	3.98
Average											**25.12**	**5.87**

Table C.7: Chloride concentration data for SSClad with four holes at 96 weeks

Specimen	Chloride Content (lb/yd^3)										Average	Standard Deviation
	1	2	3	4	5	6	7	8	9	10		
SSClad-1												
SSClad-2												
SSClad-3	15.18	11.94	14.16	11.94	9.65	15.87	16.72	23.72	8.60	17.27	14.50	4.36
SSClad-4												
SSClad-5												
SSClad-6												
SSClad-7	26.94	22.52	23.78	22.37	25.30	23.34	28.64	24.54	-	31.16	25.40	2.98
Average											**19.95**	**6.69**

Table C.8: Chloride concentration data for undamaged SSClad at 96 weeks

Specimen	Chloride Content (lb/yd^3)										Average	Standard Deviation
	1	2	3	4	5	6	7	8	9	10		
SSClad-ND-1	16.83	17.66	16.40	15.58	13.63	24.56	15.33	16.40	12.43	22.66	17.15	3.76
SSClad-ND-2	25.55	30.55	-	22.90	29.87	15.20	22.53	24.92	27.53	21.07	24.46	4.75
SSClad-ND-3	15.77	26.10	21.22	15.45	16.84	17.60	18.93	19.44	19.00	26.23	19.66	3.85
SSClad-ND-4	15.58	14.51	15.39	15.20	14.01	25.61	23.83	19.63	16.72	16.59	17.71	4.03
SSClad-ND-5	8.01	14.24	13.09	19.34	16.28	10.47	14.35	14.81	13.27	14.23	13.81	3.05
SSClad-ND-6	13.82	16.61	16.84	16.21	18.61	16.65	14.83	12.30	11.02	13.12	15.00	2.39
Average											**17.96**	**4.91**

Table C.9: Chloride concentration data for bent SSClad at 96 weeks

Specimen	Chloride Content (lb/yd^3)										Average	Standard Deviation
	1	2	3	4	5	6	7	8	9	10		
SSClad-b-1	16.34	22.96	13.93	18.73	13.69	19.56	18.48	24.72	16.40	22.36	18.72	3.76
SSClad-b-2	26.46	27.89	29.14	24.37	35.59	39.28	31.98	19.32	44.76	24.67	30.35	7.67
SSClad-b-3	23.74	23.14	19.24	19.81	20.43	29.80	21.57	16.11	19.68	19.51	21.30	3.67
SSClad-b-4	20.64	25.30	23.40	22.97	17.99	17.29	21.76	14.37	26.69	27.05	21.75	4.20
SSClad-b-5	29.78	25.57	26.18	20.25	22.28	22.71	23.03	23.34	27.76	25.49	24.64	2.85
SSClad-b-6	28.11	23.66	20.18	20.44	30.43	19.37	21.39	23.28	24.60	17.98	22.94	3.94
Average											**23.28**	**5.74**

Table C.10: Chloride concentration data for SSClad (anode) and Conventional (Cathode) at 96 weeks

Specimen	Chloride Content (lb/yd^3)										Average	Standard Deviation
	1	2	3	4	5	6	7	8	9	10		
SSClad/Conv.-1	-	31.87	32.29	29.56	26.33	28.75	29.35	30.99	28.08	24.91	29.13	2.45
SSClad/Conv.-2	13.36	16.32	13.48	17.13	19.30	-	17.75	17.37	24.88	11.46	16.78	3.94
SSClad/Conv.-3	22.73	21.67	28.78	22.36	14.92	16.21	14.64	14.19	17.00	9.33	18.18	5.63
SSClad/Conv.-4	25.36	25.87	25.36	23.53	23.97	26.24	24.04	19.94	31.86	24.85	25.10	2.97
SSClad/Conv.-5	26.25	19.09	22.27	26.61	23.60	15.52	18.74	23.56	28.39	26.68	23.07	4.17
SSClad/Conv.-6	20.69	16.53	17.22	17.54	21.20	23.34	21.58	23.53	28.45	22.84	21.29	3.60
Average											**22.26**	**5.57**

Table C.11: Chloride concentration data for conventional specimens at corrosion initiation

Specimen	Initiation Age (weeks)	Chloride Content (lb/yd^3)						Average	Standard Deviation
		1	2	3	4	5	6		
Conv.-1	16	3.91	2.78	2.02	0.63	0.57	4.82	2.45	1.80
Conv.-2	18	1.69	0.50	2.59	1.64	0.44	1.14	1.33	1.41
Conv.-3	10	1.01	1.70	1.39	1.14	0.88	0.76	1.15	0.60
Conv.-4	*4*	*0.47*	*0.91*	*0.26*	*0.63*	*0.06*	*0.51*	*Void*	*Void*
Conv.-1r	10	0.44	2.33	0.38	1.58	2.02	2.59	1.53	1.02
Conv.-5	9	1.45	3.41	2.02	0.57	0.76	0.44	1.44	0.96
Conv.-6	12	6.43	0.32	1.27	5.43	2.78	0.44	2.78	2.04
								1.78	**1.31**

Table C.12: Chloride concentration data for conventional (anode) and 2304 stainless steel (cathode) at corrosion initiation

Specimen	Initiation Age (weeks)	Chloride Content (lb/yd^3)						Average	Standard Deviation
		1	2	3	4	5	6		
Conv./2304-1	*7*	*0.57*	*0.57*	*0.67*	*0.38*	*0.32*	*0.82*	*Void*	*Void*
Conv./2304-2	5	0.99	0.74	0.52	1.54	1.14	0.35	0.88	0.43
Conv./2304-3	*5*	*0.28*	*0.29*	*0.26*	*0.51*	*0.28*	*0.19*	*Void*	*Void*
Conv./2304-4	11	5.11	2.08	1.45	1.15	1.01	1.14	1.99	1.58
Conv./2304-5	*5*	*0.50*	*0.25*	*0.38*	*0.52*	*0.38*	*0.50*	*Void*	*Void*
Conv./2304-1r	8	1.14	3.09	2.02	4.04	0.63	3.60	2.42	1.38
								1.76	**1.13**

Table C.13: Chloride concentration data for conventional (anode) and stainless steel clad (cathode) at corrosion initiation

Specimen	Initiation Age (weeks)	Chloride Content (lb/yd^3)						Average	Standard Deviation
		1	2	3	4	5	6		
Conv./SSClad-1	8	0.99	0.74	1.17	1.54	1.14	1.05	1.10	0.26
Conv./SSClad-2	10	3.03	0.44	2.33	0.38	1.58	2.02	1.53	1.02
Conv./SSClad-3	10	4.04	0.50	0.63	0.19	6.25	0.25	2.13	2.28
								1.59	**1.19**

Table C.14: Chloride concentration data for ECR specimens with holes at corrosion initiation

Specimen	Initiation Age (weeks)	Chloride Content (lb/yd^3)						Average	Standard Deviation
		1	2	3	4	5	6		
ECR-2	12	4.82	2.14	5.11	1.45	1.14	3.15	2.97	1.70
ECR-3	14	1.26	5.49	6.50	5.39	2.50	3.22	4.06	2.04
ECR-4	20	6.24	15.33	3.56	4.23	5.75	3.11	6.37	4.56
ECR-5	13	1.39	1.64	0.57	2.02	2.84	4.42	2.14	1.34
ECR-6	14	2.75	6.67	3.37	1.26	5.24	4.98	4.05	1.95
								3.92	**2.32**

Table C.15: Chloride concentration data for 2304 stainless steel specimens at corrosion initiation

Specimen	Initiation Age (weeks)	Chloride Content (lb/yd^3)										Average	Standard Deviation
		1	2	3	4	5	6	7	8	9	10		
2304-2	89	13.12	11.67	16.65	12.74	13.25	19.94					14.56	3.12
2304-3	96	20.46	13.77	18.85	18.66	21.25	28.45	26.74	20.10	20.80	20.78	20.24	4.79
2304-5	98	24.44	24.32	30.81	20.73	22.09	26.43	30.92	14.19	28.23		24.80	3.55
2304-6	116	28.96	24.79	26.81	23.03	21.88	22.21	17.85	15.14	21.01	17.03	24.61	2.81
												21.05	**3.57**

Table C.16: Chloride concentration data for 2304 stainless steel (anode) and conventional (cathode) at corrosion initiation

Specimen	Initiation Age (weeks)	Chloride Content (lb/yd^3)								Average	Standard Deviation
		1	2	3	4	5	6	7	8		
2304/Conv.-2	81	17.61	13.82	21.11	22.94	31.30	18.60	27.13	23.59	22.01	5.54
2304/Conv.-2*	69	19.4	23.3	18.6	17.9	14.4	20.3			18.99	2.93
										20.50	**4.23**

Table C.17: Chloride concentration data for stainless steel clad specimens with holes at corrosion initiation

Specimen	Initiation Age (weeks)	Chloride Content (lb/yd^3)						Average	Standard Deviation
		1	2	3	4	5	6		
SSClad-4h-1	48	18.00	21.10	14.60	13.40	8.80	11.20	8.44	2.91
SSClad-4h-2	35	6.12	5.55	9.97	7.07	7.44	8.83	8.02	1.53
SSClad-4h-3	24	3.03	4.04	6.44	9.78	9.97	8.16	6.90	2.92
SSClad-4h-4	*5*	*0.19*	*0.14*	*0.07*	*0.07*	*0.13*	*0.36*	*Void*	*Void*
SSClad-4h-4*	17	1.03	2.90	3.03	14.57	4.03	1.89	4.57	5.00
SSClad-4h-5	26	10.1	9.72	9.15	11	11.8	9.65	10.07	0.87
SSClad-4h-6	27	14.19	14.70	9.34	13.75	9.34	6.50	11.76	2.60
SSClad-4h-1r	10	4.54	2.14	3.34	3.66	1.58	1.96	3.56	1.77
								8.29	**1.42**

Table C.18: Chloride concentration data for bent stainless steel clad specimens at corrosion initiation

Specimen	Initiation Age (weeks)	Chloride Content (lb/yd^3)						Average	Standard Deviation
		1	2	3	4	5	6		
SSClad-b-2	35	9.53	12.11	11.36	19.68	13.25	16.72	14.01	2.89
SSClad-b-3	46	23.70	24.80	26.20	20.40	17.10	24.60	16.04	2.79
								15.02	**0.07**

APPENDIX D

DISBONDMENT DATA

Table D.1: Disbondment data for ECR macrocell specimens

Specimen	Macrocell				
	Site 1 Area ($in.^2$)	Site 2 Area ($in.^2$)	Site 3 Area ($in.^2$)	Site 4 Area ($in.^2$)	Average Area ($in.^2$)
ECR-1	0.18	0.14	0.13	0.13	0.15
ECR-2	0.16	0.19	0.17	0.22	0.19
ECR-3	0.11	0.21	0.10	0.26	0.17
ECR-4	0.19	0.08	0.15	0.08	0.13
ECR-5	0.06	0.32	0.09	0.09	0.14
ECR-6	0.33	0.20	0.52	0.09	0.29

Table D.2: Disbondment data for ECR in Southern Exposure specimens

Specimen		Southern Exposure			
		Top Side 1	Top Side 2	Bottom Side	Average Top Side
		Area* ($in.^2$)	Area* ($in.^2$)	Area* ($in.^2$)	Area* ($in.^2$)
ECR-1	Top Bar	1.05	1.05	1.05	1.05
	Bottom Bar	0.1	0	0	0.05
ECR-2	Top Bar	1.05	1.05	1.05	1.05
	Bottom Bar	0	0	0	0
ECR-3	Top Bar	1.05	1.05	1.05	1.05
	Bottom Bar	0.3	0	0.51	0.15
ECR-4	Top Bar	1.05	1.05	1.05	1.05
	Bottom Bar	0.16	0.03	0	0.095
ECR-5	Top Bar	1.05	1.05	1.05	1.05
	Bottom Bar	0.18	0.13	0	0.155
ECR-6	Top Bar	1.05	1.05	1.05	1.05
	Bottom Bar	0.34	0.28	0.11	0.31

*An area of 1.05 $in.^2$ corresponds to total disbondment

Table D.3: Disbondment data for ECR in cracked beam specimens

Specimen		Cracked Beam			
		Top Side 1	Top Side 2	Bottom Side	Average Top Side
		Area* ($in.^2$)	Area* ($in.^2$)	Area* ($in.^2$)	Area* ($in.^2$)
ECR-1	Top Bar	1.05	1.05	1.05	1.05
	Bottom Bar	0.46	0.7	0.45	0.58
ECR-2	Top Bar	1.05	1.05	1.05	1.05
	Bottom Bar	0	0	0	0
ECR-3	Top Bar	1.05	1.05	1.05	1.05
	Bottom Bar	0.71	0	0.18	0.355
ECR-4	Top Bar	1.05	1.05	1.05	1.05
	Bottom Bar	0.41	0.23	0.12	0.32
ECR-5	Top Bar	1.05	1.05	1.05	1.05
	Bottom Bar	0.55	0.28	0.19	0.415
ECR-6	Top Bar	1.05	1.05	1.05	1.05
	Bottom Bar	0.83	0.12	0.36	0.475

*An area of 1.05 $in.^2$ corresponds to total disbondment

APPENDIX E

COST DATA

Table E.1: Concrete and steel placement costs in new bridge decks in 2012

ODOT Project Number	Deck Area yd^2	Class AA Concrete, yd^3	Class AA Concrete Cost	Steel Reinf., lb	Steel Cost, $/lb.	ECR Cost, $/lb.
BRO-106D(116)CI	263.4	63.7	$547.50	16276	$0.90	
BRO-126D(176)CI	286.4	93.8	$575.00	16810	$0.95	
BRF-133C(105)CI	378.5	96.6	$557.50	23000	$0.89	
SSP-106C(061)SS	1009.7	260.5	$425.00	68700		$1.10
BRFY-147C(121)	1498.3	356	$585.00	114870		$0.95
BRO-119D(129)CO	600.2	141.7	$350.00	30980	$0.99	
BRF-164C(012)CI	433.1	112	$504.00	35070	$0.92	
BRF-104C(068)CI	761.1	219.2	$605.00	43860	$0.94	
BRO-171D(094)CI	238.7	58	$515.00	13037	$1.00	
BRF-154C(100)CI	135.6	32.1	$500.00	6820	$1.50	
BRO-177D(098)CI	444.4	107.8	$550.00	24748	$1.00	
BRFY-116C(098)	896.0	224.4	$420.00	60890	$1.00	$1.10
BRO-139D(101)CI	230.5	54.9	$600.00	11950	$1.25	
BRFY-152C(068)	1051.4	263.9	$542.00	81050	$1.09	
BRO-112D(058)CI	291.6	71.9	$500.00	17010	$1.00	
Average			$518.40		$1.03	$1.05

Table E.2: Steel reinforcement density in new bridge decks in 2012

ODOT Project Number	Class AA Concrete Superstructure Only, yd^3	Steel Reinforcement Superstructure Only, lb	Steel Density, lb/yd^3
BRO-106D(116)CI	63.7	16276	255.51
BRO-126D(176)CI	93.8	16810	179.21
BRF-133C(105)CI	96.6	23000	238.10
SSP-106C(061)SS	260.5	68700	263.72
BRFY-147C(121)	356	114870	322.67
BRO-119D(129)CO	141.7	30980	218.63
BRF-164C(012)CI	112	35070	313.13
BRF-104C(068)CI	219.2	43860	200.09
BRO-171D(094)CI	58	13037	224.78
BRF-154C(100)CI	32.1	6820	212.46
BRO-177D(098)CI	107.8	24748	229.57
BRFY-116C(098)	224.4	60890	271.35
BRO-139D(101)CI	54.9	11950	217.67
BRFY-152C(068)	263.9	81050	307.12
BRO-112D(058)CI	71.9	17010	236.58
Average			**246.0**

Table E.3a: Bridge deck replacement costs (concrete)

Project	Year	Bridge Deck			Class AA Concrete		Concrete Rail		
		Length (ft)	Width (ft)	Area (ft^2)	Cost per yd^3	Cost per yd^2	Cost per linear ft.	Linear ft. of rail	Cost per yd^2
SBR-105C(197)SB	2012	91.33	32.17	2938	$1,091	$242.44	$110.00	262.7	$88.52
SBR-249N(004)SB	2012	126.50	27.00	3416	$900	$200.00			
SBR-161C(246)SB SBR-161B(247)SB	2012	92.00	46.00	4232	$780	$173.33			
BHO-149D(148)CI	2012	200.50	66.83	13400	$750	$166.67	$115.00	497	$38.39
SBR-272N(020)SB	2012	522.00	49.75	25970	$800	$177.78			
SBR-136N(211)SB	2012	141.50	42.17	5967	$750	$166.67	$75.00	362.8	$41.04
SBR-166C(254)SB	2012	440.83	32.17	14180	$575	$127.78	$65.00	1442	$59.49
SSP-165C(121)SS	2011	281.50	30.17	8493	$725	$161.11	$70.00	561	$41.61
SBR-145C(168)SB	2009	125.15	42.17	5278	$550	$122.22	$85.00	370	$53.63
SAB-169C(097)BF	2006	120.50	46.17	5563	$700	$155.56	$72.50	332.5	$39.00
SBR-115A(041)SB	2006	27.00	41.58	1123	$700	$155.56	$54.00	150	$64.93
Average					$756	$168	$80.81	497	$53.33

Table E.3b: Bridge deck replacement costs (other)

Project	Guard Rail		Approach Pavement		Remove Bridge Items		Mobilization		Traffic Control	
	Total Cost	Cost per yd^2	Total Cost	Cost per yd^2	Total Cost	Cost per yd^2	Total Cost	Cost per yd^2	Total Cost	Cost per yd^2
SBR-105C(197)SB	$10,800	$33.08	$55,624	170.40	$50,625	155.09	$25,500	78.12	$9,144	28.01
SBR-249N(004)SB	$5,200	$13.70	$16,800	44.27	$40,000	105.40	$36,849	97.10	$4,659	12.28
SBR-161C(246)SB SBR-161B(247)SB	$9,400	$19.99	$54,427	115.75	$140,000	297.73	$65,000	138.23	$63,758	135.59
BHO-149D(148)CI			$42,848	28.78	$75,000	50.37	$55,000	36.94	$59,503	39.96
SBR-272N(020)SB	$8,400	$2.91	$79,120	27.42	$135,000	46.79	$110,000	38.12	$88,300	30.60
SBR-136N(211)SB	$11,880	$17.92	$63,291	95.47	$27,500	41.48			$20,296	30.61
SBR-166C(254)SB	$17,088	$10.85	$56,188	35.66	$175,000	111.07	$125,000	79.34	$84,204	53.44
SSP-165C(121)SS	$14,900	$15.79			$83,000	87.96	$40,000	42.39	$14,150	14.99
SBR-145C(168)SB	$8,400	$14.32	$42,920	73.19	$25,000	42.63	$15,000	25.58	$5,000	8.53
SAB-169C(097)BF	$12,400	$20.06	$73,812	115.75	$54,000	87.36	$25,000	40.44	$34,400	55.65
SBR-115A(041)SB			$16,800	134.67	$20,000	160.32	$15,000	120.24	$110,240	883.69
Average	$10,941	$16.51	$50,183	$84.14	$75,011	$107.84	$51,235	$69.65	$44,878	$117.58